Proceeding No.: A.15-09-010
Exhibit No.: SDG&E-14
Witness: Vanderburg

PREPARED REBUTTAL TESTIMONY OF

STEVE VANDERBURG

ON BEHALF OF

SAN DIEGO GAS & ELECTRIC COMPANY

BEFORE THE PUBLIC UTILITIES COMMISSION
OF THE STATE OF CALIFORNIA

DECEMBER 16, 2016

#310815

TABLE OF CONTENTS

PREPARED REBUTTAL TESTIMONY OF STEVE VANDERBURG

ON BEHALF OF SAN DIEGO GAS & ELECTRIC COMPANY

I. INTRODUCTION

Q. Please state your name and title.

A. My name is Steve Vanderburg. I am currently employed by San Diego Gas & Electric Company ("SDG&E") as a Meteorologist.

Q. Have you previously submitted testimony in this proceeding?

A. Yes, I submitted Prepared Direct Testimony on September 25, 2015. In that testimony, I described my educational and professional background. I included a list of my qualifications as Appendix1 to my direct testimony.

Q. What is the purpose of your rebuttal testimony?

A. The purpose of my rebuttal testimony is to respond to the testimony submitted on October 17, 2016 by the Utility Consumers' Action Network ("UCAN") witnesses Dr. Alexander Gershunov ("Gershunov Testimony") and Dr. Janice Coen ("Coen Testimony"). Both of these witnesses challenge the conclusions I reached in my direct testimony regarding the wind and weather conditions in late October 2007, when Southern California experienced a series of massive wildfire outbreaks. I also respond to the portion of the October 4, 2016 testimony of the Office of Ratepayer Advocates ("ORA") witness Mr. Nils Stannik that challenged certain aspects of my direct testimony ("Stannik Testimony").

Q. Please provide a summary of your understanding of the wind and weather issues that are in dispute in this case.

A. At a high level, the dispute is about who has provided the most accurate estimates of the wind speeds in this case. On behalf of SDG&E, both Dr. Peterka and I testify that the wind

speeds that occurred during the Santa Ana wind event in late October 2007 were extreme. For the Witch Fire, I estimated that the peak wind gusts during the Santa Ana wind event in late October 2007 reached 92 miles per hour ("mph"). Dr. Peterka calculated a peak wind gust at the Witch Fire ignition site of 78-87 mph. Mr. Stannik and Dr. Coen attempt to undermine our analyses in various ways, but they do not present any analysis of what the wind speeds were in late October 2007. Dr. Gershunov does attempt to analyze wind speeds in late October 2007, but he concludes that they were far lower (43-56 mph at the Witch Fire ignition site) than what Dr. Peterka and I calculated. According to Dr. Gershunov, "the event was extreme, but not unprecedented."[1]

The reason these wind speed estimates vary is because they are derived using different methodologies or analytical approaches. I derived my 92 mph estimate using a statistical analysis of the relationship of the actual wind speed observations from the Julian Remote Automated Weather Station ("RAWS"), which is approximately 6 miles from the Witch Fire ignition site, with observations from an SDG&E weather station installed only four poles down from that ignition site. My estimate was consistent with the results of a number of other approaches or sources of information, including:

(1) The results of the Santa Ana Wildfire Threat Index ("SAWTI"), a predictive model that SDG&E developed in partnership with the U.S. Forest Service and UCLA (Fovell and Cao) that categorizes Santa Ana wind events with respect to the anticipated potential for a large fire to occur (like the index used to categorize hurricanes) and that conclusively shows that the October 2007 Santa Ana wind event had the greatest large fire potential on record, dating back 30 years. The SAWTI's assessment is verified by the actual events – over a dozen wildfires

[1] Gershunov Testimony (Part II), p. 4.

broke out in October 2007, from a variety of ignition sources, at multiple locations across Southern California and were driven by the intense winds.[2] This was anything but an ordinary Santa Ana wind event.

(2) The results of research performed at UCLA by Dr. Robert Fovell which used mesoscale atmospheric modeling – the Weather Research and Forecast ("WRF") model –to estimate a peak wind gust at the Witch Fire ignition site of 96 mph;[3]

(3) Dr. Peterka's approach, which used WRF modeling in conjunction with a wind tunnel to model the impact of the terrain at the ignition sites on wind flow;[4]

(4) Actual observations of damage caused by the October 2007 Santa Ana wind event.

By contrast, Dr. Gershunov's estimated wind speeds are not corroborated, and his methodology is undermined in a key respect, by UCAN's other witness, Dr. Coen. According to Dr. Coen, the resolution of atmospheric modeling is important, and she criticizes Dr. Fovell's use of very fine 666 meter grid spacing.[5] I believe that even finer grid spacing would produce even higher wind speeds than what Dr. Fovell estimated. But Dr. Gershunov uses very coarse 10 kilometer grid spacing in his atmospheric modeling, which leads him to reach a number of erroneous conclusions, as I discuss below.

Q. How is your testimony organized?

---

[2] See "California Fire Siege 2007: An Overview." This report was attached as Appendix 2 to the Prepared Direct Testimony of Lee Schavrien on Behalf of San Diego Gas & Electric Company (September 25, 2015).

[3] See Appendices 1-5.

[4] See Prepared Direct Testimony of Jon A. Peterka on Behalf of San Diego Gas & Electric Company (September 25, 2015).

[5] Coen Testimony, p. 7.

A. In Section II, I respond to the criticisms of the analysis I presented in my direct testimony regarding the relationship between the RAWS located in Julian, CA with the SDG&E weather station at West Santa Ysabel, near the ignition point of the Witch Fire. I used that analysis to estimate peak wind gusts of approximately 92 miles per hour ("mph"). I provide further evidence that supports the statistical validity of my 92 mph estimate. I also respond to various challenges Dr. Gershunov and Mr. Stannik raise in an attempt to distract from this powerful evidence of the extreme wind gusts in late October 2007.

In Section III, I respond to the criticisms of the Weather Research and Forecasting ("WRF") Model that has been configured to the conditions in our service territory by Dr. Robert Fovell (formerly at UCLA, now at the State University of New York Albany), SDG&E and the U.S. Forest Service and that underlies the SAWTI. I show that WRF, as configured, provides accurate results and information.

Next, In Section IV, I respond to UCAN's and ORA's arguments regarding the SAWTI itself, none of which directly challenge the validity or use of the SAWTI, and I demonstrate that their arguments are not accurate. For instance, both Dr. Gershunov and Mr. Stannik claim that a chart depicting the SAWTI measurement of large fire potential of Santa Ana wind events that was included within Appendix 4 to my direct testimony shows that a 2011 event exceeded the October 2007 event. That assertion is wrong. The chart at issue was depicting the large fire potential in Los Angeles and Ventura County, not San Diego County. In San Diego County, the large fire potential of the October 2007 event was the greatest on record.

In Section V, I show that many of the weather and wind-related assumptions made by Dr. Gershunov in Part I of his testimony are misleading or inaccurate. Next, I show that the methodology he presents in Part II of his testimony for estimating the Santa Ana wind speeds at

the location of the ignition sites of the Witch, Rice and Guejito Fires is unreliable and biased, and that it generates wind speeds that are far too low. For instance, Dr. Gershunov estimates that the peak wind gust in October 2007 at the ignition point of the Witch Fire was 56.6 mph, which corresponds to an estimated return interval of 33 years. But actual observations from the West Santa Ysabel weather station have recorded wind gusts at or in excess of 56 mph during seven different Santa Ana Wind events in just the four-year period between October of 2012 through November 2016, which undercuts Dr. Gershunov's modeled 33 year return interval.

Finally, in Section VI, I show that the San Diego County wind gust measurements (1949-2007) that Dr. Coen presented do not contain meaningful information about Santa Ana winds generally or the wind speeds at the Witch, Rice or Guejito ignition sites.

II. THE RELATIONSHIP BETWEEN THE JULIAN RAWS AND SDG&E WEST SANTA YSABEL WEATHER STATION

Q. Please describe the relationship you presented in your direct testimony between the Julian RAWS and West Santa Ysabel weather station.

A. I performed a statistical analysis of the observed peak wind gusts at Julian RAWS and SDG&E's West Santa Ysabel weather station for 42 Santa Ana wind events since October 2012.[6] I used the results of that analysis to estimate the peak wind gust at West Santa Ysabel during the October 2007 Santa Ana wind event. I chose to perform this analysis because it provided a statistical method, using observed data only and completely independent of atmospheric model simulations, to estimate peak wind gusts during the October 2007 Santa Ana wind event. Furthermore, since this analysis was independent of any atmospheric model simulations, it can be viewed as additional evidence to assess the validity of the results of any atmospheric model simulations of the October 2007 Santa Ana wind event performed by others.

[6] Prepared Direct Testimony of Steve Vanderburg, p. 13.

Q. Please describe the UCAN and ORA criticisms of this analysis.

A. There are five basic criticisms. First, Dr. Gershunov claims that the West Santa Ysabel weather station cannot be used to estimate the wind speeds at the time and location of the Witch Fire because that weather station was built in 2011 and is 0.6 kilometers ("km") from the ignition site of the Witch Fire.[7]

Second, Dr. Gershunov argues that the relationship that I presented between the Julian RAWS and West Santa Ysabel weather station is not "strong and stable" enough to be able to accurately predict the wind speeds at the ignition of the Witch Fire.[8] Both Dr. Coen and Mr. Stannik advance similar arguments.[9]

Third, Dr. Gershunov argues that I wrongly assumed that peak gusts are representative of gusts at the time of fire ignition, and Mr. Stannik makes a similar criticism.[10]

Fourth, Mr. Stannik argues my use of RAWS data in my analysis contradicts the rejection of RAWS data by SDG&E witness Dr. Jon Peterka.[11]

Fifth, Mr. Stannik claims that the 92 mph peak gust estimate I calculate is not unprecedented.[12]

Q. How do you respond to the first criticism regarding the location of the West Santa Ysabel weather station and the time at which it was installed?

A. The West Santa Ysabel weather station is installed directly on Tie Line 637 ("TL637") a mere four spans (approximately 1,900 ft.) northeast of the ignition point of the Witch Fire. Both

---

7 Gershunov Testimony (Part I), pp. 5, 18.

8 *Id*. at pp. 5, 18-20.

9 Coen Testimony, pp. 17-18; Stannik Testimony, pp. 42-44.

10 Gershunov Testimony (Part I), pp. 5, 20-21; Stannik Testimony, p. 41.

11 Stannik Testimony, pages 36-37.

12 Stannik Testimony, page 34.

locations are situated on broadly-rounded hilltops near the summit of Dye Mountain. Figure 1 below shows both the West Santa Ysabel weather station (indicated as "WSY") and the transmission poles on either side of the ignition site (indicated by the yellow pins as Z416675 and Z416676) of the Witch Fire.

FIGURE 1 – TIE LINE 637 LOCATIONS

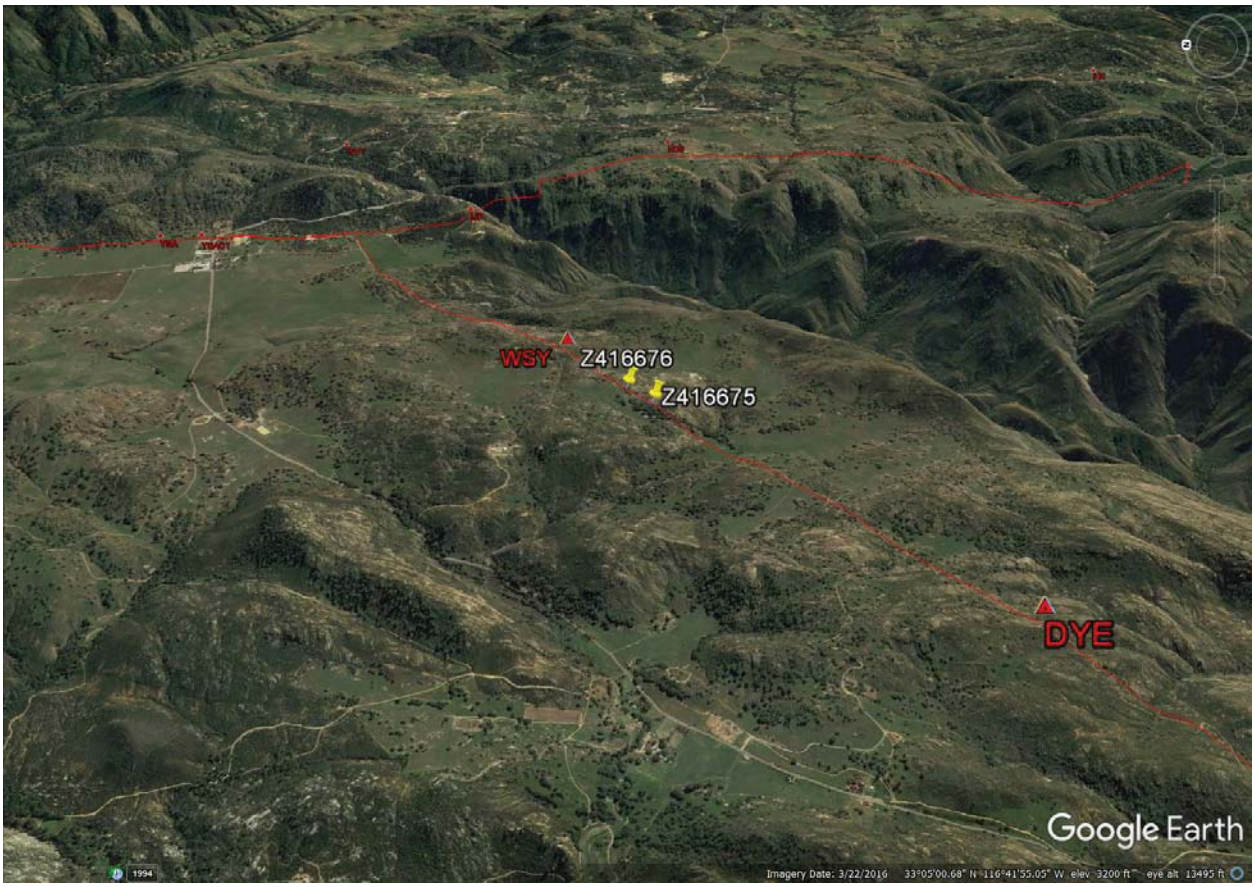

The terrain and vegetation at both locations is quite similar and both locations have excellent exposure to an easterly wind. Therefore, based on my personal and professional experience, I believe it is reasonable to conclude that peak wind gusts at West Santa Ysabel weather station are representative of the peak wind gusts at the Witch Fire ignition point during Santa Ana winds.

Q. In light of this criticism, have you done any work to corroborate your use of the West Santa Ysabel weather station?

A. Yes. In 2012, SDG&E installed another weather station on TL637 called Dye Mountain. The Dye Mountain weather station is located at 33.068817 -116.709897, approximately 9,000 FT (2.7 km) southwest of the West Santa Ysabel weather station and approximately 7,100 ft. (2.2 km) southwest of the Witch Fire ignition point. It is shown in red text in Figure 1 above as "DYE." It too is located on a broadly-rounded hilltop near the summit of Dye Mountain, similar to the West Santa Ysabel weather station. For the 42 Santa Ana wind events referenced above, the peak wind gust as measured at Dye Mountain was within 1 mph or less of the peak wind gust as measured at West Santa Ysabel 33% of the time and within 5 mph or less 81% of the time. In fact, there was only one event out of the 42 examined when the difference between the peak wind gusts at those two weather stations was greater than 10 mph.

In other words, the data show that Santa Ana wind gusts at West Santa Ysabel weather station are reasonably representative to Santa Ana Wind gusts at Dye Mountain weather station. Given the similarities in terrain and vegetation at the two weather stations and the Witch Fire ignition point, and given that the Witch Fire ignition point is directly between the West Santa Ysabel and Dye Mountain weather stations, it is reasonable to conclude that the wind gusts at the West Santa Ysabel are representative of the wind gusts at the Witch Fire ignition point.

Q. How do you respond to the second criticism regarding the stability and validity of the relationship you drew between the Julian RAWS and West Santa Ysabel Weather station?

A. There is no evidence to suggest that the fundamental behavior of Santa Ana winds has changed between October 2007 and the present day, nor has there been any significant change in the terrain or vegetation at the two sites. Therefore, any statistical correlation of wind gusts

between the two weather stations that exists today must have also existed in October 2007. Dr. Gershunov's also argues that the relationship (offset factor) is not consistent from event to event and therefore cannot be trusted.[13] The table below shows the top 10 Santa Ana wind events as measured at West Santa Ysabel since October 2012 as well as the peak wind gusts at Julian RAWS (JULC1) along with the corresponding offset factor for each of those events.

Event Start	Event End	WSY Peak Wind Gust (mph)	JULC1 Peak Wind Gust (mph)	Offset Factor
4/29/2014	5/1/2014	75	43	1.74
5/12/2014	5/15/2014	63	41	1.54
12/14/2013	12/16/2013	61	36	1.69
2/15/2013	2/16/2013	58	38	1.53
1/22/2015	1/26/2015	58	41	1.41
1/13/2014	1/17/2014	56	33	1.70
12/9/2013	12/9/2013	56	34	1.65
1/15/2013	1/17/2013	55	33	1.67
1/1/2013	1/2/2013	52	29	1.79
3/5/2015	3/7/2015	51	32	1.59

For all but one event, peak wind gusts at Santa Ysabel are more than 1.5 times stronger than at Julian RAWS, so while there is variability from event to event, the general relationship is clear: peak wind gusts at West Santa Ysabel *are considerably stronger* than peak wind gusts at Julian RAWS. If we were to use the offset factors from the top 10 events in the table above to estimate peak wind gusts at West Santa Ysabel in October 2007, nine of the ten estimates would be equal to or greater than 90 mph based on a peak wind gust of 59 mph at Julian RAWS.

Lastly, Dr. Gershunov plots hourly wind gusts and "peak event gusts" for West Santa Ysabel versus Julian RAWS during Santa Ana Wind events as evidence that the relationship between the two stations is poor.[14] This is a misleading comparison given that I was only trying

[13] Gershunov Testimony (Part I), pp. 18-21.

[14] Gershunov Testimony (Part I), p. 20.

to relate the peak wind gust at Julian RAWS to the peak wind gust at West Santa Ysabel for a given Santa Ana Wind event.

Q. Have you undertaken further analysis of the relationship you presented between the Julian RAWS and the West Santa Ysabel weather station?

A. Yes I have.

Q. Please describe that further analysis.

A. To ensure that I was thinking about the statistics the right way, I sought further SDG&E analytical support. The additional analysis corroborates not only my wind speed estimate, but also highlights the statistical significance between Julian RAWS and West Santa Ysabel weather station. The analysis attempted to estimate the speed at West Santa Ysabel by using speeds from the Julian RAWS station. To do so, the task was to find the math function with the best relationship between Julian RAWS and West Santa Ysabel.

The data used was the weather information at Julian RAWS and West Santa Ysabel from June 2011 to September 2016. The approach focused on winds similar in direction and situation to that which was seen during the 2007 event, namely winds blowing from the desert towards the coast that had a relative humidity of 30% or less. Maximum wind speeds per day (rather than per hour) were utilized due to the unknown time relationship between the two weather stations. In other words, it isn't clear how much time lag exists between when strong winds reach Julian RAWS versus West Santa Ysabel.

Using statistical software, the relationship that had the best fit was one that had a linear component and a slight exponential component. The exponential component matches our understanding of the wind patterns in this area because, during these types of wind events, the

wind accelerates as it passes across this area, and the acceleration is more prominent the stronger the wind is. The function is:

Speed at West Santa Ysabel = 1.068815 * (Speed at Julian RAWS)

+ 0.007996 * (Speed at Julian RAWS)^2

Functions that were purely linear (i.e. no exponential component) had a slightly weaker relationship, but they were not vastly different.

Importantly, the data shows a very strong correlation that would not happen by chance. There were 583 data points used, and the r-squared value is 0.71. It is our belief that a value of 0.71 is statistically significant when 583 data points are used. Using standard statistical techniques to determine the strength of relationships, the likelihood that the two weather stations are not correlated is 1 in 10^158, which is an impossibly small figure to comprehend. The data are very much correlated.

When the value of 59 mph is used for the "Speed at Julian RAWS," the value of 90.89 mph is estimated at West Santa Ysabel.

Q. How do you respond to the third criticism regarding your use of peak gusts?

A. I never claimed that the estimated peak wind gust at West Santa Ysabel corresponded to the time of ignition of the Witch Fire. I was simply trying to show how extreme the wind gusts were in the vicinity of the fire origin site during the October 2007 Santa Ana event.

Q. How do you respond to the fourth criticism regarding the alleged inconsistency with Dr. Peterka on the use of RAWS data?

A. Mr. Stannik contends that SDG&E's analysis of wind and weather as a whole cannot be relied upon because SDG&E witness Dr. Jon Peterka rejects the use of RAWS, while I use it in my comparison of wind speeds at the Julian RAWS and West Santa Ysabel weather station. In

his view, this apparent contradiction "has not been justified."[15] In making these statements, I believe he has not taken account of the differences between what Dr. Peterka and I are attempting to show.

Q. Please elaborate.

A. Dr. Peterka's analysis looks at whether the RAWS stations provided accurate wind speed measurements at the time and location of each of the Witch, Rice and Guejito Fires. I understand that he concluded that those RAWS measurements were not appropriate for those purposes because of terrain differences and obstructions that shield the RAWS anemometers from winds. I am not using the Julian RAWS as a proxy for the actual wind speeds at the location of the fires. Rather, I am using it simply as a point of comparison to the WSY weather station. The Julian RAWS serves as a reasonable point of comparison from October 2007 through the present day because the data measured there is consistent. While there may be obstructions, those obstructions are present in every wind event, and so the bias is consistent. Thus, the Julian RAWS is a good point of comparison to the West Santa Ysabel station, which did not exist in October 2007, but which provides excellent data from 2011 through the present, and it is only the relationship between the two is what matters for purposes of the statistical analysis I performed.

Q. Does Mr. Stannik make any other statements about RAWS data to which you would like to respond?

A. Yes. He claims that further investigation into Dr. Peterka's testimony is warranted because, despite Dr. Peterka's criticisms of the RAWS data, SDG&E indicated in discovery in this proceeding that it had no documented concerns about the use of RAWS data prior to the

[15] Stannik Testimony, pp. 36-37.

2007 Wildfires.[16] I believe this whole argument is irrelevant. As I understand it, the only reason RAWS data has become an issue is because the California Department for Forestry and Fire Protection and the Consumer Protection and Safety Division used RAWS data as the basis for their conclusions about the wind speeds at the time and location of each of the Witch, Rice and Guejito Fires, and Dr. Peterka has responded by showing such data cannot serve that purpose.

Q. How do you respond to the fifth criticism regarding whether the 92 mph winds were unprecedented?

A. Mr. Stannik refers to my calculation that resulted in a 92 mph peak gust estimate and then states "[b]ased on his calculation, Mr. Vanderburg claimed that 'October 2007 was unusually strong, damaging and unprecedented wind event in San Diego County.'"[17] Mr. Stannik then states my claim in this regard is undermined by a National Oceanographic and Atmospheric Administration ("NOAA") Technical Memorandum, for which I was listed as a co-author, that indicates that Santa Ana winds could have "gusts greater than 100 knots in favored areas, such as Santa Ana Canyon."[18] This testimony confuses two distinct conclusions in my direct testimony.

Q. Please elaborate.

A. As discussed above, the 92 mph peak gust estimate that I presented in my direct testimony was based on the relationship of the Julian RAWS to the West Santa Ysabel weather station. I did not say that this gust speed was "unprecedented," as Mr. Stannik claims I did.[19] Rather, I used the term "unprecedented" to refer to the October 2007 Santa Ana wind event in San Diego County as a whole, and I based that conclusion on both the regional wind speed

---

16 Stannik Testimony, pp. 41-42.

17 Stannik Testimony, p. 34.

18 Id.

19 Prepared Direct Testimony of Steve Vanderburg, p. 13.

analysis and the Large Fire Potential analysis shown later in my direct testimony.[20] With respect to the NOAA Technical Memorandum, the speed of wind gusts in Santa Ana Canyon, which separates the Chino Hills from the northern end of the Santa Ana Mountains near the intersection of Orange, Riverside and San Bernardino Counties, are frankly irrelevant to San Diego County.

Q. Mr. Stannik also uses the NOAA Technical Memorandum, and other sources of information, to support his claim that Santa Ana winds were a known local condition at the time of the 2007 Wildfires. Do you agree with that claim?

A. While knowledge of the existence of Santa Ana winds predates October 2007, I am certain that SDG&E did not know precisely how strong those winds could be in areas lacking historical weather observations or accurate wind studies, or where the strongest winds were likely to occur in its service territory from event to event, or how the risk of wildfire varied quantitatively from one Santa Ana wind event to another.

Q. Why are you certain of this?

A. Because there were no such tools in existence in October 2007 to provide that information. That is the problem we were trying to solve when we deployed the SDG&E mesonet (homogeneous network of 171 weather stations), started running WRF operationally, and developed the Santa Ana Wildfire Threat Index (which is further discussed below) in the aftermath of the 2007 Wildfires. The "where" part is especially critical. Knowing that there would be Santa Ana winds in October 2007 would provide no meaningful information about where in the 4,000 plus mile service territory the winds would be the strongest, or how strong they would be in any given location.

[20] Id., pp. 13-16.

III. WRF MESOSCALE MODELING OF THE ATMOSPHERE IN SDG&E'S SERVICE TERRITORY

Q. Please explain the role of the WRF model in the analysis and conclusions you presented in your direct testimony.

A. WRF was an integral part of the creation of the Santa Ana Wildfire Threat Index (SAWTI) and, in combination with the data collected from the SDG&E mesonet, greatly enhanced our understanding of Santa Ana Winds in San Diego County. First, with the help of Fovell and Cao, a configuration of WRF was selected which minimized errors with respect to near-surface temperatures, winds, and dew point during Santa Ana Wind events. This was accomplished by using weather station observations from the SDG&E mesonet to verify the results of numerous configurations (simulations) of WRF. Then, we used the best performing configuration of WRF to reconstruct 30+ years of hourly weather and fuels conditions at 3 km resolution across all of Southern California going back to 1984. Once complete, the 30+ year climatological dataset was then correlated to historical wildfire occurrence to create the Santa Ana Wildfire Threat Index. This effort required over one million compute core hours to complete and is the most comprehensive and detailed climatology of Santa Ana conditions relative to wildfire potential (weather and fuels) that exists to date.

Q. Please describe the arguments UCAN raises with respect to this WRF modeling.

A. Dr. Gershunov claims that WRF modeling results in overestimated wind and gust speeds, and he also claims those results are unreliable because Fovell did not use any observed data to bias-correct his modeling.[21] Dr. Coen takes issue with the use by Fovell and Cao (on which I rely) of a logarithmic wind profile to adjust the simulated winds in the model to the anemometer

[21] Gershunov Testimony (Part I), pp. 6, 22.

height level.[22] Dr. Coen claims that the gust factors used by Fovell and Cao (on which I rely) are not reasonable.[23]

Q. What is your reaction to Dr. Gershunov's claim that the WRF modeling results in overestimated wind speeds?

A. I disagree. A single WRF simulation can overestimate wind in one location and underestimate wind in another location. The amount of overestimation and/or underestimation depends largely on the configuration and resolution of WRF as well as the local terrain and site characteristics at the weather stations used to validate the simulation. For example, we have found that for well-sited weather stations in wind prone areas (i.e. Sill Hill), WRF tends to *underestimate* wind speeds. WRF wind biases at each station are systematic and quite consistent from event to event. With regards to the WRF simulations Dr. Fovell used for his analysis, the average bias at West Santa Ysabel is near zero (-0.5 m s^{-1}) which is why it was reasonable for Dr. Fovell to use the model data from that point to estimate wind gusts during the October 2007 wildfires.

Q. How do you respond to Dr. Gershunov's claim that Fovell did not use observed data to bias-correct his modeling?

A. That claim is incredibly misleading. As noted above, actual weather station observations from the SDG&E mesonet were heavily relied upon to choose the best possible configuration of WRF (based on an extensive ~50-member ensemble) as well as to validate the methods used to estimate wind gusts from model wind speeds. In fact, Dr. Fovell used far more weather stations in San Diego County to verify the results of his WRF simulations than Dr. Gershunov did to verify the results of his CaRD10 reanalysis.

---

[22] Coen Testimony, pp. 12-13.

[23] Coen Testimony, pp. 13-14.

Q. What is your response to Dr. Coen's claims about the use of a logarithmic wind profile to adjust simulated winds?

A. The use of logarithmic wind profiles to adjust model wind speed is standard practice. This adjustment is required in order to provide a fair comparison between observed winds at the anemometer height versus model winds at the lowest model height. Other methods were explored but found to have minimal impact on forecast skill when compared to actual observations from the SDG&E mesonet (Cao and Fovell 2016). As Dr. Coen herself acknowledged, "The scientific literature does not provide a better methodology."[24]

Q. What is your response to Dr. Coen's claims that the gust factors used in the WRF analysis are not reasonable?

A. Great care was taken to minimize the error associated with estimating wind gusts at certain locations, including West Santa Ysabel (WSY). An analysis of 42,230 wind observations at WSY showed that for sustained winds ≥ 12 m s^{-1} (26.8 mph), the average gust factor was 1.59, with 99.5% of observations exceeding 1.4. Furthermore, Figure 2 (below) shows decreasing variability in the gust factor with increasing wind speed, with the data converging toward a gust factor of 1.58 at the highest wind speeds. Thus, the margin of error with regards to picking a gust factor is actually reduced in strong Santa Ana wind events such as October 2007 event.

[24] Coen Testimony, p. 13.

FIGURE 2

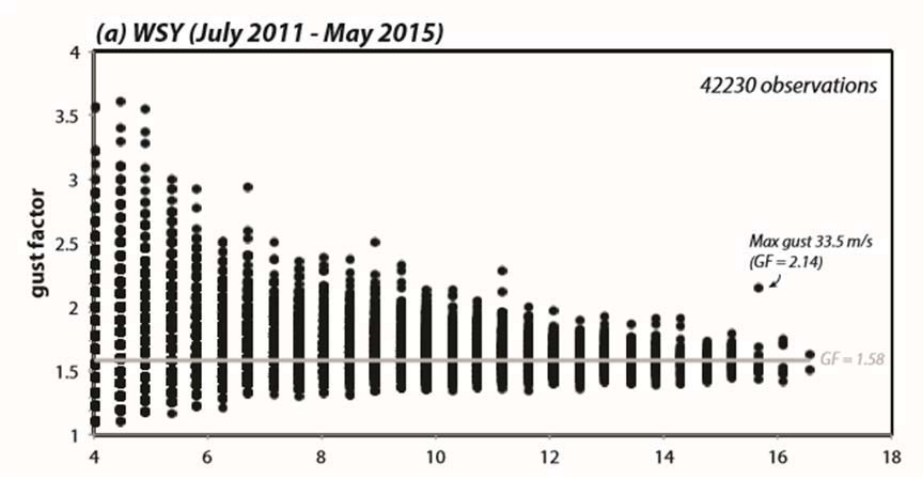

As noted above, a configuration of WRF was chosen that best represented the magnitude, special extent, and temporal variation of the winds as measured by the SDG&E mesonet. To that extent, Cao and Fovell's use of gust factors is reasonable.

IV. THE SANTA ANA WILDFIRE THREAT INDEX

Q. What is the Santa Ana Wildfire Threat Index or SAWTI?

A. As stated in my direct testimony, the SAWTI is an index that categorizes or rates Santa Ana Wind events with respect to the anticipated potential for a large wildfire to occur. The index uses a comprehensive, state-of-the-art predictive model that includes dead fuel moisture, live fuel moisture, and the greenness of annual grasses to create a detailed daily assessment of the fuel conditions across Southern California. This information is coupled with calibrated weather model output (comprised of wind speed and atmospheric moisture), to generate a 6-day forecast of Large Fire Potential. The Large Fire Potential output is then compared to climatological data and historical fire occurrence to establish the index rating. The SAWTI is somewhat analogous to the Saffir-Simpson scale used to rate the intensity of hurricanes, only in this case, we are

rating the potential for large wildfire activity based on both the severity of the Santa Ana wind event and the dryness of the vegetation. The SAWTI is produced by the U.S. Forest Service and Predictive Services. The SAWTI is used by fire agencies as a planning tool and is frequently referenced during Santa Ana wind events by local and national broadcast media, including The Weather Channel. The White House recently released a document which briefly highlighted the success of the Santa Ana Wildfire Threat Index.[25]

Q. What is the significance of the Santa Ana Wildfire Threat Index to the analysis you presented in your direct testimony?

A. The SAWTI provided us with a detailed, comprehensive climatology of Santa Ana Wind events which showed that the October 2007 Santa Ana Wind event was the most severe in our dataset for San Diego County with respect to regional wind speed. The October 2007 Santa Ana Wind event was also the highest risk event with respect to Large Fire Potential. In other words, the October 2007 Santa Ana Wind event was an extraordinary event for San Diego County.

Q. Do UCAN and ORA criticize the SAWTI?

A. They don't directly challenge its validity or use. Rather, I would say they make some criticisms around the edges of it.

Q. What do you mean by that?

A. Dr. Gershunov claims that his review of the SAWTI shows that, contrary to my direct testimony that the October 2007 Wildfires were the most extreme event in the study period (1984-2014), an event in the fall of 2011 exceeded the October 2007 Wildfires.[26] Even if Dr. Gershunov's interpretation of the Santa Ana Wildfire Threat Index data I presented were

[25] https://www.whitehouse.gov/sites/default/files/finalresilienceopportunitiesreport.pdf – page 11

[26] Gershunov Testimony (Part I), pp. 21.

accurate, it would only mean that there was another extreme event as measured by the Santa Ana Wildfire Threat Index. But Dr. Gershunov's interpretation is not accurate.

Q. Why not?

A. The figure Dr. Gershunov refers to can be found in Appendix 4 of my direct testimony – Developing and Validating the Santa Ana Wildfire Threat Index. The upper left figure in the poster shows the Large Fire Potential data for Zone 1 (LA & Ventura Counties) and *not* Zone 3 (San Diego County). For San Diego County, the October 2007 event was the most severe on record with respect to the weather conditions as well as the Large Fire Potential. I should note that the poster in Appendix 4 was not developed for this case. It was developed to publicly disseminate information about the SAWTI.

Q. Does Mr. Stannik make a claim similar to Dr. Gershunov's?

A. Yes. While Mr. Stannik also does not directly attack the validity or reliability of the SAWTI, he similarly claims that the index shows "multiple Santa Ana events since 2007 that are of a similar magnitude as the 2007 event."[27] Like Dr. Gershunov, Mr. Stannik cites to Appendix 4 of my direct testimony to support this claim.

Q. Is Mr. Stannik correct that there are multiple Santa Ana events since 2007 that are of a similar magnitude as the 2007 event?

A. No. As was the case with Dr. Gershunov, Mr. Stannik is basing his claim on data from Zone 1 (LA & Ventura Counties). For San Diego County, the strongest event to occur since October 2007 was in April 2014 when wind gusts up to 101 mph were measured at Sill Hill, and that event still does not come close to matching the intensity of 2007.

Q. Does Mr. Stannik say anything else that relates to the SAWTI?

---

[27] Stannik Testimony, pp. 34-35.

A. Again, not directly. But his testimony responding to my direct testimony about Red Flag Warnings is related to the SAWTI in that I explained that SDG&E developed the SAWTI, in part, because Red Flag Warnings did not provide enough specific information to function as a predictive tool for responding to wildfire risks in specific locations within SDG&E service territory.[28]

Q. Please describe Mr. Stannik's response to your direct testimony regarding Red Flag Warnings.

A. Mr. Stannik recites some of my statements about why Red Flag Warnings do not provide sufficient information about the likelihood of a wildfire outbreak at a specific point in time, but then he says "Red Flag Warnings are not designed specifically and exclusively for utility application," which was the very point I was trying to make in my direct testimony.[29] He then states that, despite my claims about Red Flag Warnings, SDG&E does in fact use them in its decision-making in certain circumstances, and that I misleadingly and inaccurately attempt "to distance SDG&E's procedures and decision-making processes from Red Flag Warnings."[30]

Q. What is your reaction to Mr. Stannik's claims regarding Red Flag Warnings.

A. I'm frankly somewhat confused by them. I never indicated that SDG&E does not use Red Flag Warnings for any purpose. Rather, I testified that SDG&E developed the SAWTI so that we would have a predictive tool that is specifically designed for utility applications (although it is also used by other members of the firefighting and weather communities).[31] Based on my experience as an SDG&E meteorologist, I have first-hand knowledge and

---

28 Stannik Testimony, pp.45-47; Prepared Direct Testimony of Steve Vanderburg, pp. 11-13

29 Stannik Testimony, pp. 46-47.

30 Stannik Testimony, p. 47.

31 Prepared Direct Testimony of Steve Vanderburg, pp. 8-13.

experience with using both the SAWTI and the WRF model used to generate the index to make specific departments within the company aware of wildfire threat conditions so that they can deploy resources to appropriate locations and adjust our operations as necessary.

Q. Do you believe the Red Flag Warnings in late October 2007 provided sufficient information that SDG&E could have used to avoid the ignitions of the Witch, Rice and Guejito Fires?

A. No.

Q. Why not?

A. Because Red Flag Warnings simply tell you that it is going to be windy and dry for a sustained period in San Diego County, resulting in critical fire weather conditions. Red Flag Warnings do not give specific information about the potential for large fire outbreaks, or indicate where in the SDG&E service territory as whole it will be windiest and most prone to such large fire outbreaks.

Q. Does Dr. Coen make any statements about the SAWTI?

A. Yes. Again, she does not directly criticize it. Rather, she says that it "may" exaggerate the dependence on wind speed, and that it "may also" misinterpret the impact of fuel moisture on fire spread.[32]

Q. Does Dr. Coen provide any support for the flaws that she says "may" exist in the SAWTI?

A. No.

Q. Do you agree that these flaws exist?

A. No I do not.

[32] Coen Testimony, pp. 19-21.

Q. Why not?

A. The SAWTI is a tool which categorizes the *potential* for Santa Ana Wind-driven wildfires up to 6 days in advance based on the weather and fuels forecast. Criticizing SAWTI on the basis of not accurately forecasting the rate of spread is not appropriate, because SAWTI is ultimately based on the probability of a large wildfire and is not intended to quantitatively forecast the rate of spread since the details (location, resources, time of ignition, etc.) of any potential wildfire are not known until after an ignition occurs. Clearly the risk of Santa Ana Wind-driven wildfires is greatest when wind speed is high and fuels are dry. This is captured quite well by the SAWTI and supported by historical fire occurrence.

V. DR. GERSHUNOV'S FAULTY METHODOLOGY FOR ESTIMATING WIND SPEEDS

Q. Have you reviewed the "Introduction" to Dr. Gershunov's testimony, in which he discusses wind speeds and Santa Ana winds generally?[33]

A. Yes, I have.

Q. Do you have any comments or observations regarding this portion of his testimony?

A. Yes. I found several fundamental errors or misunderstandings in that portion of his testimony.

The Coarse Resolution of Dr. Gershunov's Atmospheric Modeling: Dr. Gershunov claims that winds aloft are much less sensitive to model resolution.[34] He uses this claim to justify using a coarse model resolution of 10x10 km to estimate wind gusts at the ignition points of the various October 2007 wildfires from the modeled flow aloft. The issue here is that 10x10 km grid spacing has been definitively shown to be insufficient to properly capture the complex

[33] Gershunov Testimony (Part I), pp. 6-11

[34] Id., p. 9.

terrain of the San Diego County backcountry, something that is critically important when attempting to model terrain-amplified flows such as Santa Ana Winds. For instance, Dr. Fovell has graphically shown that model simulations using different levels of resolution (ranging from the 667 m Fovell uses to the 10 km that Dr. Gershunov uses) depict varying levels of terrain detail, which impacts how the wind estimates the mesoscale modeling generates. Coarser resolution models produce less accurate results because they do not accurately capture terrain changes, as shown in Figure 3.[35]

FIGURE 3

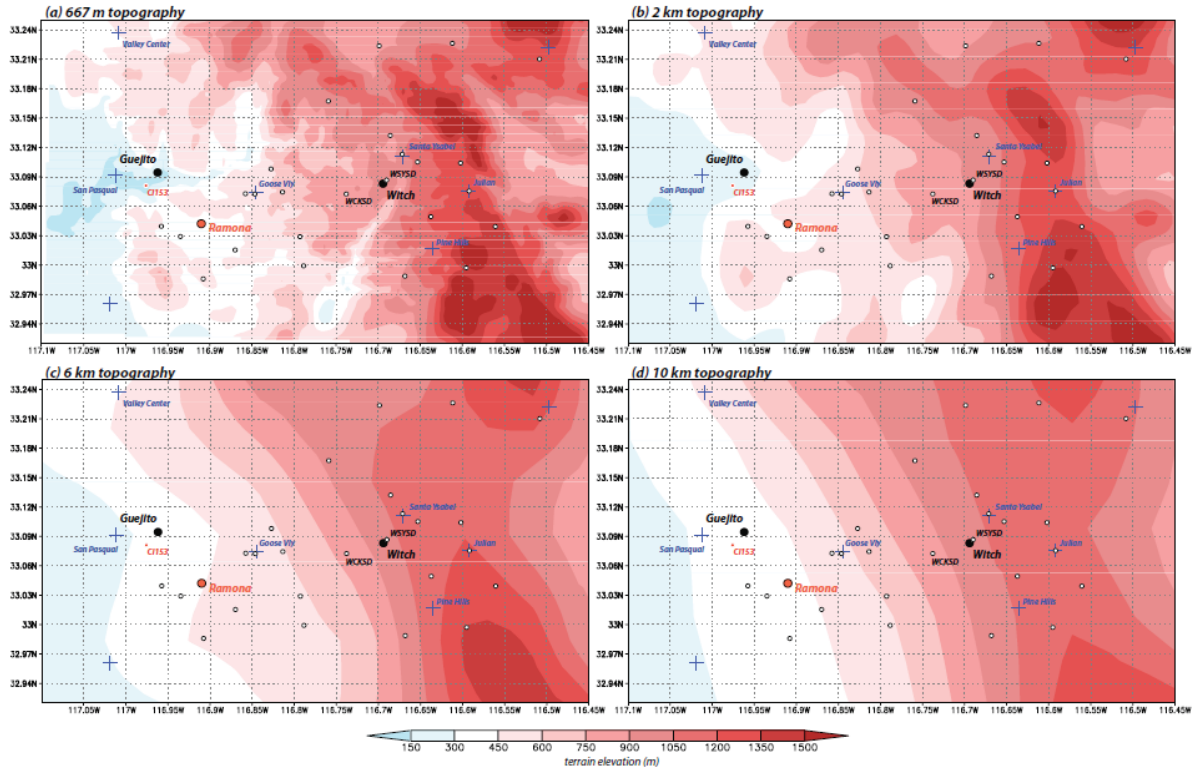

At 10 km resolution, the footprint of the strongest winds is exaggerated in the horizontal (too broad) and displaced well down the slope from where a higher resolution would place them (over Ramona instead of the Santa Ysabel area). Higher resolution simulations (2 km or greater) place

[35] See Appendix 1.

the highest winds over the Santa Ysabel area which matches what observations from publically available weather stations (including the SDG&E mesonet), as shown in Figure 4, which represents and February 2013 Santa Ana wind event.[36] This figure shows a cross section, and West Santa Ysabel (WSY) is clearly experiencing the strongest winds in the higher resolution versions.

FIGURE 4

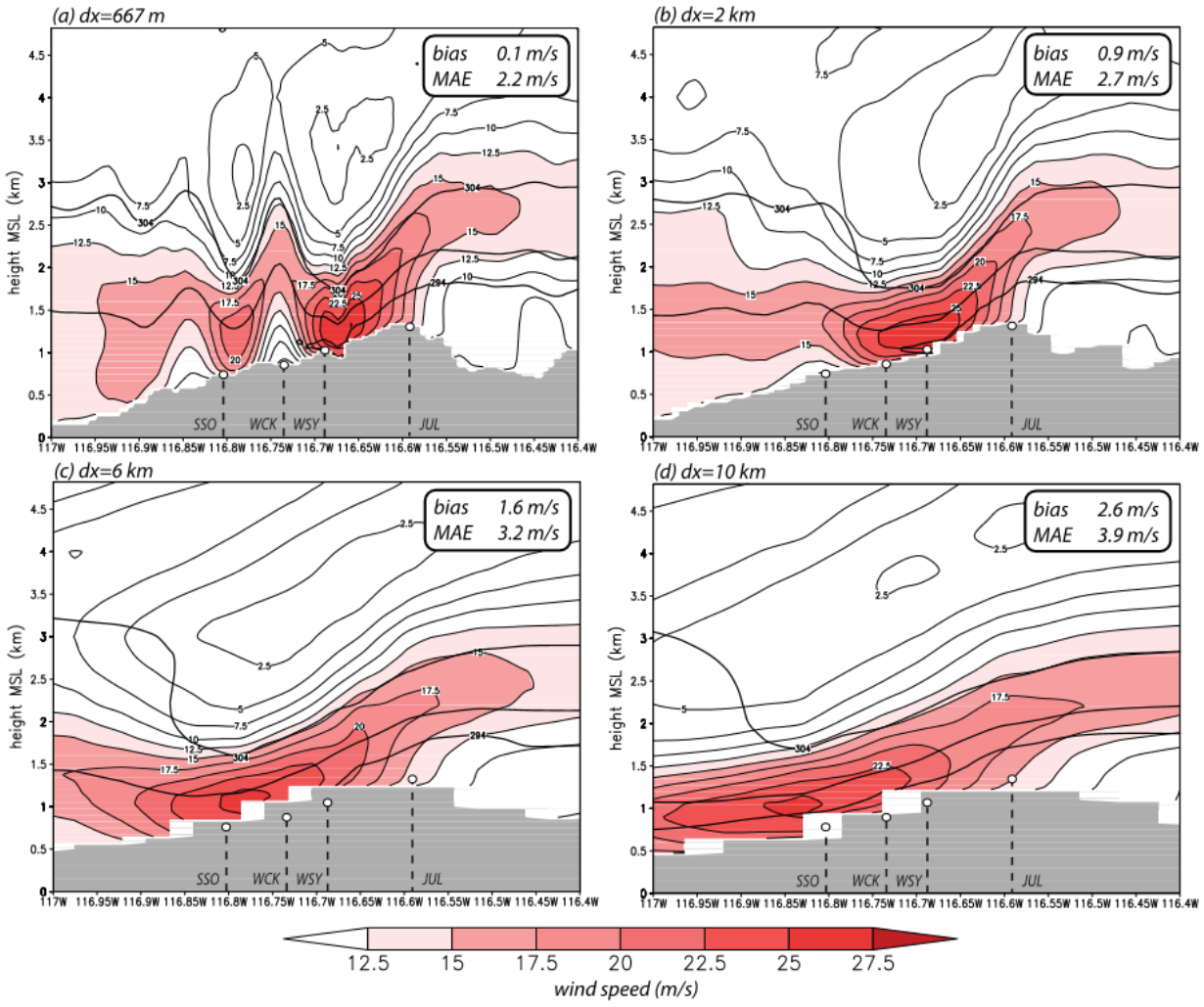

[36] See Appendix 4.

While Dr. Gershunov emphasizes the importance of terrain in Part II of his testimony,[37] it is clear that his coarse 10x10 km modeling resolution does not accurately account for changes in terrain, and as a result, cannot properly resolve the strength and extent of the Santa Ana Wind field. The CaRD10 was not designed for the type of analysis that Gershunov is attempting to perform.

Dr. Gershunov's Reliance on RAWS Data: Dr. Gershunov makes a number of inaccurate or misleading statements to justify his reliance on RAWS data. First, while I agree with Dr. Gershunov's claim that "at locations where anemometers may be obstructed (by nearby tall trees, buildings, etc.), sustained winds are expected to underestimate wind speeds of an otherwise unobstructed flow," I think he exaggerates when he states that observed gusts are "not as sensitive to obstructions."[38] I constantly monitor weather observations from the SDG&E mesonet during Santa Ana Wind events as part of my job. I have observed that Santa Ana Wind gusts are, without a doubt, sensitive to the local terrain and obstructions, even if not quite as sensitive as sustained winds. Dr. Gershunov goes on to state that near-surface wind gusts can be thought of "as being more representative of the larger-scale flow aloft."[39] But the research that Dr. Gershunov references as the source of his claims (Brasseur, O, 2001) was based on a study of synoptic-scale winter storms undergoing rapid cyclogenesis in relatively flat Belgium. Hence, it is hardly applicable to the microscale and mesoscale features of Santa Ana winds in San Diego County, where the terrain is anything but flat.

Dr. Gershunov also attempts to bolster his use of RAWS data by claiming that RAWS are strategically and carefully sited by meteorologists and fire managers with the specific goal of

---

37 See, e.g., Gershunov Testimony (Part II), p. 7.

38 Gershunov Testimony (Part I), p. 7.

39 Id.

monitoring fire weather conditions in rough terrain.[40] But I have personally participated in the siting of RAWS on numerous occasions and can say that it is not uncommon for meteorologists and fire managers to compromise on the final RAWS location based on the availability of land and other practical factors. This is the reason why so many local RAWS are located at Cal Fire stations and U.S. Forest Service stations, despite the less than ideal exposure to winds. Dr. Peterka and Dr. Fovell have both provided clear evidence that many local RAWS (including Julian, Goose Valley, and Pine Hills) are shielded from the wind by buildings and/or trees, resulting in wind measurements that are far lower than would otherwise be measured in an open field or well-exposed location.[41] Dr. Gershunov indicated in discovery that he has never visited any of the RAWS sites in San Diego County, so he has no personal knowledge of those problems.[42]

Lastly, Dr. Gershunov points to the "impressive" coverage of RAWS across Southern California, as well as the continuity of data, as reasons why these stations provide an opportunity to understand Santa Ana Winds and verify model simulations.[43] RAWS stations provide a record of observed weather data, but as noted above, it is not appropriate to use RAWS wind observations from RAWS to verify a model simulation without first considering the impact of local environmental factors such as nearby obstructions on those observations. While Dr. Gershunov might consider the RAWS coverage "impressive," none of the RAWS in existence in 2007 were in the windiest areas of San Diego County with respect to Santa Ana winds. In this regard, Dr. Gershunov has not validated the results of his model to weather observations in

---

40 Id., pp. 11-14.

41 See Appendix 1, pp. 2-3.

42 See Appendix 8 (UCAN Response to Request 17).

43 Gershunov Testimony (Part I), pp. 11-12.

locations where terrain-amplified flow is greatest, whereas Dr. Fovell has done so in his WRF atmospheric modeling that is used in the SAWTI.

Q. How do you respond to Part II of Dr. Gershunov's testimony?

A. I believe there are several fundamental errors that undermine the analysis Dr. Gershunov presents in Part II of his testimony.

Actual Observations Conflict with Dr. Gershunov's Modeling: Real world observations from the immediate vicinity of the Witch Fire ignition site undermine Dr. Gershunov's wind speed estimates shown in the Summary Table.[44] I have shown how Santa Ana Wind conditions at the West Santa Ysabel weather station are representative of the Santa Ana Wind conditions at the Witch Fire ignition site based on local terrain and environmental characteristics. Both sites are within the same 10x10 km grid cell of Dr. Gershunov's CaRD10 atmospheric model. Based on the results of the CaRD10 model simulations, Dr. Gershunov estimates that the peak wind gust in October 2007 at the ignition point of the Witch Fire was 56.6 mph, which corresponds to an estimated return interval of 33 years. In other words, winds of that magnitude are expected to recur every 33 years. This result is undermined by actual observations from the West Santa Ysabel weather station, which has measured wind gusts *at or in excess of 56 mph during seven different Santa Ana Wind events just since October of 2012 through November 2016*. In other words, Dr. Gershunov's wind gust estimates for the Witch Fire are way too low for an event that he claims was the fourth strongest Santa Ana Wind event in 65 years. This obvious flaw is further proof that the 10x10 km CaRD10 model he uses does not have the resolution necessary to adequately resolve the important details of Santa Ana Winds in San Diego County.

[44] Gershunov Testimony (Part II), p. 3.

Similarly, Dr. Gershunov concludes that peak wind gusts in wind-prone locations of San Diego County must have been "in line" with the 60 mph wind gust forecast predicted by the National Weather Service simply because wind gusts did not exceed 60 mph at a number of RAWS weather stations in the region.[45] This conclusion in not supported by an analysis of weather observations collected since 2012, or by the reports of property damage in Wynola and other backcountry communities.

In Appendix 9, I have provided a bar chart that shows the average peak wind gust and maximum peak wind gust for seven weather stations along a line from Ramona ASOS to Julian RAWS for 42 Santa Ana Wind events since 2012. It clearly shows that the strongest winds typically occur in the West Santa Ysabel area (including the Witch Fire ignition point). This point is reinforced by a second bar chart that shows the number of times each of the seven weather stations has recorded the highest wind gust of the group. West Santa Ysabel is the clear winner.

In Appendix 6, I have provided several photographs of wind damage in Wynola from the morning of October 22, 2007, which correspond to an expected peak wind gust of 75 mph. The expected peak wind gust was obtained in the same way that National Weather Service personnel conduct surveys of tornado damage. The damage caused by these peak wind gusts of 75 mph again shows that Dr. Gershunov is wrong to conclude that the wind gusts did not exceed 60 mph.

Inaccurate Modeling of the Ignition Sites: Dr. Gershunov models the ignition sites of the Witch, Guejito and Rice Fires inaccurately. He describes the Guejito and Rice ignition sites as being situated on southwest facing slopes, and he describes the Witch Fire ignition site as bring situated on somewhat flatter terrain on a broad southwest facing slope based on the actual terrain

[45] Id., p. 14.

smoothed to the 10x10 km resolution of the model.[46] This is where Dr. Gershunov runs into additional problems. First, these descriptions are do not accurately represent the actual terrain. Instead, they describe the smoothed terrain as rendered by his modeling.[47] Dr. Gershunov describes the Guejito Fire ignition site as being situated on a southwest facing slope,[48] but it is actually situated on flat terrain at the bottom of the San Pasqual Valley, with canyon walls on either side. Based on a discovery response, it does not appear that Dr. Gershunov has visited this ignition site.[49] Second, Dr. Gershunov does not actually extract the forecast wind data from the 10x10 km grid cell that corresponds to the ignition point of the Witch Fire, but instead chooses an adjacent 10x10 km grid cell based on the above interpretation of the terrain.[50] This is further evidence that his estimated wind speeds cannot be trusted.

Dr. Gershunov also downplays the significance of distance between landmarks over the significance of terrain in determining wind speed/gust since Santa Ana Winds follow the terrain. In my personal and professional experience and as observations from actual events show, distance from the mountain crests is just as important as the local terrain when determining the strength of Santa Ana winds at any given location on the landscape. This is because changes in the upstream weather conditions (temperature and wind profile in the lowest 10,000 feet) near the mountain crests greatly affect how far down the slope (toward the coast) the strongest Santa Ana Winds will blow or if the winds will even surface at all. By downplaying the significance of distance between landmarks, Dr. Gershunov makes some questionable conclusions regarding the representativeness of pre-existing weather stations and the ignition sites of the wildfires. For

[46] Gershunov Testimony (Part II), p. 7.

[47] See Appendix 8 (UCAN Response to Request 29).

[48] Gershunov Testimony (Part II), p. 7.

[49] See Appendix 8 (UCAN Response to Request 21).

[50] See Appendix 8 (UCAN Response to Request 33).

example, he claims that Ramona ASOS is broadly representative of winds at the Witch Fire ignition site based on the topographical gradient but ignores the fact that Ramona ASOS is *much* further downslope from the top of the mountain range than the ignition site.[51] An examination of actual weather station observations of Santa Ana Wind events since 2012 further shows his claimed similarity between these locations to be completely inaccurate. The table provided in Appendix 7 shows that peak wind gusts at West Santa Ysabel weather station (near the Witch Fire ignition point) are more than 1.5 times as strong as peak wind gust at Ramona ASOS in 62% of the Santa Ana Wind events examined – and more than double the peak wind gust at Ramona ASOS in 17% of the Santa Ana Wind events examined.

VI. DR. COEN'S PRESENTATION OF NATIONAL CLIMACTIC DATA CENTER WIND GUST MEASUREMENTS BETWEEN 1949-2007

Q. Please describe Dr. Coen's presentation of wind gust measurement data.

A. Dr. Coen presents what she claims to be "underutilized data that indicates gusts of the magnitude in question have occurred many times throughout the period SDG&E has operated in San Diego County."[52] This data is made available by the National Climactic Data Center and includes peak daily wind gusts at various San Diego County locations from January 1998 through September 2007. According to Dr. Coen, there are numerous instances of wind gusts over 56 mph in that dataset.[53] She further indicates that the data "demonstrate that winds of the magnitudes estimated by the testimonies of Vanderburg and Peterka are not historically unique in the area that has been served by SDG&E for over a century."[54]

---

51 Gershunov Testimony (Part II), p. 11.

52 Coen Testimony, p. 4; pp. 21-25.

53 Coen Testimony, pp. 22-24.

54 Coen Testimony, p. 23.

Q. What is your response to this testimony?

A. I believe it is flawed in several respects. First, none of the measurements are from a location anywhere near the ignition sites of the Witch, Rice or Guejito Fires.

Q. What is the significance of that observation?

A. Wind measurements at coastal stations provide no meaningful information about wind speeds near the ignition sites of the Witch, Rice, or Guejito Fires, which were inland and subject to different wind patterns. When asked in discovery which coastal stations was "close enough, in Dr. Coen's judgment, to an ignition point to either the Witch, Rice or Guejito Fires to be representative of the wind gusts experienced in the vicinity of those ignition points," she did not identify any of them. Instead, Dr. Coen said "she does not believe there is a meaningful answer to this question."[55]

Q. What other flaws have you identified?

A. Although the data is supposedly quality checked by the National Climate Data Center, the evidence shows that many of these records have been corrupted by bad data. To check the data, I obtained historical METAR observations (weather station observations) for the dates and stations listed in the table provided by Dr. Coen. When necessary, I also compared the data to weather observations from neighboring stations as well. The top three records which show wind gusts in excess of 115 mph are particularly egregious, and the first accurate record listed in the table was eighth on the list with a peak wind gust of 64.4 mph measured at KSAN on 01/17/1988. There was so much bad data, that I stopped my quality check of the table after the 20th entry. For those first 20 entries, 14 were found to be wildly inaccurate. Lastly, during discovery, SDG&E asked Dr. Coen to identify which events in the table she provided occurred during Santa Ana Wind

[55] See Appendix 8 (UCAN Response to Request 50).

conditions. Dr. Coen referenced the results of Dr. Gershunov's CaRD10 reanalysis (Guzman Morales et al.) to determine if the date listed for each entry corresponded with Santa Ana Wind conditions.[56] There were seven dates in the first 20 entries that were incorrectly labeled as occurring during Santa Ana Winds, when in reality, there was rain or winter storm conditions occurring (which never correspond to Santa Ana Wind events). This further calls into question Dr. Gershunov's CarD10 results.

VII. CONCLUSION

Q. Does this conclude your prepared rebuttal testimony?

A. Yes it does.

[56] See Appendix 8 (UCAN Response to Request 49).

Appendix 1

5.4 Downslope Windstorms of San Diego County: Sensitivity to Resolution and Model Physics*

Robert G. Fovell†
University of California, Los Angeles, California, USA

1. Introduction

The "Santa Ana" is a dry, sometimes hot, offshore wind directed from the Great Basin and Mojave Desert over the mountains and through the passes of Southern California (cf. Sommers 1978; Small 1995). Its season extends from September to April (Raphael 2003), and the winds evince terrain amplification of the mountain gap and downslope varieties (Huang et al. 2009; Hughes and Hall 2010). Fast winds combine with low relative humidities to produce substantial fire danger especially in the autumn season before the winter rains have begun (Sommers 1978; Westerling et al. 2004). Chang and Schoenberg (2011) showed that while fires occur through the year in Los Angeles, large fires cluster in the September-November time frame (see their Fig. 2). Although some attention has been paid to the phenomenon (e.g., Conil and Hall 2006; Jones et al. 2010), it remains the literature on the subject is surprisingly thin given the meteorological and economic importance of the winds.

On 21 October 2007, at or before 1930 UTC (1230 PDT), the Witch Creek fire started at 33.083083°N, 116.694139°W[1], one of 27 Southern California blazes driven by an especially strong Santa Ana wind event. Ignition was apparently caused by sparking power lines located roughly 20 m above ground level (AGL). The fire spread rapidly and merged with other blazes, becoming one of the largest in California history. This study emerged from a need to estimate ignition time and event maximum wind speeds at Witch, a location for which no meteorological data were available, but this report will focus narrowly on the peak event winds and sensitivity of Weather Research and Forecasting (WRF) model's Advanced Research WRF (ARW) core wind speed estimates to resolution and model physics.

*13th WRF Users Workshop, June 2012

†Corresponding author address: Prof. Robert Fovell, UCLA Atmospheric and Oceanic Sciences, Los Angeles, CA 90095-1565. E-mail: rfovell@ucla.edu.

[1]This location was confirmed with San Diego Gas and Electric. The California Department of Forestry and Fire Protection report lists two different origins, one clearly erroneous and the other on Hwy 78 near Witch Creek mountain, a few km from the actual ignition site.

2. Wind gust estimates

Central to this effort is the estimation of wind gusts from model output, as these short period bursts are the most likely cause of the kind of property damage that caused the Witch fire. However, models of the present type cannot capture the small-scale turbulent motions involved in gust production. Thus, model reconstructions should be compared to observed sustained winds, and gusts have to be parameterized in some fashion. Three different strategies for computing wind gusts are pursued, representing empirical, theoretical and practical approaches.

The simplest procedure is to multiply the resolved-scale wind V by a gust factor (GF) empirically determined from available observations. A typical GF for well-exposed locations in relatively smooth terrain is about 1.4, although this will depend on the gust sampling interval (3 sec is typical), the averaging period applied to the sustained wind (2 min for Automated Surface Observing System, or ASOS, stations), and possibly other factors. Wieringa's (1973) formula for a 3 sec gust

$$G \approx V + 3\sigma_u$$

presumes a normal distribution of wind fluctuations with a standard deviation σ_u that can be sampled in the field or derived from theory. It is sometimes taken as $\sigma_u \approx 2.5u^*$ (Burton and Coauthors 2011), where the friction velocity u^* is a measure of the vertical shearing stress expressed in units of wind speed (e.g., Lumley and Panofsky 1964).

The friction velocity itself depends on the speed of the sustained wind at the lowest model level V_a, the surface roughness length z_0, and the stability, and becomes relatively large on lee slopes during Santa Ana events owing to high winds and relatively low stability very near the ground. Models also use the friction velocity to estimate the wind ($F10$) at standard anemometer height (10 m) based on V_a. Since u^* and $F10$ are not completely independent, this leaves the gust factor basically a function of surface roughness and stability. Over relatively smooth terrain with $z_0 \approx 0.01$ m, $F10 \approx 16u^*$, which implies a GF of about 1.5 in neutrally stable conditions. The European Center for Medium-range Weather Fore-

casts uses the following friction velocity-based formula for nonconvective situations[2]:

$$G = \mathrm{F10} + 7.71u^*.$$

This "EC gust" again yields a GF of 1.5 over smoother surfaces.

Our practical gust estimate is termed WSMAX (for wind speed maximum), and represents the fastest resolved scale wind within the lowest six model levels above the ground (about 600 m at Witch), based on the idea that turbulence can transport high momentum air downwards. This is a simpler version of an idea advanced by Brasseur (2001). WSMAX will overestimate the gust in stable conditions, or whenever a sufficiently effective vertical transport mechanism is lacking. It may underestimate gusts in other situations, as it presumes no further acceleration by subgrid topography or other factors. The vertical distance was determined via inspection of model output, and is tailored for downslope conditions at Witch. In this situation, the fastest wind is always located very close to the surface above Witch, usually in the lowest four levels.

3. Wind corridors, wind shadows, and available surface observations

Figure 1 presents the event maximum estimated EC gust from a WRF simulation employing three domains telescoping down to 6 km horizontal grid spacing over Southern California. The simulation was initialized with the North American Regional Reanalysis (NARR; Mesinger et al. 2006) and used the YSU PBL and RUC surface parameterizations. At this resolution, the topography is fairly smooth. Note the prominent wind corridors and the equally striking wind shadows occupying much of the urban areas of Los Angeles and San Diego. Note further that the fire ignition sites are found in the wind corridors, most of which are associated with terrain gaps including the Soledad, Cajon and San Gorgonio Passes.

The terrain near the Witch Fire, however, has no pronounced gaps but this is where the simulation's strongest gusts appeared, with values exceeding 40 m/s (90 mph). Yet, the maximum wind gusts *observed* in the vicinity (Fig. 2) topped out at only 26 m/s (59 mph). We will show that the flow across the Witch and nearby Guejito fire sites had many characteristics of a classic downslope windstorm (cf. Klemp and Lilly 1975; Durran 1986) and the terrain-accelerated flow was strongest in the immediate vicinity of the Witch ignition site. Furthermore, there are reasons to be skeptical of the representativeness of the observed winds, especially at the Remote Automated Weather Station (RAWS) sites.

First, RAWS stations measure the wind at a height of only 6.1 m (20 ft) AGL, and report ten-minute average winds once per hour, which leaves over 80% of the hour unsampled for the sustained wind. Other factors being equal, RAWS winds should be slower than those from ASOS stations, most of which report 10 m (33 ft) winds each minute, averaged over a two-minute period. In validation exercises, adjustments dependent on vertical stability and surface roughness have to be made to the model's standard 10 m wind diagnostic to avoid a false conclusion of overprediction. Also keep in mind the relevant height for Witch is 20 m, so the winds should be even stronger than at 10 m anyway.

Additionally, even a cursory examination of RAWS site photos hosted by the Desert Research Institute (DRI)[3] reveals numerous stations shielded by buildings and/or trees, among other siting issues. The most important RAWS station for the Witch event is Goose Valley (GOSC1), as it is located immediately downwind and downslope from the ignition location. At this writing, there are no photos for GOSC1 on the DRI website, but Google Earth reveals the station is partly shielded by tall trees when the winds have an easterly component (Fig. 3), as occurs during Santa Ana events.

These trees appear to significantly slow the sustained wind during Santa Ana episodes. Subsequent to October 2007, the San Diego Gas and Electric (SDGE) company deployed numerous stations at wind-prone areas in the county, including several in the immediate vicinity of Witch. These stations adhere to the RAWS wind standard (10 min averages taken at 6.1 m height) but report every 10 min. One such station, GOSSD, is presently located 0.7 km down Black Canyon Road from GOSC1, but is better exposed to the winds[4]. During a moderately strong Santa Ana wind event in December 2011, GOSSD's winds were about 80% faster than those at the nearby RAWS station (Fig. 4), based on the arguable assumption that they would report calm winds simultaneously, and its gusts were 40% stronger (not shown).

In August 2010, station WCKSD was installed near Witch Creek mountain, 4.2 km southwest and 244 m downslope from the Witch ignition site. This station was in place for a moderately strong Santa Ana wind event that occurred in early February 2011. At 26.8 m/s (60 mph), WCKSD reported the fastest gust in

[2]http://www.ecmwf.int/research/ifsdocs/CY37r2

[3]http://www.raws.dri.edu/

[4]Before November 2011, GOSSD was sited even closer to GOSC1, in a less well-exposed area intended to mimic the RAWS installation (S. Vanderburg, pers. comm.).

the entire region (Fig. 5). Note that this value was 30% stronger than for the Goose Valley RAWS and 81% larger than the fastest gust recorded at Ramona airport. However, note further that the wind speeds reported at the ASOS and RAWS are considerably below those recorded during October 2007 (33 vs. 56 mph, or 14.8 vs. 35 m/s, for Ramona, for example). This was a significantly less intense event.

4. Sensitivity to resolution

Terrain gap and downslope flows are significantly modulated by the shape of the topography, which is in turn dependent on the resolution of the model grid and the topographic database. Resolution sensitivity is demonstrated using four simulations, employing grid spacings of 667 m, and 2, 6 and 10 km. The finest grid, shown in Fig. 6a (also seen in Figs. 2 and 5), employs a very high resolution (≈10 m) terrain database that is available from USGS. This dataset sharpens up some of the topographic features, and overall it compares very well with the terrain as rendered within Google Maps (not shown).

In particular, note the presence of a narrow northeast-southwest oriented canyon immediately east of Witch, and an even narrower north-south canyon very close to the Guejito site. It is conceivable that these terrain features are important to the winds at the ignition sites, in which case they should be resolved. These features are notably absent in the 2 km topography (Fig. 6b), which utilized the 30 sec USGS terrain database, but otherwise the rendition appears acceptable. Note, however, that further resolution degradation profoundly changes the slope of the terrain west of the ridge (Figs. 6c, d). At 6 km, Ramona's small valley has been smoothed away (Fig. 6c). The coarsest grid flattens the ridge into a mesa, and pushes Witch up onto it (Fig. 6d).

Figure 7 presents hourly time series of near-surface winds from simulations employing the topographic representations shown in Fig. 6. The simulations were made using WRF version 3.2 with the YSU PBL and thermal diffusion (TD) surface scheme, initialized with the NARR. For Witch, the model-diagnosed 10 m wind is shown, although we already mentioned the relevant height for this site is 20 m. For Ramona, the winds were reduced to 7.9 m using the logarithmic wind profile with a surface roughness length $z_0 = 0.01$ m, which the TD scheme uses in late October for the USGS land use category applicable to the site (category 9, shrubland/grassland). (A small urban area, category 1, resides immediately east of the airport.) In neutral conditions, which is valid for most of the event, this represents a downward adjustment of 3%.

At 10 km resolution (Fig. 7a), the model suggests winds peaked at about 26.8 m/s (60 mph) for Ramona airport. These are raw model outputs, and so should be compared to the *sustained winds* at the site, as the model cannot resolve the small-scale turbulence that drives wind gusts. Yet, the 10 km reconstruction greatly exceeds the fastest sustained wind observed, which was only 17.4 m/s (39 mph). It also exceeds the fastest observed gust, which was 24.6 m/s (55 mph). Even more importantly, the 10 km simulation is suggesting the winds were stronger at Ramona than at the Witch ignition site. This immediately seems quite unreasonable, especially given recent observations provided by the SDGE mesonet.

The 6 km simulation (Fig. 7b) predicts roughly equal winds at Ramona and Witch, although the model's sustained winds still compare better to the observed gusts at the airport. With a 2 km grid spacing, in contrast, the model suggests Witch's sustained winds were 50% stronger than at Ramona. Note the model reconstruction at the airport no longer systematically exceeds the event maximum value, and the sustained winds at Witch are comparable to Ramona's strongest *gusts*. The ignition site was well-exposed to winds from the east and northeast, so the gusts at Witch could be expected to be about 40% larger than the sustained wind, representing a gust factor of about 1.4, which yields an event maximum gust of about 37.6 m/s (84 mph). This gust factor is supported by observations at SDGE station WCKSD during the moderately strong 1-3 February 2011 Santa Ana wind event (Fig. 8).

Finally, we see intermittently stronger winds appear in the 667 m simulation (Fig. 7d), but the overall magnitude and evolution of the event resembles the 2 km result far better than the latter compared with the 6 and 10 km reconstructions. The sustained winds at Ramona do not exceed the maximum observed values, and a peak gust at Witch of about 42 m/s (94 mph) might be anticipated from a gust factor of 1.4. We will soon see the reason why the winds increased at Witch in this simulation is that we began resolving relatively high frequency wave activity that can act to amplify the resolved-scale winds, and thus the unresolvable gusts as well.

Vertical cross-sections, taken west-east across Witch, demonstrate why the coarser resolution simulations overpredict the winds at Ramona, and underpredict them farther upslope (Fig. 9). Shown is the horizontal wind field at 1900 UTC 21 October, shortly before the Witch fire onset. For the 667 m simulation (Fig. 9a), the fastest wind speed in the plane at this time is 27 m/s (60 mph), located immediately above Witch. The red shaded area depicts where Richardson number is less than 0.25. It is conceivable that small scale eddies, unresolvable even at

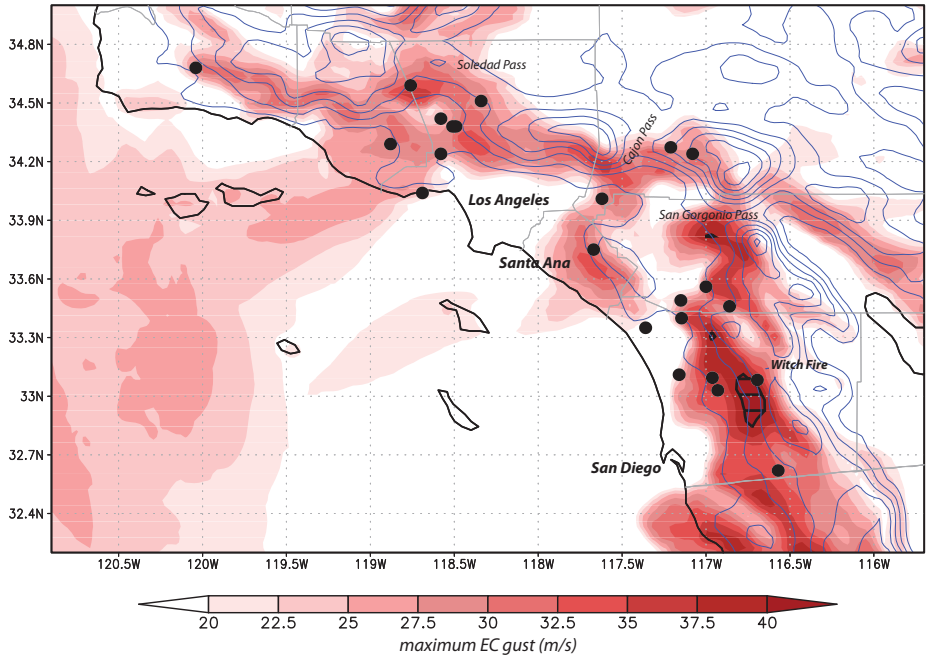

Fig. 1: Event maximum EC wind gusts (colored) for the October 2007 Santa Ana wind event from a 6 km WRF-ARW simulation. Values exceeding 40 m/s (90 mph) are hatched. Topography shown in blue (300 m contours). Black dots indicate locations of most ignition sites; Witch fire site is labeled. Only part of the 6 km domain shown.

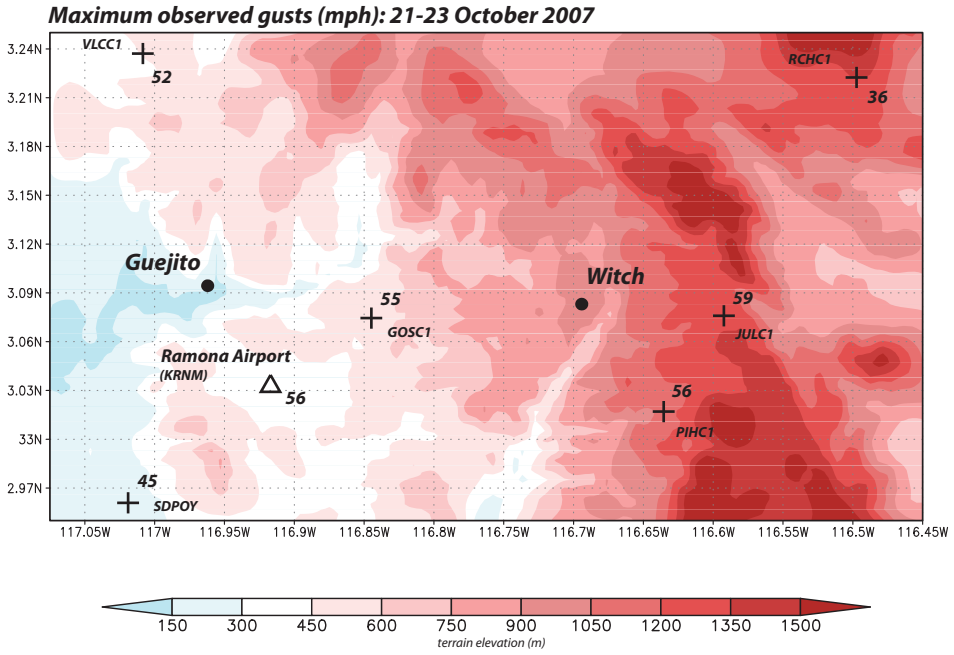

Fig. 2: Maximum observed gusts (mph) for the 21-23 October 2007 period, superposed on topography for 667 m Domain 5. Stations with names ending with "C1" are RAWS sites. Locations of the Witch and Guejito fires are indicated.

Fig. 3: Satellite imagery of the Goose Valley RAWS (GOSC1) immediate area. From Google Earth.

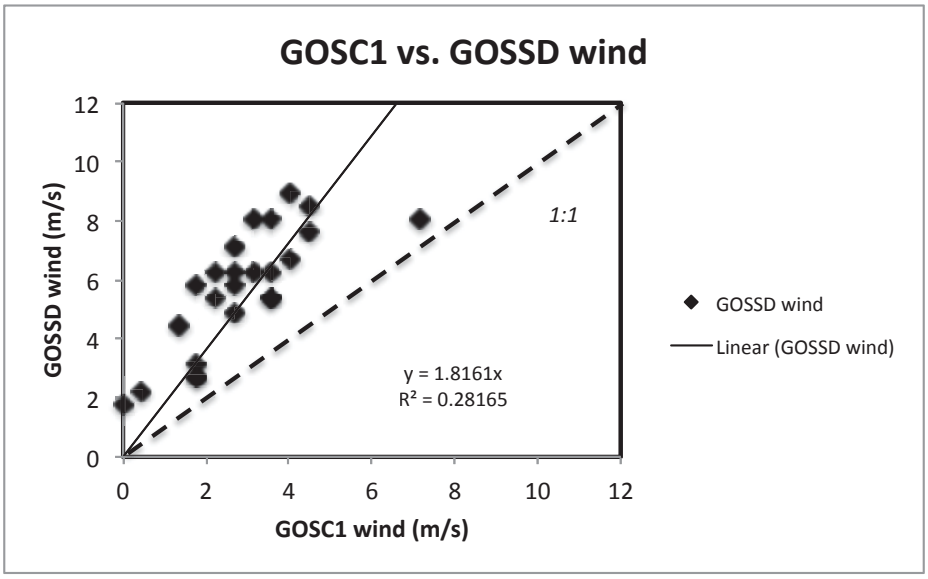

Fig. 4: Scatterplot of hourly sustained winds measured at the Goose Valley RAWS (GOSC1) and SDGE (GOSSD) sites for the period between 00 UTC 6 December to 00 UTC 7 December 2011, with zero-intercept least squares and 1:1 correspondence lines. If the single strongest hourly observation at GOSC1 is removed, the slope of the no-intercept least squares line becomes 2.00 with an R^2 of 0.6, and the fit with intercept is 4.0+1.44*GOSC1, with $R^2 = 0.7$.

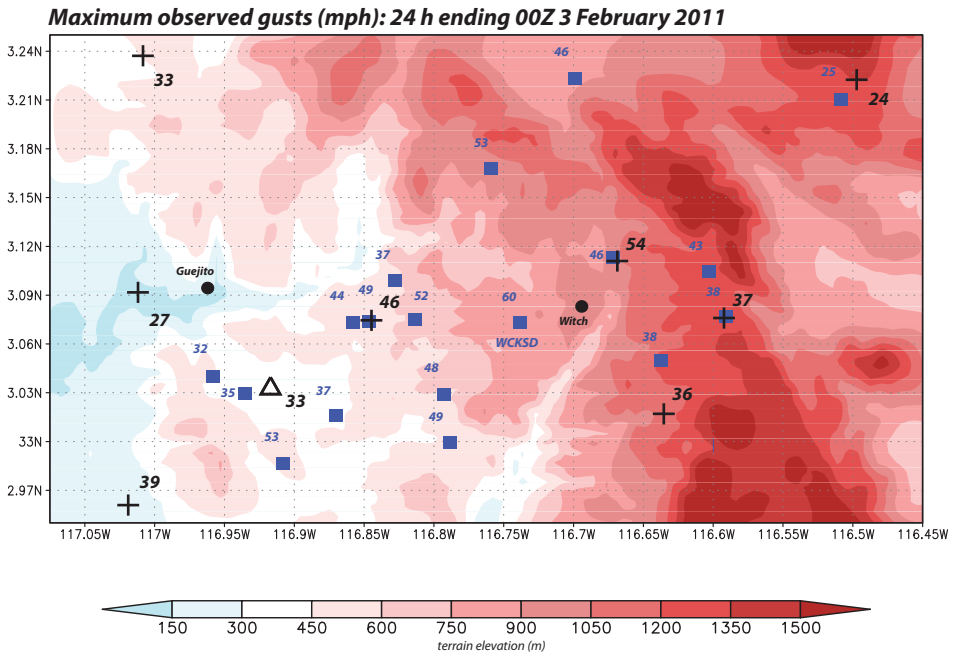

Fig. 5: As in Fig. 2, but for the 2 February 2011 Santa Ana wind event. Blue markers indicate SDGE stations; WCKSD is labeled. GOSSD, near GOSC1 (see Fig. 2), was not in its present location during this event.

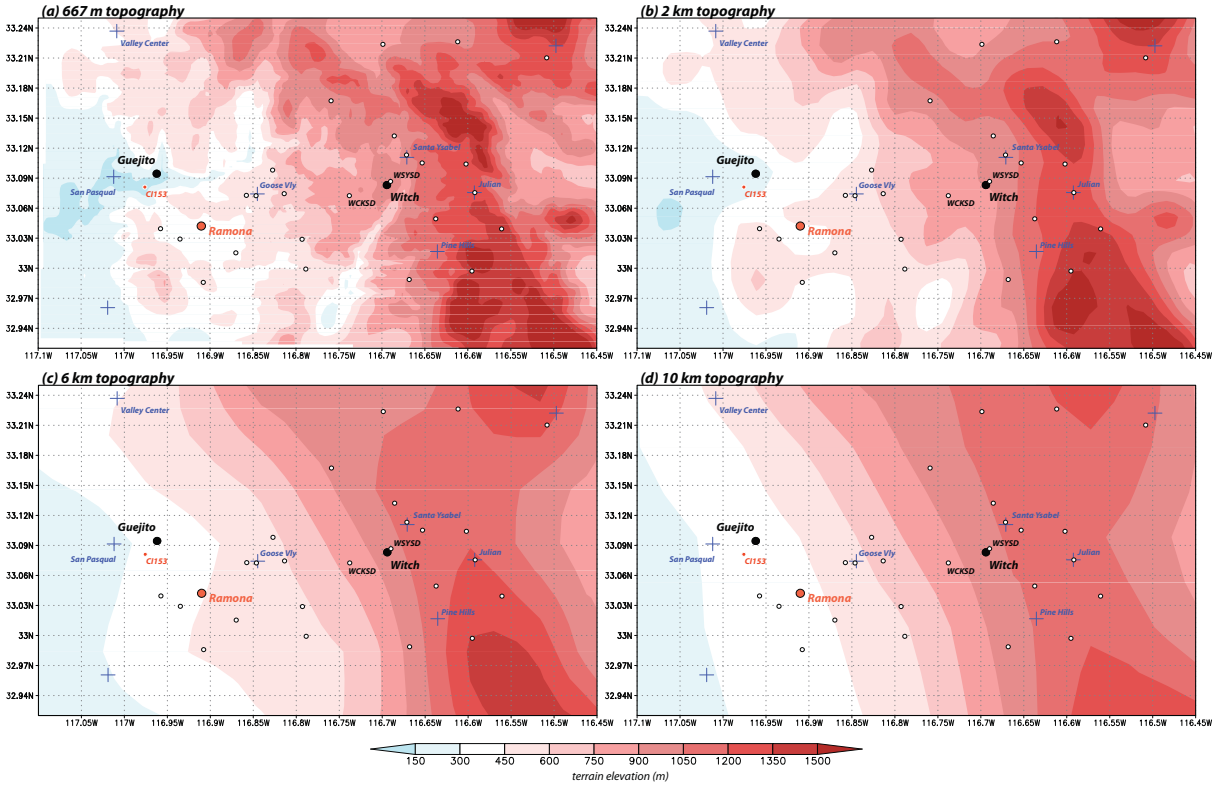

Fig. 6: Topography of the Witch area as rendered in model simulations with maximum resolution of: (1) 667 m; (b) 2 km; (c) 6 km; and (d) 10 km. Small black and white circles indicate some SDGE stations; WCKSD and WSYSD are labeled. WSYSD is located 0.6 km from the ignition site, at the same elevation, but was not installed until August 2011.

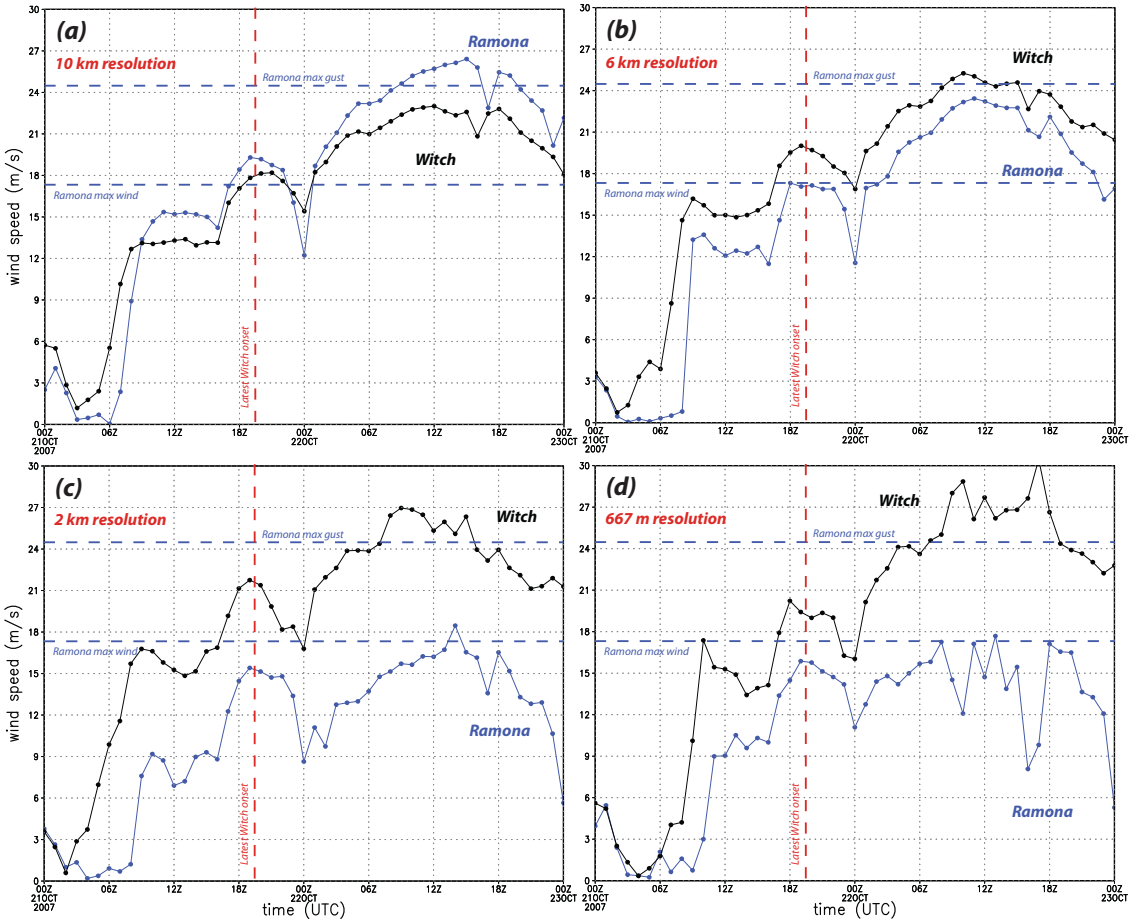

Fig. 7: Time series of hourly simulated at 7.9 m for Ramona and 10 m for Witch, for four simulations differing by the finest grid spacing over the Witch region. At Ramona, the diagnosed 10 m wind was adjusted via the standard logarithmic wind profile. Observed maximum gust and sustained wind at Ramona indicated.

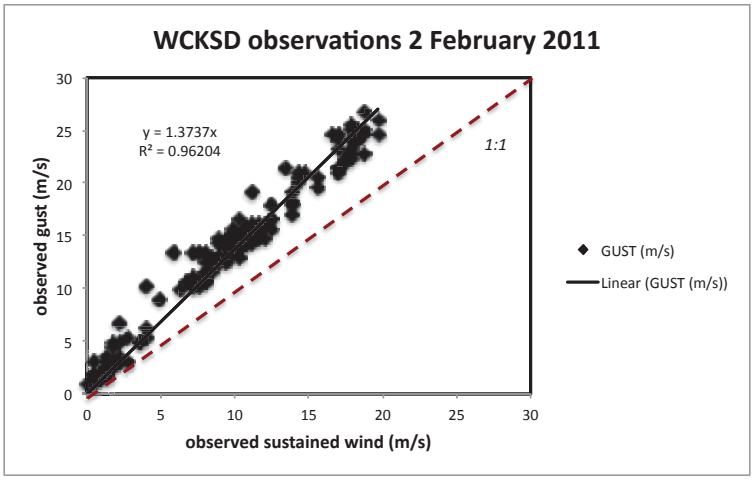

Fig. 8: Observed winds vs. gusts (m/s) at WCKSD for 2 February 2011, based on 10 min sustained winds and 5 sec maximum gusts, both reported every 10 min, with zero-intercept least squares and 1:1 correspondence lines.

this grid spacing, could become established at the top of the high-wind layer and cause the downward transport (if not further amplification) of momentum, enhancing the already fast winds above the ignition site.

Comparing this result with the other panels of Fig. 9, we see that as the grid spacing becomes coarser, the terrain-accelerated flow becomes substantially larger in horizontal extent (although not stronger), and the fastest wind speeds are found farther down the lee slope. In the 10 km simulation, we see why the winds are stronger above Ramona than Witch. As suggested in Fig. 6d, Witch is located on the broadened ridge. If one's goal is to assess wind speeds at a particular time and place, accurately resolving the terrain shape is of paramount importance. Based on these results, it is concluded that grid spacing wider than 2 km cannot reliably place the fastest winds at the most likely correct locations.

5. Sensitivity to model physics

Hundreds of simulations were made for this study, which has included variations in the initialization data source (including NARR, NNRP, FNL, NAM analyses and forecasts, RUC, CFSR, ERA-INTERIM datasets), WRF-ARW model version (3.2 through 3.4), model start time, grid and topographic resolution, and the size, configuration and placement of the model nests. The physics sensitivity simulations in this section were made with WRF version 3.4 using five domains telescoping to 667 m grid spacing in the Witch-Guejito vicinity, and initialized with NARR at 0000 UTC 21 October 2007. The finest resolution domain is slightly larger than shown in Figs. 2 and 6a.

Observations recorded every minute at the Ramona ASOS station are shown in Fig. 10 (grey curve), up until the station ceased reporting at 1931 UTC on the 22nd[5]. There are two peaks, nearly corresponding with the Witch and Guejito fire ignitions, and the maximum value of 17.4 m/s (39 mph) occurs during the second surge. A WRF reconstruction using the YSU PBL and RUC surface schemes is superimposed (black curve), derived from approximately one-minute outputs. This is one of 16 members of a physics ensemble that varied the PBL (also including MYJ, QNSE, and ACM2) and surface (also comprising TD, Pleim-Xiu or PX, and Noah) parameterizations, and was selected as the benchmark run on the basis of this figure.

The event appears to start several hours early in the simulation, but congruence with the observations is acceptable after about 1500 UTC on the 21st, at which time the surface layer becomes (and remains) neutrally stable. The simulation has little high-frequency temporal variation, at least at first. The higher-frequency episode that commences around 0800 UTC on October 22nd is the subject of Sec. 7.

[5]Although these are one-minute data, the sustained winds plotted represent two-minute averages.

Table 1: Roughness lengths employed by the surface schemes for USGS land use category 9 in the late October simulations in YSU, ACM2 runs.

Surface scheme	Roughness length (m) in October
TD	0.01
Noah	0.024
RUC	0.11
PX	0.20

Figure 11 incorporates the remaining ensemble members from this experiment. It is clear that the ensemble spread is very large. All of the members start the event too early, and several consistently overpredict the winds through the period shown while others indicate speeds that are much too low during the core of the event. This could be very discouraging, but two things need to be noted: (1) the ensemble spread is smaller and less important at Witch; and (2) the variation of the winds at Ramona is largely a function of how the surface scheme handles the roughness of the lee slope.

The first point is illustrated in Fig. 12, which presents the WSMAX gust estimates at Witch, for comparison with the sustained winds at Ramona. The ensemble spread is relatively small, as all members produce a downslope windstorm with winds peaking above or near Witch. The vertical cross-sections in Fig. 13 are valid at 0900 UTC 22 October, which is near the event peak. In addition to the YSU/RUC benchmark (Fig. 13b), the other two members selected include YSU/Noah (Fig. 13a) and ACM2/PX (Fig. 13c), which produce the strongest and weakest winds at Ramona, respectively (see next section). As far as Ramona is concerned, the principal difference among these simulations is how far downslope the strong winds remain relatively close to the surface. The variation closer to Witch is comparatively minor.

The largest contributor to the variation of simulated sustained winds at Ramona is the roughness length specified by the surface scheme (Table 1). The local landscape is dominated by USGS land use category 9 (scrubland/grassland). As mentioned earlier, the TD scheme uses the wintertime z_0 value listed in LANDUSE.TBL of 0.01 m, which seems small. The Noah scheme reads data from VEGPARM.TBL and applies a somewhat larger value for this landuse type. The RUC and PX schemes treat scrubland

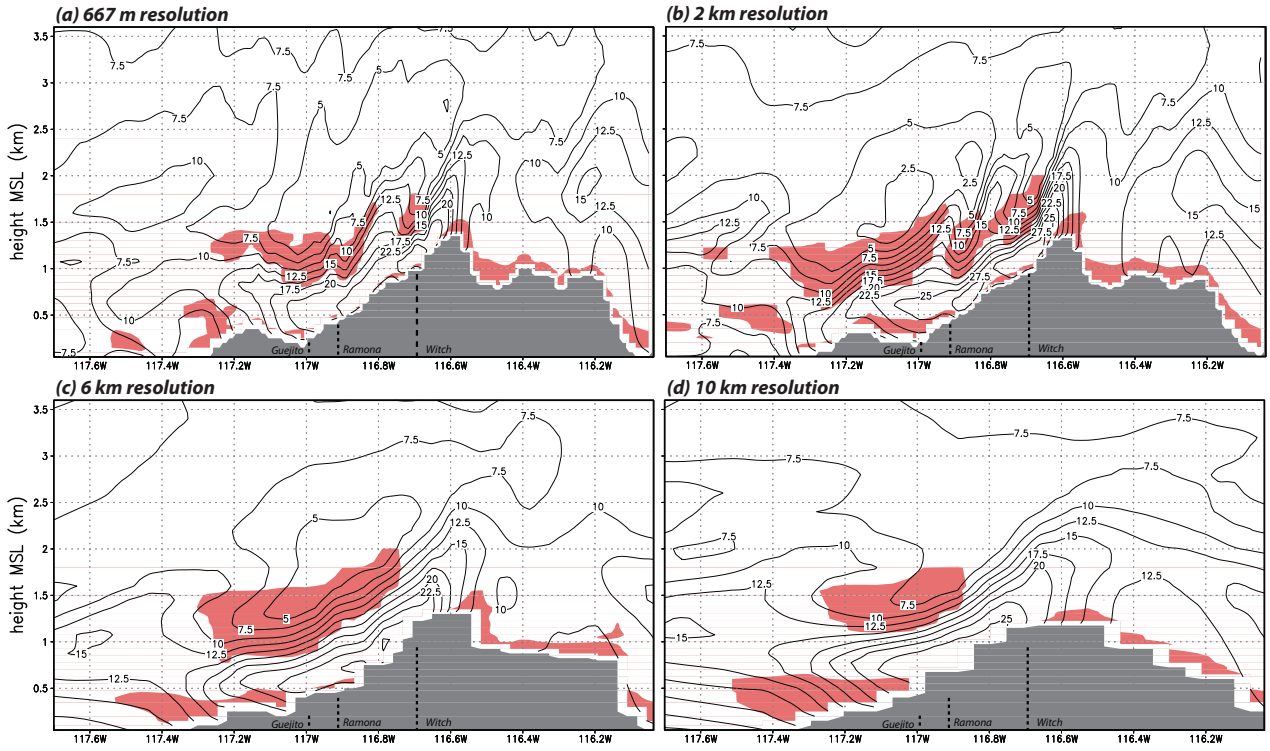

Fig. 9: Vertical cross-sections of horizontal wind speed (2.5 m/s contours) for 1900 UTC 21 October 2007, taken west-east across Witch for the simulations shown in Fig. 7. Red shaded field indicates where Richardson number Ri < 0.25; grey shaded area depicts topography. Approximate locations of Witch, Ramona and Guejito are shown. Guejito and Ramona reside 1.3 km north and 5.1 km south, respectively, of the plane shown. The 667 m simulation shown in panel (a) is taken from the 2 km parent domain, for conformity with the other panels.

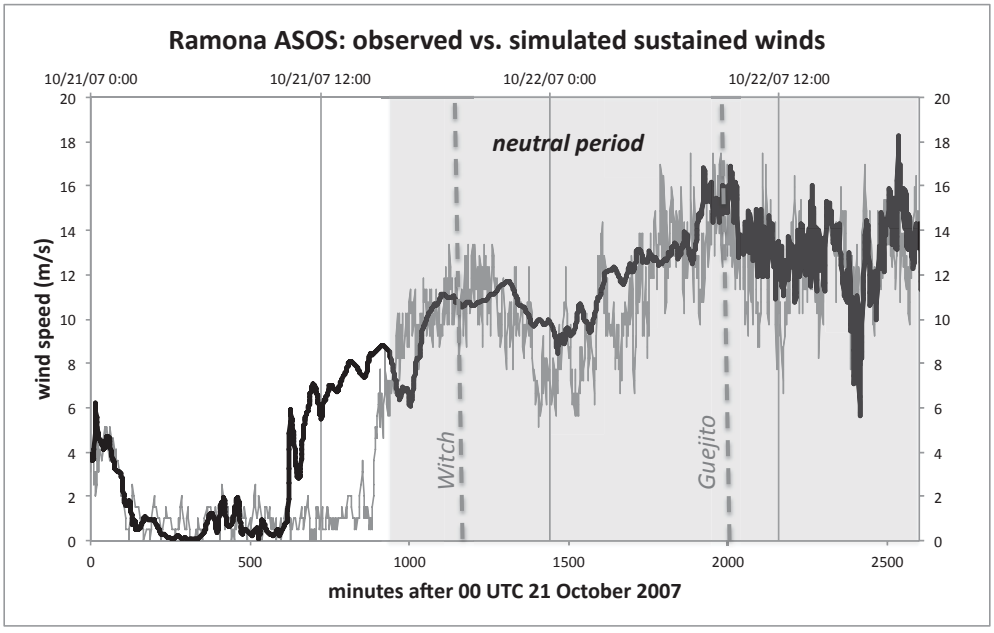

Fig. 10: Time series of observed (grey) and simulated (black) winds at Ramona airport, commencing at 0000 UTC 21 October 2007. The observed winds are two-minute average sustained winds measured at 7.9 m AGL, reported every minute. The model winds are instantaneous 10 m values, adjusted for the anemometer height, and plotted approximately every minute (59 s), from a NARR-initialized (benchmark) simulation using the YSU PBL and RUC surface schemes. The grey-shaded area represents the time period for which the surface layer possesses neutral stability in the simulation. Ramona stopped reporting at 1931 UTC 22 October, the time at which this plot ends. Witch and Guejito fire onset times marked.

and grassland as 11 and 20 times rougher than TD, and yield the slowest winds at Ramona[6].

The Noah scheme results in the largest winds at Ramona in part because it gives a smaller roughness to the urban area (Ramona city) immediately upwind of the ASOS station. A test was carried out in which a YSU/TD simulation was repeated with a LANDUSE.TBL modified to use the RUC scheme's z_0 values for all categories. This simulation resulted in much slower winds at Ramona than observed through the peak of the event, although winds at Witch were little affected (not shown). Although validation is important, there may be less value in the effort than usually presumed, and it is possible incautiously trusting the observations leads one to some erroneous conclusions.

6. Maximum gust estimates for Witch

Table 2 presents maximum event gust estimates for Witch from the 667 m ensemble. The GF gust was created by applying a gust factor of 1.4 to the 20 m wind V_{20}, which was derived from V_a via the logarithmic wind profile

$$V_{20} = V_a \frac{\ln(20/z_0) - \psi_{20}}{\ln(Z_a/z_0) - \psi_a}.$$

In the above, $Z_a \approx 26$ m is the height of the lowest model level and ψ_x are stability functions. The EC gust may be less applicable at other altitudes, and by its nature, WSMAX is height-independent.

The estimated maximum gust range listed on Table 2 is 38-49 m/s (85-110 mph). Among the three estimates, WSMAX is the only one that *directly* incorporates information above the lowest model level and, apart from the PX scheme members, produces the smallest gusts. The WSMAX range, at 41-45 m/s (93-100 mph), is also relatively small. Although the Witch fire started hours before the event peak, our interest here is in the maximum, and a reasonable estimate for the fastest gust at the Witch site is about 43 m/s or 96 mph.

7. High-frequency episode near the event peak

All of the 667 m ensemble members possess a high-frequency episode that commences around 1000 UTC 22 October, around the event peak, and lasts for hours (cf. Fig. 10). West-east vertical cross-sections past Witch over a 6 minute period from the benchmark run reveal the temporal variation is associated with a wave-like feature forming over, and then passing downwind, of Witch with a phase speed of roughly 12 m/s and a period of about 8 min. These

[6]MYJ and QNSE recompute $F10$ with an "effective z_0" which increases the diagnosed wind speed. The effect appears to be proportional to z_0 but is cosmetic.

Table 2: Estimated maximum event gusts at Witch (m/s). (MYJ, QNSE values based on pre-adjusted z_0.)

Surface	PBL	WSMAX	EC gust	GF gust
TD	YSU	43	46	49
TD	ACM2	43	45	47
TD	MYJ	44	41	46
TD	QNSE	44	43	46
NOAH	YSU	42	46	48
NOAH	ACM2	44	45	47
NOAH	MYJ	44	42	45
NOAH	QNSE	44	44	47
RUC	YSU	41	45	43
RUC	ACM2	44	47	45
RUC	MYJ	43	42	43
RUC	QNSE	44	43	44
PX	YSU	45	46	39
PX	ACM2	42	46	40
PX	MYJ	44	44	41
PX	QNSE	43	42	38

appear to be gravity waves, mechanically forced by a shear instability (note region of Ri < 0.25) immediately above the high wind layer that are trapped within the downsloping flow, and are very well resolved both spatially and temporally. Thus, this phenomenon is ostensibly similar to the high frequency disturbances discussed in Scinocca and Peltier (1989) and Smith (1991).

The waves did not form in the 2 km simulations, although some (lower frequency) oscillations did appear (not shown). Therefore, higher resolution appears necessary to capture this feature, These waves deserve further study as it is clear that they represent locally concentrated zones of horizontal velocity that could be transported vertically the surface turbulence, further amplifying near-surface gusts.

8. Concluding discussion

From close inspection of WRF model simulations, we have seen that the infamous Santa Ana wind event of October 2007 possessed many characteristics of downslope windstorms in the Laguna mountains of San Diego county. The terrain-amplified flow was largest in the immediate vicinity of the ignition site of the Witch Creek fire, as long as the regional topography is adequately rendered. Model horizontal grid spacings wider than 2 km were determined insufficient to properly capture the terrain shape. The simulations were sensitive to model physics, mainly due to variations in the surface roughness that determines how far downslope the accelerated flow can remain close to the ground. High resolution simulations reveal the event peak was also marked by relatively high-frequency, well-resolved gravity waves apparently provoked by shear instability immediately above the downsloping flow. This feature is likely relevant to gustiness and deserves further study.

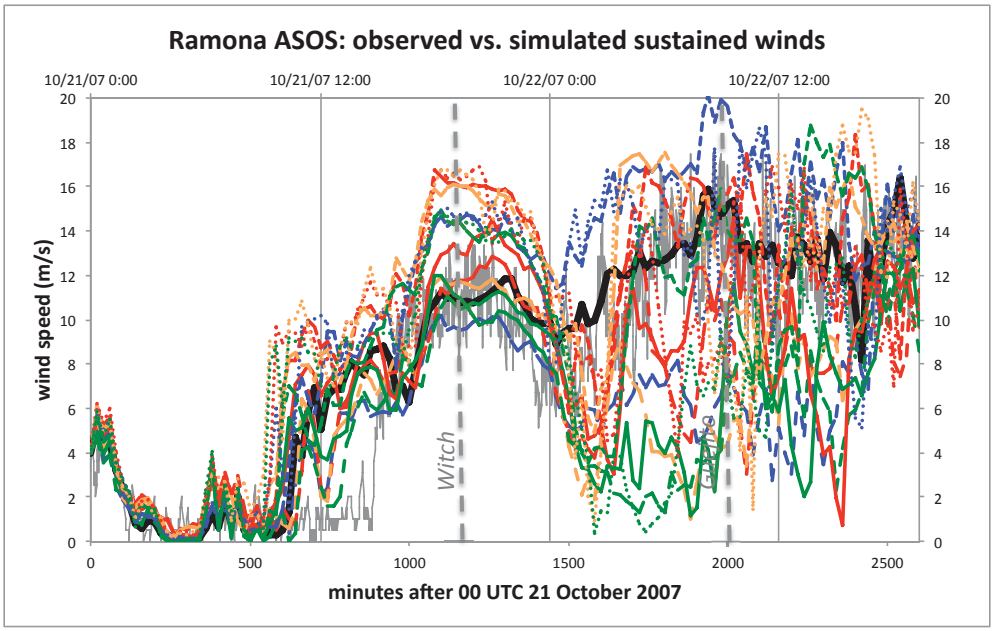

Fig. 11: As in Fig. 10, but including the remaining ensemble members. Simulated winds are based on 20 min outputs. Benchmark run highlighted.

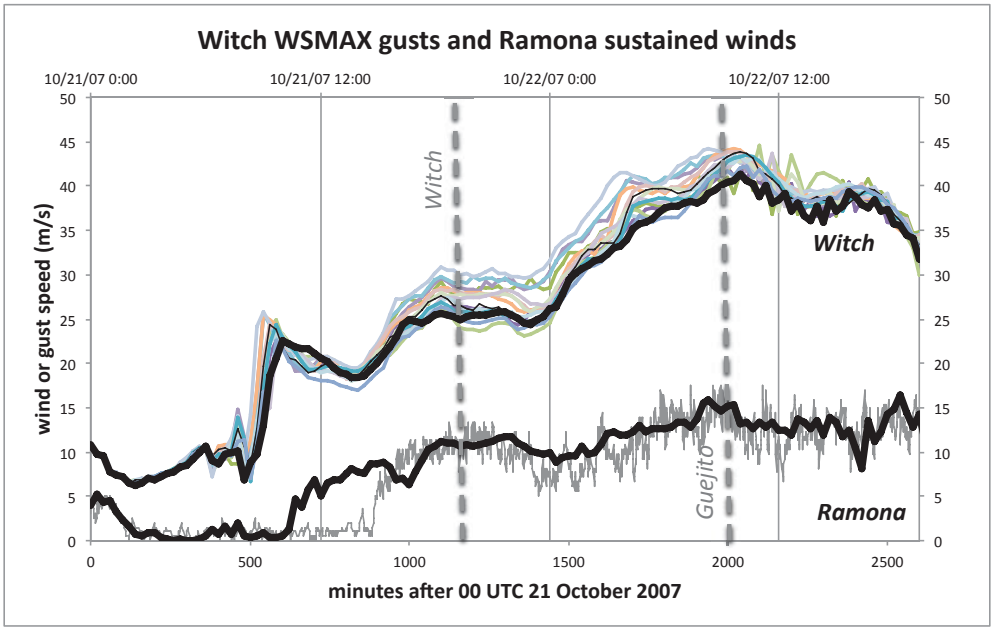

Fig. 12: As in Fig. 11, but for the WSMAX gust estimates at Witch. The benchmark run is highlighted. Sustained winds observed and simulated in the benchmark run for Ramona included for comparison. Based on 20 min outputs. By its nature, WSMAX partially masks the high-frequency episodes.

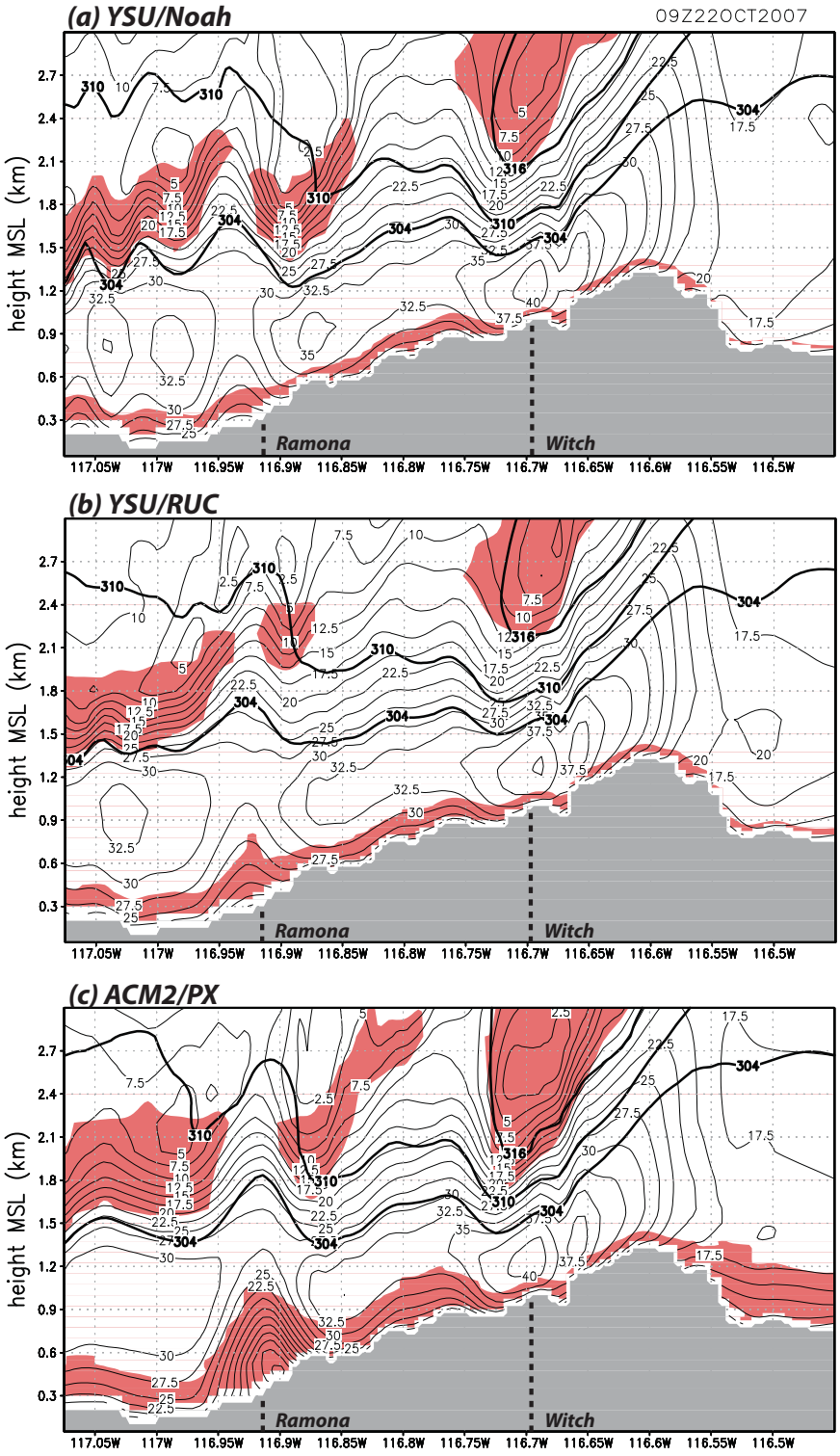

Fig. 13: Similar to Fig. 9, but horizontal velocity (2.5 m/s contours) for three members of the 667 m ensemble, at 0900 UTC 22 October 2007. Thick black contours are the 304, 310 and 316 K isentropes. The shaded field shows where Richardson number < 0.25. Members are: (a) YSU/Noah; (b) YSU/RUC (benchmark); and (c) ACM2/PX.

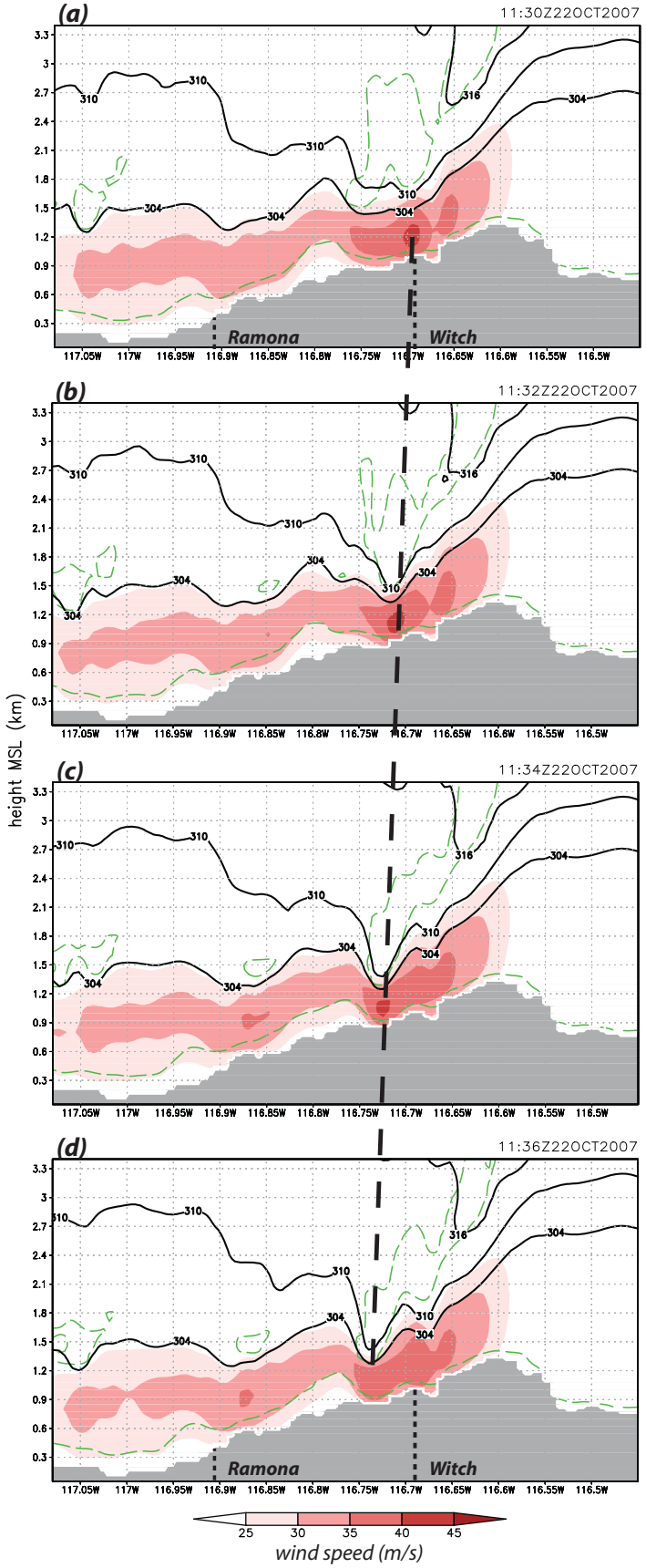

Fig. 14: Similar to Fig. 13, but for 667 m benchmark run (YSU/RUC), at four times during the high-frequency episode. Shaded field is horizontal wind speed (m/s). Thick black contours are the 304, 310 and 316 K isentropes. The green contour encloses are with Richardson number < 0.25.

9. References

Brasseur, G., 2001: Development and application of a physical approach to estimating wind gusts. *Mon. Wea. Rev.,* **129**, 5–25.

Burton, T., and Coauthors, 2011: *Wind Energy Handbook*, WIley, Chichester, UK.

Chang, C.-H., and F. P. Schoenberg, 2011: Testing separability in marked multidimensional point processes with covariates. *Ann Inst Stat Math*, **63**. 110–1122.

Conil, S., and A. Hall, 2006: Local Regimes of Atmospheric Variability: A Case Study of Southern California. *J. Climate*, **19**, 4308–4325.

Durran, D. R., 1986: Another look at downslope windstorms. Part I: The development of analogs to supercritical flow in an infinitely deep, continuously stratified fluid. *J. Atmos. Sci.,* **43**, 2527–2543.

Huang, C., Y.-L. Lin, M. L. Kaplan, and J. J. Charney, 2009: Synoptic-scale and mesoscale environments conducive to forest fires during the October 2003 extreme fire event in Southern California. *J. Appl. Meteor. Clim.,* **48**, 553–579.

Hughes, M., and A. Hall. 2010: Local and synoptic mechanisms causing Southern Californias Santa Ana winds. *Clim. Dyn.* **34:6**, 847–857.

Jones, C., F. Fujioka, and L. M. V. Carvalho, 2010: Forecast skill of synoptic conditions associated with Santa Ana Winds in Southern California. *Mon. Wea. Rev.,* **138**, 4528–4541.

Klemp, J. B., and D. K. Lilly, 1975: The dynamics of induced downslope winds. *J. Atmos. Sci.,* **32**, 320–339.

Lumley, J. L. and Panosfky, H. A., 1964: *The Structure of Atmospheric Turbulence*, Interscience, London, UK.

Mesinger, F., and Coauthors, 2006: North American Regional Reanalysis. *Bull. Amer. Meteor. Sci.,* **87**, 343–360.

Raphael, M. N., 2003: The Santa Ana Winds of California. *Earth Interact.*, **7**, 1–13.

Scinocca, J. F., and W. R. Peltier, 1989: Pulsating downslope windstorms. *J. Atmos. Sci.,* **46**, 2885–2914.

Small, I. J., 1995: Santa Ana Winds and the fire outbreak of fall 1993. Tech. Memo., NOAA/NWS, 48 pp.

Smith, R. B., 1991: Kelvin-Helmholtz instability in severe downslope wind flow. *J. Atmos. Sci.,* **48**, 1319–1324.

Sommers, W. T., 1978. LFM forecast variables related to Santa Ana Wind occurrences. *Mon. Wea. Rev.,* **106**, 1307–1316.

Westerling A. L., D. R. Cayan, T. J. Brown, B. L. Hall, and L. G. Riddle, 2004: Climate, Santa Ana winds and autumn wildfires in Southern California. *EOS* **85**, 289–296.

Wieringa, J., 1973: Gust factors over open water and built-up country. *Boundary Layer Meteor.*, **3**, 424–441.

Acknowledgments. This research was sponsored by Aspen Reinsurance, Catlin Group, and AEGIS. Steve Vanderburg and Brian D'Agostino of San Diego Gas and Electric helped confirm fire ignition locations and SDGE mesonet information. Thanks also to Travis Wilson and Yang Cao (UCLA); Joe Klemp, Jimy Dudhia and Bob Sharman (NCAR); and Doug King (Aspen).

Appendix 2

7.6 Predictability and Sensitivity of Downslope Windstorms in San Diego County

Yang Cao and Robert G. Fovell*

Department of Atmospheric and Oceanic Sciences, University of California, Los Angeles

ABSTRACT

A case study of downslope flow during a moderately intense Southern California weather event known as the Santa Ana winds is presented, making use of an exceptionally dense network of near-surface observations in San Diego county to calibrate and validate a numerical weather prediction model, which in turn is used to help understand and fill in the many gaps in the observations. This case is shown to be particularly sensitive to the physical parameterizations and landuse database employed in the model, as well as to small random perturbations mimicking the action of unresolved turbulence.

1. Introduction

Southern California is famous for its "Santa Ana" winds, which were named after a city and canyon in Orange County. Santa Anas are very dry, sometimes hot, offshore winds (Glickman 2000) that can produce gusts exceeding 25 m s^{-1} (56 mph) in favored areas (Chow et al. 2012). Events occur most frequently between October and February, with December being the peak month, although its season extends from September through April (Raphael 2003). Although Santa Anas tend to form most frequently in midwinter, the most dangerous events often occur in autumn, before the winter rains have begun. At that time, the vegetation tends to be extremely dry, and autumn fires historically have the potential to be very large in area, being fanned by the Santa Ana winds (Chang and Schoenberg 2011).

Santa Ana events result when cooler air spills across the Great Basin, becoming partially dammed by the mountains that encircle Southern California. This increases the horizontal gradient in sea-level pressure (SLP) and helps increase flow speeds through prominent terrain gaps such as the Cajon Pass (leading to Santa Ana) and through the Soledad Gap (northwest of Los Angeles), creating prominent wind corridors in the northern part of the Los Angeles basin (Fig. 1). Wind speeds can also be very large in San Diego county, where the terrain gaps appear less prominent but also terrain heights are generally lower. We will see that in this part of Southern California, the flow across the topography shares many characteristics of classic downslope windstorms.

Downslope windstorms are a type of large amplitude mountain wave that can produce strong, often gusty winds on the lee side of a mountain barrier. Subsidence of air can cause very low relative humidities near the surface, particularly if the air mass starts with low absolute humidity. The necessary ingredients for downslope windstorms are a sufficiently large mountain barrier, as well as strong cross-barrier winds and a stable atmosphere, both near the mountaintop level (Chow et al. 2012). Downslope windstorms are observed in many areas of the world, and carry such names as the Bora, Chinook, Foehn, Zonda and Taku winds (Schamp 1964).

In complex terrain, the wind can vary greatly over small distances and gustiness is common in downslope windstorms, which may be caused by subrotors embedded

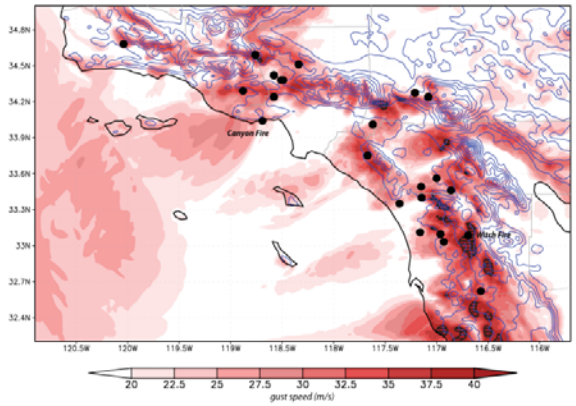

Fig. 1. Event maximum estimated wind gusts (colored) for the October 2007 Santa Ana wind event from a 2 km WRF-ARW simulation, illustrating wind corridors and shadows in Southern California. Values exceeding 40 m s^{-1} (90 mph) are hatched. Topography is shown in blue (300m contours). Black dots denote locations of fire ignition sites. Witch and Canyon fire sites are labeled.

in the flow (Doyle and Durran 2007). Wind forecasts in this region are extremely important, since the gusty winds can knock down trees and power lines, starting and spreading fires. As an example, on 21 October 2007, the Witch Creek fire was sparked by wind-whipped power lines located about 20 m above ground level (AGL), and was driven by an especially strong Santa Ana wind event to become one of the largest fires in California history. This was but one of more than 25 fires that started during this event, all initiated in the regions characteristic wind corridors (Fig. 1).

There is great need to know, in advance, when the electrical grid is in danger, to reduce the risk of fire to this very fire-prone area. The purpose of this study is to understand how predictable the winds are in the San Diego area region and how skillfully a regional-scale weather prediction model can forecast the winds and especially the gusts that they even cannot resolve. The Weather Research and Forecasting (WRF) models Advanced Research WRF (ARW) core is selected for this exercise. Model validation and calibration will be carried out using a newly installed surface observing network of perhaps unprecedented density.

2. Available surface observations

Observations are crucial for vetting a numerical model, but there are several significant challenges involved. The surface wind observation station network has historically been relatively sparse and few stations have very long record lengths. Each network tends to measure the wind differently, with respect to sensor height and sampling, averaging and reporting intervals. Unfortunately, numerous stations have anemometers that are shielded by buildings and/or trees, or simply were not installed in the areas of greatest wind and/or hazard. Furthermore, above ground wind information is in even shorter supply.

In the last few years, the San Diego Gas and Electric (SDGE) company has deployed over 140 stations across San Diego county, purposefully placed in wind-prone areas (Fig. 2). These stations were designed to follow the RAWS (Remote Automated Weather Station) standard with respect to anemometer height (6.1 m or 20 ft AGL) and averaging interval for the sustained wind (10 min). Every 10 min, SDGE stations report sustained winds as well as maximum gusts based on 3-sec samples; this contrasts with the RAWS networks hourly reporting interval. The SDGE network may be the densest surface wind observations on the planet at this time, and captured a moderately strong Santa Ana wind event that occurred in middle of February 2013.

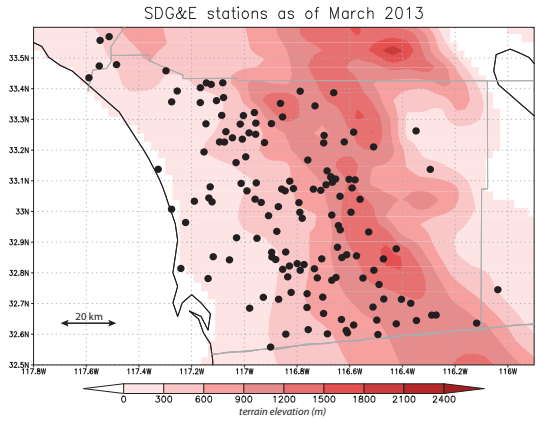

FIG. 2. SDGE surface station locations (black dots), with underlying topography shaded.

3. The 14-16 February 2013 event

In 2007, very high winds rushed through San Diego county, starting and spreading the infamous Witch Fire. At the time, however, few well-positioned and exposed stations existed, limiting our ability to calibrate and validate the model. Our strategy is to examine more recent Santa Ana events captured in the SDGE network. At this writing, these events have been considerably weaker than the October 2007 windstorm, but may provide important insights into the optimal model configuration with respect to model physics and resolution that are applicable to more intense events. Even though the current SDGE mesonet only provides us with information from a few meters above the ground, its high station density such as this will help us understand the spatial and temporal variation of the winds across this region, and can test the accuracy of the model simulations.

Although likely only moderate in overall strength as a Santa Ana event, some very impressive winds and gusts were recorded in the SDGE network during the mid-February event. For example, at 1830 UTC (1030 AM PST) on 15 February 2013, SDGE station Sill Hill (SIL) recorded a 41 m s^{-1} (91 mph) wind gust (Fig. 3), at a time when no other stations in this region recorded a wind gust greater than 26 m s^{-1} (57 mph). Indeed, the winds were 50% weaker at Boulder Creek (BOC), the SDGE station just 1.6 km to the south.

It would be easy to dismiss such a high wind observation. The wind record at that station (Fig. 4) shows, however, that the 91 mph gust was not an isolated occurrence. Over a 2-hour period, the SIL gust averaged 75 mph (34 m s^{-1}) and was frequently in the 80 mph (36 m s^{-1}) range before the 91 mph observation was recorded. (Note how similar the sustained wind at SIL is to the wind

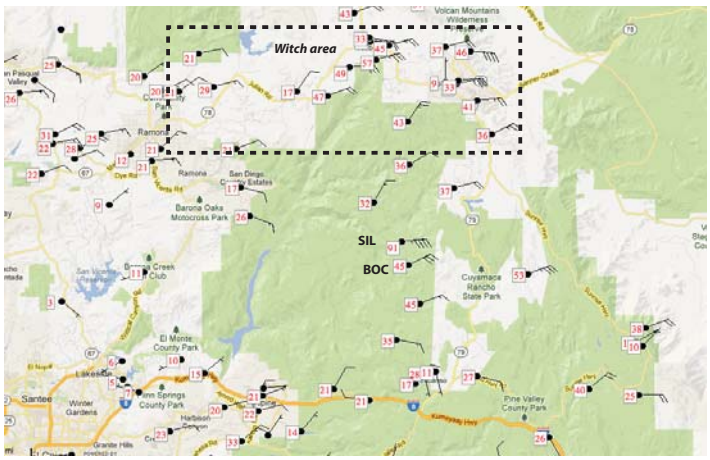

FIG. 3. Surface wind gusts (red numbers) and sustained winds (flags), both mph, at 1830 UTC (1030 AM PST) on 15 Feburary 2013, superposed on topography for the area. Distance between station SIL and BOC is 1.63 km (1 mile). Source: MesoWest and Google Maps.

gusts from BOC.) Furthermore, two SDGE meteorologists, Brian DAgostino and Steven Vanderburg, were at the site an hour before the fastest winds were recorded, and measured winds around 73 mph (33 m s^{-1}) at eye level with hand-held anemometers. A close inspection at the topographic map in the vicinity of SIL and BOC (not shown) indicates that SIL is sited on a small local ridge while BOC is in a local terrain crease, very small-scale factors that may be relevant to the wind speeds and exposures. This comparison helps illustrate the challenge that is faced in simulating and validating the winds across this area, as these very subtle terrain features would require extremely high resolution to capture.

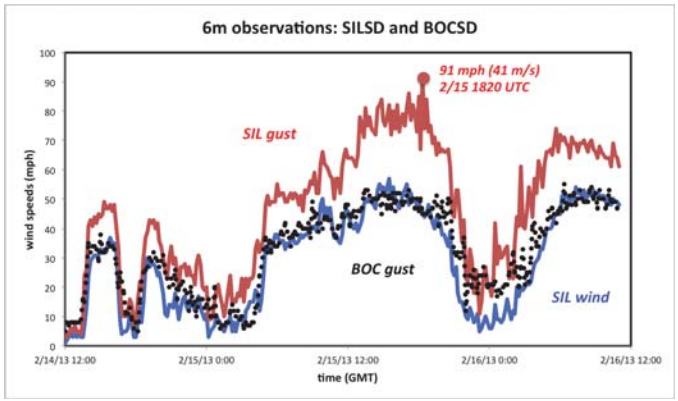

FIG. 4. Time series of observed winds (mph) at SIL and BOC over 2 days. Red and blue lines depict SIL gust and sustained wind, respectively; black dots denote BOC gust.

We now shift focus to the Witch Creek area, where there are many more SDGE stations available (Fig. 3). Station West Santa Ysabel (WSY) is located on the west-facing slope of the mountain, about 9-10 km down from the ridge (see Fig. 5a). Wind gusts observed there over a two-day period (Fig. 5b) reveal a Santa Ana episode consisting of two pulses separated by a protracted lull. The first phase peaked at 26 m s^{-1} (58 mph) at 1800 UTC (10 AM PST) on 15 Feb. After declining to as slow as 3 m s^{-1} (7 mph) during the afternoon, the gusts achieved similar strength by midnight local time before finally slowing as the event wound down.

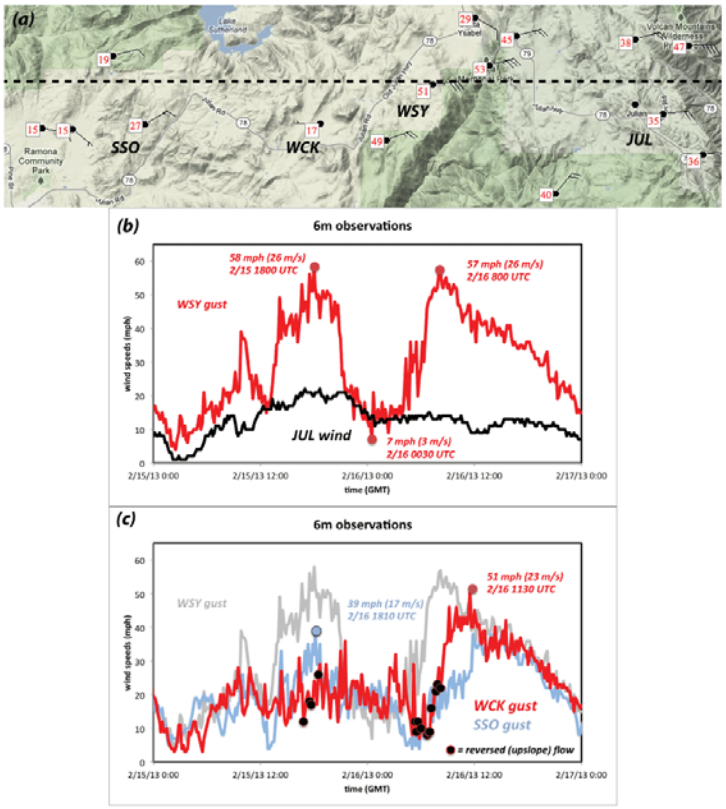

FIG. 5. (a) As in Fig. 3, but for surface wind (mph) observations at 1740 UTC (940 AM PST) on 15 February 2013 (source MesoWest), and time series of observations of (b) WSY gusts (red) and JUL sustained winds, and (c) WSY (black), WCK (red), and SSO (blue) gusts, over a period of 2 days. On (c), black dots indicate winds directed upslope at WCK.

In contrast, the sustained winds recorded at SDGE station Julian (JUL), which is near the top of the mountain ridge, reveal little in the way of temporal trend, apart from a long, slow decline through the period depicted (Fig. 5b). The winds also behaved very differently at Witch

Creek (WCK) station (Fig. 5c), which is less than 5 km downslope from WSY. During the first peak, WCKs winds remained much weaker than WSYs. Occasionally, the wind direction at WCK reversed to upslope (at times indicated by the black dots), suggesting a rotor or hydraulic jump may have formed there. During the lull between the two peaks, WSY and WCKs winds were comparably weak. WCK finally recorded strong winds during the second peak, but the winds lagged about 3 hours after WSY. While the winds were rising farther upslope, more wind reversals were observed at Witch Creek station.

Station Sunset Oaks (SSO) is 7 km farther downslope from WCK. Note that, during the first peak, its gusts were weaker than WSYs, but peaked at about the same time and were generally stronger than at WCK (Fig. 5c). The lull lasted longer at this station, and reached its second peak after the gusts at both WSY and WCK had started to decline. Taken together, these stations suggest a two-part Santa Ana event in which winds were largely in phase early in the event, apart from a suspected jump at WCK, and had a second part consisting of a marked downslope progression as the overall winds waned.

4. Vertical structure of the downslope flow

Although it provides no information above 6 m AGL, the dense SDGE surface observation network enables us to evaluate the realism of the model simulations of the terrain-amplified winds. This is important, as we have determined from hundreds of WRF simulations of this event alone that important characteristics of the downsloping flow are quite sensitive to resolution, landuse characteristics, model physics, and even random noise. Based on a systematic validation of model vs. observed winds, which will be explored in the next section, the physics ensemble member that appears to best represent the surface observations with respect to magnitude and temporal and spatial variation employed the Pleim-Xiu (PX) land surface model, ACM2 planetary boundary layer, and RRTMG radiation schemes. A simulation using this configuration in WRF version 3.5 and was initialized with North American Mesoscale (NAM) model forecasts at 1200 UTC 14 February 2013 (to represent an operational environment) will be examined in this section. A five-domain telescoping grid arrangement, with a 667 m nest that extended about 80 km west-east by 70 km north-south and covered roughly 70% of the SDGE network, is employed. The landuse database used was derived from MODIS observations.

Figure 6 presents the west-east vertical cross-sections across WSY (see Fig. 5a), with SSO, WCK, and JUL marked but being slightly out of the vertical plane depicted. At 0800 UTC 15 Feb 2013 (Fig. 6a), the downslope windstorm had started, but the winds near the ground at WSY and stations farther downslope had not yet begun to rise. Recall that by 1740 UTC, winds recorded at WSY and SSO had reached their first-phase peaks, but WCKs gusts remained weaker (Fig. 5c). Note the model simulation has developed a jump-like feature almost directly above WCK at this time (Fig. 6b), rendering relatively weak (and even occasionally reversed) winds there and stronger winds at WSY and SSO, consistent with the observations. Note also that, as expected, the wind speeds had not strengthened very much at JUL, which is located at the top of the ridge and at the very edge of the terrain amplification.

Five hours later, there was a brief period (around 2130 UTC) during which the winds at WCK were actually stronger than at the other stations (Fig. 5c). The winds at WSY and SSO were entering the lull period around that time, while the gusts at WCK had finally reached their first-phase peak of 36 mph (16 m s^{-1}). While the timing is not perfect, a similar phenomenon occurred in the model simulation. During this interval, the jump-like feature retreated upslope, passing over WCK (Fig. 6c).

As the jump retreated farther upslope, it also weakened and appeared to become more elevated (Fig. 6d). The model shows the lull period was one in which strong near-surface winds still existed, but became concentrated close to the ridge and in an area where there were no stations. The retreat occurred during the afternoon hours, and it is likely the shift in the character of the downsloping flow was responding to environmental changes on the upwind side. This is a subject of continuing research.

The second phase of the Santa Ana event ensued as the reintensifying flow began progressing downslope again after 0500 UTC (Figs. 5, 6e). Note another, smaller amplitude jump formed in the vicinity of WCK, again consistent with the observations. By midnight, however, that feature had disappeared and the downsloping flow became "flatter" and, eventually, shallower as the Santa Ana event eventually wound down (Figs. 6f-h). The observations indicated a westward progression in the peak near-surface wind speeds (Fig. 5c) occurred, and the model has largely captured this behavior.

5. Sensitivity to model physics and random perturbations

The physics sensitivity experiment in this section was conducted with WRF version 3.4.1, also using five domains telescoping to 667 m grid spacing but with the innermost nest focused more tightly on 25 stations in the Witch Creek vicinity. These simulations were also initialized with the aforementioned NAM model forecasts but utilized the USGS landuse database. Creating a physics ensemble involves an exhaustive examination of available model physical parameterizations, such as the land surface schemes, planetary boundary layer schemes, radiation schemes etc. In all, almost one hundred

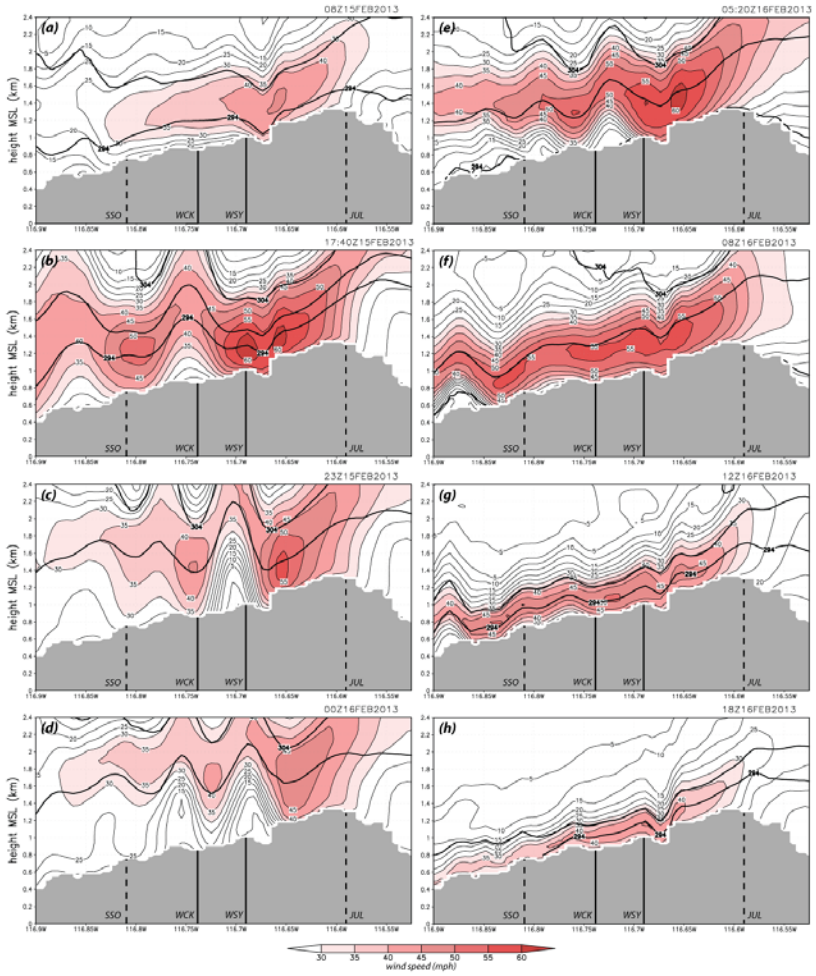

FIG. 6. Vertical cross-section of horizontal wind speed (5 mph interval thin contours), taken west-east across WSY with underlying topography shaded (see Fig. 5a). Red shaded field indicates wind speed. Thick contours denote isentropes (5K interval). Approximate locations of JUL, WSY, WCK and SSO are marked. WCK, SSO and JUL are a bit out of the vertical plane depicted.

combinations of model physics were examined.

As Fig. 7 reveals, not all model configurations are created equal. Shown is mean absolute error (MAE) of wind speed, relative to hourly observations from the SDGE network, averaged over the 54 h simulation period. The average event MAE spans 2.0-4.3 m s^{-1} (about 5-10 mph), with simulated wind speeds invariably overpredicted (not shown). Part of this is because the observed winds, recorded at 6 m (20 ft.), are being compared to the models 10 m flow speeds, which are computed diagnostically from the models lowest sigma level (about 26 m AGL) using the logarithmic wind relationship. Even correcting for the height difference does not completely mitigate the positive forecast bias, however (not shown).

The simulations are clearly sensitive to model physics, especially the land surface (LSM) scheme. Overall, the PX LSM was involved in the majority of the most accurate wind reconstructions when averaged over the 95 SDGE stations in the 667 m nest, with the Noah and MYJ schemes common among the poorest performers. It is perhaps not surprising that different model physics produces different wind speeds near the ground. Our analysis, however, suggests the most important aspect of the LSM was in how it handled the surface roughness (z_0). In the WRF model, the roughness for a particular location depends on the landuse category and database origin (such as USGS or MODIS). The PX scheme increases z_0 for many landuse categories, especially those most common on the west-facing slopes in San Diego county. We have found that altering other LSMs to increase the roughness of

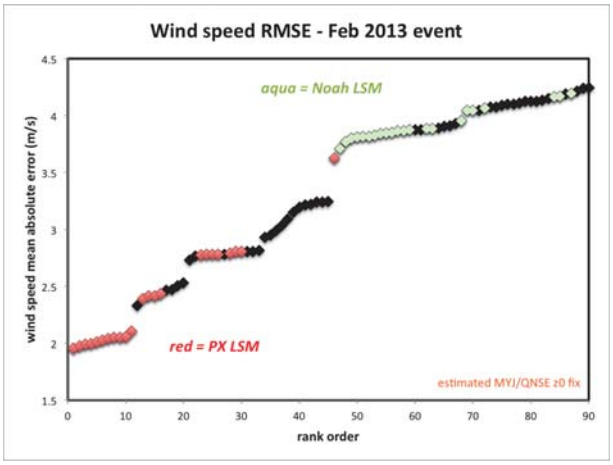

FIG. 7. Physics ensemble sustained wind speed mean absolute error (m s^{-1}), validated against SDGE network, in rank order. Red and aqua colors indicate PX and Noah LSM members, respectively. For members using the MYJ scheme, a standard but cosmetic recalculation of the near-surface winds was overridden.

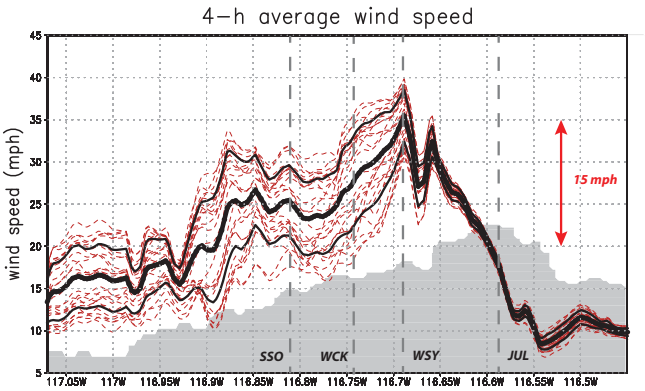

FIG. 8. Physics ensemble 4-hour average winds (mph) adjusted to SDGE anemometer height and centered on the WSY gust's first peak time (1800 UTC 15 February). Black lines are the ensemble mean, and ±1 standard deviations. Also shown is the underlying terrain (shaded).

those categories improved their MAE and bias scores (not shown).

It is intuitive that increasing the surface roughness should slow down the winds. However, it also changes the nature of the downsloping flow, at least in this case. One of the remarkable characteristics of the 14-16 February event, especially its first phase, was the development of the jump-like feature and wind reversal above WCK. It has emerged that only the LSMs that employed relatively larger z_0 values were able to capture this feature, which the observations indicate was prominent and persistent. The smoother the terrains lee side, the faster and more uniform the flow that developed there was, preventing the WCK jump from forming and resulting in faster than observed winds farther down the slope.

Figure 8 presents four-hour average winds from about 40 of the physics ensemble members, centered on the time of WSYs first peak and WCKs first wind reversals. The winds have been adjusted to SDGE anemometer height using the logarithmic wind profile, which is a function of z_0, stability, and the diagnosed 10 m wind. Note the variation among the ensemble members was quite small upwind of, and past, the ridge, until the flow passed the narrow canyon just upslope from WSY. From that point downslope, the variation has become quite substantial, in the very region where the need for skillful forecasts is crucial. As suggested by the figure, few of the physics ensemble members have reconstructed weak winds for the Witch Creek area, although a local minimum is indicated between WCK and SSO.

We have found that wind speed MAEs and positive biases were reduced by adopting the MODIS landuse database instead of the WRF default USGS dataset. Although these databases categorize the landscape somewhat differently, the MODIS version narrows a zone of high roughness ($z_0 \approx 0.5$ m) near the ridge but also generally increases the drag across the west-facing slope, including placing a locally rough area ($z_0 \approx 0.24$ m) just upslope from WCK (not shown). In contrast, the USGS surface roughness during winter in this area is only 0.01 m, with no variation at all in the vicinity of WCK. The PX LSM increases these MODIS values further almost everywhere, with WCK area roughnesses being as large as 0.75 m, 7500% larger than the USGS specification. It is surmised that increasing the surface drag played a major role in the ability of the PX ensemble members to create the Witch Creek jump.

That being said, it has also emerged that the wind reconstructions for this case possessed a tremendous amount of inherent uncertainty as well. This was demonstrated by introducing random noise into the simulations using the stochastic kinetic energy backscatter scheme (SKEBS) in WRF (Shutts 2005). This scheme inserts its perturbations where and when turbulence is diagnosed, which is substantial on the downslope side, especially at and below WSY. We examined two perturbation ensembles, using WRF version 3.5, the large 667 m resolution domain, and the MODIS database. The first ensemble employed the popular Noah/YSU physics combination, while the second adopted the PX/ACM2 physics combination, which was judged as the best one among the physics ensemble.

Figure 9 shows the 4-hour averaged anemometer-level winds around the occurrence of the first wind peak at WSY for the Noah/YSU random perturbation ensemble, for comparison with Fig. 8. Note the structure of the winds across the upper part of the terrain is now different; this reflects the adoption of the MODIS roughnesses. Again, the spread increased at and past WSY, and now uncertainty was largest near WCK, with winds spanning 7-38 mph. Vertical cross-sections (not shown) reveal that some of the members still did not produce jumps over WCK, while many others did, although obviously with a variety of positions relative to the station (Fig. 9).

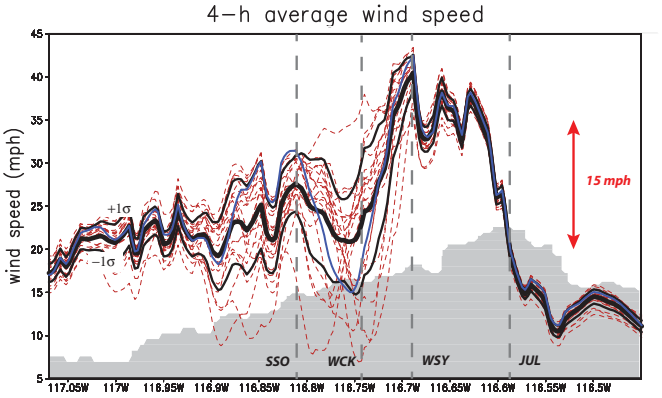

FIG. 9. As in Fig. 8, but for the Noah/YSU MODIS-based perturbation ensemble.

The magnitude of the perturbation ensembles variability is remarkable, as it exceeds that seen in the physics ensemble. It is speculated that the generally rougher surface assumed by the MODIS database is important to enhancing this sensitivity. Increasing the roughness further, however, appears to start dampening the sensitivity, which appears sensible. The PX/ACM2 physics combination (Fig. 10) produced slower and less variable winds overall, with a greater likelihood of positioning the jump over WCK. Again, revising z_0 values in Noah/YSU simulations tended to make the flow patterns and speeds more like those produced by PX/ACM2 (not shown).

6. Gust estimation

Short period (3-sec) gusts cause severe damage, yet mesoscale models are not able to directly simulate them. The winds generated by the model should be compared to sustained winds, as even with the small time steps associated with the high-resolution simulations fail to capture high-frequency variability associated with turbulence. A variety of techniques, ranging from simple and sophisticated, can be employed to diagnose the gusts from the model (e.g., Fovell 2012), one of these involving

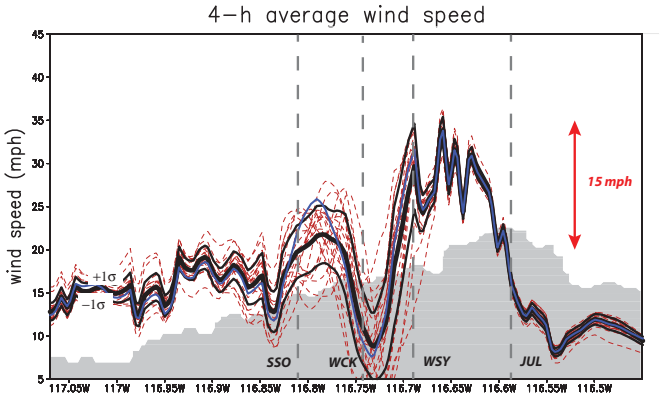

FIG. 10. As in Fig. 8, but for the PX/ACM2 MODIS-based perturbation ensemble.

the application of a gust factor (GF) to the models diagnosed winds (after sensor height adjustment). This is not a particularly rewarding strategy when a gridded output field is needed, as the GF will vary from place to place, reflecting locational characteristics, and is also generally dependent on the magnitude of the sustained wind.

The literature suggests that a typical GF for a well-exposed site in flat terrain is about 1.4-1.5, although this depends on atmospheric stability, the sustained wind speed, surface roughness, observation height, and averaging interval for the sustained wind as well as the sampling interval for the gust (e.g., Durst 1960; Wieringa 1973; Schroeder et al. 2002). As an example, Fig. 11 displays the distribution of GF with sustained wind for SDGE station SIL calculated from 38600 observations recorded during 2012 and 2013. We see that as the 10-min average wind gets stronger, the GFs magnitude and range both decrease, to roughly 1.25 for the very fastest observations. This hints the commonly used typical GF value of 1.4 may be not generally appropriate. Certainly, some polynomial function could be fitted to these data, providing some insight into the gust strengths that might be expected given a particular model-predicted sustained wind. However, the 91 mph gust mentioned in Sec. 3 that occurred with the sustained wind was only 45 mph (20 m s^{-1}), so such a function would have seriously underpredicted that very fast wind sample.

There are a variety of techniques for relating observed near-surface gusts to some function of the resolved flow speeds in the boundary layer (e.g., Brasseur 2001). Thus far, we have found a fair amount of success using the simulations wind speed at the first model level alone (approximately 26 m AGL) to represent the gust, at least when the PX and ACM2 schemes are used with their

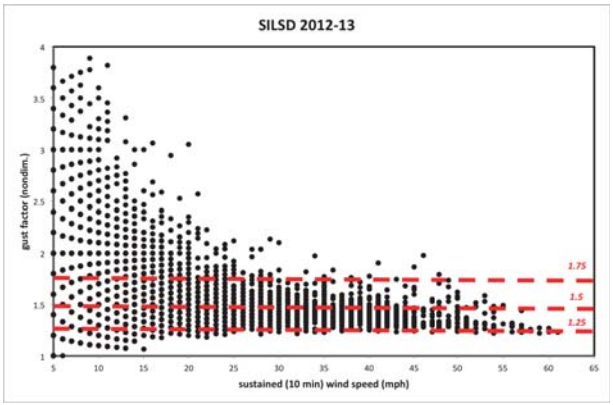

FIG. 11. Gust factors (nondimensional) calculated from 38600 observations for the SDGE station at Sill Hill (SIL) for observations collected during parts of 2012 and 2013, plotted against the sustained 10 minute wind speed (mph).

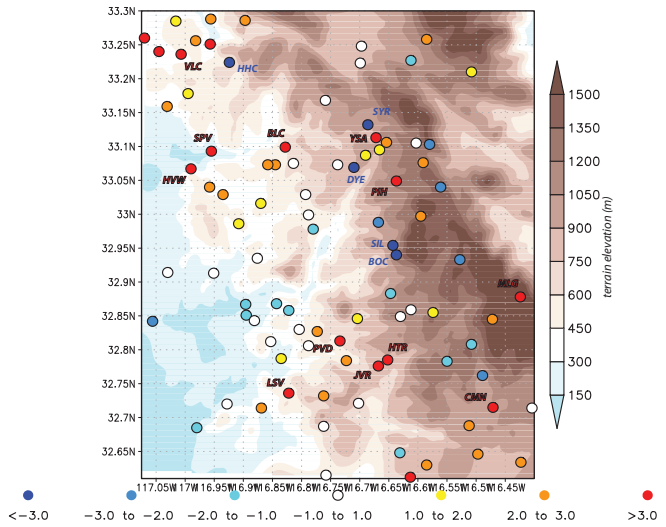

FIG. 12. Average event gust bias (m s^{-1}) map for the 14-16 February 2013 event for the gust proxy using the first model level simulated wind. Warm colors denote stations with overpredicted gusts, while cold colors indicate underpredicted locations, with underlying topography shaded.

revised MODIS roughnesses. Our validations are limited to 95 SDGE stations in the 667 m domain, comparing the 26 m simulated wind on the hour to the fastest 6 m wind gust reported during the previous hour.

Figure 12 shows the average event bias map for this wind gust proxy over the February 2013 Santa Ana event. Clearly, some stations are systematically over- or underpredicted, reflecting terrain variations that are subgrid, even at this relatively high resolution. Overforecasted station YSA is sited very close to a sharply rising hill, and thus probably in a very localized wind shadow. Station SYR, just 2.5 km away, is sited a little farther away from this same north-south terrain feature, and its winds were substantially underforecasted. PIH resides downslope of perhaps the thickest canopy of trees remaining in the San Diego backcountry, bringing roughness values and logarithmic wind profile applicability into question, while MLG, near the ridge, is known to have been improperly sited immediately behind trees. The model gusts at SIL were consistently stronger than the simulated winds anywhere in the boundary layer; both SIL and DYE have small-scale terrain features that may be helping locally amplify the flow. As a consequence of this, multiple techniques for gust forecasts are being considered. There is no "one size fits all" method, indicating a demand for an ensemble approach for gust predictions.

A major goal of this work is to produce a wind map of San Diego county, to determine how fast the wind has been at various places using model simulations of the past, calibrated against modern observations. A preliminary example that was developed from 41 high wind past events is shown in Fig. 13. Ultimately, to determine the wind threat, we also need to investigate the sensitivity of the Santa Ana winds to potential, near-term climate change. This represents future work.

7. Summary

We have closely examined the 14-16 February 2013 Santa Ana event, which was characterized by a moderately intense downslope windstorm in the Laguna mountains of San Diego county. The unprecedented, dense SDGE mesonet is enabling enhanced insights into the terrain-amplified wind events. We have shown that the windstorm flow speeds and patterns were sensitive to model configuration, especially the land surface schemes and landuse database, which determine the surface roughness that modulates the strength of the downslope flow at the surface. Sensitivity to random noise was also substantial. The models 26 m sustained wind showed promise for forecasting gusts recorded at anemometer-level, at least for certain model configurations and during downslope windstorms. In addition to implementing an operational gust forecasting capability, we also intend to produce a wind map for San Diego, providing guidance on maximum potential winds and recurrence intervals.

Acknowledgments.

This research was sponsored by San Diego Gas and Electric company.

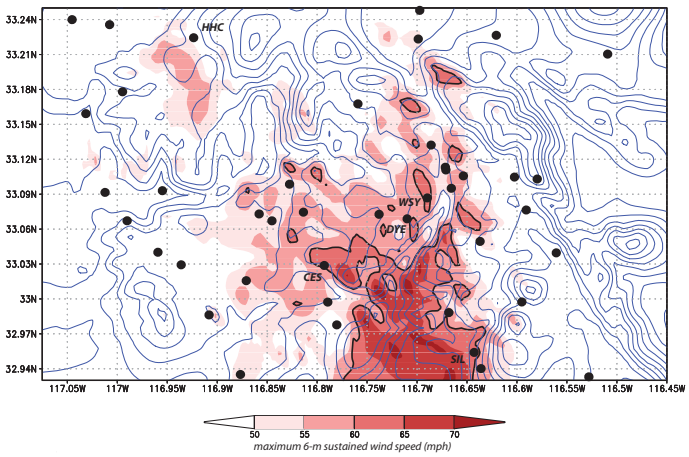

FIG. 13. Preliminary maximum wind map over the Witch area, representing a composite of high wind events over a 60-year period. Maximum 6-m wind speeds (mph) are shaded, with superposed topography contoured. Some SDGE station locations are indicated.

REFERENCES

Brasseur, G., 2001: Development and application of a physical approach to estimating wind gusts. *MWR*, **129**, 5–25.

Chang, C.-H. and F. P. Schoenberg, 2011: Testing separability in marked multidimensional point processes with covariates. *Ann. Inst. Stat. Math.*, **63**, 1103–1122.

Chow, F. K., S. F. D. Wekker, and B. J. Snyder, 2012: *Mountain Weather Research and Forecasting: Recent Progress and Current Challenges*. Springer, 750 pp.

Doyle, J. D. and D. R. Durran, 2007: Rotor and subrotor dynamics in the lee of three-dimensional terrain. *J. Atmos. Sci.*, **64**, 4202–4221.

Durst, C. S., 1960: Wind speeds over short periods of time. *Meteor. Mag.*, **89**, 181–186.

Fovell, R. G., 2012: Downslope windstorms of San Diego county: Sensitivity to resolution and model physics. *13th WRF Users Workshop*, Boulder, CO, Nat. Center for Atmos. Res.

Glickman, T., 2000: *Glossary of Meteorology*. Amer. Meteor. Soc., 855 pp.

Raphael, M. N., 2003: The Santa Ana Winds of California. *Earth Interact.*, **7**, 1–13.

Schamp, H., 1964: *Die Winde der Erde und ihre Namen*. Franz Steiner Verlag, 94 pp.

Schroeder, J. L., M. R. Conder, and J. R. Howard, 2002: Additional Insights into Hurricane Gust Factors. *25th Conf. on Hurricanes and Tropical Meteorology*, San Diego, CA, Amer. Meteor. Soc., 39–40.

Shutts, G., 2005: A kinetic energy backscatter algorithm for use in ensemble prediction systems. *Quart. J. Roy. Meteor. Soc.*, **131**, 3079–3102.

Wieringa, J., 1973: Gust factors over open water and built-up country. *Boundary Layer Meteor.*, **3**, 424–441.

Appendix 3

5A.2 Wind and Gust Forecasting in Complex Terrain

Robert G. Fovell and Yang Cao

Department of Atmospheric and Oceanic Sciences, University of California, Los Angeles

ABSTRACT

The mid-May 2014 Santa Ana event is investigated to evaluate the ability of high-resolution WRF-ARW simulations in predicting winds and gusts in complex terrain. Model reconstructions of sustained wind are calibrated and validated against the exceptionally dense and homogeneous SDGE mesonet in San Diego county. A large model physics ensemble reveals the land surface model to be most crucial in skillful wind predictions, which are particularly sensitive to the surface roughness length. A surprisingly simple gust parameterization is proposed for the San Diego network, based on the discovery that this homogeneous mesonet has a nearly invariant network-averaged gust factor.

1. Introduction

The "Santa Ana" winds of Southern California are a very dry, sometimes hot, offshore wind (Glickman 2000; Fovell 2012; Cao and Fovell 2013) that can produce wind gusts exceeding 100 mph (45 m s^{-1}) in favored areas[1]. Events are associated with the partial damming of a cool or cold Great Basin air mass by the mountains that separate Southern Calfiornia from the inland deserts. In the San Diego area, the Santa Anas possess characteristics of downslope windstorms (Fovell 2012; Cao and Fovell 2013). Santa Ana season is typically thought of as extending from September to April (Raphael 2003), but the last two years (2013 and 2014) have seen events of significant strength during the month of May.

Fire danger is elevated during Santa Ana events, owing to the combination of low-to-very low humidity and strong winds that can spark and spread flames. Owing to this danger, accurate forecasts of winds and gusts are crucial. We have previously shown that simulations of downsloping winds in the San Diego mountains are sensitive to model physics and even the introduction of random noise (Cao and Fovell 2013). Furthermore, weather prediction models such as WRF [the Weather Research and Forecasting model; Skamarock and co authors (2007)] that are designed for use on regional scales cannot capture wind gusts, which produce much of the damage.

In this paper, we examine the skill of the WRF model's Advanced Research WRF (ARW) core in forecasting Santa Ana winds in San Diego county. Model forecasts are validated against sustained wind observations reported by the San Diego Gas and Electric (SDGE) mesonet, a network of more than 140 stations cited primarily in well-exposed, wind-prone areas on the west-facing slopes of the county's mountains. This research has involved large model physics, landuse database, and perturbation ensembles, as described in Cao and Fovell (2013). Although several events of varying strengths have been examined, we will mainly focus on the recent event of mid-May 2014 as an illustrative example. A surprisingly simple gust parameterization is proposed, that is perhaps applicable solely to this homogeneous and exceptionally dense mesonet.

[1]Examples: On 21 October 2007, the weather station on Laguna Peak, overlooking Pt. Mugu, recorded a 111.5 mph (50 m s^{-1}) wind gust. More recently, on 30 April 2014, the Sill Hill station in San Diego reported a 101 mph (45 m s^{-1}) gust, and remained above 90 mph for a total of five nonconsecutive hours.

2. Data and methods

a. *Available observations*

Validating a numerical simulation against available observations is not as straightforward as it might appear. Historically, the surface wind observation network has possessed low station density, especially relative to the expected spatial variation of winds owing to topography in places such as San Diego county. Furthermore, observational networks vary with respect to sensor hardware, mounting height, intervals employed for sampling, averaging and reporting, and station siting philosophies, all of which can dramatically impact the magnitudes of winds and gusts that are reported. The unfortunate fact is that the anemometers at many stations are improperly shielded by buildings and/or trees, or simply were not installed in the areas of greatest wind and/or hazard.

In pointed contrast, the mesonet installed by the San Diego Gas and Electric (SDGE) placed stations in

well-exposed areas that are known to be windy (Fig. 1). The network currently consists of over 140 stations and is homogeneous with respect to hardware employed, mounting height, and data collection and reporting. The stations adhere to the RAWS (Remote Automated Weather Station) standard with respect to anemometer height (6.1 m or 20 ft AGL) and averaging interval for the sustained wind (10 min). Every 10 min, SDGE stations report sustained winds as well as maximum gusts based on 3-sec samples; this contrasts with the RAWS networks hourly reporting interval.

b. Model experimental design

All simulations in this report employed recent versions of WRF-ARW, using telescoping nests to 667 m horizontal resolution. The 667 m domain covers about two-thirds of the SDGE mesonet, and its parent 2 km grid encompasses the entire network. The physics ensemble mainly focuses on the role of land surface models (LSMs) and planetary boundary layer (PBL) schemes on forecast skill; see Cao and Fovell (2013) for more information. Simulations of the 13-15 May 2014 Santa Ana wind event used version 3.5 and were initialized with the 12 km North American Mesoscale (NAM) model gridded analysis and forecasts for initial and boundary conditions, respectively. For simplicity, only the MODIS landuse database is considered herein.

c. Validation strategy

The SDGE wind data were employed to validate model output available at hourly intervals. SDGE mesonet data were obtained at full temporal resolution (10 min intervals) from the MADIS (Meteorological Assimilation Data Ingest System) archive. We elected to replace observed winds and gusts on the hour with the largest values of each reported in the previous 50 min. However, this was found to have relatively little impact on the results and conclusions.

The WRF model reports a 10 m wind diagnostic that requires adjusting prior to validation against the SDGE network's 6.1 m wind observations, lest an entirely artificial high wind bias would very likely be found. Adjustments were made during post-processing, utilizing the logarithmic wind profile assumption,

$$V_{6.1} = V_{10} \frac{\ln \frac{6.1}{z_0} - \psi_{6.1}}{\ln \frac{10}{z_0} - \psi_{10}}, \qquad (1)$$

where $V_{6.1}$ and V_{10} are the winds at 6.1 and 10 m, respectively, z_0 is the surface roughness length, and $\psi_{6.1}$ and ψ_{10} represent stability correction functions that vanish when the surface layer is neutrally stratified. The latter is often presumed true when wind speeds exceed about 5 m s^{-1} or so (e.g., Wieringa 1976; Verkaik 2000), which does appear valid among our model simulations.

Although somewhat dependent on the LSM and landuse database (e.g., USGS vs. MODIS) employed, we have found network-averaged z_0 to vary between 0.16 and 0.27 m, which result in adjustments to the 10 m wind of about 14%. It is noted that Eq. (1) could have been written with a zero-plane displacement modification of the anemometer heights, which is sometimes used in areas with significant obstacles. We neglect this adjustment because of the siting characteristics of the SDGE mesonet.

We will show that most model physics configurations generate a high wind bias relative to the observed sustained winds, even after anemometer height adjustment. The worst offenders were ostensibly those employing the MYJ PBL scheme. However, we discovered the MYJ code recomputed the LSM's 10 m wind values, specifying smaller roughness length than employed in the model calculations. This purely cosmetic adjustment (shared by the QNSE PBL scheme) exacerbated the high wind bias, and removing the code made physics ensemble members employing the MYJ scheme much more competitive.

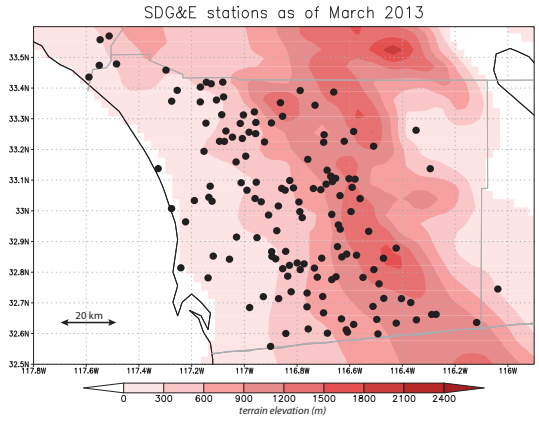

FIG. 1. SDGE surface station locations (black dots), with underlying topography shaded. Stations in place as of March 2013.

3. The 13-15 May 2014 Santa Ana wind event

In mid-May, 2014, a major Santa Ana wind event sparked several fires in the Rancho Bernardo, Oceanside and Camp Pendleton areas. The first fire to ignite was the Bernardo fire, which occurred as strong winds and gusts pushed to the coastline (Fig. 2). We will contrast simulations of this event using the Pleim-Xiu (PX) LSM coupled with the ACM2 PBL scheme (shown in Fig. 2) against runs using the Noah LSM and YSU PBL options. The latter likely represents the most commonly adopted configuration employed with WRF-ARW, while the former has proven to validate well against SDGE wind

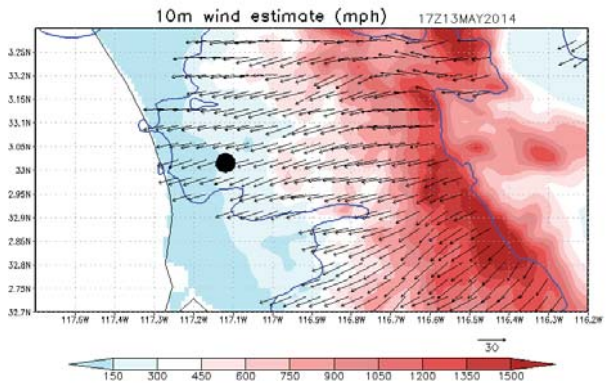

FIG. 2. Model predicted sustained winds at 10 m above ground level, valid at 1700 UTC 13 May 2014, around the initiation time of the Bernardo fire, from a simulation made with the PX LSM and ACM2 PBL schemes. Blue contour represents 20 mph wind speed and red shading is topography. Grid points with speeds < 20 mph are not shown, and vectors have been thinned for clarity. Fire ignition location indicated by large black dot.

observations. As an example, Figure 3 shows results from the physics ensemble of an earlier event, revealing the expected positive correlation between mean absolute error (MAE) and bias for height-adjusted sustained winds. The PX/ACM2 member had one of the smallest event-averaged MAEs for that event, along with an only slightly negative bias, in contrast with YSU/Noah, which was the worst-performing ensemble member overall.

Simulations for the 13-15 May event spanned 55 h, initialized at 0600 UTC on 13 May 2014. Network-averaged wind from the PX/ACM2 and YSU/Noah simulations (Fig. 4) show the former had greater overall agreement with the observations for this event as well. Still, some stations were systematically over- or underpredicted, as illustrated in Fig. 5, although the mean network bias was very small (0.18 m s^{-1}). Clearly, more stations were overpredicted in the YSU/Noah simulation (Fig. 6), which had a mean network bias of 1.63 m s^{-1}.

The region around Santa Ysabel has a particularly large number of stations, a total of 14 in a roughly 15 km by 10 km area. Even for the PX/ACM2 member, wind bias varied enormously (Fig. 7). There was no mean bias at WSYSD (Fig. 8) over the 55 h event, while at IJPSD (Fig. 9) and YSASD (Fig. 10), residing about 3 km from WSYSD, winds were somewhat underpredicted and very overpredicted, respectively. The YSU/Noah member's general high wind bias exacerbated the overprediction at YSASD and also had a positive bias for WSYSD (Fig. 6). We tested whether WRF-ARW's "topo_wind" option, which presently only works with the YSU PBL, would help to mitigate the YSU/Noah member's high wind bias. However, we found that both versions available in WRF v.3.5 reduced the network-averaged winds by about 50% (Fig. 11), resulting in a systematic low wind bias, not only as a function of time (Fig. 12), but also for most stations (not shown).

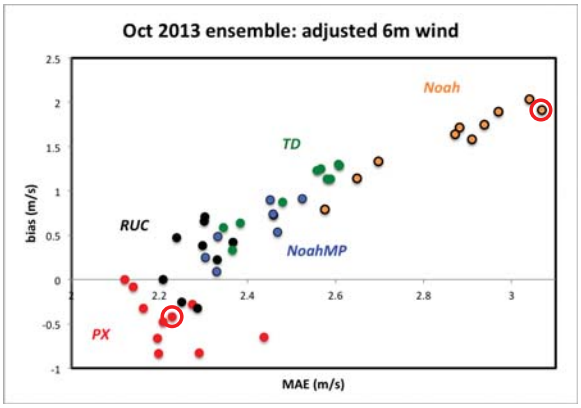

FIG. 3. Mean absolute error (MAE) vs. bias (both m s^{-1}) from an October 2013 event's physics ensemble incorporating 5 LSMs and 10 PBL schemes. Points represent event-averaged values, and are color-coded by LSM, with the PX/ACM2 and YSU/Noah members highlighted.

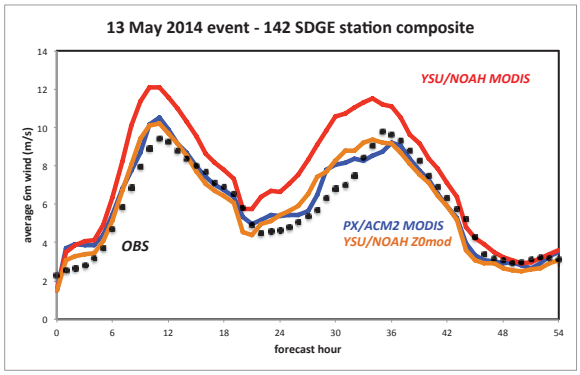

FIG. 4. Time series of SDGE network-averaged sustained wind (m s^{-1}) observations (black dots), for comparison with predictions from the PX/ACM2 and YSU/Noah, along with a YSU/Noah run employing roughness lengths mimicking those employed by PX (YSU/Noah/Z0mod). All three simulations used the MODIS landuse database.

4. Improving wind reconstructions for the 13-15 May 2014 event

The ensembles for various Santa Ana wind events has revealed that the single most important physics option

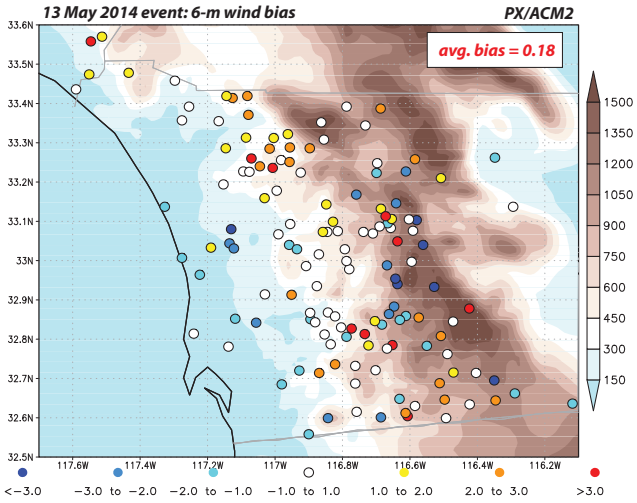

FIG. 5. Spatial distribution of event mean sustained wind bias for SDGE stations for the PX/ACM2 simulation, using the MODIS landuse database. Deep red and blue colors indicate the model overestimates and underestimates the event-averaged 6m wind by 3 m s^{-1}. Brown shading indicates model topography.

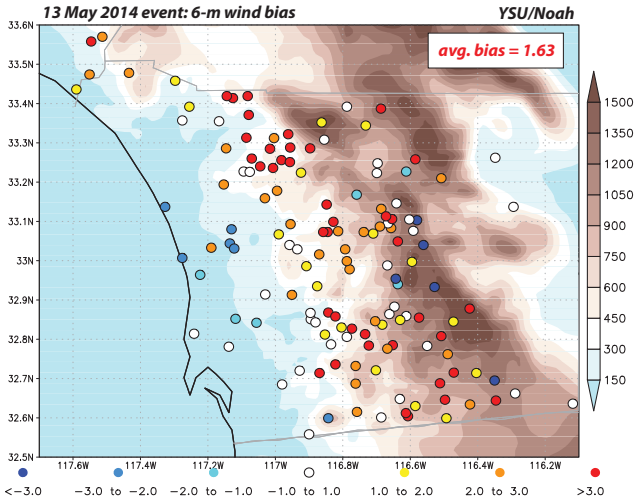

FIG. 6. As in Fig. 5, but for the Noah/YSU simulation, using the MODIS landuse database.

controlling the quality of the mean wind reconstruction is the LSM (Fovell 2012; Cao and Fovell 2013). Analysis has indicated that LSMs differ most with respect to how they handle the roughness of the surface. Table 1 lists the relative fraction of various landuse categories occurring in the 2 km nest that encompasses the SDGE network, along with tabled values of z_0 (from `LANDUSE.TBL` and/or `VEGPARM.TBL`) employed in "summer" simulations (applicable to the present Santa Ana case) and roughness values as assigned in `module_sf_pxlsm_data.F`. Two-thirds of the 2 km nest's land areas are shrublands, which are presumed rougher in the PX LSM than in the MODIS default. Although LSMs like Noah subsequently modify these tabled values, it remains this scheme employed lower roughnesses for many of the categories occurring in the SDGE network.

The importance of z_0 in an LSM is demonstrated by modifying the Noah scheme to mimic PX. This simulation, dubbed "YSU/Noah/Z0mod", yielded a much more faithful reconstruction of the network-averaged wind (Fig. 4) as well as a much lower mean bias of 0.07 m s^{-1} (Fig. 13). The correlation between PX/ACM2 and YSU/Noah Z0mod is very high but not perfect, in part because the PBL scheme does influence the results, and also because the PX and Noah LSMs handle fractional landuse differently. However, using PX-inspired roughness values in Noah clearly resulted in superior wind

TABLE 1. Default roughness lengths employed by surface schemes for MODIS landuse categories occurring in the SDGE network for summer season simulations. Water areas of the 2 km nest excluded.

Landuse index	Fraction (%) of network	PX z_0	Tabled z_0	Type
1	5.9	1	0.5	Evergreen needleleaf
2	0.2	0.9	0.5	Evergreen broadleaf
5	6.0	1	0.5	Mixed forests
6	11.8	0.15	0.05	Closed scrublands
7	54.4	0.15	0.06	Open shrublands
8	0.2	0.25	0.05	Woody savannas
9	0.3	0.15	0.15	Savannas
10	2.3	0.07	0.12	Grasslands
11	0.1	0.2	0.3	Permanent wetlands
12	0.4	0.1	0.15	Croplands
13	11.2	0.8	0.8	Urban
16	7.3	0.05	0.01	Barren/sparse

performance and a very small network-averaged bias.

We are compelled to consider z_0 as a tunable parameter, and feel that the high quality, density and homogeneity of the SDGE network will permit us to improve the land representation in the WRF simulations for this area. However, it is not clear that fine-scale adjustments of the roughness length will be all that useful. The reason is that the remaining wind bias is moderately anti-correlated (R^2 = 0.40) with the event mean wind, with positive biases at stations with relatively weaker winds and negative ones at windier locations (Fig. 14), while the correlation of bias with z_0 is nearly zero (R^2 = 0.14, not shown). In the next section, we offer an explanation for this trend in the bias, and argue that a fair fraction of the remaining wind bias may be "unfixable" (apart from bias correction).

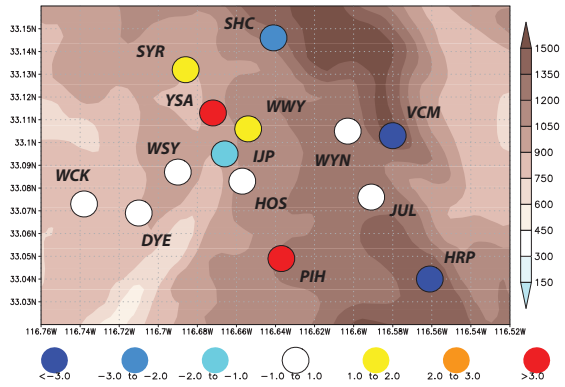

FIG. 7. As in Fig. 5, but zoomed into the region around Santa Ysabel (YSA). Labels indicate names of SDGE stations, with "SD" suffix omitted.

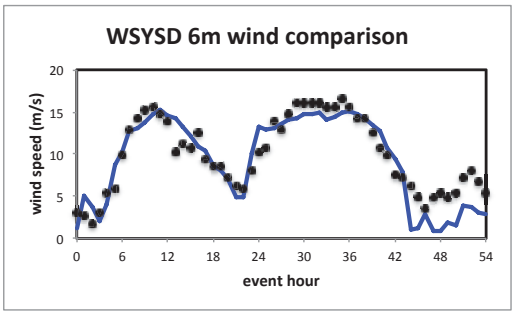

FIG. 8. Time series of observed (black dots) and predicted (blue curve) 6 m sustained winds (m s^{-1}) at WSYSD (see Fig. 7) , from the PX/ACM2 simulation.

5. Further analysis

The *gust factor*, or GF, is the ratio of the gust and the sustained wind. GF should be a function of sampling interval, anemometer hardware and mounting height, anemometer exposure, and perhaps surface roughness as well (Ashcroft 1994). It may also be a function of the sustained wind itself, and vary among stations, and perhaps from event to event.

Averaged over the entire SDGE network, however, we have found the GF to be nearly constant, with a value of nearly 1.7 and virtually no dispersion (Fig. 15). There were 330 observation times between 0510 UTC on 13 May to 1200 UTC on the 15th, at 10-min intervals. For each time, the sustained wind and gust observations were averaged over the 142 station network, and the results are shown in the figure. The R^2 of the fit is 0.997. Although GFs do vary with station, sustained wind speed, and time, *the network-averaged GF can be represented by a single number*, independent of the magnitude of the network-averaged wind.

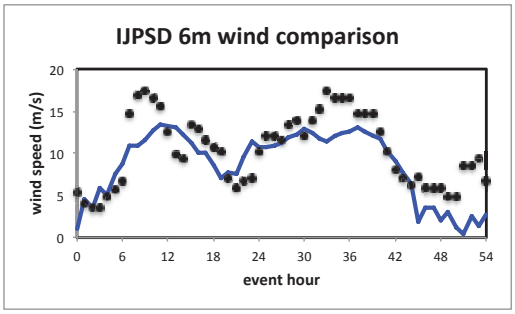

FIG. 9. As in Fig. 8, but for the station at IJPSD.

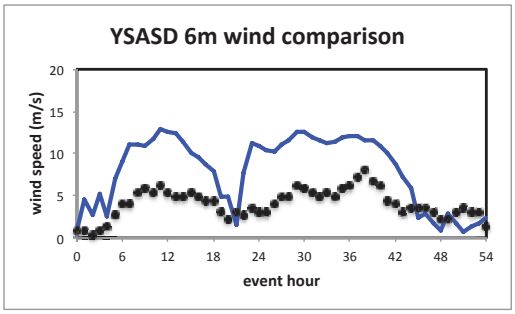

FIG. 10. As in Fig. 8, but for the station at YSASD.

This surprising result is not confined to Santa Ana wind events. Figure 16 presents a composite of 10-min observations over three months, representing summer (June 2013), autumn (October 2013) and winter (February 2014) examples[2]. Santa Ana events did occur during the latter two months, but represent a small fraction of the 12324 observations plotted. This result is not entirely understood, but we will take the SDGE network-averaged GF as 1.7, and refer to it as "G".

The reality is that GFs should and will vary among stations, and it is important to understand why. At any given site, the mean GF tends to decrease (if only very weakly) with increasing sustained wind speed (e.g., Cao and Fovell 2013). Over the SDGE network, GF has a more robust negative association with event-averaged wind (Fig. 17). However, given that the *overall* (network-averaged) gust factor G is nearly insensitive to factors such as offshore vs. onshore winds, day vs. night, cloudy vs. sunny, etc., we hypothesize that stations having individual GFs that vary significantly from the network average may, at least in part, represent the influence of very localized factors. Furthermore, to the degree that these localized factors

[2]For February 2014, observations from two thunderstorm days were removed, as they clearly deviated from the remaining observations. The fact that thunderstorm gusts might have a substantially different character is anticipated from Wieringa (1973).

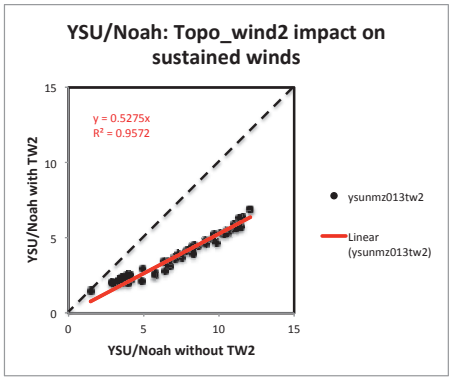

FIG. 11. Scatterplot of hourly network-averaged sustained winds for YSU/Noah simulations before and after application of the topo_wind = 2 option (TW2) .

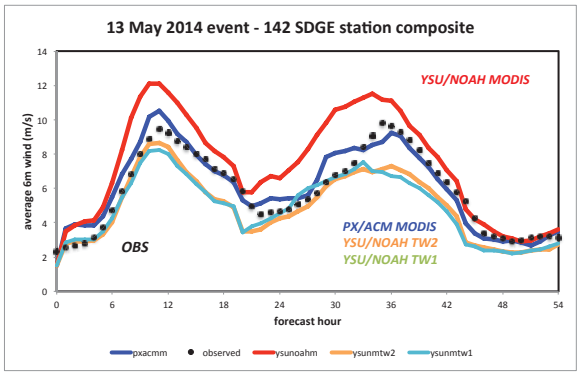

FIG. 12. As in Fig. 4, but adding YSU/Noah simulations made with topo_wind = 1 and 2 (TW1 and TW2), with the MODIS landuse database.

are unresolvable, even on a very high resolution grid, we may find that even a model that is properly configured overall will be more likely to have systematic biases at these stations.

Thus, other factors being equal, *we anticipate overpredicting the sustained wind at stations with GF > G, while underpredicting winds at stations with GF < G*, for the reasons demonstrated in Fig. 18. Figure 18a illustrates the standard case. The wind profile is described by the log wind profile (1), being calm at height z = z_0. A parcel possessing faster horizontal velocity is transported downward, and manifested at anemometer level as a gust (U_{max}) exceeding the sustained wind ($\bar{U}$). If gust factor for this station is comparable to the network average, we anticipate that a properly configured model will be able to represent the winds at this location without significant bias.

Despite best efforts regarding siting, however, some stations will experience at least very localized obstructions.

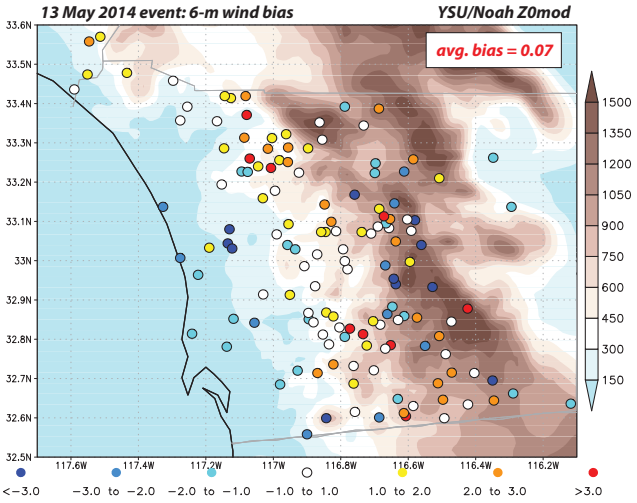

FIG. 13. As in Fig. 5, but for the Noah/YSU Z0mod simulation, using modified roughness values inspired by the PX LSM.

For example, anemometers might have to be installed relatively close to landforms that might partially shield them, or be placed in an area with denser and/or taller vegetation than is representative of the grid cell in which it is found. In those cases, we anticipate that the sustained wind is slowed more than would be expected given the z_0 value employed for the grid cell. However, a parcel from farther aloft has less time to be influenced by the obstructions, and thus would appear stronger relative to $\bar{U}$, resulting in a larger station GF, as illustrated in Fig. 18b. If these obstructions cannot be resolved on the model grid, or represented by the grid's z_0, we anticipate overpredicting the wind at these stations.

Alternatively, some stations may be located with areas with landforms that serve to further accelerate the wind, including flow through favorably-oriented canyons, near steep ravines, or over small hills. These may serve to enhance the sustained wind at anemometer level, such that a descending parcel has a relatively smaller speed advantage over the mean flow there, resulting in GF < G (Fig. 18c). If those features are unresolvable, we hypothesize that we will underpredict the wind there.

The hypothesis is tested in Fig. 19, which presents station gust factor for the 13-15 May 2014 event plotted against event-averaged bias from the YSU/Noah simulation with PX-inspired roughness lengths. For each station, the GF from an intercept-suppressed least squares fit was determined. The largest value (3.15) was for station MLGSD near Mt. Laguna, which is known to be directly impacted by trees (S. Vanderburg and B. D'Agostino,

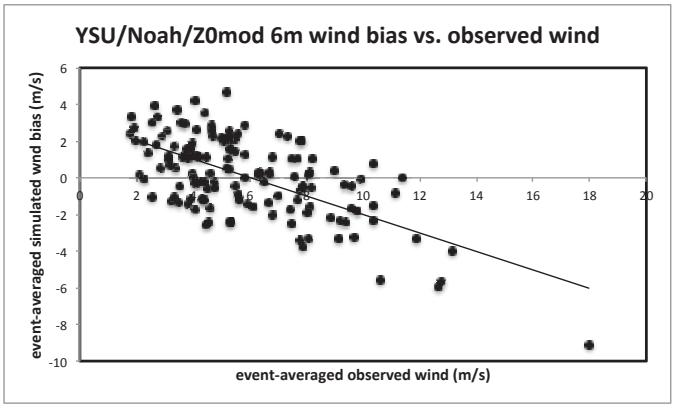

FIG. 14. Scatterplot of event-mean observed wind vs. mean bias in the YSU/Noah/Z0mod simulation for SDGE stations. A least-squares fit is shown for reference.

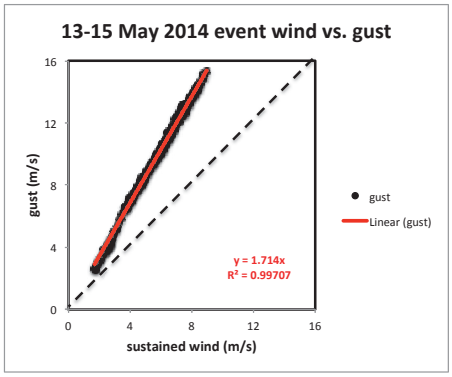

FIG. 15. Scatterplot of network-averaged sustained wind vs. gust for the 13-15 May 2014 Santa Ana wind event. 330 observation times are plotted, each representing a 142-station average. The intercept-suppressed least squares fit is also shown, with slope 1.714 and $R^2 = 0.997$.

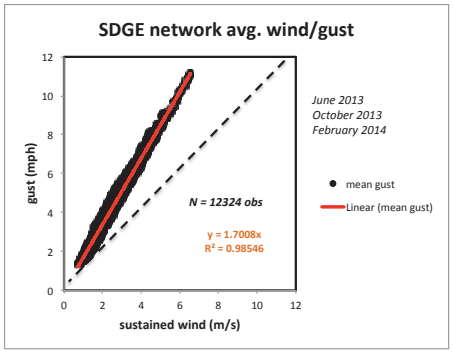

FIG. 16. As in Fig. 14, but for three non-consecutive months, June and October of 2013, and February of 2014, representing 12324 total observation times. Two thunderstorm days in late February were excluded.

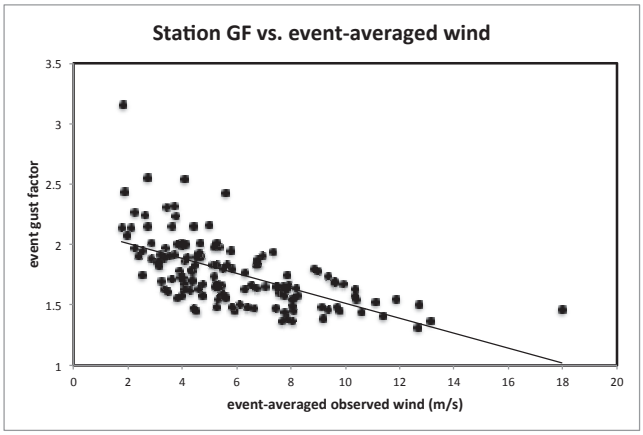

FIG. 17. Scatterplot of GF vs. event-averaged wind from the 13-15 May 2014 Santa Ana case, for the 142 SDGE stations. The least squares line is shown for reference only. The linear association is $R^2 = 0.37$.

personal communication) and routinely overpredicted in our simulations. The smallest value (1.31) was for VCMSD, a station in the Santa Ysabel area (Fig. 7) that is substantially underpredicted in nearly all WRF model reconstructions. The station-averaged GF for this event was 1.77, which is fairly close to G. Curiously, we have found that station GF and assigned z_0 to be very nearly uncorrelated.

If our hypothesis is correct, the network stations should preferentially cluster into the lower left and upper right quadrants. For the YSU/Noah/Z0mod simulation, 76% of the stations do fall into those quadrants (52 underpredicted with GF < G and 56 overpredicted having GF > G), and many of the remainder do not stray far into the other two quadrants. Very similar results hold for the PX/ACM2 reconstruction (not shown). That said, stations falling well into the other two quadrants are likely candidates for closer examination, either of the surface landuse category or roughness length assigned to them, or for station siting and/or quality factors. Still, the figure indicates there are probably too few of those to matter in a network of this size. For the correctly assigned stations, we feel that the simulation bias largely represents *uncorrectable error* that must be handled subsequently via bias correction (or possibly further resolution enhancement).

6. A very simple gust parameterization for the SDGE network

Owing to the preceding, we suggest a very simple gust parameterization for use by properly configured model

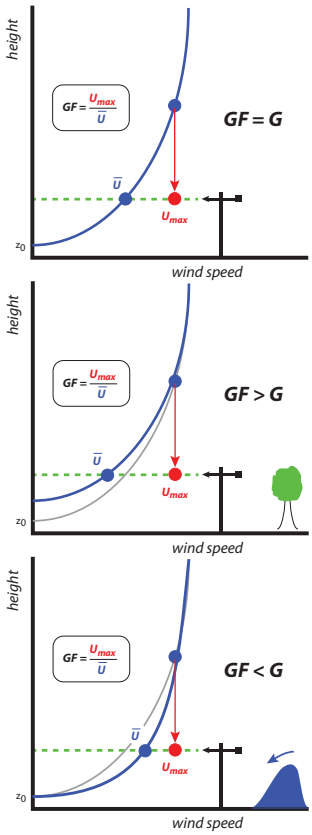

FIG. 18. Illustration of wind bias concept, based on station GF relative to network average G: (a) standard case; (b) obstructed case; (c) enhanced case.

simulations of winds in the SDGE mesonet. It seems most reasonable to apply a GF of about 1.7 to all stations, i.e., equal to G, at all times (except possibly during thunderstorms, which are rare in Southern California). When sustained winds are lighter, larger GFs are probably appropriate, but the threat from weak gusts is not very substantial. Figure 20 shows how well this simple gust scheme reproduces the event-averaged wind gusts observed at the 142 SDGE stations.

It is clear that the employment of a constant GF works to remove the dependence of wind forecast bias on sustained wind speed (see Fig. 14). To a large degree, stations with GF > G tend to be overpredicted already, so using a smaller GF value than justified from the observational record works to mitigate the positive sustained wind forecast bias at those locations. Similarly, underpredicted stations we generally have GF < G, so using a larger than observed GF helps correct the negative sustained wind forecast bias. Certainly, a more sophisticated treatment could be designed, and the results

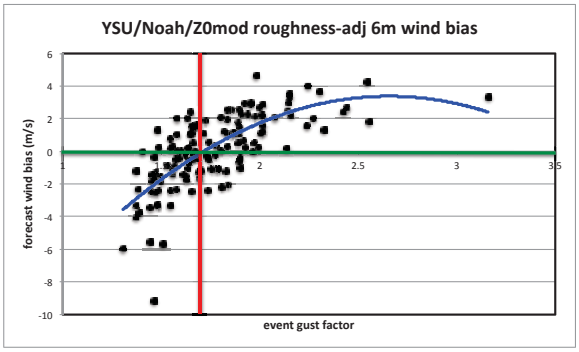

FIG. 19. Scatterplot of event-mean sustained wind bias from the YSU/Noah/Z0mod simulation vs. 13-15 May 2014 event GF. The red vertical line represents the SDGE network gust factor average, G ≈ 1.7. The blue curve represents a curvilinear least squares fit, predicting model bias from station GF.

presented herein need to be tested against more Santa Ana wind events, but we are encouraged that an attractively simple gust parameterization could be utilized with skillful sustained wind forecasts in this region.

7. Summary

We seek to skillfully predict winds and gusts during Santa Ana wind events in rural San Diego county, with model configurations validated and calibrated against the dense, homogeneous SDGE network. Large physics ensembles for past events have revealed that skill depends most crucially on the LSM, far more than on other factors such as the PBL scheme, radiation, and the landuse database. However, at least for wind, the role of the LSM depends mainly on how the surface roughness is handled. Most WRF simulations result in a high wind bias because the surface is treated as too smooth.

To our surprise, we have discovered that the SDGE network-averaged gust factor, which we termed G, is nearly constant with season, time, and event (apart from thunderstorm activity), with a value of about 1.7. While this finding is not well-understood, we anticipated, and demonstrated, that stations with gust factors (GF) smaller than G were likely to be underpredicted in the model, while the winds at stations with GF > G were likely overpredicted. This was used to separate the forecast error into that which might still be rectified, by modifying surface characteristics and perhaps model physics, and that which was probably "unfixable" other than via *ex post facto* bias correction. Thus, we propose a simple gust parameterization, with a GF of 1.7, for all stations in the network, because the constant GF works to mitigate wind biases found at the more problematic stations.

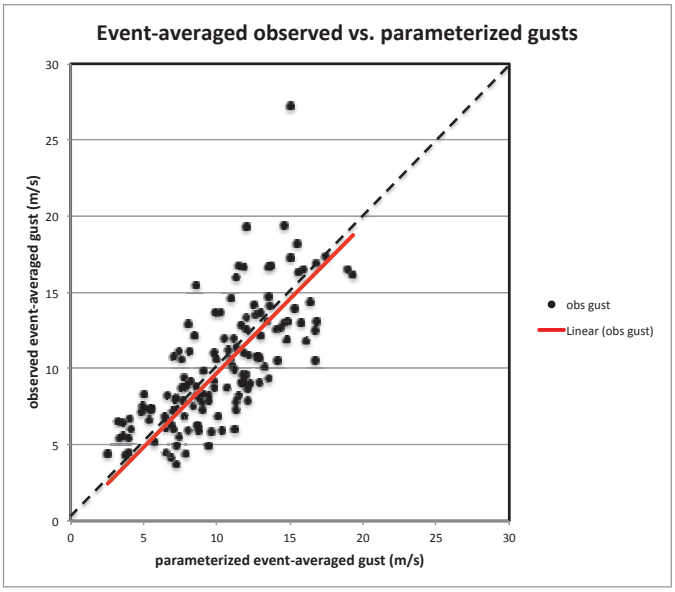

FIG. 20. Scatterplot of observed event-averaged gust (vertical axis) vs. parameterized gust, based on event-averaged wind multiplied by a station-independent GF of 1.7. The least-squares fit is shown for reference. R^2 is 0.50.

It is cautioned that the constant network GF may reflect, and very likely depend on, the homogeneity of the SDGE network, with respect to hardware, mounting height, sampling interval and siting philosophy, and therefore may not be applicable outside of the San Diego mesonet.

Acknowledgments.

This research was sponsored by San Diego Gas and Electric company. The authors thank Brian D'Agostino, Steve Vanderburg, Tom Rolinski, and Scott Capps for helpful discussions.

REFERENCES

Ashcroft, J., 1994: The relationship between the gust ratio, terrain roughness, gust duration and the hourly mean wind speed. *J. Wind. Eng.*, **53**, 331–355.

Cao, Y. and R. G. Fovell, 2013: Predictability and Sensitivity of Downslope Windstorms in San Diego County. *15th Conf. on Mesoscale Processes*, American Meteorological Society.

Fovell, R. G., 2012: Downslope windstorms of San Diego county: Sensitivity to resolution and model physics. *13th WRF Users Workshop*, Boulder, CO, Nat. Center for Atmos. Res.

Glickman, T., 2000: *Glossary of Meteorology*. Amer. Meteor. Soc., 855 pp.

Raphael, M. N., 2003: The Santa Ana Winds of California. *Earth Interact.*, **7**, 1–13.

Skamarock, W. C. and co authors, 2007: A description of the Advanced Research WRF Version 2. NCAR Tech. Note NCAR/TN-468+STR, 88 pp.

Verkaik, J. W., 2000: Evaluation of Two Gustiness Models for Exposure Correction Calculations. *J. Appl. Meteor.*, **39**, 1613–1626.

Wieringa, J., 1973: Gust factors over open water and built-up country. *Boundary Layer Meteor.*, **3**, 424–441.

Wieringa, J., 1976: An Objective Exposure Correction Method for Average Wind Speeds Measured at a Sheltered Location. *Quart. J. Roy. Meteor. Soc.*, **102**, 241–253.

Appendix 4

Downslope Windstorms of San Diego County. Part I: A Case Study

Article *in* Monthly Weather Review · February 2016

DOI: 10.1175/MWR-D-15-0147.1

2 authors:

Yang Cao
The University of Arizona
12 PUBLICATIONS **9** CITATIONS
SEE PROFILE

Robert G. Fovell
University at Albany, The State University of …
84 PUBLICATIONS **1,810** CITATIONS
SEE PROFILE

Downslope Windstorms of San Diego County. Part I: A Case Study

YANG CAO AND ROBERT G. FOVELL

Department of Atmospheric and Oceanic Sciences, University of California, Los Angeles, Los Angeles, California

(Manuscript received 9 April 2015, in final form 27 October 2015)

ABSTRACT

The "Santa Ana" wind is an offshore flow that affects Southern California periodically during the winter half of the year, typically between September and May. The winds can be locally gusty, particularly in the complex terrain of San Diego County, where the winds have characteristics of downslope windstorms. These winds can cause and/or rapidly spread wildfires, the threat of which is particularly acute during the autumn season before the onset of winter rains. San Diego's largest fires, including the Cedar fire of 2003 and Witch Creek fire of 2007, occurred during Santa Ana wind events.

A case study of downslope flow during a moderately intense Santa Ana event during mid-February 2013 is presented. Motivated by the need to forecast winds impinging on electrical lines, the authors make use of an exceptionally dense network of near-surface observations in San Diego County to calibrate and verify simulations made utilizing the Advanced Research version of the Weather Research and Forecasting (WRF) Model, which in turn is employed to augment the observations. Results demonstrate that this particular Santa Ana episode consists of two pulses separated by a protracted lull. During the first pulse, the downslope flow is characterized by a prominent hydraulic jumplike feature, while during the second one the flow possesses a clear temporal progression of winds downslope. WRF has skill in capturing the evolution and magnitude of the event at most locations, although most model configurations overpredict the observed sustained wind and the forecast bias is itself biased.

1. Introduction

Southern California is known for its "Santa Ana" winds, which were named after a city and canyon in Orange County, California. The Santa Anas are very dry, sometimes hot, offshore winds directed from the Great Basin and Mojave Desert over the mountains and through the passes of Southern California (cf. Sommers 1978; Small 1995) that can produce gusts exceeding 45 m s^{-1} (100 mph) in favored areas.[1] The winds evince terrain-associated amplification of the mountain gap and downslope varieties (Huang et al. 2009; Hughes and Hall 2010). Santa Ana events occur most frequently between October and February, with December being the peak month (Raphael 2003; Jones et al. 2010). Its season is often thought of as extending from September to April, although recent years (2013 and 2014) have seen events of significant strength during the month of May.

Although the Santa Anas tend to form most frequently in midwinter, the most dangerous events often occur in autumn, before the winter rains have begun (Sommers 1978; Westerling et al. 2004). At that time, the vegetation tends to be extremely dry, and fire danger is elevated owing to the combination of low to very low humidity and strong winds that can spark and spread flames. Autumn fires historically have the potential to be very large in area, being fanned by the Santa Ana winds (Chang and Schoenberg 2011).

Santa Ana events result when cooler air spills across the Great Basin, becoming partially dammed by the mountains that separate Southern California from the inland deserts. This increases the horizontal gradient in sea level pressure (SLP) and helps to enhance flow speeds through prominent terrain gaps such as the Cajon Pass (leading to

[1] Examples: On 21 October 2007, the weather station on Laguna Peak, overlooking Pt. Mugu, recorded a 50 m s^{-1} (111.5 mph) wind gust. More recently, on 30 April 2014, a station in San Diego County (Sill Hill, SILSD) reported a 45 m s^{-1} (101 mph) gust, and remained above 40 m s^{-1} (90 mph) for a total of five nonconsecutive hours.

Corresponding author address: Robert Fovell, Atmospheric and Oceanic Sciences, University of California, Los Angeles, 405 Hilgard Ave., Los Angeles, CA 90095.
E-mail: rfovell@ucla.edu

DOI: 10.1175/MWR-D-15-0147.1

Santa Ana) and through the Soledad Pass (northwest of Los Angeles), creating prominent wind corridors in the northern part of the Los Angeles basin (Jackson et al. 2013). Wind speeds can also be very large in San Diego County, where the terrain gaps appear less prominent but mountain heights are also generally lower. The flow across this topography shares many characteristics of classic downslope windstorms (e.g., Huang et al. 2009).

Downslope windstorms are a type of large-amplitude mountain wave that can produce strong, often gusty winds on the lee side of a mountain barrier (Durran 1990, 2003; Jackson et al. 2013). They are observed in many areas of the world, and carry such names as the bora, chinook, foehn, zonda and taku winds (e.g., Schamp 1964; Durran 2003). Windstorms require a sufficiently large mountain barrier, and a terrain-dependent magnitude of cross-barrier winds, along with another ingredient such as an elevated inversion (e.g., Vosper 2004; Sheridan and Vosper 2006), Scorer parameter layering (e.g., Durran 1986), or a critical level either associated with the mean state (e.g., Durran and Klemp 1987) or generated by wave breaking (e.g., Peltier and Clark 1979). Subsidence associated with downslope windstorms can cause very low relative humidities near the surface, particularly if the air mass starts with low absolute humidity.

In complex terrain, the wind can vary greatly over small distances and gustiness is common in downslope windstorms, which may include rotors and subrotors embedded in the flow (Doyle and Durran 2004; Jackson et al. 2013). Terrain-amplified winds and gusts can knock down trees and power lines, starting and spreading fires, making accurate forecasts in this region extremely important. Proper model verification, however, can be hampered by the sparseness of the surface network, the absence of stations in wind-prone areas, as well as deficiencies in anemometer placement. As an example, on 21 October 2007, the Witch Creek fire was sparked by wind-whipped power lines located about 20 m above ground level (AGL), and was driven by an especially strong Santa Ana winds to become one of the largest fires in California history.[2] It is nearly certain that the meteorological stations that existed at the time did not fully capture the ferocity of the winds experienced at the initiation site of that or other fires that started during this windstorm.

[2] According to information obtained from the California Department of Forestry and Fire Protection (Cal Fire), the Witch Creek fire was the third largest California wildfire since 1932 upon its containment, and is ranked sixth largest as of this writing.

Despite steady improvement in operational numerical weather prediction models over the last several decades as well as advancements in the understanding of mountain meteorology dynamics, forecast skill for downslope windstorms is still limited by several factors, including dependence and/or sensitivity to model resolution (e.g., Reinecke and Durran 2009b; Jackson et al. 2013), numerical schemes (e.g., Reinecke and Durran 2009b), vertical coordinates and diffusion (e.g., Smith et al. 2007), physical formulations [especially the boundary layer; see Smith (2007)] and initial condition uncertainties (e.g., Reinecke and Durran 2009a). Our work was motivated by the need to forecast winds that could affect electrical transmission lines in San Diego County operated by the San Diego Gas and Electric (SDG&E) company. Operational products were viewed by the meteorologists tasked with anticipating wind threats in the electric network as insufficiently skillful (B. D'Agostino and S. Vanderburg 2012, personal communication). In particular, even available high-resolution (4-km horizontal grid spacing or better) products permitted the strong near-surface winds to extend downslope too far and too often, resulting in false alarms and a waste of resources.

In this part, we examine the skill of the Advanced Research version of the Weather Research and Forecasting (WRF) Model (Skamarock et al. 2008) core in forecasting Santa Ana winds in San Diego County. High spatial resolution is focused over this area, especially over the area's roughly north–south mountain range that serves to amplify the winds. Model forecasts are verified against wind observations reported by the SDG&E mesonet, a recently installed and exceptionally dense surface observing network of (presently) more than 140 stations sited primarily in well-exposed, wind-prone areas on the west-facing slopes of the county's mountains. Numerous combinations of model physical parameterizations were examined, for this and similar events, to identify the configuration that best captures the magnitude, temporal evolution, and spatial extent of the winds. Although the verification observations are still confined near the surface, we will show that the SDG&E network helps reveal model weaknesses and suggest remedies that might not have been detectable from a less-extensive set of observations.

The structure of this paper is as follows. The available observations, model experimental design, and verification strategy are presented in section 2. The mid-February 2013 event is described via SDG&E network observations in section 3. Section 4 presents the model simulations and comparisons with the observations, and the summary composes the final section.

2. Data and methods

a. Available observations

Observations are crucial for vetting a numerical model, but there are several significant challenges involved. First of all, most of the data available for verification are located very close to the surface, and even these have historically been relatively sparse. With respect to airflow, the relevant information comes in the form of "sustained winds," which are temporally averaged quantities composed of discrete samples measured by anemometers. While the WMO (2010) provides some guidelines for sustained wind collection at synoptic stations (specifying a 10-m anemometer mounting height above local open ground and removed from obstacles, and a 10-min averaging period), it remains that networks tend to differ with respect to sensor hardware, mounting height, station siting guidelines and sampling, and averaging and reporting intervals. All of these can dramatically impact the magnitudes of winds and gusts that are reported, complicating the verification process.

As an example, most (not all) ASOS stations report sustained winds at 10 m AGL, but averaged over a 2-min period, with data available at 1-min intervals (NOAA 1998).[3] The WRF provides a wind diagnostic for this height, which typically resides between the lowest model level and the surface. However, most available measurements in complex terrain come from the Remote Automated Weather Stations (RAWS) network that employs anemometers mounted closer to the surface (6.1 m AGL) and transmit longer (10 min) averages for the sustained wind once per hour (leaving over 80% of the hour unsampled). Thus, regardless of other factors, contemporaneous and collocated RAWS and ASOS sustained wind reports can be expected to disagree. In verification exercises, adjustments dependent on vertical stability and surface roughness have to be made to the model's standard 10-m wind diagnostic to avoid a potentially false conclusion of overprediction.

The WMO (2010) notes that "the most difficult aspect of wind measurement is the exposure of the anemometer." Even a cursory examination of RAWS site photos hosted by the Desert Research Institute (DRI)[4] reveals numerous examples of problematic anemometer placement with respect to buildings and/or trees. During the aforementioned Witch Creek fire, the RAWS station at Goose Valley (GOSC1) occupied an important location immediately downwind and downslope from the ignition location, but at the time was closely surrounded by significant obstacles (verified by inspection). It is not known how much larger its event maximum sustained wind (15 m s^{-1}) and gust (25 m s^{-1}) might have been had the station not been sited close to large trees.

Since 2009, SDG&E has deployed surface stations in wind-prone areas across San Diego County (Fig. 1). Sites were carefully selected in order to accurately and properly gauge the wind threat to well-exposed electrical installations. These stations conform to the RAWS standard (National Wildfire Coordinating Group 2014) with respect to anemometer height (20 ft or about 6.1 m AGL) and sustained wind formulation (10-min averages from 3-s samples), but report every 10 min instead of hourly. For each 10-min interval, the sample resulting in the largest wind speed is reported as the gust. Station identifiers consist of five characters, terminating with "SD." (This suffix will be ignored when convenient.)

As a test, SDG&E station GOSSD was purposely placed at a better-exposed location 0.7 km along Black Canyon Road from GOSC1's original location.[5] For the month of December 2011, which included several moderate Santa Ana wind events, the 10-min-averaged sustained winds at GOSSD were about 50% stronger than at the more sheltered RAWS station (Fig. 2), even though they were measured at the same height. Indeed, among the 744 contemporaneous observations of sustained wind during that month, 639 SDG&E observations were larger than their corresponding RAWS wind speed, 48 observations were the same, and only 56 of the RAWS observations (<8% of the total) exceeded the SDG&E reports. As demonstrated clearly below, even closely spaced and well-exposed stations can exhibit wind variability of this magnitude, so part of the GOSSD-GOSC1 discrepancy might have been due to an unappreciated terrain effect. However, this result motivated us to use the SDG&E network exclusively to verify our model results, owing to its high density and optimal siting philosophy. The purpose of our work, after all, is to forecast winds impinging upon electrical lines at risk of igniting wildfires in well-exposed terrain.

b. Model experimental design

The simulations examined herein were made using WRF version 3.5. To represent an operational environment, the model was initialized with the North American Mesoscale Forecast System (NAM) gridded

[3] The sampling interval for these stations was shortened from 5 to 3 s between 2005 and 2009 (Tyner et al. 2015).

[4] http://www.raws.dri.edu.

[5] Prior to November 2011, GOSSD was sited even closer to GOSC1, in a less well-exposed area intended to mimic the RAWS siting issues (S. Vanderburg 2012, personal communication). GOSC1 was subsequently moved.

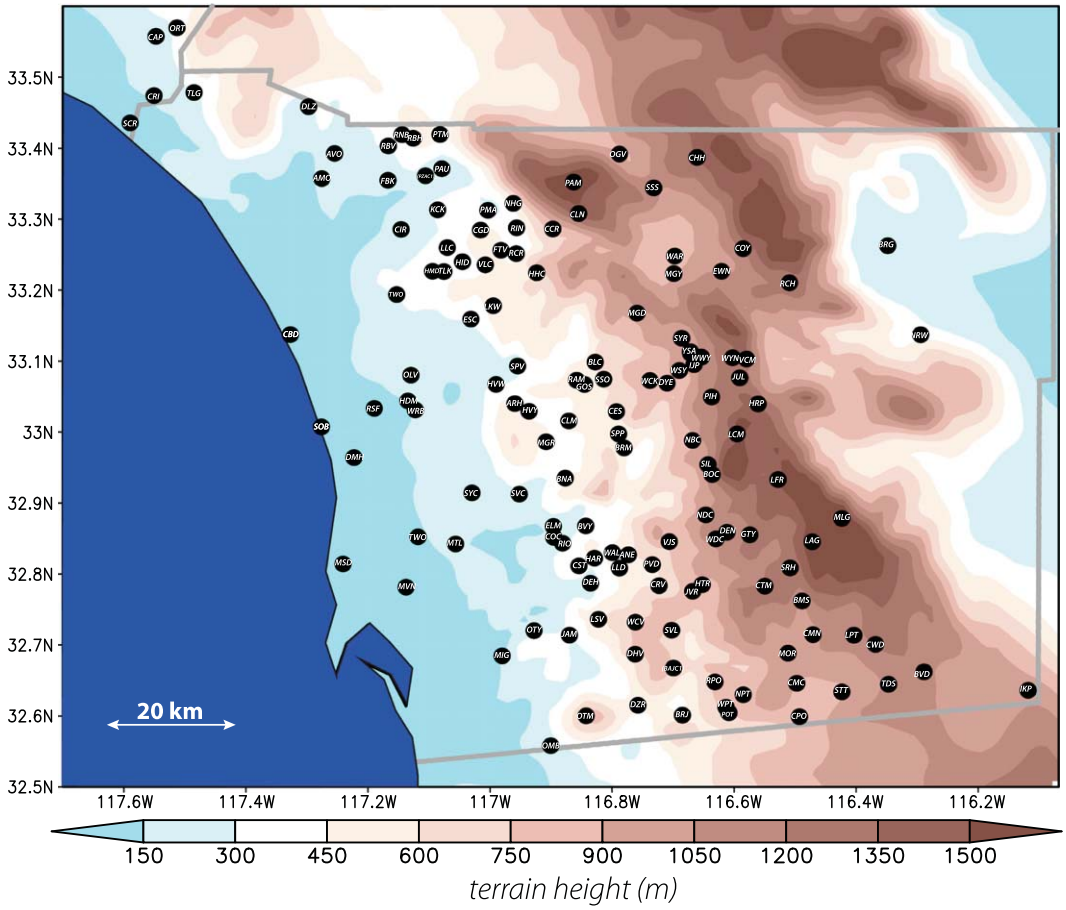

FIG. 1. SDG&E surface station locations (black dots), with underlying topography shaded. Station labels omit "SD" suffix. Stations were in place as of February 2013.

analysis and forecasts from its 1200 UTC 14 February 2013 cycle, and integrated for 54 h. A five-domain telescoping grid arrangement (denoted D1–D5) is used with horizontal grid spacings of 54, 18, 6, 2, and 0.667 km, respectively (Fig. 3). The innermost 667-m nest extends about 80 km west–east by 70 km north–south and covers roughly 70% of the SDG&E mesonet, while its parent 2-km grid encompasses the entire network. The highest resolution (~10 m) U.S. Geological Survey (USGS) terrain database available was used in the construction of the topography of the innermost two domains,[6] permitting the model to capture finer-scale features (see Fig. 3 inset) than the USGS database distributed with WRF makes possible.

The model top is 10 hPa, with 50 layers (51 full-sigma vertical levels) employed, focusing the highest resolution in the lower troposphere in the usual fashion. By default, the WRF real-data initialization program (real.exe) places about 7 half-sigma (wind and scalar) levels in the lowest kilometer AGL, with the first level (Z_a) at about 27 m above the surface. The placement of the lowest model wind level can influence surface fluxes (Wei et al. 2001), modulate the operation of the planetary boundary layer (PBL) scheme (Shin et al. 2012), and have a particularly strong impact on downslope windstorms (Zängl et al. 2008). We utilize the default setup of Z_a = 27 m for the simulations referenced herein, for the reasons discussed in section 2c.

Although it provides no information above 6.1 m AGL, the exceptionally dense SDG&E surface observation network enables us to evaluate the realism of the model simulations of the terrain-amplified winds. This is important, as we have determined from many hundreds of WRF simulations of this and other events that important local and county-wide characteristics of the downslope flow are quite sensitive to resolution, land-use assumptions, model physics, and even random noise (cf. Cao 2015). Our experiments for each event have included combinations of 5 land surface models (LSMs)

[6] http://nationalmap.gov/viewer.html.

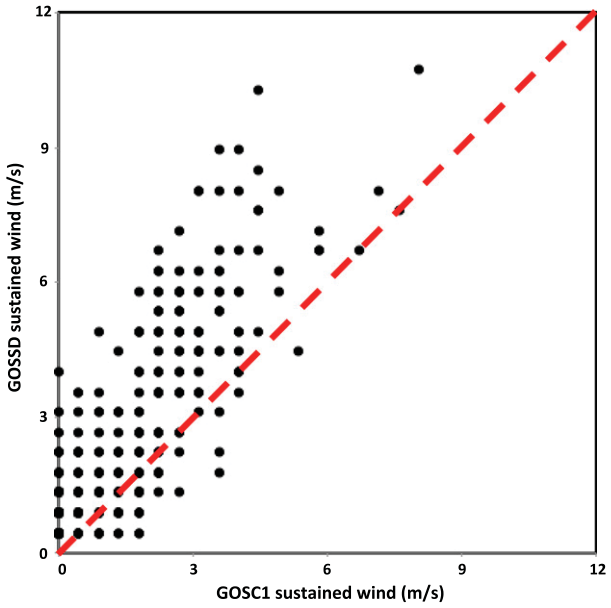

FIG. 2. Scatterplot of hourly sustained winds measured at the Goose Valley RAWS (GOSC1) and SDG&E (GOSSD) sites for December 2011, with a 1:1 correspondence line (red). Owing to rounding, there are numerous overlapping observations.

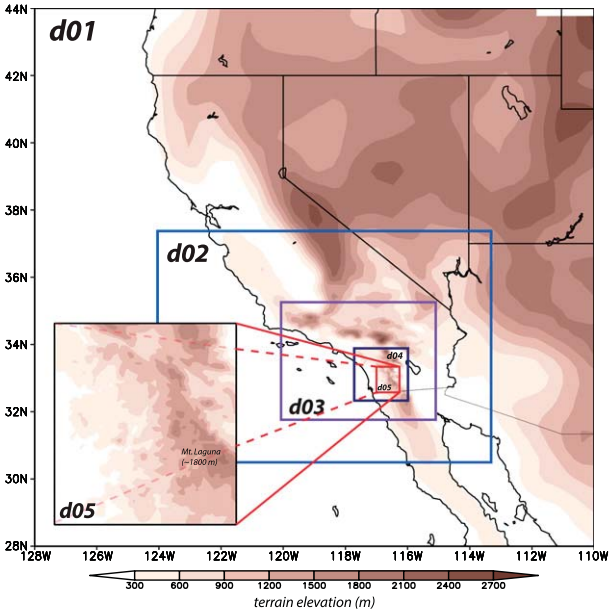

FIG. 3. Domain configuration for the WRF simulations, with topography shaded. Domains 1–5 employ horizontal grid spacings of 54, 18, 6, 2, and 0.667 km over Southern California, respectively. The inset shows an enlarged version of domain 5.

and 10 PBL schemes as well as 2 land-use databases (USGS and MODIS); for each PBL scheme, the recommended and/or most frequently adopted surface layer parameterization was employed. Simulations were nearly insensitive to some other physics options, such as the microphysics and cumulus schemes (Cao 2015).

The physics combination that consistently best represented the sustained wind observations over a set of events with respect to magnitude and temporal and spatial variation employed the Pleim–Xiu (PX; Pleim and Xiu 1995; Xiu and Pleim 2001) LSM and surface layer scheme, along with the Asymmetric Convection Model, version 2 (ACM2; Pleim 2007a,b) PBL parameterization. This ''standard'' configuration, labeled PX–ACM2, also utilized the MODIS land-use database, the Rapid Radiative Transfer Model for General Circulation Models (RRTMG; Iacono et al. 2008) radiation parameterization, and explicit horizontal diffusion was not applied. Neither the land-use nor diffusion choice had much impact on the results (Cao 2015) for this combination.

While the physics sensitivity experiment will be explored more fully in Part II, we will also reference herein results using the Noah (Chen and Dudhia 2001; Ek et al. 2003) and thermal diffusion (TD; Skamarock et al. 2008) LSMs, and the Yonsei University (YSU; Hong et al. 2006), Mellor–Yamada–Janjić (MYJ) PBL scheme (Janjić 1994), and total energy–mass flux (TEMF; Angevine et al. 2010) PBL parameterizations. In particular, the Noah–YSU combination, along with the surface layer scheme derived from MM5 (Noah–YSU),[7] is of interest because it is likely the most commonly used configuration in WRF.

c. *Verification strategy*

As noted above, SDG&E stations were intentionally placed at wind-prone sites. An unavoidable assumption being made in this study is that the SDG&E stations are representative of the landscape as a whole—or at least as it is rendered in the model. At a given grid spacing, the model is trying to capture the gross features of the terrain, which enter into parameterizations such as the LSM via such factors as the surface roughness length. It cannot directly incorporate subgrid-scale features such as trees, buildings, small hills, and terrain creases that can act to locally modulate the wind in the immediate vicinity of an anemometer. We believe that one advantage of SDG&E observations over their RAWS counterparts is that they are less likely to be influenced by small-scale features that we know we cannot represent on the grid, and thus may be more representative of the landscape we are capable of resolving.

SDG&E mesonet observations were obtained from the Meteorological Assimilation Data Ingest System (MADIS) archive and interpolated to station locations using the Developmental Testbed Center's MET

[7] This surface scheme was modified for WRF, version 3.6.

software. For wind, we compared instantaneous model predictions computed on the hour with sustained wind observations, which is the standard (if not often explicitly acknowledged) practice. Comparisons of model winds with observed gusts are not appropriate because the model's resolution, configuration, and filters preclude its ability to resolve small-scale turbulent motions. In theory, model fields could be averaged over time periods comparable to the sustained wind averaging period, but in practice this makes very little difference. The goal is to faithfully capture the overall temporal evolution and spatial characteristics of the event.

WRF computes a wind diagnostic relating the lowest model level wind V_a at height $z = Z_a$ to the WMO standard height of 10 m ($V_{10\mathrm{m}}$) via the logarithmic wind profile assumption (e.g., Oke 1987):

$$V_{10\mathrm{m}} = V_a \frac{\ln\dfrac{10}{z_0} - \psi_{10\mathrm{m}}}{\ln\dfrac{Z_a}{z_0} - \psi_a}, \tag{1}$$

where z_0 is the surface roughness length, and ψ_a and $\psi_{10\mathrm{m}}$ represent stability correction functions at Z_a and 10 m that vanish when the surface layer is neutrally stratified. However, proper comparison with the SDG&E network winds requires further adjustment to its anemometer mounting height at 6.1 m AGL level ($V_{6.1\mathrm{m}}$), that is,

$$V_{6.1\mathrm{m}} = V_{10\mathrm{m}} \frac{\ln\dfrac{6.1}{z_0} - \psi_{6.1\mathrm{m}}}{\ln\dfrac{10}{z_0} - \psi_{10\mathrm{m}}}, \tag{2}$$

where $\psi_{6.1\mathrm{m}}$ is the stability correction computed at anemometer level.[8] Although somewhat dependent on the land surface model and surface layer scheme, land-use database (e.g., USGS vs MODIS) employed and season, z_0 values range between 0.05 m and 0.9 m at SDG&E stations, resulting in wind speed reductions of 10%–20% from the 10-m values even when conditions are neutral.

An acknowledged limitation of this study is our assessments are being made solely with near-surface observations and presume a wind profile [Eq. (2)] that is implicitly or explicitly relied upon (e.g., Mass et al. 2002), but not well tested (cf. Stensrud 2007), in complex terrain. An alternative to the latter would be to shift the vertical coordinate so the lowest model wind level resides at $Z_a = 6.1$ m, permitting a direct comparison with the observations. This has been investigated for a number of events, but we have found that 1) shifting PX–ACM2 did not change its forecast skill very much; 2) PX–ACM2 retained its skill advantage relative to other physics combinations, even after shifting; and 3) most importantly, the shifted PX–ACM2 setup encountered linear instability issues in a subset of events (including the one examined herein) necessitating the use of much smaller time steps. As a consequence, we retain the default Z_a placement for this study. Finally, it is noted that Eqs. (1) and (2) could have been written with the zero-plane displacement modification of the anemometer heights that is sometimes used in areas with significant obstacles; we neglect this adjustment because most SDG&E stations were installed in well-exposed areas.

Event-averaged mean absolute error (MAE) and bias statistics, defined for station j and time i as

$$\mathrm{MAE} = |f_{j,i} - y_{j,i}| \tag{3}$$

and

$$\mathrm{bias} = (f_{j,i} - y_{j,i}) \tag{4}$$

are employed as tools to measure how close pointwise model predictions f_i are to their corresponding observations y_i. Model gridded winds are first interpolated to the SDG&E station locations using hourly information,[9] representing the initial time and 54 subsequent forecasts. From these data, network averages for each verification time are computed, and the event-averaged MAE and bias represent the mean network average over the 55-h event window. Using these measures, we will show that most model physics configurations generate a high wind bias relative to the observed sustained winds, even after anemometer or model level height adjustment, with the worst offenders ostensibly being those employing the MYJ PBL. However, we discovered the MYJ code was recomputing the 10-m wind values, specifying smaller roughness lengths than actually employed in the model integrations. This purely cosmetic adjustment, shared by the QNSE PBL scheme (Sukoriansky et al. 2006), exacerbated the high

[8] Neutrality is often presumed when wind speeds exceed about 5 m s^{-1} or so (e.g., Wieringa 1976; Verkaik 2000), which does appear valid among our model simulations. The stability corrections in Eq. (2) were retained for simulations examined in detail in this report, but these was found to have relatively little impact on the results and no influence on the conclusions.

[9] Mesonet data were obtained at full temporal (10 min) resolution and we elected to replace observed winds on the hour with the largest values reported during the previous 50 min, motivated by the relatively larger high-frequency variability present in the observations and our practical concern with the high wind threat. However, this was found to have relatively little impact on the results and no influence on the conclusions.

wind bias, and removing the code (as done for this study) made physics ensemble members employing MYJ and QNSE much more competitive.

3. The 14–16 February 2013 event observations

Although only moderate in overall strength as a Santa Ana episode, some very impressive winds (~26 m s^{-1}) and gusts (~41 m s^{-1}) were recorded in the SDG&E network during the 14–16 February 2013 event. More interestingly, this event was a two-phase episode, with the first phase characteristic of the development of a well-developed hydraulic jumplike feature associated with wind reversals, and the second one being a normal downslope progression of winds.

Certain synoptic-scale conditions interacting with local topography contribute to Santa Ana occurrence (Yoshino 1975; Sommers 1978; Hughes and Hall 2010). This mid-February Santa Ana wind event commenced around 0000 UTC 15 February 2013, as maximum sea level pressures exceeded 1028 hPa in the Great Basin (Fig. 4a), and a midlevel ridge approached the western United States, bringing northeast winds over the mountains encircling Southern California (Fig. 4d). Some stations reported their fastest offshore winds around 1800 UTC 15 February 2013, when the Great Basin high and the 700-hPa ridge reached peak magnitudes (Figs. 4b and 4e). During the next 24 h, the high pressure migrated eastward (Fig. 4c), away from Southern California, the surface offshore winds weakened, and the 700-hPa ridge flattened (Fig. 4f).

Figure 5 presents the maximum wind gusts observed in the SDG&E network for the event. The strongest gusts are found to be located along the western slopes, close to but not at the ridgelines. The great spatial variability of the winds can be detected in Fig. 5b, which focuses on the ''central area'' that comprises the stations of greatest present interest. Peak gusts varied between 10 and 30 m s^{-1} within a 5-km distance, suggesting each station is representative only of a small local area, at least with respect to the winds. The event-maximum sustained winds (not shown) are similar in pattern although naturally weaker in magnitude.

Figure 6a presents a time series of winds and gusts recorded at central area stations Sill Hill (SIL) and Boulder Creek (BOC). The event as a whole was characterized by two peaks separated by a protracted lull that occurred during the afternoon and early evening hours of 15 February. At 1830 UTC (1030 PST) on 15 February, SIL recorded a 41 m s^{-1} wind gust, at a time when no other stations in this region had a gust exceeding 26 m s^{-1}. Indeed, the winds were 50% weaker at BOC, which is just 1.6 km to the south (Fig. 5b). (Keeping in mind that the sustained wind represents 10-min averages and the gusts are single 3-s samples, note how similar the sustained wind at SIL is to the wind *gusts* from BOC.) It would be easy to dismiss such a high wind observation, but the station record shows that gusts exceeding 36 m s^{-1} were frequently recorded occurrence (Fig. 6a), and eye-level gusts of 33 m s^{-1} had been measured with hand-held anemometers at the site about an hour earlier (B. D'Agostino and S. Vanderburg 2013, personal communication). A close inspection of the topography in the vicinity of SIL and BOC (not shown) indicates that SIL is sited on a small local ridge while BOC resides in a narrow terrain crease, very small-scale features that may be relevant to the wind speeds and exposures and illustrate the challenge that is faced in simulating and verifying the winds across this area.

We now shift focus to the Witch Creek (WCK) area, where the SDG&E station density is particularly high (Fig. 5b). At West Santa Ysabel (WSY; Fig. 6b), located on the west-facing slope about 9–10 km down from the ridge, gusts during the first phase peaked at 26 m s^{-1} at 1800 UTC (1000 PST) on 15 February and regained comparable strength by midnight local time before finally slowing as the event wound down. Although about 40% weaker than the gusts, the sustained winds at WSY followed a similar trend. At SDG&E station Julian (JUL), close to the ridge, the gusts were much weaker than WSY's during the first phase, stronger (although still fairly slow) during the afternoon lull, and markedly weaker again during the second phase. This hints that there is something structurally and/or dynamically different about the second half of the event.

The winds also behaved very differently at the WCK station (Fig. 6c), which is less than 5 km downslope from WSY. Through the first phase, WCK's gusts remained much weaker than WSY's. Note the wind direction at WCK occasionally reversed to upslope (at times indicated by the black dots) during this period, including at and around the time of WSY's peak gusts. During the lull between the two phases, the WSY and WCK winds were comparably weak. While the winds remained downslope at WCK during the lull, they often reversed to upslope at WSY (at times indicated by the gray squares). Wind reversals reappeared at WCK during the onset of the second phase before downsloping became firmly reestablished there. WCK recorded its event maximum gust of 23 m s^{-1} at 1130 UTC 16 February, during the second pulse and about 3 h after the winds at WSY started to decline.

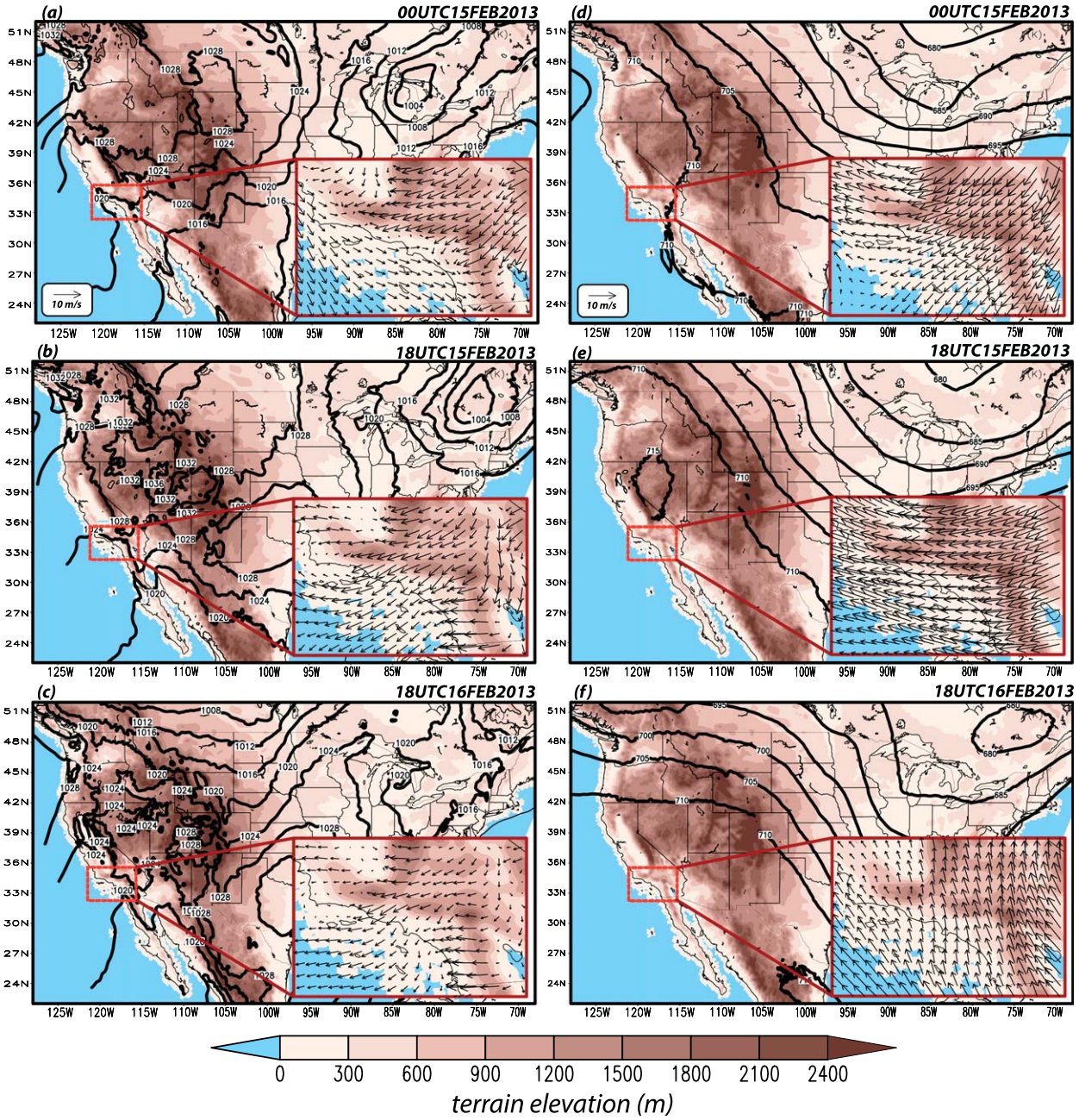

FIG. 4. NAM model sea level pressure analyses for (a) 0000 UTC 15 Feb, (b) 1800 UTC 15 Feb, and (c) 1800 UTC 16 Feb 2013; and 700-hPa analyses for (d) 0000 UTC 15 Feb, (e) 1800 UTC 15 Feb, and (f) 1800 UTC 16 Feb 2013. The insets show the total (left) 10-m and (right) 700-hPa winds of Southern California (the red box). Only a subset of vectors are plotted for clarity. Topography is shaded.

Station Sunset Oaks (SSO) is located 7 km farther downslope from WCK. Note that, during the first pulse, its gusts were weaker than, but in phase with, WSY's. The wind reversals at WCK during this time occurred with while downslope flow was observed both uphill (at WSY) and downhill (at SSO), indicating a rotor or jump may have formed there. The upslope shift of the wind reversals during the lull period from WCK to WSY could be explained by a change in the rotor or jump position. Station SSO emerged last from the lull, and its second peak was reached after the gusts at both WSY and WCK had started to decline. Taken together, these stations suggest a two-part Santa Ana event in which winds were largely in phase early in the event, apart from the suspected jump at WCK, and had a second pulse

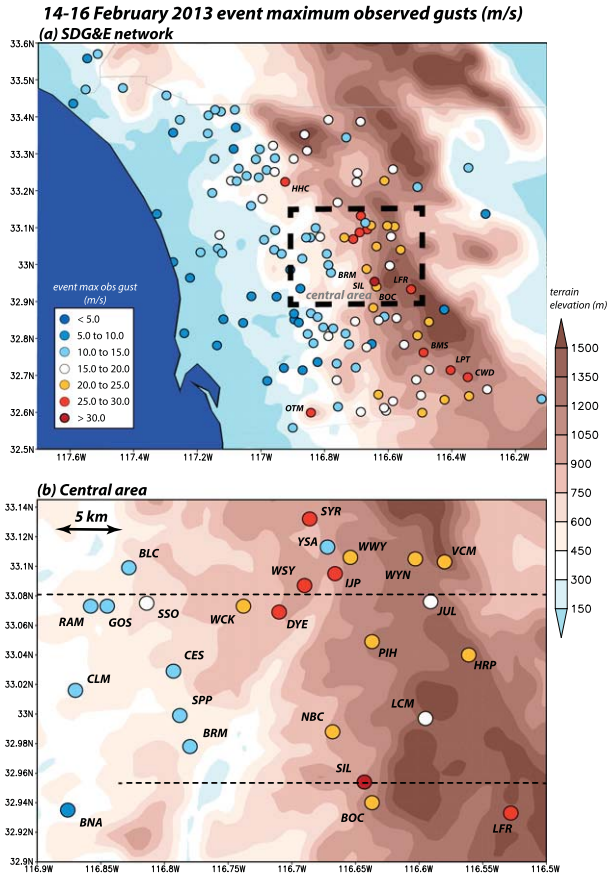

FIG. 5. Spatial distribution of 14 Feb 2013 event maximum observed wind gusts ($m\,s^{-1}$) with topography (shaded) for SDG&E stations in (a) the entire network and (b) the central area identified in (a). Black dotted lines denote locations of cross sections across WSY and SIL shown in Figs. 13 and 15.

consisting of a marked downslope progression as the overall winds abated.

4. Model simulations and verifications

In sections 4a–c, the standard run is verified and examined, and its configuration is justified.

a. *Verification of the standard run*

To a large extent, the standard PX–ACM2 simulation captured the magnitude and temporal evolution of the SDG&E network-averaged sustained winds (the mean of 138 sites), at least after the first 12 h (Fig. 7). Over the entire simulation period, the linear correlation between the network-averaged hourly observations and forecasts was 0.85, and the network- and event-averaged MAE and bias were 2.23 and 0.07 $m\,s^{-1}$, respectively. Individual stations having relatively large and small errors or biases are ostensibly dispersed randomly in space (Fig. 8). Like the network as a whole, the spatially averaged bias is nearly zero in the aforementioned central area, although clearly very variable in space (Fig. 9), so that overpredicted stations reside in close proximity to underpredicted ones. This hints at the value of high network density and the danger of drawing conclusions from a limited number of stations.

However, these plots may obscure some potentially important aspects of the sustained wind reconstructions. Among the 138 stations employed in the verification, MAE is positively correlated with the event-averaged observed wind (Fig. 10a; $R^2 \sim 0.5$ for the red curve) while the bias is negatively related (Fig. 10b; $R^2 \sim 0.5$ for the red line) to the wind. Both of these relationships are largely driven by the stations recording the highest wind speeds, and are much smaller ($R^2 \sim 0.1$ and 0.2, respectively), although still significant at the 99% level, if the windiest 10 locations (7% of the network) are removed. The uniqueness of the windy station subset can be seen when MAE and bias are presented in rank order (Figs. 10c,d); the majority of the locations (indicated by the red dots) comprise the blades of hockey stick–like structures. Six of these high-wind stations (SIL, LFR, VCM, BOC, HRP, and IJP) reside in the central area (Fig. 9).

Still, if the windiest locations are excluded, the network- and event-averaged MAE and bias are only slightly changed (to about 2.1 and 0.4 $m\,s^{-1}$, respectively). Furthermore, we will show later (in section 4c) that this result is a common characteristic of Santa Ana WRF simulations overall, independent of model physics and not unique to this event, so that exclusion of the windy subset would not alter our findings. Instead, it does not appear possible to accurately predict the winds at the windiest locations without simultaneously overpredicting the wind speed nearly everywhere else. The standard model configuration was selected to maximize network-averaged skill at reproducing the 6.1-m wind integrated over the network and through the event (as well as through other episodes not explicitly considered herein). It needs to be borne in mind that the model will require bias correction at the most wind-favored locations.

b. *Spatial and temporal variation of the winds in the standard run*

Figure 11 (left column) compares hourly time series of simulated sustained wind at stations WSY, WCK, and SSO, with the observations used in the verification. Overall, the simulation captures the evolution and magnitude of the winds at each station to a good degree, although there are some clear timing issues. At WSY, the magnitude of the second pulse was underpredicted, although the phasing was skillful (Fig. 11a). The second phase's winds ramped up too early at both

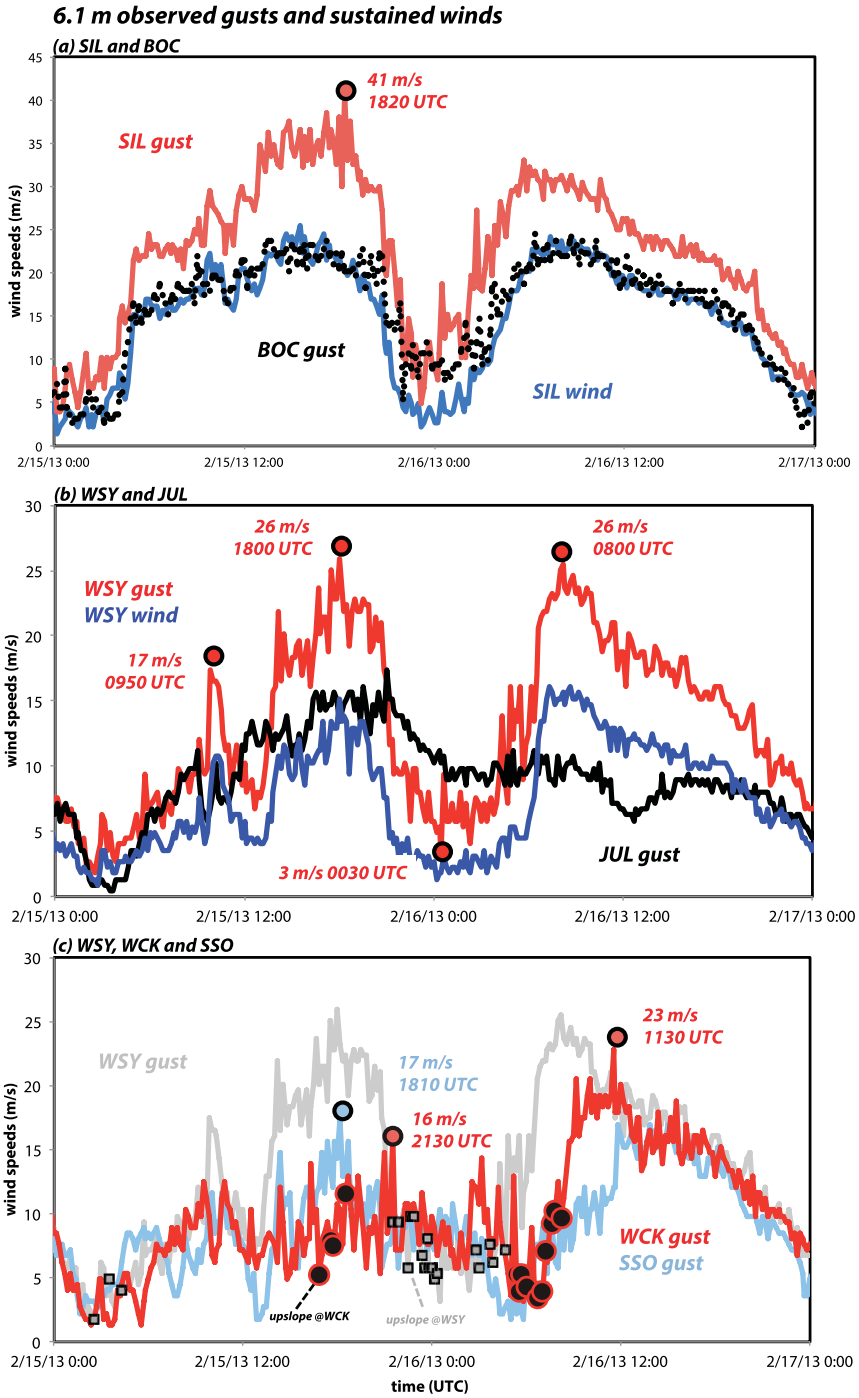

FIG. 6. Time series of observed gusts and sustained winds ($m\,s^{-1}$) over 2 days at (a) SIL and BOC; (b) WSY and JUL; and (c) WSY, WCK, and SSO. Some maxima and minima are highlighted. In (c), black dots indicate times when winds were directed upslope at WCK and gray squares indicate times when winds were directed upslope at WSY.

WCK and SSO (Figs. 11b and 11c). That said, however, the model captured the overall event evolution (Fig. 11d) as manifested by the observed winds (Figs. 11a–c) and gusts (Fig. 6c): during the first pulse, wind speeds remained markedly weaker at WCK than at stations both upslope and downslope, and the second pulse was characterized by a downslope progression of the flow with time.

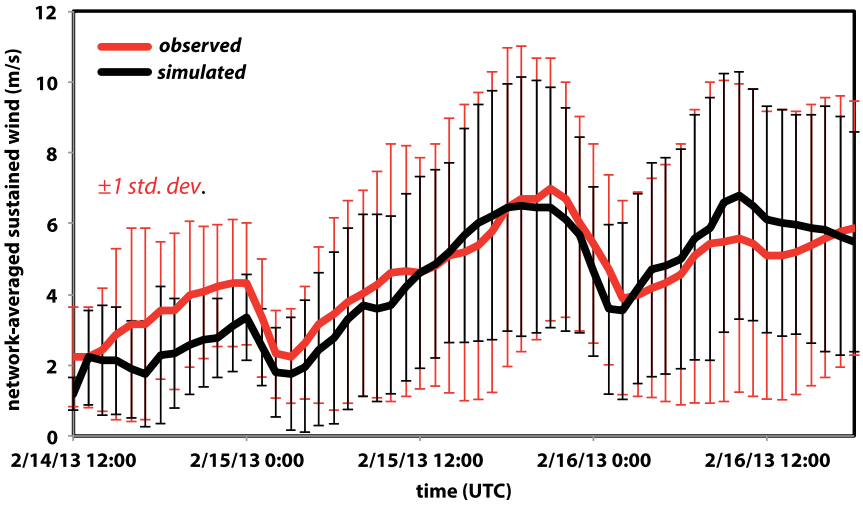

FIG. 7. Time series of SDG&E network-averaged sustained wind ($m\,s^{-1}$) observations (red line) at 6.1 m AGL over 2 days, for comparison with predictions from the standard (PX–ACM2) run (black line). Red and black color bars are plus and minus one standard deviation for observations and the standard run, respectively. The plot spans the entire 54-h simulation period.

Having demonstrated reasonable fidelity with the available observations, the simulation will be used to complete the horizontal wind field (Fig. 12), and provide insight into the vertical dimension that is missing from the observations (Figs. 13 and 15). By 0800 UTC 15 February 2013 (Fig. 12a), the downslope windstorm had already started, but the winds near the ground at WSY and stations farther downslope had not yet begun to rise. The model indicates that significant easterly flow was already present above WSY and WCK, but had not yet reached the surface (Fig. 13a). Recall that by 1740 UTC, winds recorded at WSY and SSO had reached their first-phase peaks, but WCK's winds remained quite weak (Figs. 6c and 11b). The simulation has indeed developed a jumplike feature almost directly above WCK at this time (Fig. 13b), rendering relatively weak winds there and upslope nearby (see the square and blue arrows in Fig. 12b). The reversed upslope winds indicate the existence of a local horizontal roller and characterize a turbulent and clearly defined hydraulic jump (e.g., Chanson 2009). Note also that, as expected, the wind speeds had not strengthened very much at JUL, which is located at the top of the ridge and at the very edge of the terrain-induced flow amplification.

Five hours later, there was a brief period (around 2130 UTC) during which the observed gusts at WCK were actually stronger than at the other stations (Fig. 6c), having reached their first-phase peak of $16\,m\,s^{-1}$. The winds at WSY and SSO had already entered the lull period, and the wind at WSY was directed upslope at and after this time. While the timing is not perfect, the model suggests this occurred as the jumplike feature retreated upslope, relocating the reversed flow to WSY (Fig. 13c; see square in Fig. 12c). As the windstorm subsequently retreated even farther eastward, it also weakened and became more elevated (Fig. 13d). The model reveals that strong near-surface winds still existed during the lull, but became concentrated close to the ridge and in an area where there were no stations (see between WSY and JUL in Figs. 12d and 13d).

The second phase of the Santa Ana event ensued as the reintensifying flow began progressing downslope again after 0500 UTC 16 February (Figs. 13e and 12e). Note another, smaller-amplitude jump formed in the vicinity of WCK, again consistent with the wind reversals seen in the observations (Fig. 6c). By midnight local time (0800 UTC), however, that feature had disappeared and the downsloping flow became "flatter" and, eventually, shallower as the Santa Ana event eventually wound down (Figs. 13f–h). The observations indicated that a westward and downslope progression in the peak near-surface wind speeds (Fig. 6c) had occurred, and the model has largely captured this behavior (Figs. 11d and 12f–h).

The retreat separating the two phases likely responds, at least in part, to temporal variations upstream of the mountain ridge, some of which are diurnal in character and some are associated with the evolution of the synoptic-scale environment. Figure 14 presents a time versus height view of stability and temperature (at top) and winds (at bottom) at the location marked "E" in Fig. 13, just east of the ridge. The figure reveals that an elevated inversion atop a less

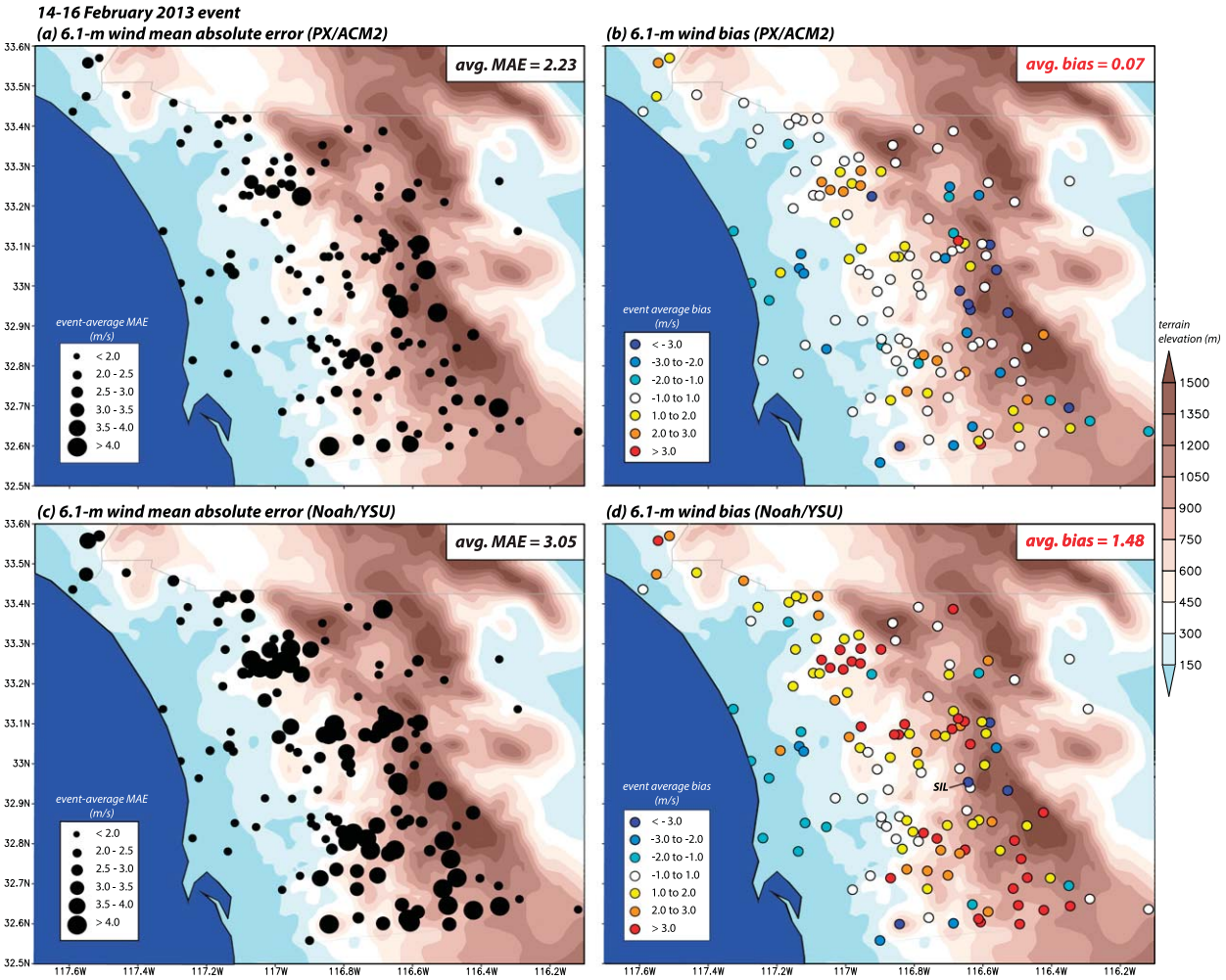

FIG. 8. As in Fig. 5a, but for (a) event-mean sustained wind MAE against observations and (b) event-mean sustained wind bias against observations, for the standard simulation. (c),(d) As in (a),(b), but for the Noah–YSU run.

stable layer was present through most of the Santa Ana episode, similar to the situation studied by Vosper (2004). Elevated inversions also occur during high-wind events at Boulder, Colorado (e.g., Brinkmann 1974; Klemp and Lilly 1975). The inversion had appeared prior to 0000 UTC 15 February, and the winds just east of the ridge had already acquired an easterly component, but the simulated winds at WSY (superposed for reference) did not rise until the inversion and cross-ridge flow both strengthened during the next 12 hours.[10]

After the maximum winds were reached at WSY, note that the easterlies above point E subsequently changed relatively little through 0600 UTC 16 February, spanning the entire interperiod lull. While a closer examination is required, the windstorm's upstream retreat appears to be associated with the erosion and descent of the inversion that occurred after 1800 UTC on the 15th, in the hours after sunrise (around 1430 UTC). Part of this evolution is a consequence of daytime heating, which is evident in the evolution of the temperature contours below about 3.5 km MSL (2.4 km AGL) in Fig. 14a. The increasing separation between the 298- and 306-K isentropes in Fig. 14b during this time is also consistent with surface-based heating, and indicative of a weakening and repositioning of the inversion.

The second phase commenced after the inversion again ascended after 0400 UTC 16 February, a few hours after sunset (around 0130 UTC). Through the second

[10] A critical level with respect to the cross-ridge wind appeared above 4 km above mean sea level (MSL) prior to WSY's first peak, but did not persist. A mean state critical level was present at 7 km MSL throughout the event; not shown.

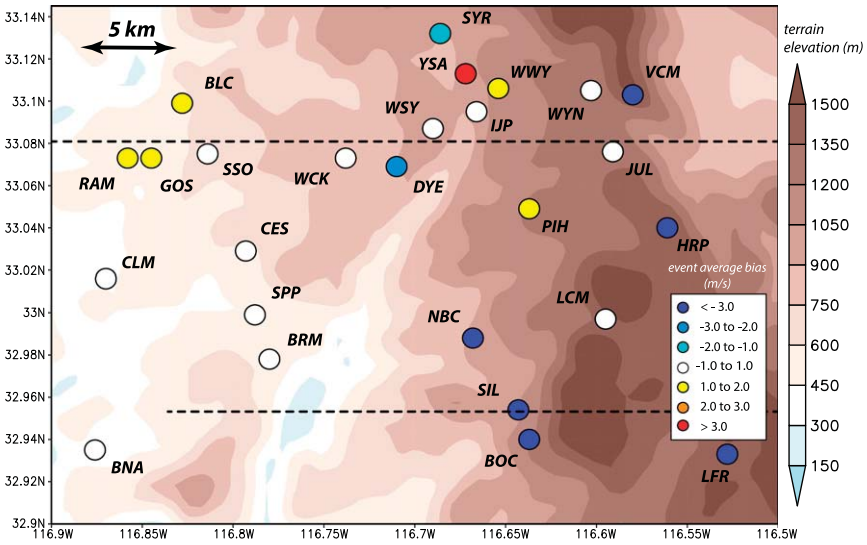

FIG. 9. As in Fig. 8b, but zoomed into the central area. Labels indicate names of SDG&E stations, with the "SD" suffix omitted. Black dotted lines denote cross sections across WSY and SIL shown in Figs. 13 and 15.

pulse, however, the easterly winds were not only weaker but also located closer to the surface, and the stability structure evolved further, becoming surface based after sunrise on 16 February as the simulated downsloping winds became shallower (Figs. 13g,h). This shift in the stability structure, which appears to reflect the evolving large-scale environment, may explain the different character of the downslope winds during the two phases. Vosper (2004) and Durran (1986) have demonstrated that the structure and intensity of windstorms can be very sensitive to even subtle shifts in characteristics such as inversion height and stable layer depth.

Figure 15 switches focus to the west–east vertical cross sections across SIL (see Fig. 12a), the focus of Fig. 6a. During the first phase of the event (Figs. 15a–d), the downslope winds were not able to progress beyond this station, at least at this latitude, prior to the afternoon retreat upslope. It is recalled that SIL's observed peak gust (41 m s^{-1}) occurred at 1820 UTC (Fig. 6a), the time of Fig. 15c. The winds extended farther downslope during the second pulse, fitfully forming jumplike features (Figs. 15e–g) in areas lacking stations (e.g., between BRM and SIL in Figs. 12e–g). The event winds waned more quickly in this portion of the central area than the subzone around WCK (Figs. 12h and 15h).

As seen earlier, SIL and BOC were among the most severely underpredicted sites (Fig. 9). Reconstructions for these two stations are very similar (Fig. 11e), which is unsurprising due to their small separation (1.6 km) relative to the 667-m resolution of D5. A nearby station, North Boulder Creek (NBC), was also underpredicted (Fig. 11f), with a delayed windstorm onset, although the model accurately captured the fact the NBC site was less windy than both SIL and BOC. At Barona Mesa (BRM), located farther downslope (Fig. 9), both the simulated and observed winds remained generally weak during the episode (Fig. 11g), suggesting that the model's rendition of the spatial extent of the strong winds is reasonable.

c. *Justification of the standard configuration*

Our standard configuration employs a sub-1-km nest placed over the heart of the SDG&E network. It is well appreciated that terrain gap and downslope flows are significantly modulated by the shape of the topography, which is in turn dependent on the resolution of the model grid and the topographic database. Horizontal resolution sensitivity is demonstrated using vertical cross sections taken west–east across station WCK for PX–ACM2 simulations employing horizontal grid spacings between 667 and 10 km (Fig. 16). The fields shown are 4-h averages taken between 1500 and 1900 UTC 15 February, straddling the peak of the event's first phase at WSY (Fig. 6b), and network- and event-averaged bias and MAE are also reported.

The previously noted jump over WCK (Fig. 13b) is revealed to be a persistent feature in the highest-resolution run (Fig. 16a), which also has the smallest bias and MAE of the four simulations shown. Although it does not capture the jump, the 2-km simulation (Fig. 16b) does resemble a spatially smoothed version of the 667-m run's flow, and the strongest winds are still correctly positioned near station WSY. Further resolution

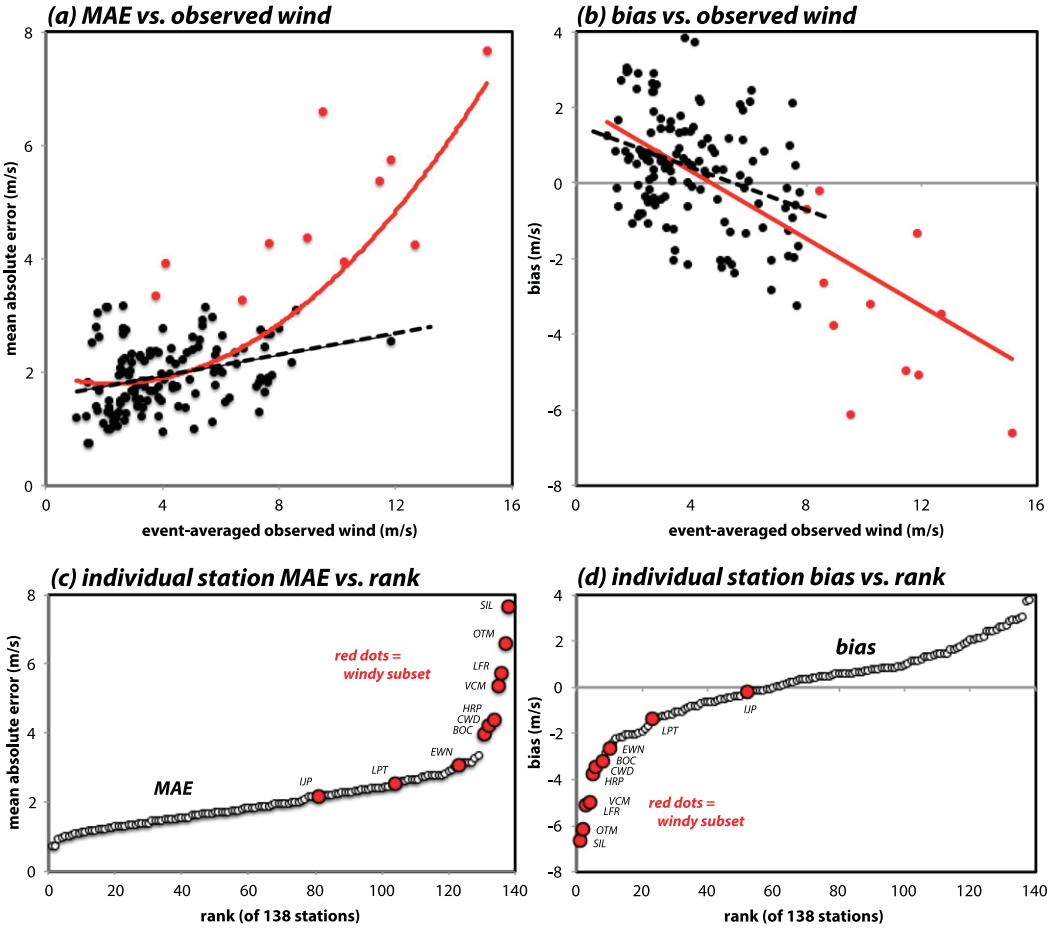

FIG. 10. (a) Scatterplot of event-mean observed wind vs MAE in the PX–ACM2 simulation for the 138 SDG&E stations. Red points identify the 10 windiest stations (see text). Least squares fits including all stations are shown in red, and those including only the black points are shown in black. (b) As in (a), but for event-mean observed wind vs mean bias. (c) Station MAE shown in rank order, with red points again identifying the windiest stations (identified by name). (d) As in (c), but for bias.

degradation, however, profoundly alters the shape of the terrain and improperly changes the location and horizontal extent of the maximum winds, leading to larger MAEs and sizable high wind biases (Figs. 16c,d). (Recall from the introduction that operational models tended to push high winds too far down the slope too often; clearly lower resolution can contribute to that.) Based on these results, it is concluded that 2-km resolution is acceptable but wider grid spacing cannot reliably place the fastest winds at the most likely correct locations. We elected to deploy a sub-1-km domain within the SDG&E mesonet to capture relatively subtle features such as the narrow northeast–southwest-oriented canyon immediately east of WSY and the terrain depression near WCK that can be seen in Fig. 16a.

As mentioned earlier, PX–ACM2 was selected for the standard run owing to its small MAE and nearly zero bias for the event-averaged sustained wind, in this as well as other cases (cf. Cao 2015, and below). Nearly all other physics combinations resulted in a positive wind bias as well as larger MAE for this event (Fig. 17). The members have clearly clustered with respect to LSM, with the choice of the PBL scheme having only a secondary effect (especially after the cosmetic MYJ–QNSE fix; see section 2c). For a given LSM, we have often found the largest error to be associated with the TEMF PBL parameterization, as also occurred in this experiment. This is believed to be another cosmetic result, being a consequence of TEMF's surface layer scheme not incorporating stability corrections [ψ in Eq. (1)] into its near-surface wind diagnostic, thereby rendering it slightly less competitive relative to the alternatives. Keep in mind that these winds have been adjusted to the 6.1-m level; a straight comparison with the model's 10-m wind diagnostic would have suggested even larger overpredictions.

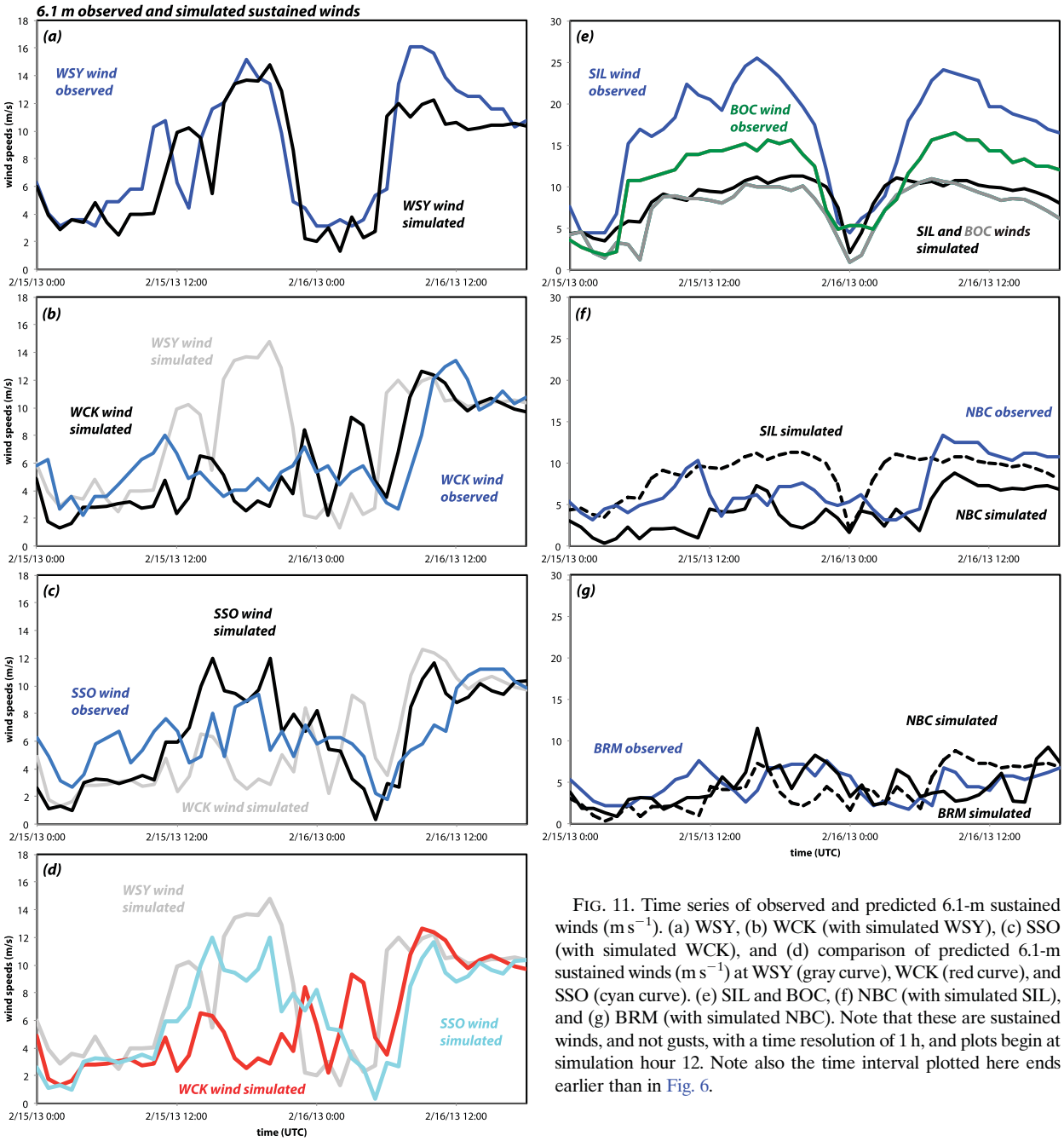

FIG. 11. Time series of observed and predicted 6.1-m sustained winds ($m\,s^{-1}$). (a) WSY, (b) WCK (with simulated WSY), (c) SSO (with simulated WCK), and (d) comparison of predicted 6.1-m sustained winds ($m\,s^{-1}$) at WSY (gray curve), WCK (red curve), and SSO (cyan curve). (e) SIL and BOC, (f) NBC (with simulated SIL), and (g) BRM (with simulated NBC). Note that these are sustained winds, and not gusts, with a time resolution of 1 h, and plots begin at simulation hour 12. Note also the time interval plotted here ends earlier than in Fig. 6.

The commonly employed Noah–YSU combination resided in the middle of our 48-member physics ensemble (Fig. 17), with obviously larger MAE at most stations (Fig. 8c). While SIL was still substantially underpredicted (Fig. 8d), over three-quarters of the sites had a positive wind bias (Fig. 18b). We note that this Noah–YSU run's bias and MAE were comparable to PX–ACM2's values from its 6-km run (see Fig. 16c).

Earlier, we demonstrated (Fig. 10) that while the network-averaged bias was nearly zero, the standard PX–ACM2 simulation's bias (and MAE) were functions of observed event-average sustained wind speed, driven primarily by a handful of particularly windy locations. Figure 18, which compares the PX–ACM2 configuration with two others, Noah–YSU and TD–TEMF, for the present as well as two other strong Santa Ana wind episodes, shows this tendency is a common occurrence. For

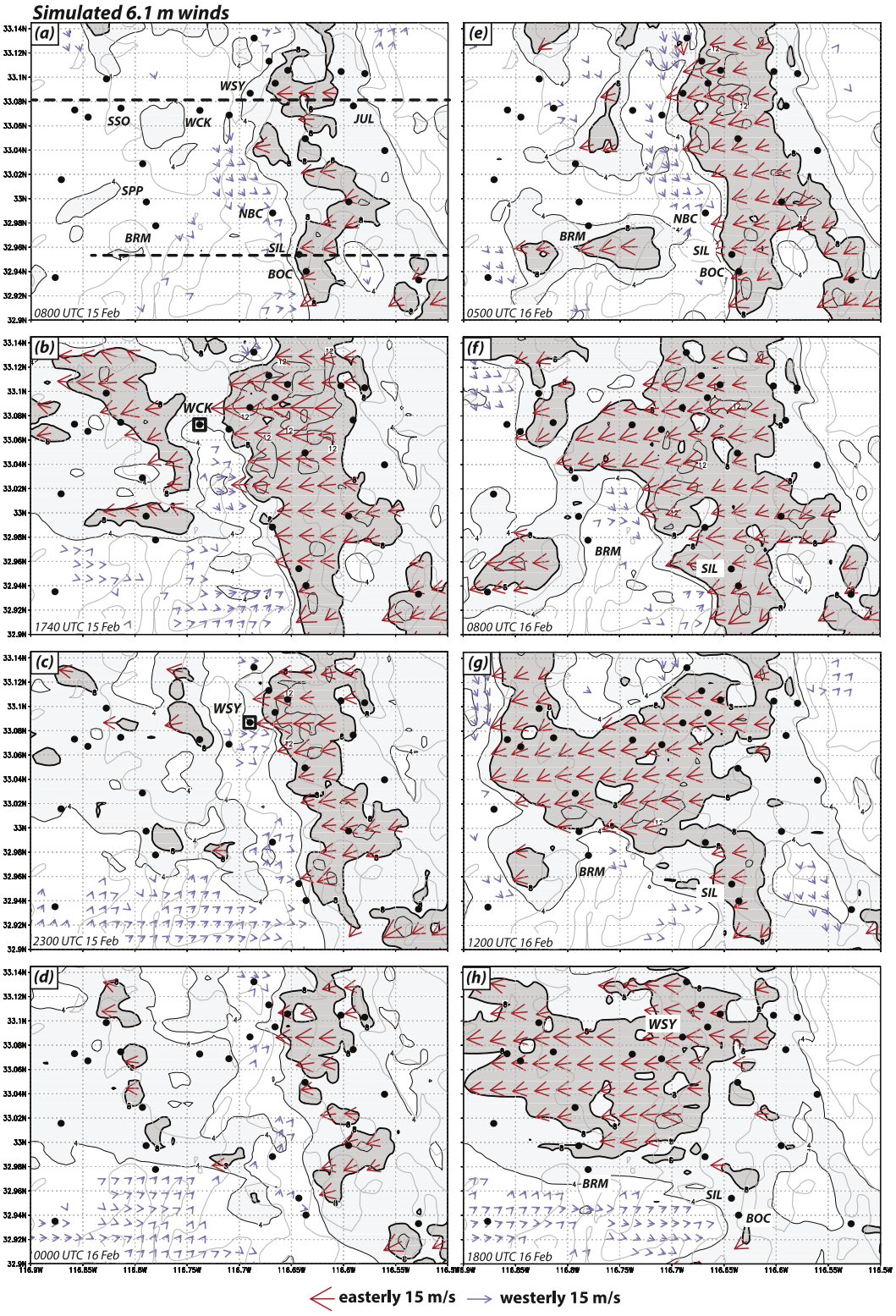

FIG. 12. Simulated 6.1-m horizontal wind speed (4 m s^{-1} interval, 8 m s^{-1} contour bolded) for (a) 0800 UTC 15 Feb, (b) 1740 UTC 15 Feb, (c) 2300 UTC 15 Feb, (d) 0000 UTC 16 Feb, (e) 0500 UTC 16 Feb, (f) 0800 UTC 16 Feb, (g) 1200 UTC 16 Feb, and (h) 1800 UTC 16 Feb 2013, with topography (300-m gray contours). Black dots denote SDG&E surface stations. Dashed lines in (a) denote locations of vertical cross sections shown in Figs. 13 and 15. Blue arrows denote winds with a westerly component ≥0.5 m s^{-1}, and red arrows denote winds with an easterly component ≥8 m s^{-1}. Many vectors are omitted for clarity.

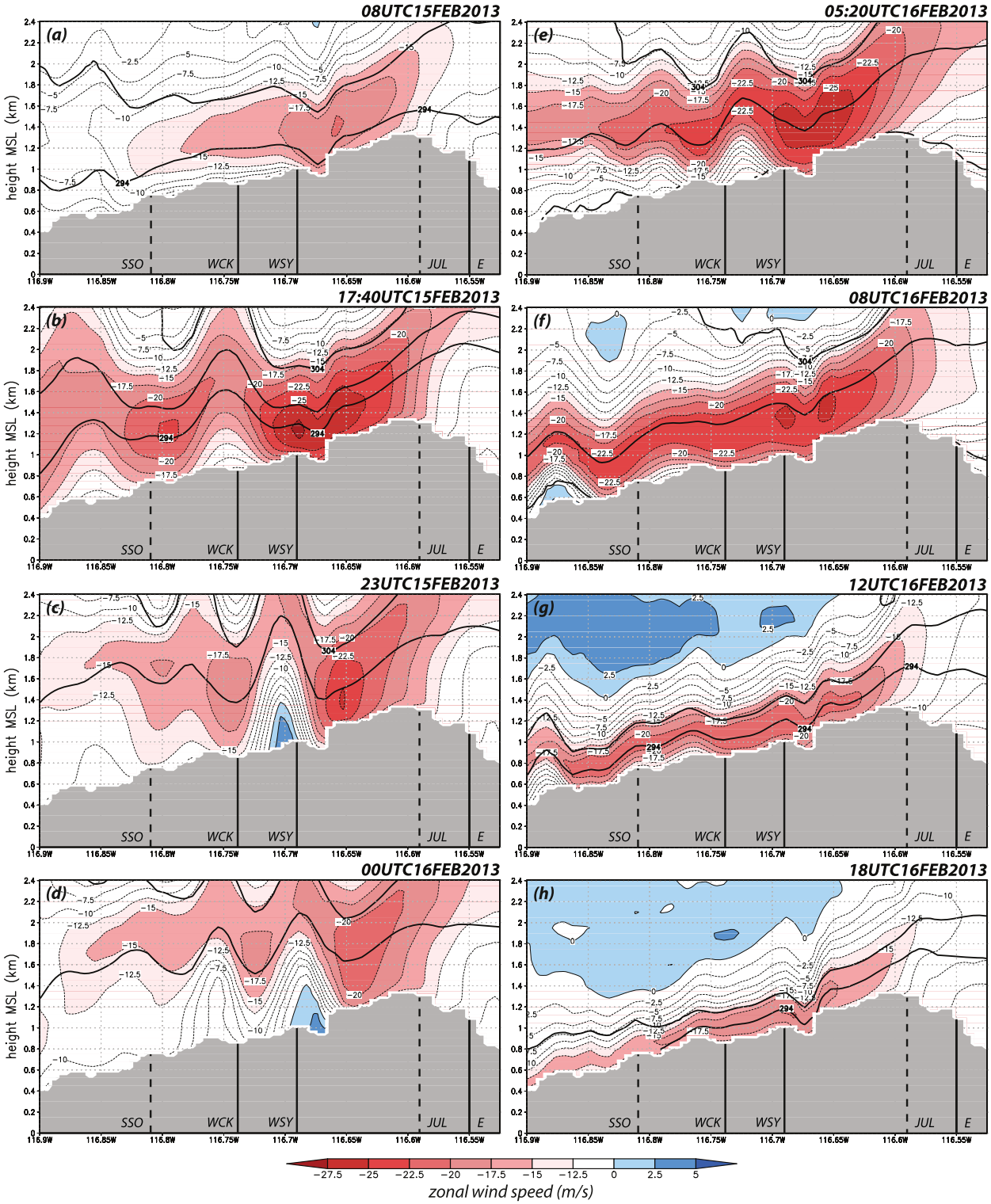

FIG. 13. Vertical cross section of zonal wind speed (shaded, with 2.5 m s^{-1} interval thin contours), taken west–east across WSY with underlying topography in gray (see Fig. 12a). Thick contours denote isentropes (5-K interval). Approximate locations of stations JUL, WSY, WCK, and SSO are marked. WCK, SSO, and JUL are displaced somewhat from the vertical plane depicted. The location for Fig. 14 is marked "E."

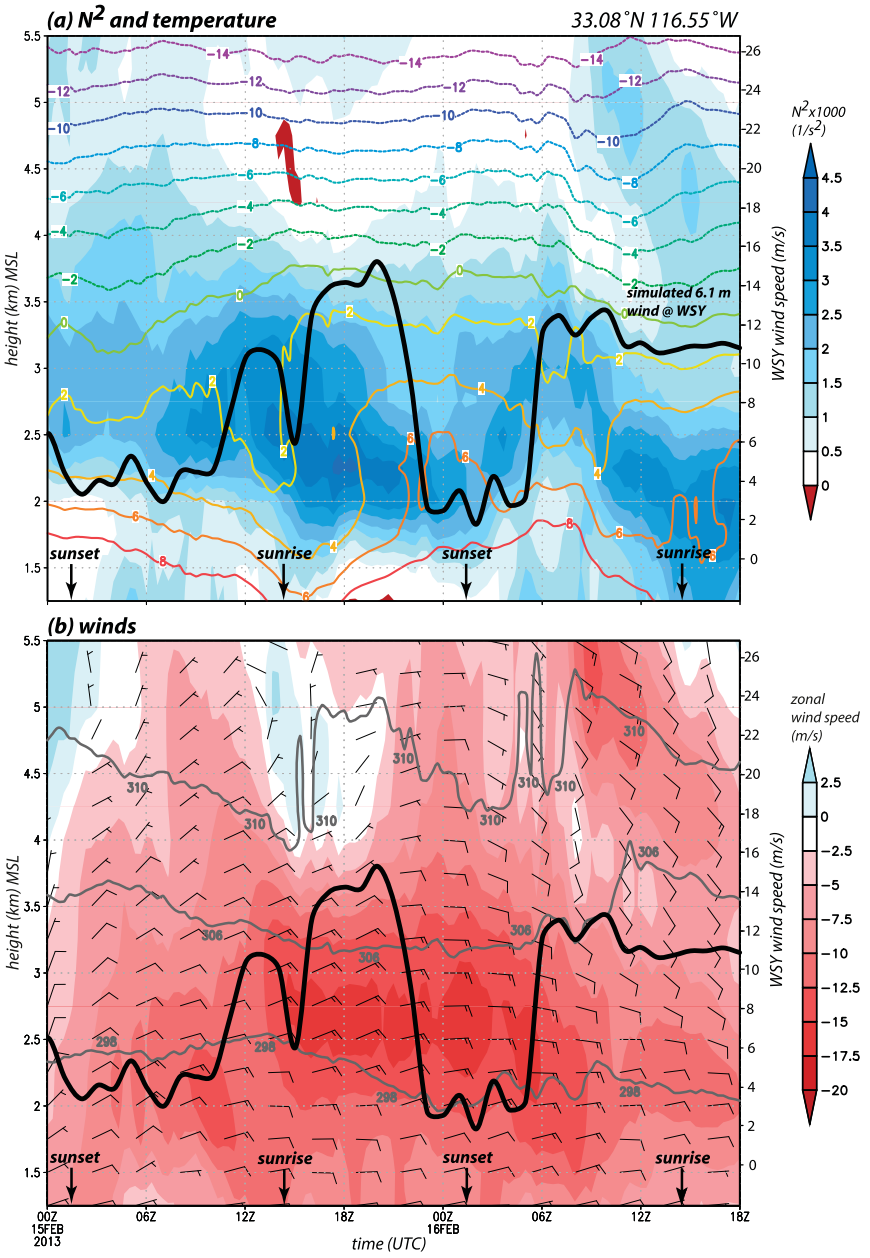

FIG. 14. Time–height plot of simulated (a) stability (dry squared Brunt–Väisälä frequency N^2, shaded as indicated) and temperature (2°C contours); and (b) zonal winds (shaded as indicated), horizontal wind barbs (in m s^{-1}), and selected potential temperature contours (298, 306, and 310 K) for location marked "E" in Fig. 13. Simulated sustained winds at WSY from Fig. 11a superposed for convenience; scale at right. Note that the plot does not start at model initiation time and fields have been vertically interpolated and thus wind barbs do not necessarily correspond to model levels.

PX–ACM2, aggregation of the three events still yields a roughly zero network-average bias, whether or not the windy subset is removed. The other two configurations, however, tend to have larger biases (e.g., TD–TEMF overpredicts the wind at over 80% of the stations among the three events) even before the windiest stations are removed, as well as larger spreads.

5. Discussion and summary

We have examined the 14–16 February 2013 Santa Ana event, which possessed many characteristics of a moderately intense downslope windstorm on the west-facing slopes of San Diego County, as part of an effort to improve wind forecast skill in this area. This study was made possible by observations from the San Diego Gas

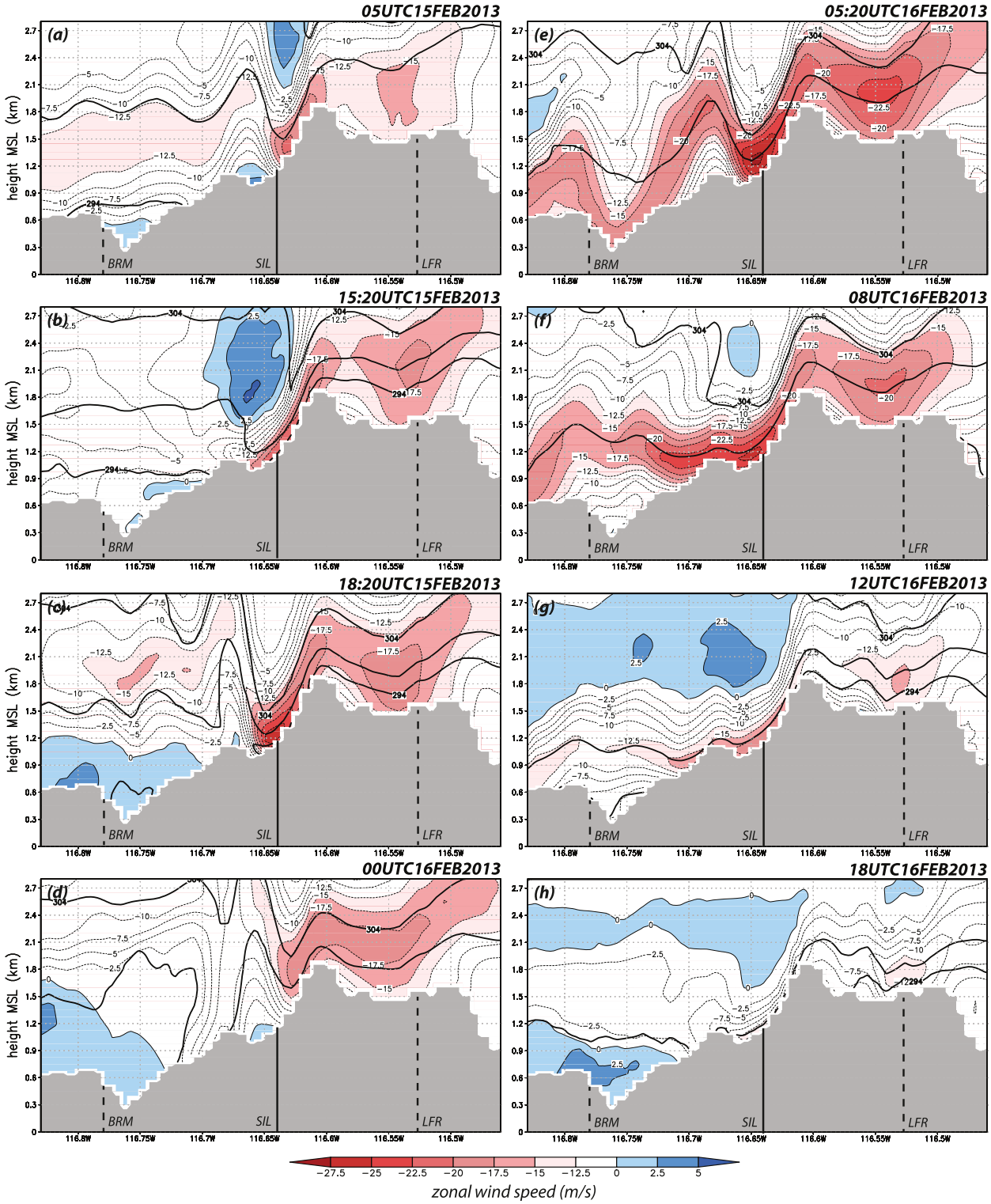

FIG. 15. As in Fig. 13, but across station SIL. Note that some times do not match those in Figs. 13a–h.

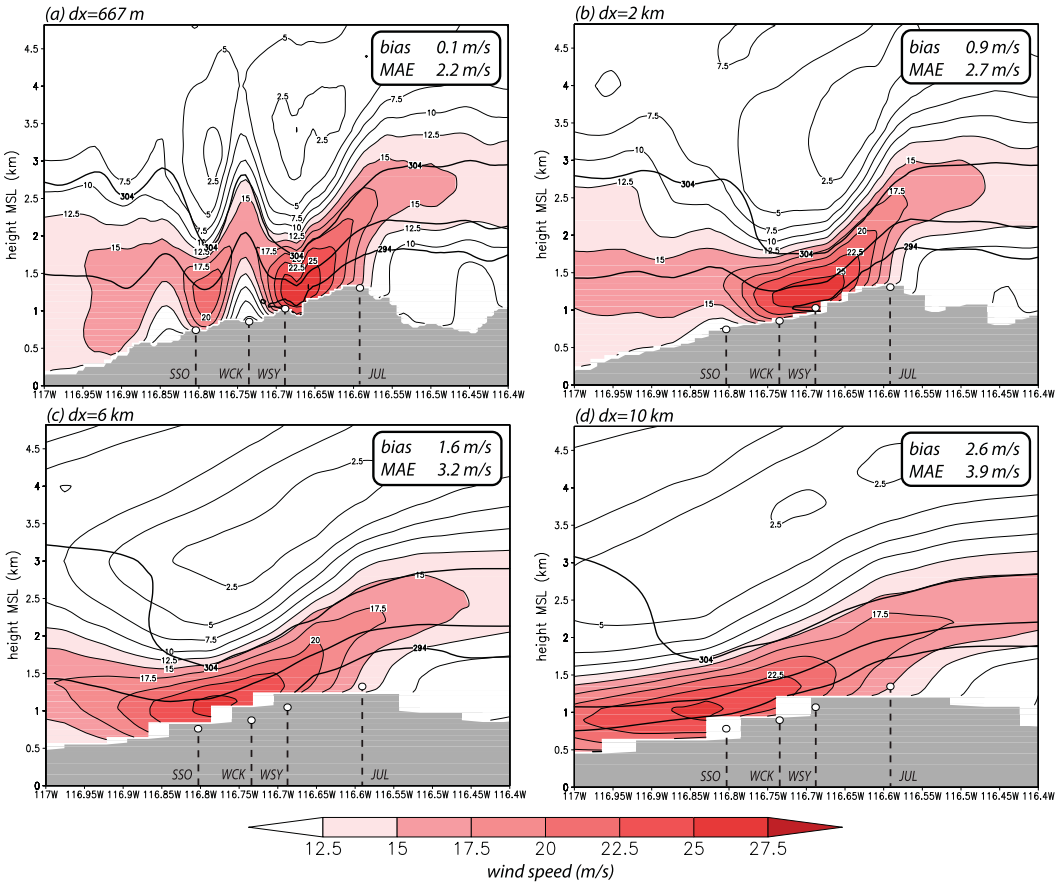

FIG. 16. Vertical cross sections of 4-h averaged horizontal wind speed (2.5 m s^{-1} contours and red shaded fields) for 1500–1900 UTC 15 Feb 2013, taken west–east across Witch Creek for the (a) 667-, (b) 2-, (c) 6-, and (d) 10-km horizontal grid spacing simulations. Thick black contours are the 294-, 299-, and 304-K isentropes. Gray shaded area depicts topography. The network- and event-averaged sustained wind MAE and bias are given in the box. The local rise in topography around 116.5°W longitude in the 2-km rendition results from a nearby topographic feature encroaching into the plane depicted owing to smoothing.

and Electric (SDG&E) mesonet, an unprecedented dense, homogeneous, and reliable observation network of ~140 stations sited in wind-prone areas, especially in the mountainous backcountry of San Diego County. These observations revealed that the 14–16 February 2013 Santa Ana episode consisted of two pulses separated by a protracted lull, and suggested that the first phase possessed a hydraulic jumplike flow in part of the network, while the second was characterized by a clear downslope progression of the winds with time as the event itself wound down.

The motivation of this study was to improve wind forecast skill in the area, and the WRF was selected for this effort. WRF provides many PBL and land surface parameterizations, permitting a very wide range of model configurations, many of which were tested for this and other recent Santa Ana wind events. Simulations were verified against SDG&E sustained wind observations, and the principal tools employed were the mean absolute error (MAE) and bias (mean error), averaged over the event at each station, and also averaged over the entire network. For this and other events, the Pleim–Xiu LSM with the ACM2 PBL scheme (PX–ACM2) combination performed well, typically minimizing MAE with a nearly zero bias with respect to the sustained wind when averaged over the network and event.

Telescoping nests were used with horizontal grid spacing of 2 km over San Diego County and 667 m over the county's highest terrain. While the 667-m grid permitted the model to capture the observed jumplike flow feature during the first pulse that was missing in the 2-km simulations, it otherwise had little influence on the network-averaged verification statistics. Horizontal resolution coarser than 2 km, however, exaggerated the spatial extent of the downslope flow, resulting in higher wind biases. Resolution also influences how well models

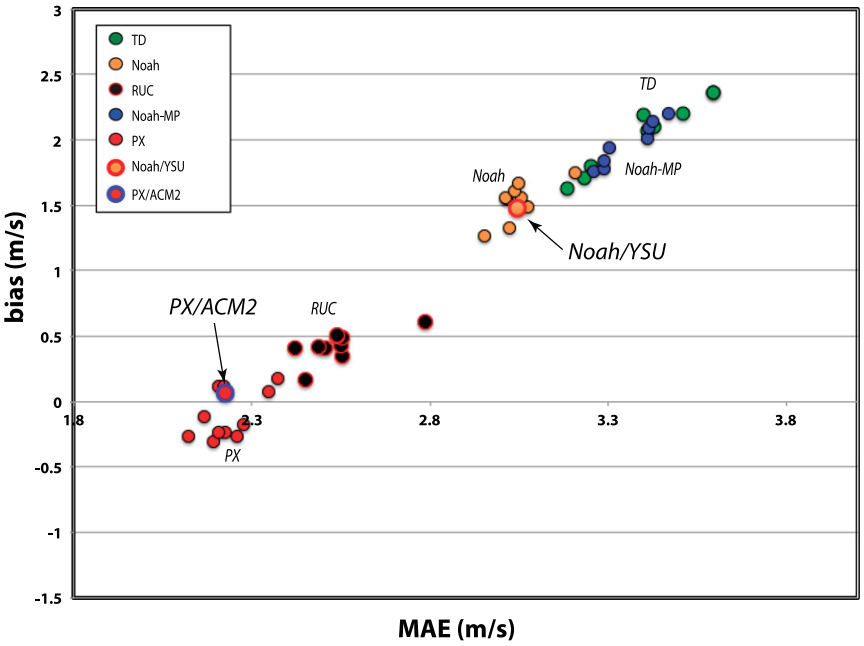

FIG. 17. Scatterplot of network- and event-averaged 6.1-m sustained wind bias vs MAE (both m s^{-1}) from the 48 physics ensemble members for the 14–16 Feb 2013 episode, color coded by LSM. For each PBL scheme, the recommended and/or most frequently adopted surface layer parameterization was employed. For members using the MYJ PBL scheme, a standard but cosmetic recalculation of the near-surface winds was removed, as noted in text. Horizontal diffusion option is turned off. The land-use database is derived from MODIS.

can capture other aspects of terrain-induced flow (e.g., Jackson et al. 2013; Reinecke and Durran 2009b) as well.

Even with adequate resolution, nearly all model configurations were found to consistently overpredict the winds at most stations in the SDG&E network, despite the adjustments for the nonstandard anemometer height (6.1 m AGL) that were made. Although it could be anticipated that the boundary layer was an important contributor (e.g., Smith 2007), this result was driven largely by the land surface model (LSM). Even the PX–ACM2 configuration had some issues, including possessing larger MAEs for windier stations, and the tendency to simultaneously overpredict less windy sites and underpredict flow speeds in windier areas of the network. In other words, the bias itself was biased. Other physics combinations, including the popular Noah–YSU configuration, resulted in a similar wind speed-dependent bias, just superposed on a larger, positive network-average mean error.

We infer from these results that event-averaged station bias represents the convolution of correctable and inherent errors, and that the PX–ACM2 combination has minimized the former relative to other configurations. In the next part of this study, we pursue the idea that the inherent error represents very small-scale influences that cannot possibly be resolved, even on a 667-m grid, features that permit the wind to vary over such small scales as previously discussed in the context of Fig. 5b. Part II will also explain why some LSMs outperformed others with respect to wind forecast skill.

It remains, however, that the PX–ACM2 simulation did a reasonable job of capturing the evolution and characteristics of this event. The model was then used to fill in gaps in the observations, especially the vertical structure of the wind field. Vertical cross sections revealed that the aforementioned jumplike feature did form on the west-facing slope, and did appear to be a hydraulic jump with reversed (upslope) near-surface flow. As observed, the simulated jump subsequently progressed upslope during the conclusion of the first phase of the event. The model also showed that while the winds were observed to be weak across the network during the afternoon lull, they actually stayed relatively strong near the ridgeline, in an area largely devoid of stations. Also captured by the model was the more uniform downslope flow that occurred during the event's second phase. These variations are of interest to local meteorologists as they help them understand what kinds of winds can occur at various places and times.

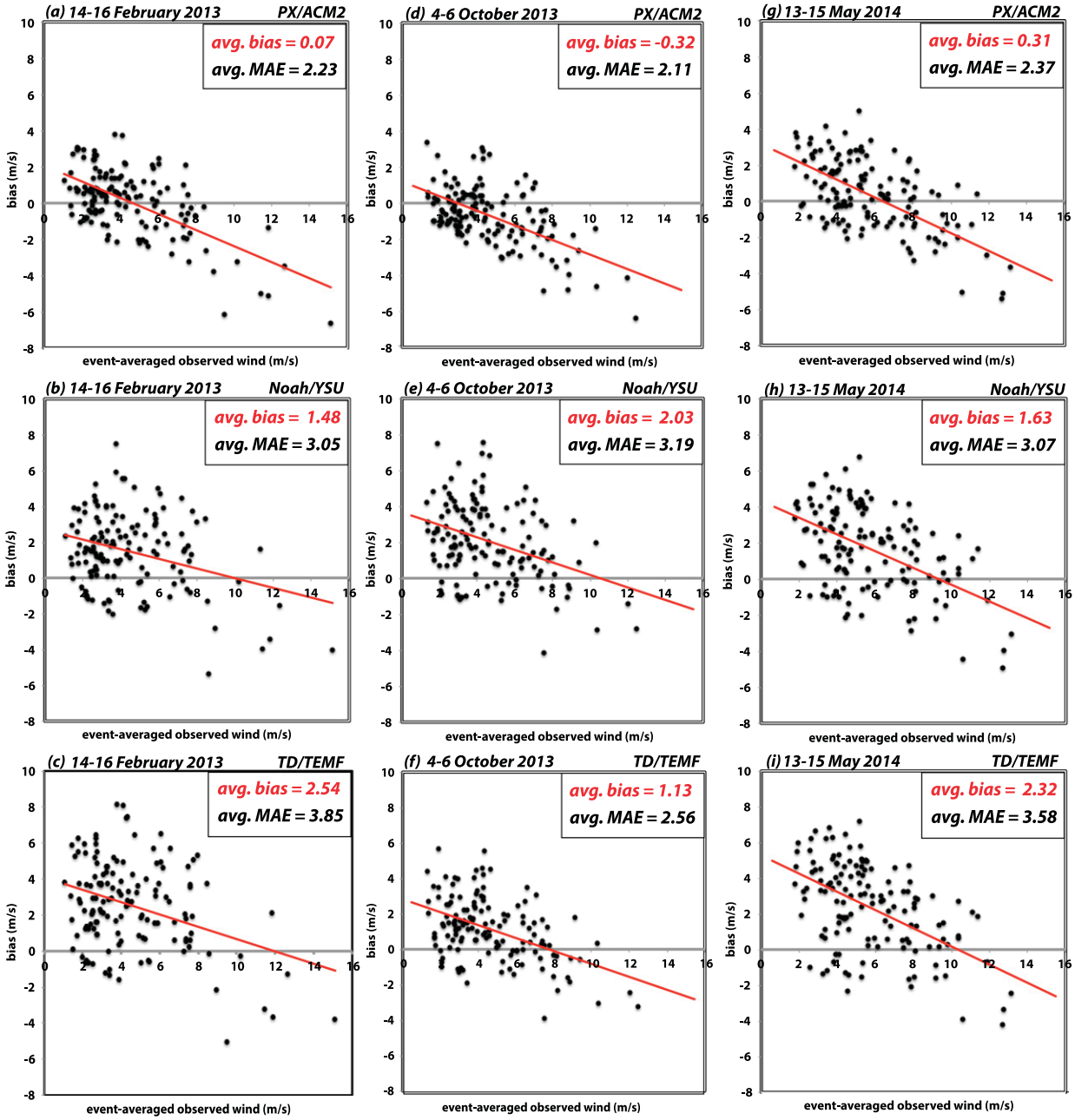

FIG. 18. Scatterplots of event-mean observed wind vs bias for SDG&E stations for three different Santa Ana wind events (columns), and three different LSM/PBL configurations (rows). A least squares fit (red line) is shown on each figure for reference. A version of (a) also appeared in Fig. 10.

Clearly, other variables such as temperature and humidity are also important for fire weather, and our experience has been that the Noah-based schemes, including Noah–MP (Niu et al. 2011), generally emerge as better with respect to MAE and bias (not shown). This motivates us to further investigate the difference among LSMs in predicting winds. Accordingly, the next part of this study will examine how and why model physics influences forecast skill with respect to the sustained winds, what needs to be done to the Noah-based schemes to improve their wind forecast skill, and will address the important issue of gust parameterization, as the greatest concern is the impact of these high-frequency, small-scale wind bursts that models of the present time cannot resolve. As in the present study, a key role will be played by the exceptionally dense and homogeneous SDG&E network.

Acknowledgments. This research was sponsored by the San Diego Gas and Electric Company. The authors thank Steve Vanderburg and Brian D'Agostino of San Diego Gas and Electric for their assistance and support. Travis Wilson designed many scripts involved in the verification, which employed the Model Evaluation Tools (MET) package from the Developmental Testbed Center. The authors would also like to acknowledge high-performance computing support from Yellowstone (ark:/85065/d7wd3xhc) provided by NCAR's Computational and Information Systems Laboratory, sponsored by the National Science Foundation. The authors thank the three anonymous reviewers for their constructive suggestions.

REFERENCES

Angevine, W. M., H. Jiang, and T. Mauritsen, 2010: Performance of an eddy diffusivity-mass flux scheme for shallow cumulus boundary layers. *Mon. Wea. Rev.*, **138**, 2895–2912, doi:10.1175/2010MWR3142.1.

Brinkmann, W. A. R., 1974: Strong downslope winds at Boulder, Colorado. *Mon. Wea. Rev.*, **102**, 592–602, doi:10.1175/1520-0493(1974)102<0592:SDWABC>2.0.CO;2.

Cao, Y., 2015: The Santa Ana Winds of Southern California in the context of fire weather. Ph.D. thesis, University of California, Los Angeles, 173 pp.

Chang, C.-H., and F. P. Schoenberg, 2011: Testing separability in marked multidimensional point processes with covariates. *Ann. Inst. Stat. Math.*, **63**, 1103–1122, doi:10.1007/s10463-010-0284-7.

Chanson, H., 2009: Current knowledge in hydraulic jumps and related phenomena. A survey of experimental results. *Eur. J. Mech.*, **28B**, 191–210, doi:10.1016/j.euromechflu.2008.06.004.

Chen, F., and J. Dudhia, 2001: Coupling an advanced land surface-hydrology model with the Penn State–NCAR MM5 modeling system. Part I: Model implementation and sensitivity. *Mon. Wea. Rev.*, **129**, 569–585, doi:10.1175/1520-0493(2001)129<0569:CAALSH>2.0.CO;2.

Doyle, J. D., and D. R. Durran, 2004: Recent developments in the theory of atmospheric rotors. *Bull. Amer. Meteor. Soc.*, **85**, 337–342, doi:10.1175/BAMS-85-3-337.

Durran, D. R., 1986: Another look at downslope windstorms. Part I: The development of analogs to supercritical flow in an infinitely deep, continuously stratified fluid. *J. Atmos. Sci.*, **43**, 2527–2527, doi:10.1175/1520-0469(1986)043<2527:ALADWP>2.0.CO;2.

——, 1990: Mountain waves and downslope winds. *Atmospheric Processes over Complex Terrain*, *Meteor. Monogr.*, No. 45, Amer. Meteor. Soc., 59–81.

——, 2003: Downslope winds. *Encyclopedia of Atmospheric Sciences*, G. North, J. Pyle, and F. Zhang, Eds., Elsevier Science, 644–650.

——, and J. B. Klemp, 1987: Another look at downslope winds. Part II: Nonlinear amplification beneath wave-overturning layers. *J. Atmos. Sci.*, **44**, 3402–3412, doi:10.1175/1520-0469(1987)044<3402:ALADWP>2.0.CO;2.

Ek, M. B., K. E. Mitchell, Y. Lin, E. Rogers, P. Grunmann, V. Koren, G. Gayno, and J. D. Tarpley, 2003: Implementation of Noah land surface model advances in the National Centers for Environmental Prediction operational mesoscale Eta model. *J. Geophys. Res.*, **108**, 8851, doi:10.1029/2002JD003296.

Hong, S.-Y., Y. Noh, and J. Dudhia, 2006: A new vertical diffusion package with an explicit treatment of entrainment processes. *Mon. Wea. Rev.*, **134**, 2318–2341, doi:10.1175/MWR3199.1.

Huang, C., Y. L. Lin, M. L. Kaplan, and J. J. Charney, 2009: Synoptic-scale and mesoscale environments conducive to forest fires during the October 2003 extreme fire event in Southern California. *J. Appl. Meteor. Climatol.*, **48**, 553–579, doi:10.1175/2008JAMC1818.1.

Hughes, M., and A. Hall, 2010: Local and synoptic mechanisms causing Southern California's Santa Ana winds. *Climate Dyn.*, **34**, 847–857, doi:10.1007/s00382-009-0650-4.

Iacono, M. J., J. S. Delamere, E. J. Mlawer, M. W. Shephard, S. A. Clough, and W. D. Collins, 2008: Radiative forcing by long-lived greenhouse gases: Calculations with the AER radiative transfer models. *J. Geophys. Res.*, **113**, D13103, doi:10.1029/2008JD009944.

Jackson, P. L., G. Mayr, and S. Vosper, 2013: Dynamically-driven winds. *Mountain Weather Research and Forecasting*, F. K. Chow, S. F. J. D. Wekker, and B. J. Snyder, Eds., Springer-Verlag, 121–218.

Janjić, Z. I., 1994: The step-mountain Eta coordinate model: Further developments of the convection, viscous sublayer, and turbulence closure schemes. *Mon. Wea. Rev.*, **122**, 927–945, doi:10.1175/1520-0493(1994)122<0927:TSMECM>2.0.CO;2.

Jones, C., F. Fujioka, and L. M. V. Carvalho, 2010: Forecast skill of synoptic conditions associated with Santa Ana winds in Southern California. *Mon. Wea. Rev.*, **138**, 4528–4541, doi:10.1175/2010MWR3406.1.

Klemp, J. B., and D. R. Lilly, 1975: The dynamics of wave-induced downslope winds. *J. Atmos. Sci.*, **32**, 320–339, doi:10.1175/1520-0469(1975)032<0320:TDOWID>2.0.CO;2.

Mass, C. F., D. Ovens, K. Westrick, and B. A. Colle, 2002: Does increasing horizontal resolution produce more skillful forecasts? *Bull. Amer. Meteor. Soc.*, **83**, 407–430, doi:10.1175/1520-0477(2002)083<0407:DIHRPM>2.3.CO;2.

National Wildfire Coordinating Group, 2014: Interagency Wildland Fire Weather Station Standards and Guidelines (PMS 426-3). National Wildfire Coordinating Group, 52 pp. [Available online at http://www.nwcg.gov/publications/interagency-wildland-fire-weather-station-standards-and-guidelines.]

Niu, G.-Y., and Coauthors, 2011: The community Noah land surface model with multiparameterization options (Noah-MP): 1. Model description and evaluation with local-scale measurements. *J. Geophys. Res.*, **116**, D12109, doi:10.1029/2010JD015139.

NOAA, 1998: Automated Surface Observing System (ASOS) user's guide. National Oceanic and Atmospheric Administration, 72 pp. [Available online at http://www.nws.noaa.gov/asos/pdfs/aum-toc.pdf.]

Oke, T. R., 1987: *Boundary Layer Climates.* Routledge, 435 pp.

Peltier, W. R., and T. L. Clark, 1979: The evolution and stability of finite-amplitude mountain waves. Part II: Surface wave drag and severe downslope windstorms. *J. Atmos. Sci.*, **36**, 1498–1529, doi:10.1175/1520-0469(1979)036<1498:TEASOF>2.0.CO;2.

Pleim, J. E., 2007a: A combined local and nonlocal closure model for the atmospheric boundary layer. Part I: Model description and testing. *J. Appl. Meteor. Climatol.*, **46**, 1383–1395, doi:10.1175/JAM2539.1.

——, 2007b: A combined local and nonlocal closure model for the atmospheric boundary layer. Part II: Application and evaluation in a mesoscale meteorological model. *J. Appl. Meteor. Climatol.*, **46**, 1396–1409, doi:10.1175/JAM2534.1.

——, and A. Xiu, 1995: Development and testing of a surface flux and planetary boundary layer model for application in mesoscale models. *J. Appl. Meteor.*, **34**, 16–32, doi:10.1175/1520-0450-34.1.16.

Raphael, M., 2003: The Santa Ana winds of California. *Earth Interact.*, **7**, doi:10.1175/1087-3562(2003)007<0001:TSAWOC>2.0.CO;2.

Reinecke, P. A., and D. R. Durran, 2009a: Initial-condition sensitivities and the predictability of downslope winds. *J. Atmos. Sci.*, **66**, 3401–3418, doi:10.1175/2009JAS3023.1.

——, and ——, 2009b: The overamplification of gravity waves in numerical solutions to flow over topography. *Mon. Wea. Rev.*, **137**, 1533–1549, doi:10.1175/2008MWR2630.1.

Schamp, H., 1964: *Die Winde der Erde und ihre Namen (The Winds of the Earth and Their Names)*. Franz Steiner Verlag, 94 pp.

Sheridan, P. F., and S. B. Vosper, 2006: A flow regime diagram for forecasting lee waves, rotors and downslope winds. *Meteor. Appl.*, **13**, 179–195, doi:10.1017/S1350482706002088.

Shin, H. H., S. Y. Hong, and J. Dudhia, 2012: Impacts of the lowest model level height on the performance of planetary boundary layer parameterizations. *Mon. Wea. Rev.*, **140**, 664–682, doi:10.1175/MWR-D-11-00027.1.

Skamarock, W. C., and Coauthors, 2008: A description of the Advanced Research WRF version 3. Tech. Note NCAR/TN-475+STR, 113 pp., doi:10.5065/D68S4MVH.

Small, I. J., 1995: Santa Ana winds and the fire outbreak of fall 1993. NOAA Tech. Memo., National Oceanic and Atmospheric Administration, National Weather Service Scientific Services Division, Western Region, 30 pp. [NTIS PB-199520.]

Smith, R. B., 2007: Interacting mountain waves and boundary layers. *J. Atmos. Sci.*, **64**, 594–607, doi:10.1175/JAS3836.1.

——, J. D. Doyle, Q. Jiang, and S. A. Smith, 2007: Alpine gravity waves: Lessons from MAP regarding mountain wave generation and breaking. *Quart. J. Roy. Meteor. Soc.*, **133**, 917–936, doi:10.1002/qj.103.

Sommers, W. T., 1978: LFM forecast variables related to Santa Ana wind occurrences. *Mon. Wea. Rev.*, **106**, 1307–1316, doi:10.1175/1520-0493(1978)106<1307:LFVRTS>2.0.CO;2.

Stensrud, D. J., 2007: *Parameterization Schemes: Keys to Understanding Numerical Weather Prediction Models.* Cambridge University Press, 488 pp.

Sukoriansky, S., B. Galperin, and V. Perov, 2006: A quasi-normal scale elimination model of turbulence and its application to stably stratified flows. *Nonlinear Processes Geophys.*, **13**, 9–22, doi:10.5194/npg-13-9-2006.

Tyner, B., A. Aiyyer, J. Blaes, and D. R. Hawkins, 2015: An examination of wind decay, sustained wind speed forecasts, and gust factors for recent tropical cyclones in the mid-Atlantic region of the United States. *Wea. Forecasting*, **30**, 153–176, doi:10.1175/WAF-D-13-00125.1.

Verkaik, J. W., 2000: Evaluation of two gustiness models for exposure correction calculations. *J. Appl. Meteor.*, **39**, 1613–1626, doi:10.1175/1520-0450(2000)039<1613:EOTGMF>2.0.CO;2.

Vosper, S. B., 2004: Inversion effects on mountain lee waves. *Quart. J. Roy. Meteor. Soc.*, **130**, 1723–1748, doi:10.1256/qj.03.63.

Wei, H., M. Segal, W. J. Gutowski, Z. Pan, R. W. Arritt, and J. W. A. Gallus, 2001: Sensitivity of simulated regional surface thermal fluxes during warm advection snowmelt to selection of the lowest model level height. *J. Hydrometeor.*, **2**, 395–406, doi:10.1175/1525-7541(2001)002⟨0395:SOSRST⟩2.0.CO;2.

Westerling, A. L., D. R. Cayan, T. J. Brown, B. L. Hall, and L. G. Riddle, 2004: Climate, Santa Ana winds and autumn wildfires in Southern California. *Eos, Trans. Amer. Geophys. Union*, **85**, 289–296, doi:10.1029/2004EO310001.

Wieringa, J., 1976: An objective exposure correction method for average wind speeds measured at a sheltered location. *Quart. J. Roy. Meteor. Soc.*, **102**, 241–253, doi:10.1002/qj.49710243119.

WMO, 2010: Guide to Meteorological Instruments and Methods of Observation. WMO Rep. 8, Secretariat of the WMO (World Meteorological Organization), Geneva, Switzerland, 716 pp.

Xiu, A., and J. E. Pleim, 2001: Development of a land surface model. Part I: Application in a mesoscale meteorological model. *J. Appl. Meteor.*, **40**, 192–209, doi:10.1175/1520-0450(2001)040<0192:DOALSM>2.0.CO;2.

Yoshino, M. M., 1975: *Climate in a Small Area: An Introduction to Local Meteorology.* University of Tokyo Press, 549 pp.

Zängl, Z., A. Gohm, and F. Obleitner, 2008: The impact of the PBL scheme and the vertical distribution of model layers on simulations of Alpine foehn. *Meteor. Atmos. Phys.*, **99**, 105–128, doi:10.1007/s00703-007-0276-1.

Appendix 5

The Santa Ana winds of Southern California: Winds, gusts, and the 2007 Witch fire

Robert G. Fovell[1,*] and Yang Cao[2]

[1]*Department of Atmospheric and Environmental Sciences, University at Albany, State University of New York, Albany, NY, USA*
[2]*Department of Atmospheric Sciences, University of Arizona, Tucson, AZ, USA*

(Received XXX, Revised YYY, Accepted ZZZ)

Abstract. The Santa Ana winds occur in Southern California during the September-May time frame, bringing low humidities across the area and strong winds at favored locations, which include some mountain gaps and on particular slopes. The exceptionally strong event of late October 2007, which sparked and/or spread numerous fires across the region, is compared to more recent events using a numerical model verified against a very dense, limited-area network (mesonet) that has been recently deployed in San Diego County. The focus is placed on the spatial and temporal structure of the winds within the lowest two kilometers above the ground within the mesonet, along with an attempt to gauge winds and gusts occurring during and after the onset of October 2007's Witch fire, which became one of the largest wildfires in California history.

Keywords: complex terrain; downslope winds; numerical weather prediction

1. Introduction

The "Santa Ana" is a dry, sometimes hot, offshore[1] wind directed from the Great Basin and Mojave Desert (**Fig. 1**) over the mountains and through the passes of Southern California (Sommers 1978, Small 1995). Its season is often thought of as extending from September to April (Raphael 2003), although prominent May events have occurred in recent years. At various places in the Los Angeles basin, fast winds are associated with terrain gaps and/or particular mountain slopes (Huang *et al*. 2009, Hughes and Hall 2010, Cao and Fovell 2016), resulting in both wind corridors and shadows. Although some attention has been paid to the phenomenon (Conil and Hall 2006, Jones *et al*. 2010), the literature on the subject is surprisingly thin given the meteorological and economic importance of the winds.

In particular, the fast winds combine with low relative humidities to produce substantial fire danger, especially in the autumn season before the winter rains have begun (Sommers 1978, Westerling *et al*. 2004). Chang and Schoenberg (2011) showed that while fires occur through the year in Los Angeles, large fires cluster in the September-November time frame (see their Fig. 2). On 21 October 2007, at or before 1930 UTC (1230 local daylight time), the Witch Creek fire

[1] In meteorology, winds are identified by their origin, so an "offshore" wind blows from land towards sea, in contrast to an "onshore" wind, or sea-breeze.

started at 33.083083˚N, 116.694139˚W in San Diego County[2], one of more than two dozen Southern California blazes driven by an especially strong Santa Ana wind event. Ignition was apparently caused by the wind-induced faulting (arcing) of power lines located roughly 20 m above ground level (AGL). The fire spread rapidly and merged with other blazes, becoming one of the largest in California history.

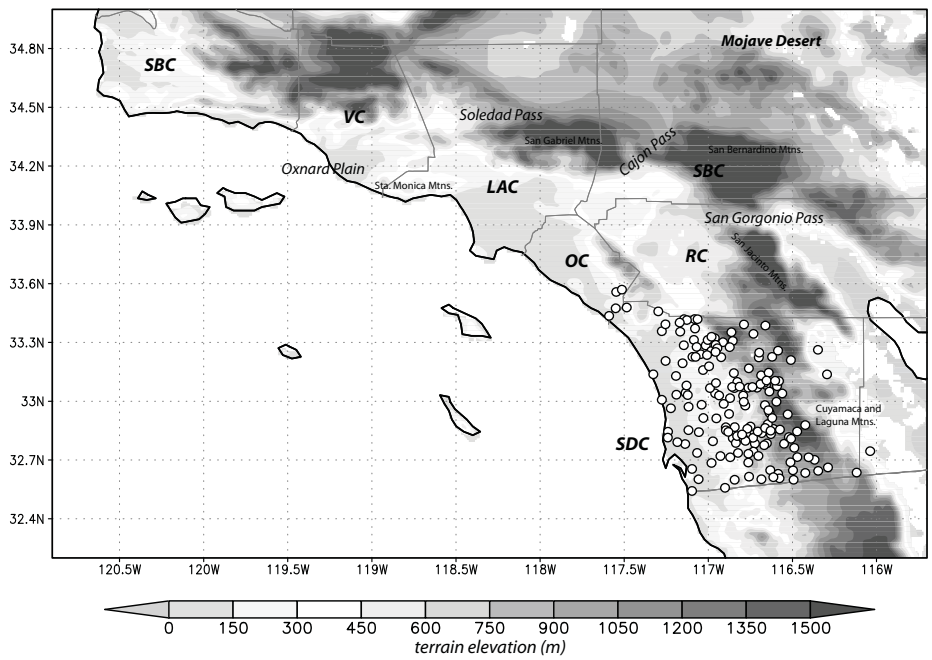

Fig. 1 Topography of Southern California (longitude on abscissa, latitude on ordinate), with selected place names. County outlines in grey; identifiers are Santa Barbara (SBC), Ventura (VC), Los Angeles (LAC), Orange (OC), San Bernardino (SBC), and Riverside (RC).

This study emerged from a need to estimate the event maximum wind speeds (sustained winds and gusts) at the Witch fire ignition site, a location for which no good, representative meteorological data were available. Existing stations were too far away and/or negatively influenced by obstacles such as buildings or trees (cf. Cao and Fovell 2016). Even if all observing sites were well-exposed and handled uniformly, it remains that winds are very strongly influenced by terrain, and thus can vary substantially even over rather short distances. This is where numerical modeling can help fill the spatial and temporal observational gaps, but models need to be verified and calibrated, which can be a problem when observing systems tend to vary with respect to sensor hardware, averaging, sampling and reporting intervals, and even (and perhaps especially) mounting height.

[2] This location was confirmed with San Diego Gas and Electric. The California Department of Forestry and Fire Protection report lists two different origins, one clearly erroneous and the other on Hwy 78 near Witch Creek mountain, a few km from the actual ignition site.

Subsequent to the 2007 firestorm, the San Diego Gas and Electric (SDG&E) company started building a high density, limited-area observational network (a "mesonet") in San Diego County, consisting of instruments installed on electrical poles at a height of 6.1 m AGL in wind-prone areas (see white dots on **Fig. 1**). The roughly 140 stations presently in this mesonet employ uniform hardware as well as siting and sampling strategies. We will examine the spatial and temporal structure of the October 2007 event, using model simulations verified and calibrated against SDG&E mesonet using more recent (albeit somewhat weaker) Santa Ana episodes, two of which (occurring during April and May 2014) are also investigated herein. Another such event (from February 2013) was studied in detail by Cao and Fovell (2016), which developed the experimental design used in this study. They showed that most model configurations tended to overpredict the wind, and that relatively high resolution (2 km or better) was needed to properly represent the terrain shape that helped determine the magnitude and location of the fastest downslope winds.

The structure of this paper is as follows: Section 2 provides information regarding the model simulations and observations used to verify them, and Sec. 3 provides background on two particular stations of interest in the SDG&E mesonet. Sections 4-6 focus on particular Santa Ana events, including the October 2007 windstorm, identifying potentially contributing factors to the production of intense gusts. Section 7 examines vertical wind profiles and related issues, and the summary is presented in Sec. 8.

2. Data sources and experimental design

As in Cao and Fovell (2016), version 3.5 of the Weather Research and Forecasting (WRF) model's Advanced Research WRF (ARW) core (Skamarock *et al*. 2007) was used with telescoping grids having horizontal resolutions as fine as 667 m over the complex topography of San Diego County (**Fig. 2**). The model was initialized using either forecast and/or analysis grids from the North American Mesoscale (NAM) model, the NCEP[3] operational mesoscale model, or the North American Regional Reanalysis (NARR) dataset (Mesinger *et al*. 2006). NAM-based runs employed the NAM's analysis for the initial time and its 3-hourly forecasts for the outer domain's boundary tendencies, except for the October 2007 event, for which forecasts were not available, so 6-hourly analysis grids were used. For recent events, SDG&E mesonet data were obtained from the Meteorological Assimilation Data Ingest System (MADIS) archive. SDG&E stations report sustained winds representing 10-min averages of 3-s samples, with the fastest 3-s sample in each 10-min interval representing the gust. Simulated and observed sustained winds were compared hourly, in the manner described in Cao and Fovell (2016).

The WRF model uses a terrain-influenced coordinate system with a staggered "C" grid (Arakawa and Lamb 1977). In typical use, the WRF vertical grid is stretched, concentrating highest resolution near the surface, but with the lowest model level for scalars and the horizontal wind components ($z = Z_a$) placed at about 27 m AGL, well above the height at which the vast majority of wind observations are taken $\leq$ 10 m). The standard practice is to assume a logarithmic wind profile between Z_a and the observation height (Z_{obs} = 6.1 m for the SDG&E network) of the form:

[3] National Centers for Environmental Prediction.

$$V_{obs} = V_a \frac{\ln\left(\frac{Z_{obs} - \delta}{z_0}\right) - \varphi_{obs}}{\ln\left(\frac{Z_a - \delta}{z_0}\right) - \varphi_a}, \quad (1)$$

where V_{obs} and V_a are the winds at the anemometer and lowest model levels, respectively, z_0 is the surface roughness length, δ is the so-called zero-plane displacement (typically neglected), and ψ_{obs} and ψ_a represent stability correction functions evaluated at the two heights that vanish when the surface layer is neutrally stratified, which usually occurs when the wind speeds exceed about 5 m s^{-1} (Wieringa 1976, Verkaik 2000). The roughness lengths are derived from the Moderate Resolution Imaging Spectroradiometer (MODIS) landuse database, and a United States Geological Survey (USGS) terrain database with higher resolution than the standard distributed with the WRF model is employed in San Diego County. While the assumptions inherent in the logarithmic wind profile have not been well tested in complex terrain (cf. Stensrud 2007), Cao and Fovell (2016) investigated shifting Z_a to 6.1 m, obviating the need for such assumptions, and found it not worth the extra computational expense (coming in the form of smaller model time steps) for Santa Ana wind events.

Model physical parameterizations in WRF include land surface models (LSMs), planetary boundary layer (PBL) and radiation schemes, and treatments for resolved-scale and subgrid clouds, among others, allowing an enormous number of potential configurations. Based on extensive, ~50 member model physics ensembles (Cao 2015, Cao and Fovell 2016), we have selected the Pleim-Xiu ("PX"; Pleim and Xiu 1995, Xiu and Pleim 2001) LSM and the Asymmetric Convection Model version 2 ("ACM2"; Pleim 2007) PBL options for the standard setup. This combination best represented the magnitude, spatial extent and temporal variation of the winds in the SDG&E network over a set of recent offshore wind events, including but not limited to episodes in February, October, and November 2013, and January, April, and May 2014. Most of the other physics combinations resulted in high wind biases and larger mean absolute errors with respect to the observations (Cao 2015, Cao and Fovell 2016). In many cases, that resulted from the model producing flows that remained too strong, too far down the slope.

A few caveats need to be borne in mind. Based on an extensive examination of past Santa Ana events, the October 2007 winds were very likely the strongest in San Diego County since the November 1957 episode, which means that the model was calibrated against winds that were necessarily weaker. Additionally, we only have near-surface data available for our verification, although we have been able to make logical inferences about wind patterns present farther aloft (Cao and Fovell 2016). Finally, owing to an inability to resolve subgrid scale turbulence, and relatively little spectral power at fine temporal and spatial scales, the WRF model's winds should be compared with sustained winds and not gusts (Cao and Fovell 2016).

Therefore, the properly calibrated model may still underestimate the true wind threat, which can come in the form of particularly violent wind "bursts". We will define a wind burst as a notably gusty period spanning three or more consecutive reporting intervals (i.e., 30 min), to lessen the chance that any single strong wind reading is in fact a bad observation. Starting in Sec.

4.2, gust predictions will be obtained by multiplying the sustained winds by reasonable, constant gust factors, applying a non-convective gust equation in operational use, and examining the resolved-scale winds near the surface. These estimates will be compared to available observations.

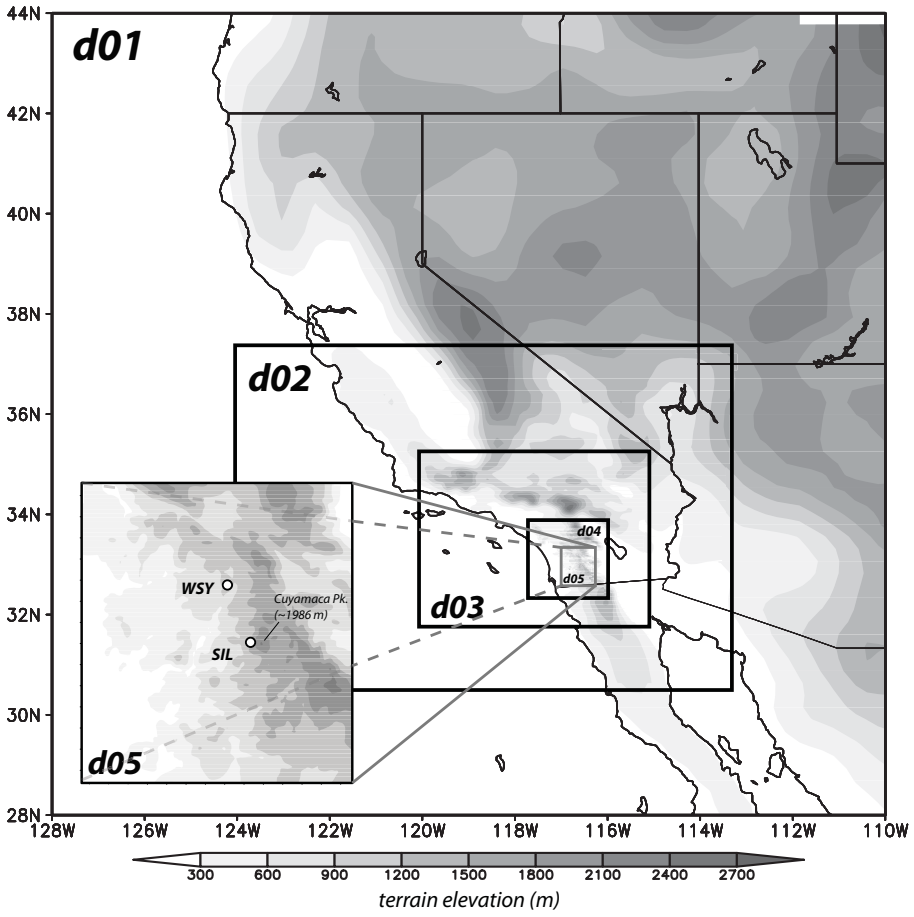

Fig. 2 Model domain configuration for the WRF-ARW simulations, with topography shaded. Domains 1-5 employ grid spacings of 54, 18, 6, 2 and 0.667 km, respectively. Locations of WSY and SIL are shown on Domain 5 inset (d05).

3. West Santa Ysabel and Sill Hill

Of the roughly 140 stations in the SDG&E mesonet, two are singled out for special attention: West Santa Ysabel (WSY) and Sill Hill (SIL), both being on west-facing slopes, which is the lee side during a Santa Ana episode. WSY was installed in July 2011 at 1003 m above mean sea level (MSL), approximately 0.6 km northeast of the Witch fire ignition site. This location is in a region of sparse, low-lying vegetation just downslope of a deep, narrow canyon that will be seen to be moderately well captured on the 667-m grid. Although not resolved, the ground surface also

drops appreciably just to the south and southwest of the ignition location (not shown), more so than at WSY. Located 15.3 km SSE of WSY, Sill Hill has emerged as the windiest station in the network since its October 2012 installation and resides at 1084 m MSL on a steep slope west of Cuyamaca Peak (1986 m), the second highest point in San Diego County. The terrain also drops steeply immediately north of this site, which is unresolved but perhaps contributes to its especially windy conditions, and vegetation is also relatively sparse, but somewhat more dense than that in the WSY/Witch area.

Since the model cannot directly predict gusts, we need to know something about how observed gusts vary with the sustained wind. We will do this by applying reasonable gust factors (GFs), representing the ratio of the gust to the sustained wind, to the model predictions that are calibrated to remove biases. GFs can be expected to vary from site to site and time to time, reflecting specific site characteristics, vertical stability, measurement averaging periods, and also be inversely related to the sustained wind at a given location (cf., Monahan and Armendariz 1971). For the period ending 31 May 2015, there were 42230 and 33847 reports for which the sustained wind of 4 m s^{-1} or faster at WSY and SIL, respectively, the smaller count for SIL reflecting its shorter record. At both, GF variability decreased with increasing wind speed (**Fig. 3**), and over all observations with sustained winds $\geq$ 4 m s^{-1}, the average GF was 1.68 at WSY and 1.59 at SIL. At WSY, the 858 observations with sustained winds $\geq$ 12 m s^{-1} had an average GF of 1.59 with 99.5% of observations exceeding 1.4 and 15.0% $\geq$ 1.7; at much windier SIL, fully 5588 observations surpassed that threshold, with a GF average of 1.44 and all but eight samples exceeding a factor of 1.2.

However, the very strongest gusts at these sites (all occurring during Santa Ana wind events) have been associated with GFs surpassing the above-cited averages (**Table 1**), suggesting that higher GFs do need to be considered. At both WSY and SIL, the fastest winds were recorded on April 30, 2014, reaching 34 and 45 m s^{-1}, respectively. The WSY observation had a GF of 2.14, which represented something of an outlier during the record (**Fig. 3a**), but still would have been 2.03 had it been associated with the (larger) sustained wind reported 10 min later[4]. The other record gusts were also associated with larger than average GFs, suggesting that gust factors between 1.7 and 2.0 can occur at WSY during especially severe conditions. The SIL gusts also at least equaled that location's average GF (1.44) during windier conditions.

As illustrated in **Fig. 4**, the strongest gusts exhibit a pronounced diurnal cycle, with the highest frequencies occurring between 1500 and 1800 UTC at both locations and a secondary peak between 0500 and 0700 UTC that is more prominent at SIL. The observations employed were limited to observed gusts exceeding 20 m s^{-1} at WSY and 30 m s^{-1} at SIL, representing 826 and 741 instances, respectively. During the winter half-year, the 1500-1800 UTC interval follows sunrise, and the other period falls in the evening before local midnight. At both locations, fast winds are rarely observed in the afternoon hours (around 0000 UTC). Although the winds were not controlled for wind direction, the substantial majority of the included observations occurred during Santa Ana events, and thus this distribution can be taken as typical of such conditions. In their case study, Cao and Fovell (2016) showed that although the February 2013 event spanned

[4] WSY gusts observed in the intervals immediately preceding and following this observation were both 27 m s^{-1}, representing GFs of 1.91 and 1.62.

multiple days, the downslope winds were punctuated by pronounced "lull" periods that occurred around 0000 UTC (see their Fig. 6). The diurnal variation is likely tied to boundary layer evolution, which responds to diabatic surface forcing [cf. Smith and Skyllingstad (2011)].

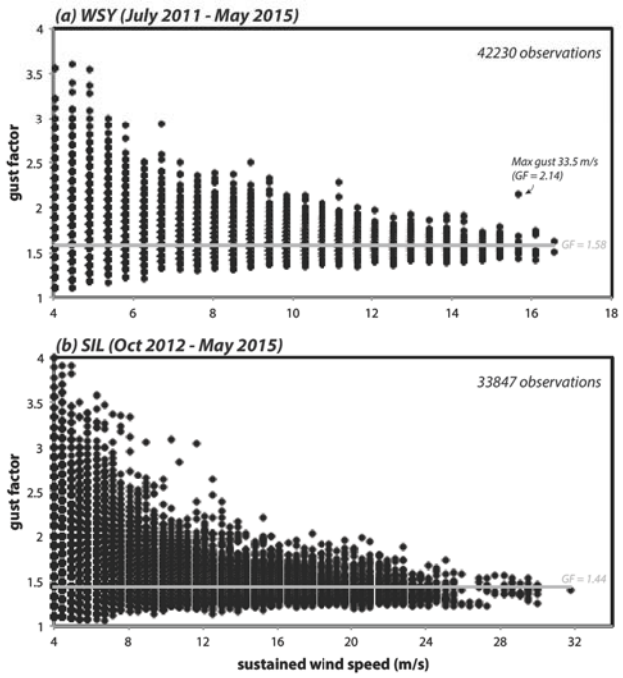

Fig. 3 Gust factors (non-dimensional) calculated from (a) 42230 observation times for the SDG&E station WSY for observations collected during July 2011-May 2015, and (b) 33847 observations times at SDG&E station SIL for observations collected during Oct 2012-May 2015, plotted against the sustained 10-min interval wind speed (m s^{-1}). Grey lines denote constant gust factors of (a) 1.58 and (b) 1.44 respectively. Note horizontal axes have different ranges.

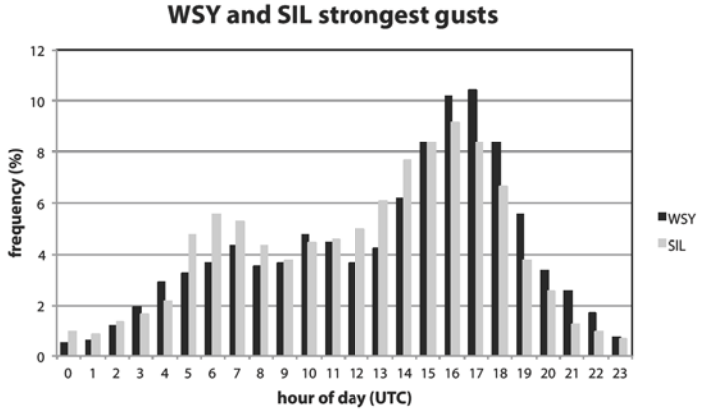

Fig. 4 Hourly frequency of the strongest observed wind gusts at WSY (black bars) and SIL (grey bars). Data from station installation through May 2015 were used, independent of season and wind direction, representing 826 observations ≥ 20 m s^{-1} at WSY and 741 observations ≥ 30 m s^{-1} at SIL.

4. The 13-15 May 2014 Santa Ana wind event

4.1 Event evolution

Southern California has a Mediterranean type climate, consisting of hot and usually quite dry summers. As a consequence, the majority of the most destructive fires associated with Santa Ana wind events have occurred in the autumn, prior to the onset of the winter rains (Sommers 1978, Westerling *et al*. 2004). A glaring exception was the mid-May 2014 Santa Ana event, which was notable for sparking as many as 15 fires, including five exceeding 1000 acres (4 km^2) and a smaller one (the Poinsettia fire) responsible for destroying more than a dozen structures[5,6]. High temperatures and very low humidities combined with prolonged drought conditions to make the landscape more susceptible than usual to fierce downslope winds. This episode ranked second by event maximum observed gust at WSY (Table 1), and produced the 11 of the 22 fastest gust samples in this station's record. It was SIL's fifth-ranked episode, producing that station's 45th largest wind gust observation.

The May 2014 episode's network-averaged sustained winds reveal two peaks of roughly equal strength both occurring around 1700 UTC (10 AM local daylight time), about 4 hours after sunrise, separated by a pronounced lull in the early evening at 0400 UTC, about 90 min after sunset (**Fig. 5**). Both the magnitude and the temporal variation of the mesonet-averaged winds are well captured in the simulation, which was initialized with NAM grids at 0600 UTC on 13 May and integrated for 54 h. While the figure demonstrates that the network-averaged wind bias is nearly zero, **Fig. 6a** reveals some stations are better handled than others. As was shown in Cao and Fovell (2016), the wind bias is quite variable in space, especially in the "central area" (**Fig. 6b**). Note that while WSY is well-predicted with respect to the event-averaged wind, SIL and several other stations are dramatically underforecasted and the simulated YSA (Santa Ysabel) and PIH (Pine Hills) winds are too strong.

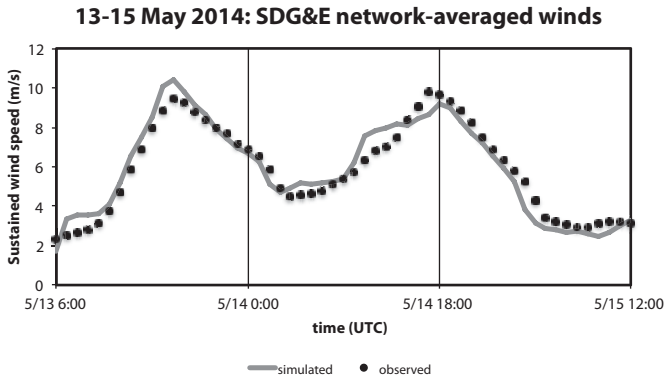

Fig. 5 Time series of SDG&E network-averaged sustained winds observed (black dots) and simulated (grey curve) for the 13-15 May 2014 Santa Ana wind event, based on 142 stations.

5 https://en.wikipedia.org/wiki/May_2014_San_Diego_County_wildfires.

6 http://www.carlsbadca.gov/news/displaynews.asp?NewsID=769&TargetID=1.

Somewhat similar to Cao and Fovell (2016), the May 2014 event's two phases evinced different evolutions in the vicinity of WSY (**Fig. 7a**) with respect to observed winds and gusts. During the first phase, the gusts waxed and waned nearly simultaneously at stations JUL, WSY, WCK, and SSO, which are aligned east to west along the northernmost dashed line shown in **Fig. 6b**, with JUL being close to the ridgeline. Magnitudes were also comparable among those sites, although WSY's winds were more variable and more subject to relatively short-period wind bursts, as defined earlier. The wind gust observed at WSY at 1500 UTC on May 13th was the 12th fastest recorded during the station's period of record, and tied for 5th for this particular event.

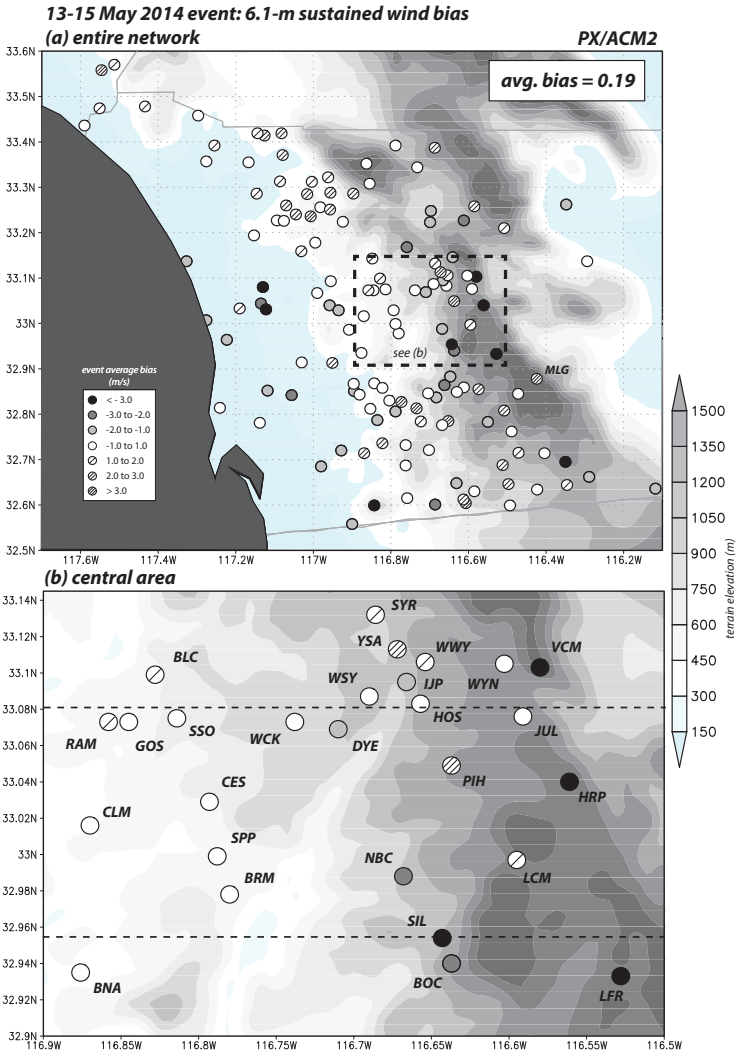

Fig. 6 Event-average wind bias relative to the observed wind for the 13-15 May 2014 Santa Ana wind event, using the control model configuration (including the PX/ACM2 physics combination) showing (a) the full SDG&E network, and (b) stations in the central area including WSY and SIL. Model topography of the 2 km domain (longitude on abscissa, latitude on ordinate) is shown as the shaded field.

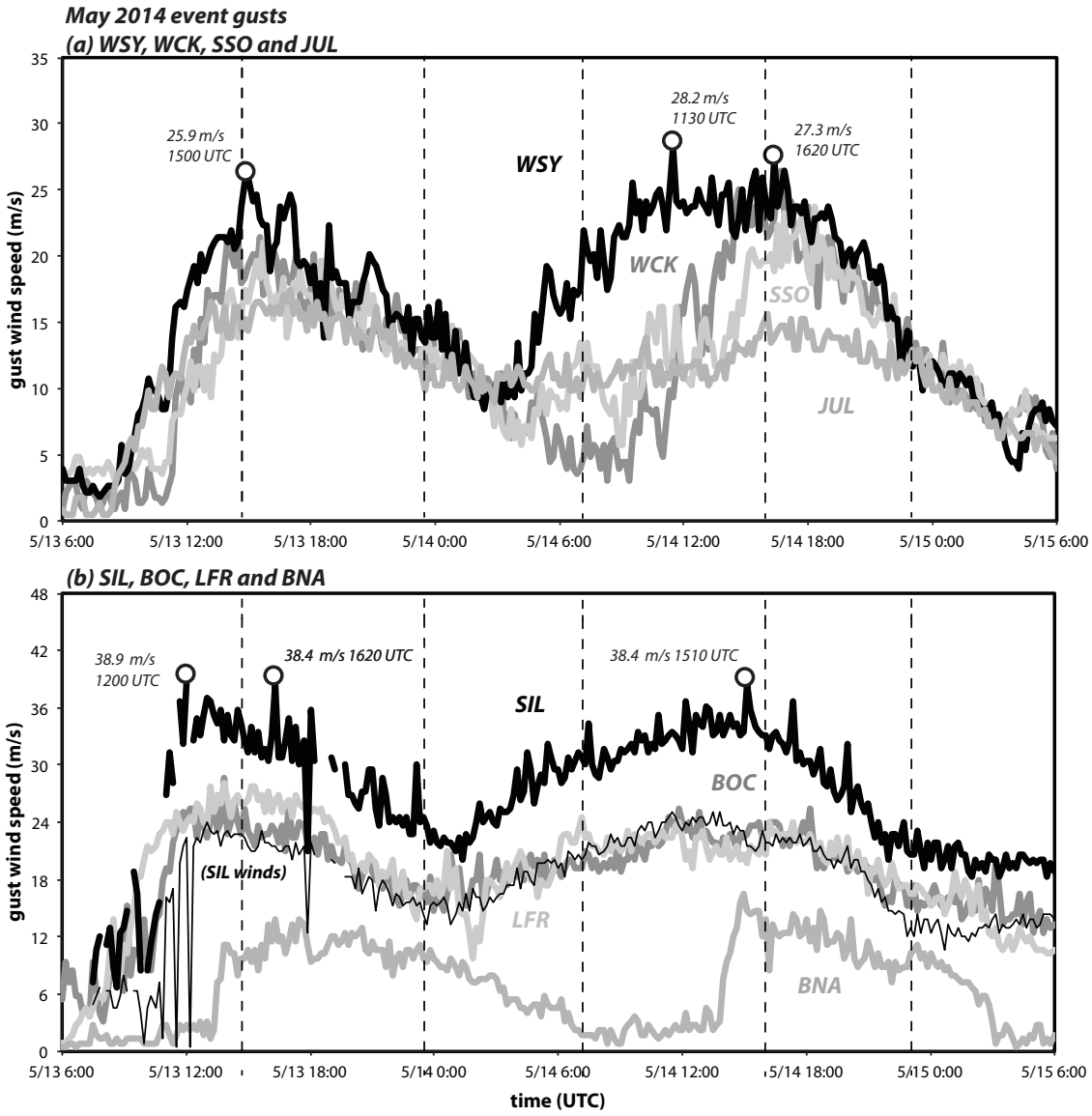

Fig. 7 Time series of observed gusts (m s^{-1}) over two days at (a) WSY, WCK, SSO and JUL; and (b) SIL, BOC, LFR and BNA. On (b), sustained winds (thin black line) for SIL are superposed. Vertical dashed lines correspond to times of Fig. 8. Some maxima are highlighted.

Figure 8 presents vertical cross-sections of the westerly wind component (with negative values for east-to-west flow), taken along **Fig. 6b**'s northernmost dashed line. Superposed are isentropes, being isolines of virtual potential temperature (θ_v), a property defined as

$$\theta_v = T\left(1.0 + 0.61 q_v\right)\left[\frac{p_0}{p}\right]^{R_d/c_{pd}} \quad (2)$$

where T is absolute temperature, q_v is the water vapor specific humidity (kg of vapor per kg of air), p is the pressure, the reference pressure p_0 is 1000 hPa, and R_d and c_{pd} are the dry air gas constant and specific heat at constant pressure, respectively. θ_v is conserved in the absence of diabatic heating and mixing, and can be used to roughly visualize flow streamlines (rather than trajectories) as well as stability (via their vertical variation). During this phase, the model produced a deep and spatially extensive layer of strong easterly winds west of the ridgeline (**Fig. 8a**). Note that westbound parcels passing over the crest are subject to considerable descent. The winds extended far along the slope before and after this time (not shown), and even reached the coastline where the Bernardo fire started (at about 1700 UTC on May 13th). In many Santa Ana wind events, the winds have lofted well above the ground by the time the flow has reached the ocean.

By 0000 UTC May 14th (**Fig. 8b**), the winds had diminished almost everywhere. The observations (**Fig. 7a**) and simulation (**Figs. 8c-d**) both suggest the second phase exhibited a clear downslope progression, as faster winds appeared earlier (i.e., the lull ending sooner) higher up on the slope. During this second phase, wind speeds remained decidedly weaker at the ridge (JUL). This is reminiscent of the second half of the February 2013 episode (Cao and Fovell 2016), and is captured in the model cross-sections. The weak flow seen at 0000 UTC May 15th (**Fig. 8e**) is not just a lull, but also the end of this roughly 2-day event.

At SIL (**Fig. 7b**), gusts exceeded 38 m s^{-1} during both phases, representing the fastest winds observed in the mesonet during this event. Like WSY, the Sill Hill site evinced frequent, short-period spikes in the reported gusts. Note that the flow at anemometer level was much weaker at BOC, only 1.6 km away and slightly farther (at 1130 m MSL) up the slope, and at LFR (11 km away, at 1445 m MSL). In fact, as occurred in the February 2013 episode, SIL's sustained winds were comparable to BOC's (also LFR's) *gusts*. There is good reason to believe that the reported winds are characteristic of the site, and the equipment is operating properly (Brian D'Agostino and Steve Vanderburg, personal communication, 2013). As SIL and BOC represent neighboring grid points on the 667 m grid (and the same point at coarser resolution), forecasts for the two sites are nearly identical, so it would be impossible to accurately simulate the winds at both sites simultaneously. The topographic feature that ostensibly helps SIL's winds to often be so much stronger than BOC's during Santa Ana wind events is not resolvable in the current experiment.

The broader-scale topography in the west-east plane crossing SIL is much steeper than it was across WSY, and the model suggests that the strong flow tended to be shallower as well as to conform more closely to the terrain during the first phase of the event (**Fig. 8f**). This characteristic places faster winds closer to the surface in the vicinity of Sill Hill. Following the lull, the simulated winds were lofted to the west of SIL as the second phase commenced (**Figs. 8g-h**), but subsequently descended to the surface again (**Fig. 8i**). This is consistent with the observations recorded at BNA, located farther down the slope (**Figs. 6, 7b**). (Note the sudden increase in wind speeds following 1400 UTC May 14th, which falls between the times of **Figs. 8h and i.**) At all times, the strongest winds tend to be found in the local terrain depression located just downslope of SIL, in an area devoid of stations. It is possible the windiest spot in San Diego County is actually just downslope from the Sill Hill site.

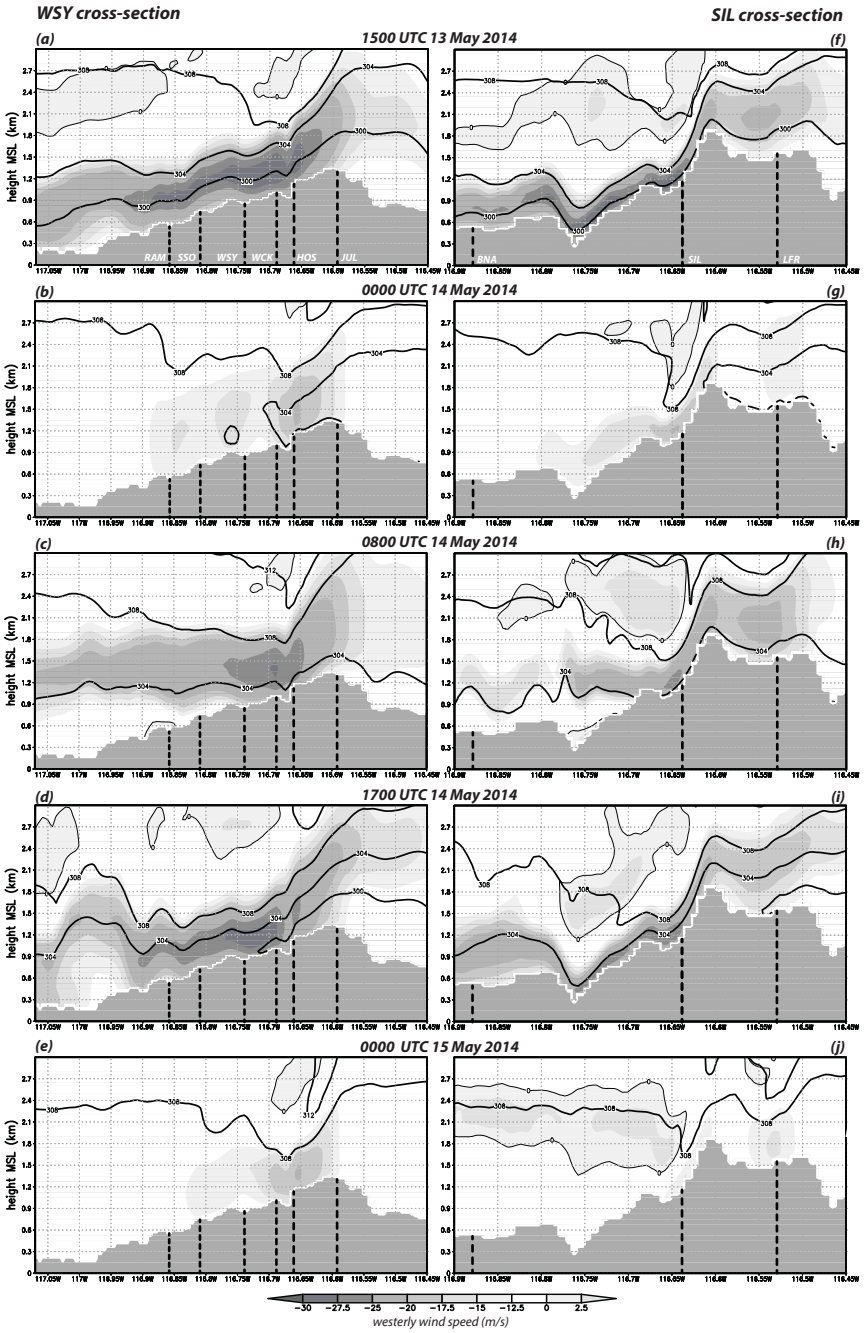

Fig. 8 West-east vertical cross-sections (longitude on abscissa) of zonal wind speed (shaded, with zero thin contours) for five times during the 13-15 May 2014 event, taken west-east across (a-e) WSY and (f-j) SIL with underlying topography in grey (see Fig. 6b). Thick contours denote isentropes of virtual potential temperature (4 K interval). Approximate locations of some SDG&E stations are marked. Stations WCK, SSO, JUL, RAM, HOS, BNA, and LFR are displaced somewhat from the vertical plane depicted.

4.2 Inferring wind gusts from sustained wind forecasts

Accurate predictions of winds and gusts for locations in San Diego County, particularly for the Witch fire site during the October 2007 event, are essential since winds and gusts help spread fires. An important part of this exercise is model calibration, to identify and mitigate (if not eliminate) biases from the sustained wind reconstructions. Because gusts can fluctuate so rapidly with time at some stations, as demonstrated above for WSY and SIL, we have to accept that any particular forecast may possess considerable error, but our expectation is we can learn something useful about how fast an event's maximum winds might be and when they might occur.

Figure 9 compares simulated with observed sustained winds at WSY, SIL, and three other nearby stations for the May 2014 case. Both the magnitude and the evolution of the winds are well simulated at WSY but are significantly underpredicted at SIL. As suggested by **Fig. 6b**, forecasts at stations IJP and VCM are also negatively biased while YSA is overpredicted by 100%. As with SIL, the negative biases at IJP and VCM likely represent unresolved landforms that serve to amplify the offshore wind at those sites. Station YSA is sited just west of a very steep cliff that is not rendered properly even in the 667 m domain, placing the actual site in an unresolved wind shadow.

The most poorly handled stations are quite consistent from event to event. **Figure 10** presents average event sustained wind biases aggregated over five separate episodes (February and October 2013, April and May 2014, and January 2015) for 137 stations consistently available since 2013. The distribution of errors among stations is essentially Gaussian with (as in the May 2014 case) a mean bias that is statistically indistinct from zero. YSA has second-highest positive average forecast error (3.2 m s^{-1}) among the 137 stations included in this analysis[7] while SIL's is -8.4 m s^{-1}. Much of the west-facing slope is shrubland but the vegetation density around PIH is greater than in other areas and higher than suggested by the model's landuse database, likely explaining its weaker-than-predicted winds. These systematic biases most likely represent unfixable localized exposure issues and terrain features that are unresolvable on the model grid. The biases at WSY and WCK are -0.4 and -0.5 m s^{-1}, respectively, which we consider negligible.

Figure 11 presents gust forecasts for WSY and SIL for the May 2014 Santa Ana and two other events that will be examined later. For WSY, the gust predictions were obtained by multiplying the sustained wind forecasts by 1.7, representing the average GF for all observations from this site with sustained winds exceeding 4 m s^{-1}. While **Fig. 3a** suggests a smaller multiplier might be appropriate, the 1.7 GF appears to work well. Some events are captured somewhat more faithfully than others, but the magnitude and timing of event's largest gusts are adequately identified. For SIL, the multiplier used was 1.6, again being representing the average GF for winds $\geq$ 4 m s^{-1}, applied to bias-corrected sustained winds (i.e., increased by 8.4 m s^{-1}). The plots suggest that underprediction remains an issue with this multiplier.

---

[7] The largest positive bias, 3.7 m s^{-1}, is at station MLG, a ridgetop site closely surrounded by trees; see Fig. 6a.

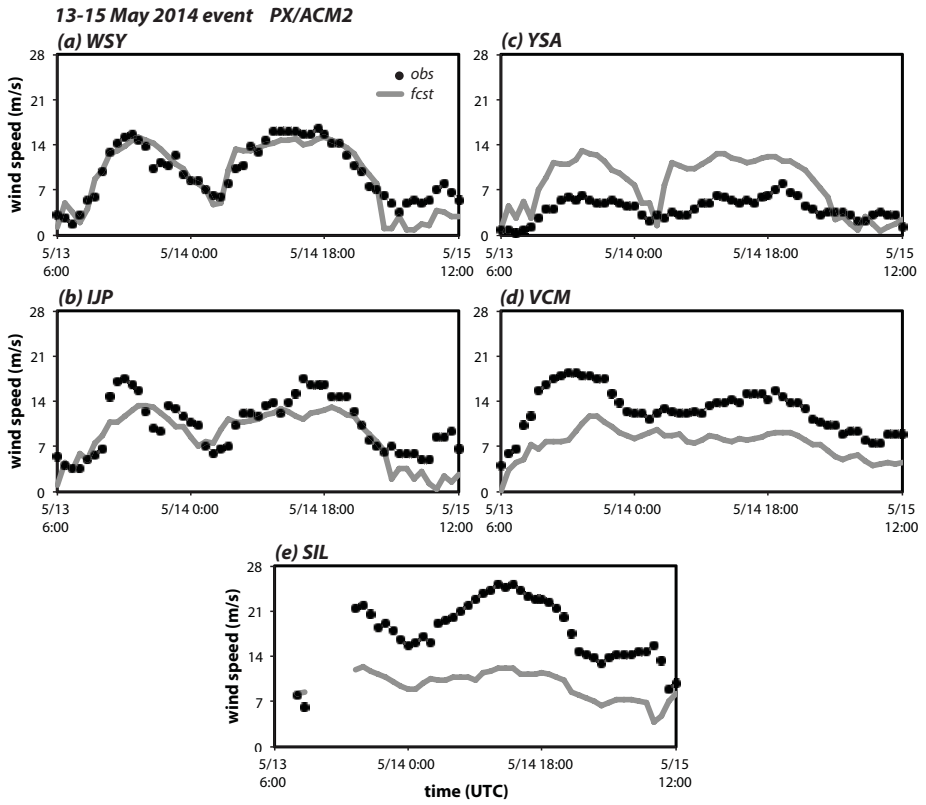

Fig. 9 Time series of observed (black dots) and predicted (grey curves) 6.1-m sustained winds (m s^{-1}) for the 13-15 May 2014 event at stations (a) WSY, (b) IJP, (c) YSA, (d) VCM, and (e) SIL.

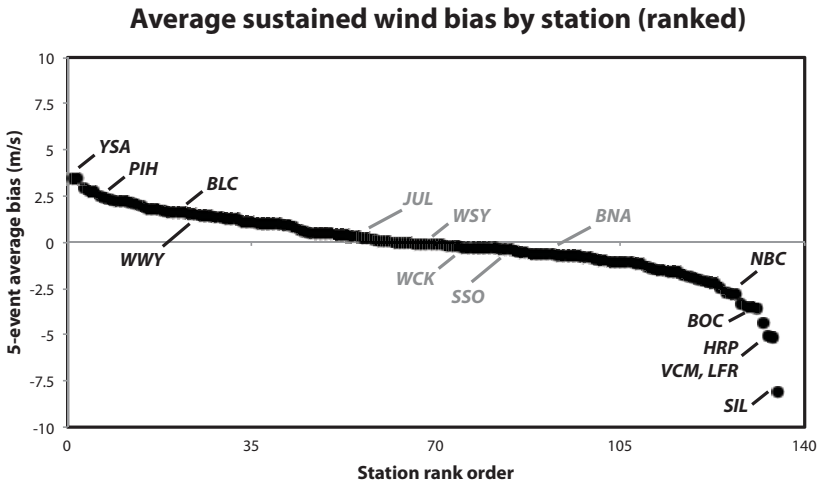

Fig. 10 Sustained wind bias, averaged over five Santa Ana events (February and October 2013, April and May 2014, and January 2015), in rank order with selected stations identified. Only the 137 stations available for all five events are included.

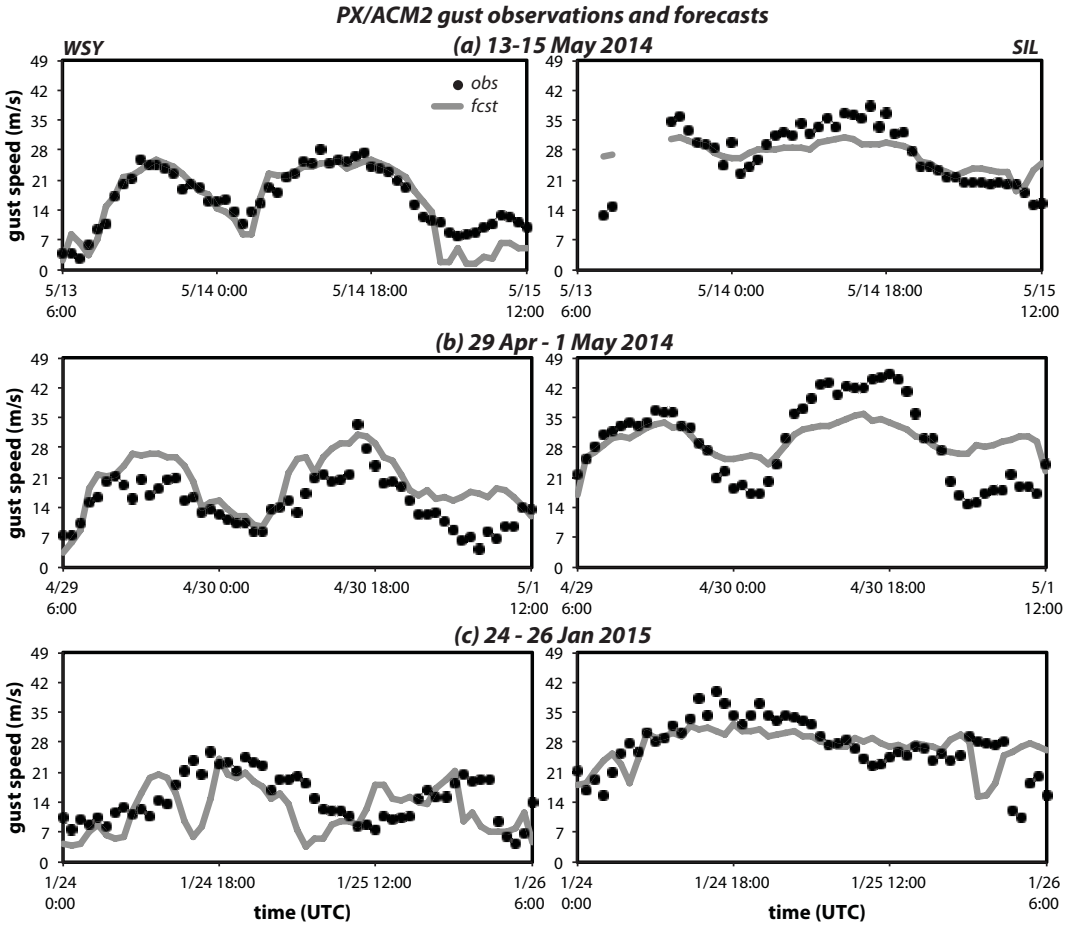

Fig. 11 Time series of observed (black dots) and predicted (grey curves) 6.1-m wind gusts (m s^{-1}) at stations WSY (left) and SIL (right) for the (a) 13-15 May 2014, (b) 29 Apr-1 May 2014, and (c) 24-26 Jan 2015 events. Gust factors used to forecast gusts are 1.7 for WSY and 1.6 for SIL respectively.

5. The late-April 2014 Santa Ana wind event

The windstorm that began on 29 April 2014 yielded the fastest recorded wind and gust observations at both WSY and SIL (**Table 1**) during their relatively short histories. The observations (**Fig. 12**) reveal the episode also had two phases separated by a lull between 0000 and 0600 UTC on April 30th. In terms of evolution, both halves of the event resembled the May 2014 episode's first phase in that the winds at WSY, JUL, WCK and SSO remained in sync and of relatively similar strength. WSY's fastest gust, 33 m s^{-1}, occurred at 1600 UTC on April 30th, during a particularly dramatic wind burst that lasted about 60 min, represented the top six gust reports for this event, and included 4 of the 7 largest values in station history. At SIL, the largest gust report was 45 m s^{-1} for 1710 UTC on April 30, but gusts exceeded 40 m s^{-1} repeatedly during a roughly ten-hour period stretching between 0950 and 2000 UTC. This event accounted for the top 23 gust observations at this site, and 40 of the top 44 readings, all of which surpassed 39 m s^{-1}.

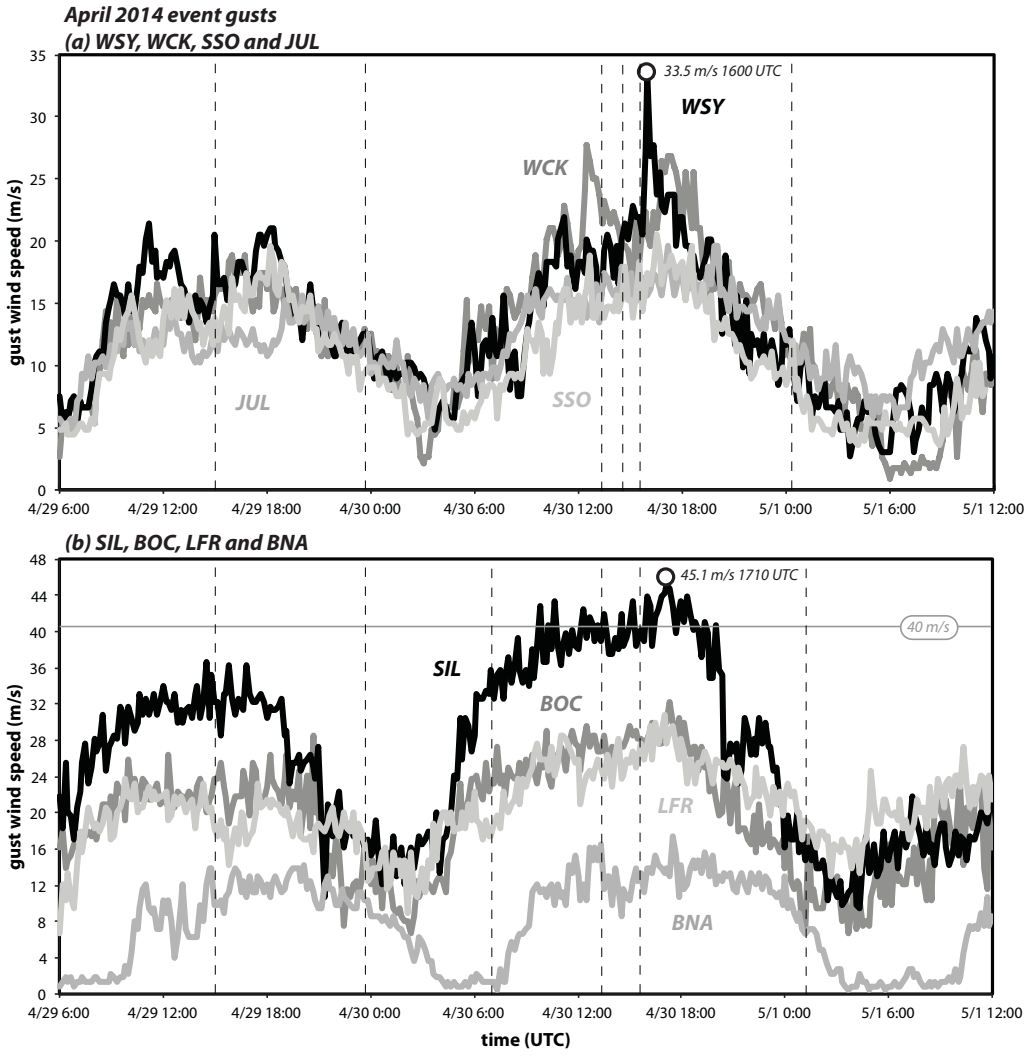

Fig. 12 Time series of observed gusts (m s^{-1}) over two days and six hours at (a) WSY, WCK, SSO and JUL; and (b) SIL, BOC, LFR and BNA. Some maxima are highlighted. Grey line denotes gust threshold of 40 m s^{-1}.

The evolution of the downslope flow in the west-east cross-section including WSY is shown in **Fig. 13**, from a NAM-initialized simulation commencing at 0600 UTC on 29 April. The strong winds that were seen at 1500 UTC on April 29th, roughly the midpoint of the first phase, had already largely disappeared by 0000 UTC April 30th, the early part of the lull (**Figs. 13a, b**). During the peak of the second phase, an *absolutely unstable* layer develops above WSY, which is revealed by the folding of the 296 K isentrope at 1520 UTC (**Fig. 13e**) and thus represents a θ_v minimum not far above the local ground surface. In subsaturated air, absolute instability is indicated by θ_v decreasing with height. This feature is short-lived but of interest because it might not only assist in the delivery of higher momentum air from aloft downward to the anemometer level but also help further intensify wind gusts through buoyancy-generated turbulence. At WSY,

the top of the unstable layer resides at 180 m AGL, which is at or just below the level of maximum winds at this location.

In **Fig. 14**, isotherms of temperature (in ˚C) are shown along with full horizontal wind speed (dominated by the west-east component in this cross-section) for six times spanning the development of the absolutely unstable layer. Temperature is not a conserved quantity, but the isotherms help illustrate where temperature advection is occurring. Wind speeds are weak at 0400 UTC on April 30th (**Fig. 14a**), which is during the lull, and the horizontal temperature gradient across the mountain is relatively small. However, the sun had already set (by 0230 UTC) and the desert region east of the ridge cools more quickly during the evening hours, so the temperature gradient and winds both start increasing.

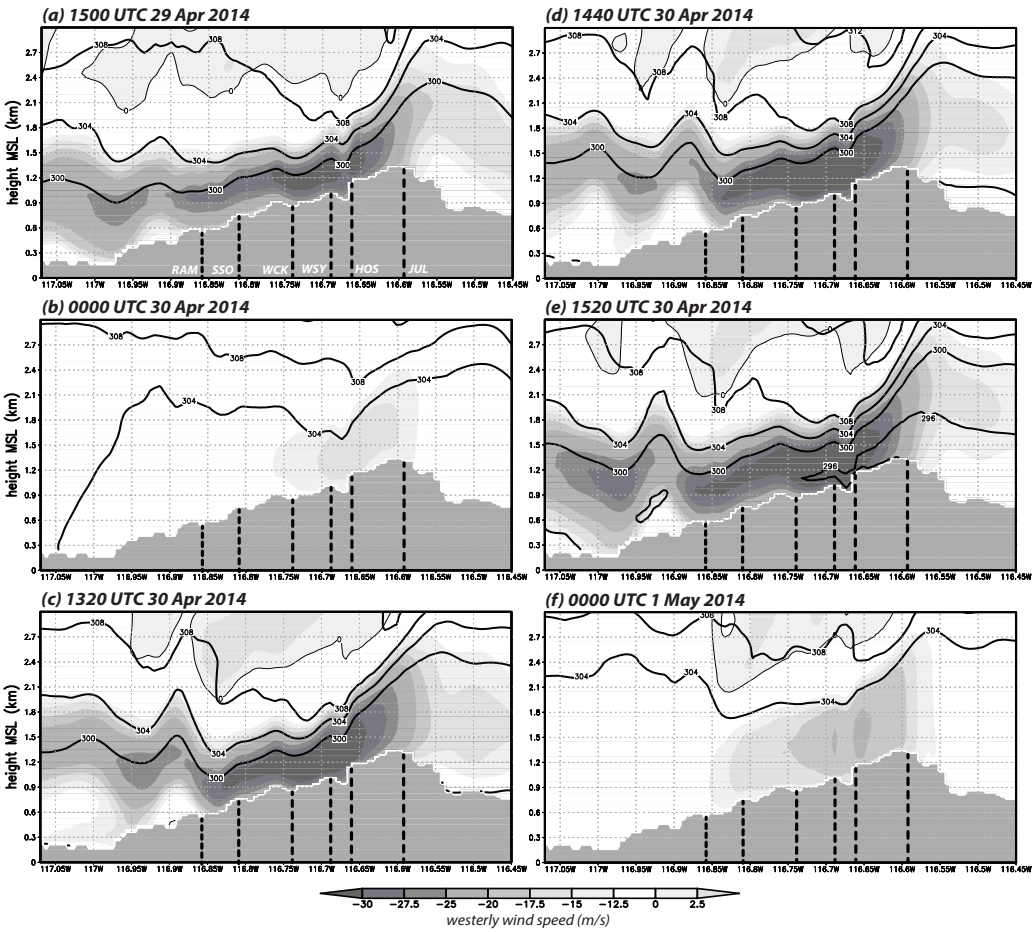

Fig. 13 West-east vertical cross-sections (longitude on abscissa) of zonal wind speed (shaded, with zero thin contours) for six times during the late April 2014 event, taken west-east across WSY with underlying topography in grey (see Fig. 6b). Thick contours denote isentropes of virtual potential temperature (4 K interval). Stations WCK, SSO, JUL, RAM, and HOS are displaced somewhat from the vertical plane depicted.

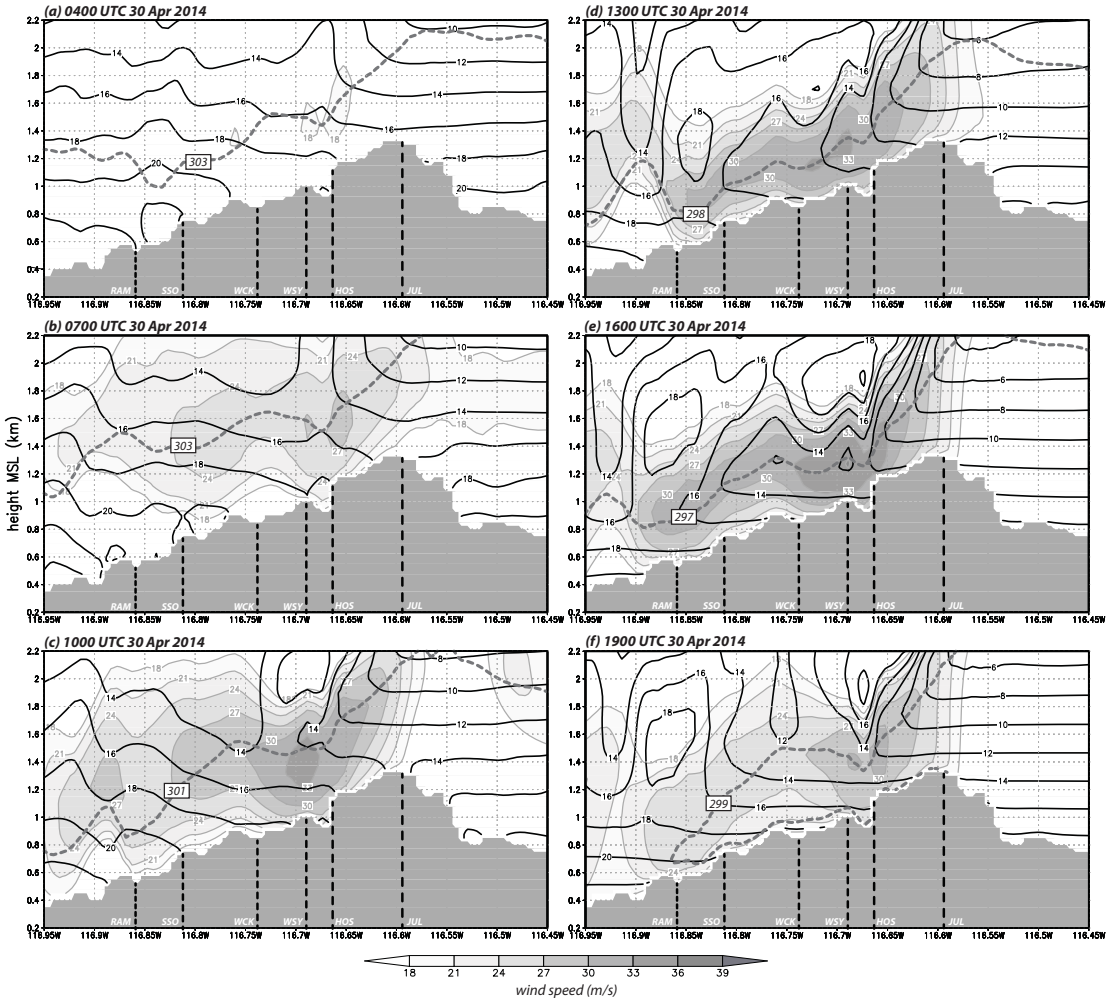

Fig. 14 West-east vertical cross-sections (longitude on abscissa) of full horizontal wind speed for six times during the late April 2014 event (shaded, with 3 m s^{-1} interval grey contours), taken west-east across WSY with underlying topography in grey (see Fig. 6b). Black contours denote isotherms of temperature (2˚C interval). Grey dotted contours denote isentropes of virtual potential temperature. Approximate locations of stations JUL, HOS, WSY, WCK, SSO, and RAM are marked. WCK, SSO, JUL, RAM, and HOS are displaced somewhat from the vertical plane depicted.

As the downslope flow strengthens, note the isotherms take on a concave shape above the upper portion of the lee slope (see especially **Figs. 14d,e**). This is a consequence of *differential* cold advection: the strong winds are pushing colder temperatures from the mountain's windward side down the slope, but less effectively near the surface where the winds are relatively weaker (if only owing to friction). This result is not particularly sensitive to the boundary layer parameterization employed, and occurs despite the vertical mixing it produces. As a consequence, the vertical stability in the layer extending up to the level of maximum winds is being reduced on part of the lee slope during the second episode's peak, to the point where it becomes absolutely unstable.

At favored locations, including WSY, adiabatic cooling is augmenting this destabilization; the selected isentropes (especially on **Figs. 14d,e**) show that the generally descending flow tends to follow the terrain contours. The wind impinging on the uneven terrain induces ascent above WSY (and other hills farther downslope), accounting for the temperature minimum that appears at the maximum wind level by 1600 UTC (**Fig. 14e**). That particular time is a few hours after sunrise (around 1300 UTC), and destabilization disappears as the desert side of the mountain heats up and the winds subside (**Fig. 14f**).

Figure 15a presents vertical profiles of virtual potential temperature for the atmosphere above WSY before and during the development of the absolutely unstable layer. At time #① (1400 UTC), although differential cold advection has been occurring, the vertical stratification is still stable, especially very close to the surface (the model predicted temperature at 2 m AGL is depicted with circles). However, this time is about an hour after sunrise and solar insolation is increasing the surface temperature even as continued cold advection causes the 180 m temperature to fall markedly. Over the next 40 min (to time #②), the vertical lapse rate of the 0-180 m layer becomes absolutely unstable and the instability continues to increase as temperatures at the layer top do not reach minimum until between 1500 and 1600 UTC (the time of **Fig. 14e**). We note that in the observations, the largest gusts and GFs were recorded around this time.

While absolute instability in a shallow layer very close to the surface is common in boundary layers heated from below (especially later in the day), and occurs at other locations around this time, the destabilization in the vicinity of WSY represents particularly effective differential cold advection. The isochrones in **Fig. 16** demonstrate the penetration of potentially cold air at 180 m AGL from the desert side through a terrain gap between Volcan Mountain and North Peak between 1436 and 1500 UTC, and arriving at WSY by 1454 UTC, using θ_v values motivated by **Fig. 15**. During this period, solar insolation is causing temperatures closer to the surface to rise (**Fig. 15a**), thereby decreasing the vertical stability, most dramatically where the 180 m AGL virtual potential temperature is lowest. As the wind speed remains strong through this period (see **Figs. 14d** and **e**), we believe that this could enhance the likelihood of strong winds and gusts occurring in this locality, which might appear in the station record associated with atypically large gust factors, as those tend to be higher under unstable conditions (e.g., Suomi *et al*. 2013).

Figure 17 illustrates how the downslope flow evolves in the west-east plane crossing Sill Hill. As in the May 2014 case, the flow can be intense but often remains shallow, following the terrain closely, particularly in the vicinity of SIL. Panels (c)-(e) sample the extended period of very strong winds and gusts notes earlier (**Fig. 12b**). Again, we believe that part of the reason why sustained winds are so much higher at SIL is that the terrain shape helps bring the strongest winds closer to the surface than occurs at other locations, such as WSY.

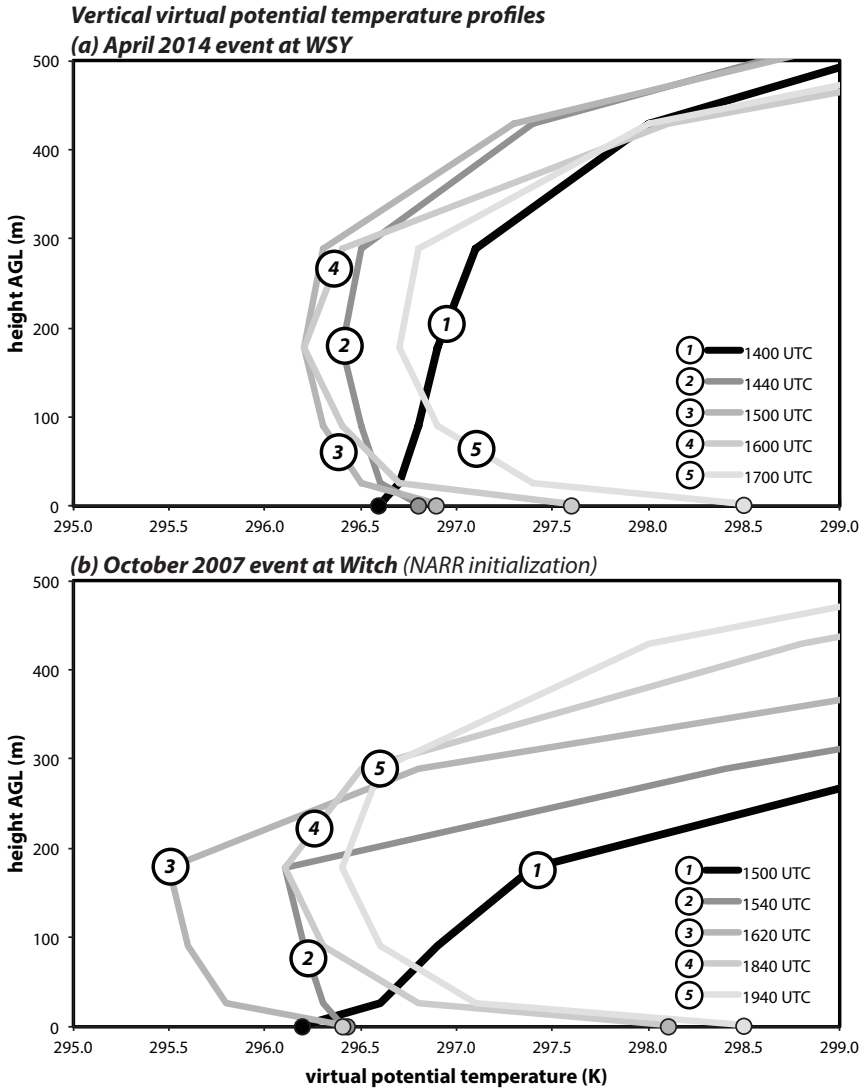

Fig. 15 Vertical profiles over the lowest 500 m AGL of virtual potential temperature for five times (a) above WSY for the April 2014 event and (b) above the Witch ignition site for the October 2007 event. Circles on the horizontal axes represent predictions at 2-m AGL.

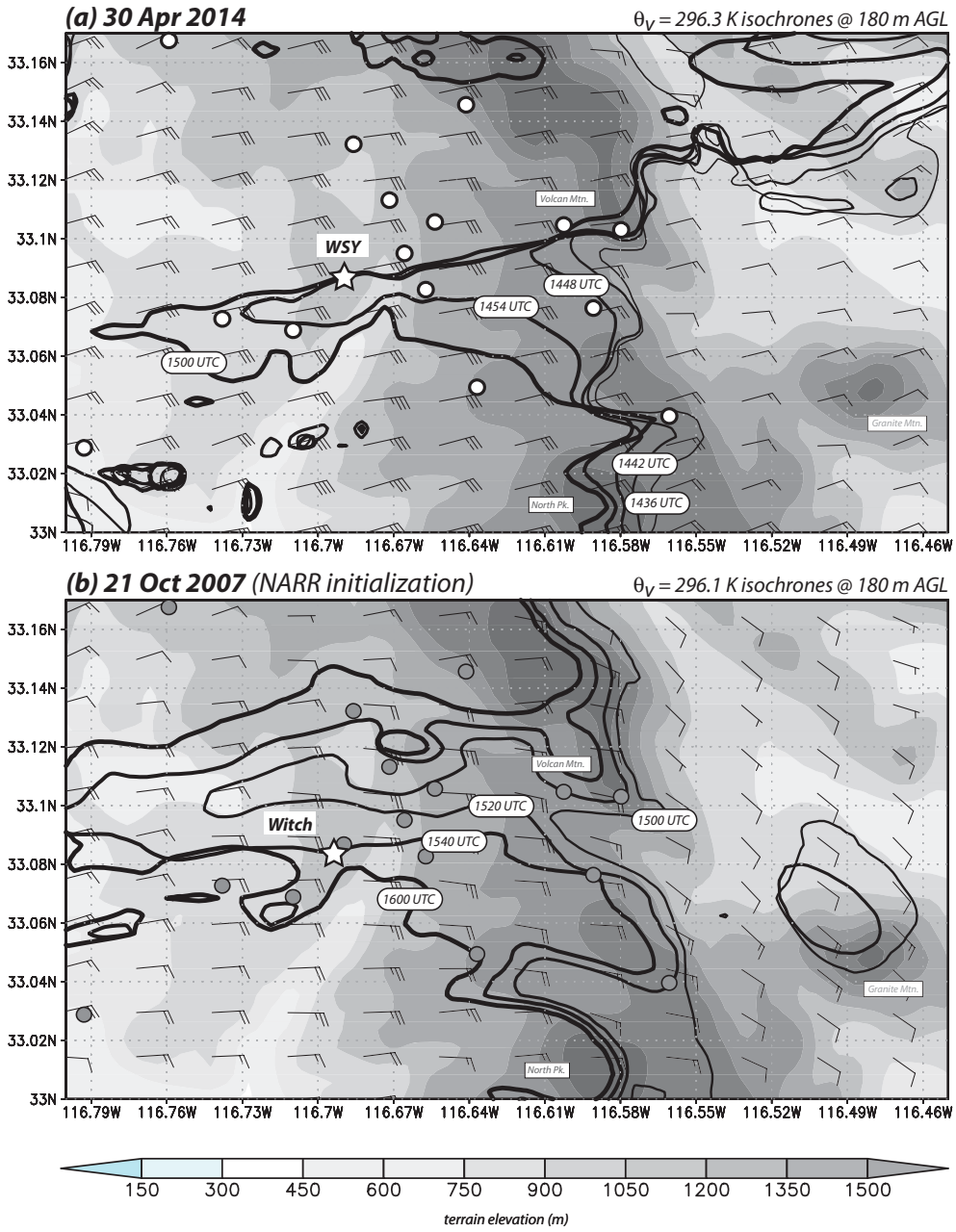

Fig. 16 Isochrones of (a) 296.3 K virtual potential temperature for the 30 April 2014 event, and (b) 296.1 K virtual potential temperature for the 21 October 2007 event, both at 180 m AGL, with topography shaded. Location of WSY on (a) is indicated with a star, and other SDG&E sites with white circles. On (b), the Witch ignition site is indicated with a star, and locations of subsequently installed SDG&E stations with grey circles are shown for reference. Simulated winds at 180 m also shown, with full and half barbs representing 10 and 5 m s^{-1}, respectively.

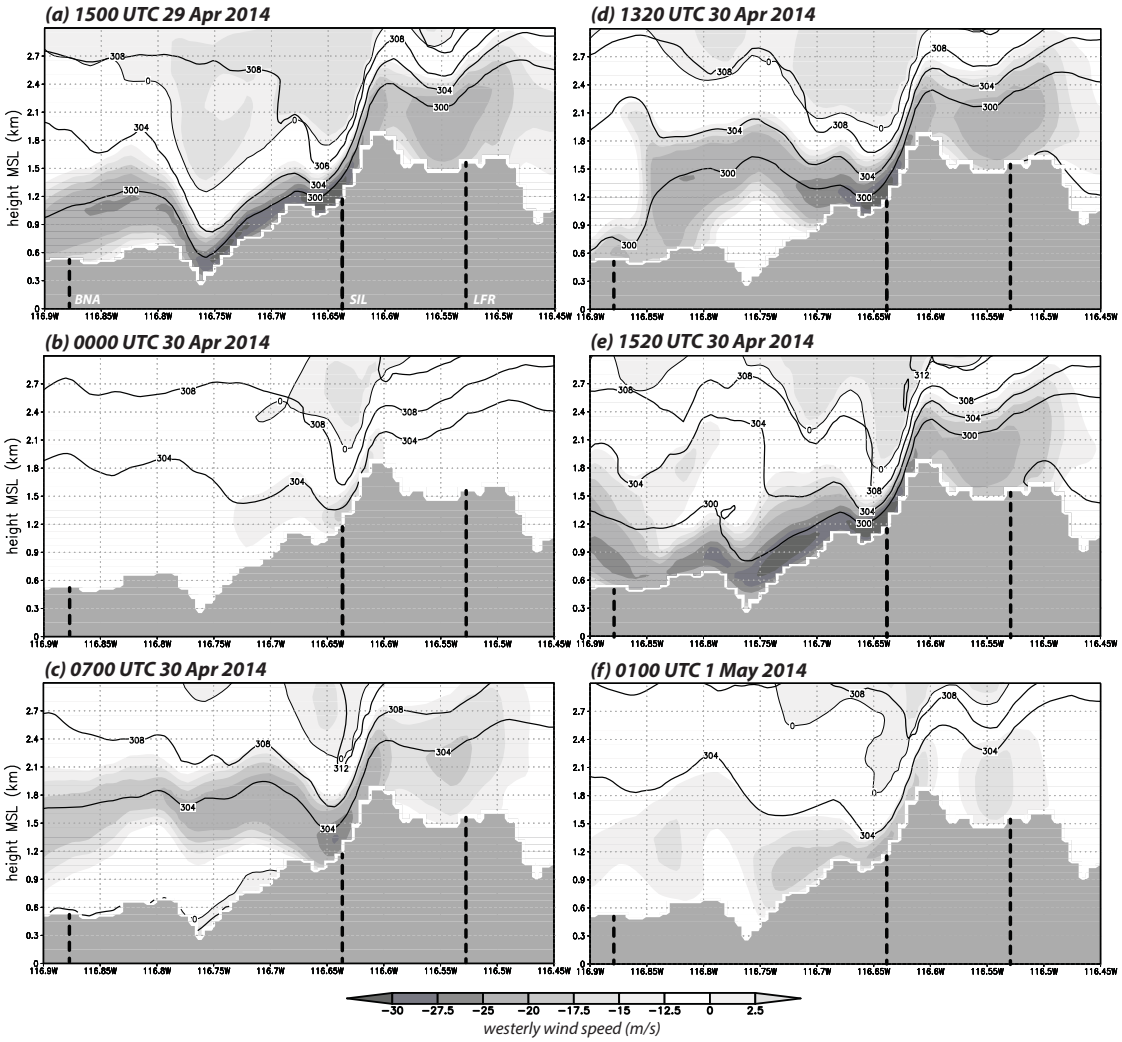

Fig. 17 Similar to Fig. 13, but for the west-east vertical plane across station SIL.

6. The October 2007 Santa Ana wind event

As noted earlier, the October 2007 Santa Ana sparked and spread numerous wildfires in Southern California, including the Witch fire that started 0.6 km from subsequently-installed station WSY. In this section, we will examine two simulations of the episode, configured as described for the two 2014 cases discussed above but initiated with different data sources. One (the NAM initialization) employed the analysis and forecast grids produced by the operational NCEP model in real time. That is consistent with the manner in which the other events were initialized, but it should be borne in mind that the operational model changed significantly between 2007 and 2014. The other utilized the NARR reanalysis. Both simulations were started at 0000 UTC on October 21st.

Although they disagree somewhat with respect to intensity and timing, both October 2007 simulations generate an extremely strong Santa Ana wind event, at its peak far more intense than the April 2014 episode. Peak 6.1-m winds at the Witch ignition site were 25 m s^{-1} in both (**Fig. 18**), occurring between 1040 and 1400 UTC on October 22nd, significantly exceeding the largest observation in the WSY record (16.5 m s^{-1}; see **Table 1**). Of particular relevance are the winds at power line height, 20 m AGL, again obtained using Eq. (1). The first significant wind maximum occured around 1800-1900 UTC on October 21st, which coincided with incidents of reported power line sparking or faulting (indicated by the vertical dashed lines). The onset time of the Witch fire is not precisely known, but it must be before 1929 UTC October 21st, as a witness reported the flames at that time.

Also shown on **Fig. 18** are three 20-m gust estimates made using gust factors derived from the WSY observations. As discussed earlier, GFs of 1.4 and 1.7 were exceeded by 99.5 and 15% of all reports at WSY with sustained winds $\geq$ 12 m s^{-1}, and the 2.0 factor represents exceptional bursts, as was observed during the April 2014 event (cf. **Table 1**) when the simulated near-surface layer was absolutely unstable (**Fig. 15a**). For WSY, the 1.7 factor appeared reasonable with respect to both the observations (**Fig. 3a**) and the reconstructions (**Fig. 11**), given the model's lack of bias there. One complicating issue is that GFs could be anticipated to decrease somewhat with height (e.g., Deacon 1955, Monahan and Armendariz 1971, Suomi *et al*. 2013), although it is not clear that would also occur in highly sheared, mountain-driven windstorms. Indeed, there are also reasons to believe that the 1.7 and even 2.0 GF estimates might be too *low* because the model sustained winds could be negatively biased for the Witch fire site. The SIL-BOC comparison illustrates that the wind can differ substantially during a windstorm at two neighboring, well-exposed sites and recall that the Witch fire site is close to a locally steep but to the model unresolvable drop in terrain, and thus in that respect resembles the Sill Hill landscape.

With respect to the 1.7 GF estimate, the simulations suggest that 20-m gusts on the order of 35-38 m s^{-1} could have been expected around the Witch fire onset time, leading up to event-maximum gusts of about 53 m s^{-1}. If the 2.0 GF estimate is justifiable, gusts of 40-45 m s^{-1} could have occurred during the sparking period. During that time, and in a similar manner as for the April 2014 event, an absolutely unstable layer *did* form over the site, as demonstrated in **Fig. 19** for the two simulations at their respective times of maximum winds above Witch/WSY. Focusing for convenience on the NARR-based simulation, note that at 1500 UTC (profile #① in **Fig. 15b**), 63 min after sunrise, the atmosphere above the Witch site was still stable, but absolute instability in the 0-180 m layer was already present by 1540 UTC (profile #②). The first power line fault was reported shortly thereafter (at 1553 UTC). Temperatures at the top of this layer reached minimum around 1620 UTC (profile #③), but the instability persisted past the sparking period's wind maximum for this simulation (1840 UTC, profile #④) and even the latest onset time for the Witch fire (1940 UTC, profile #⑤). As in the April 2014 case, this instability was exacerbated by the opportunistic intrusion of a potentially cold airmass from the desert over the Witch/WSY area after the sun was already heating the surface beneath (**Fig. 16b**).

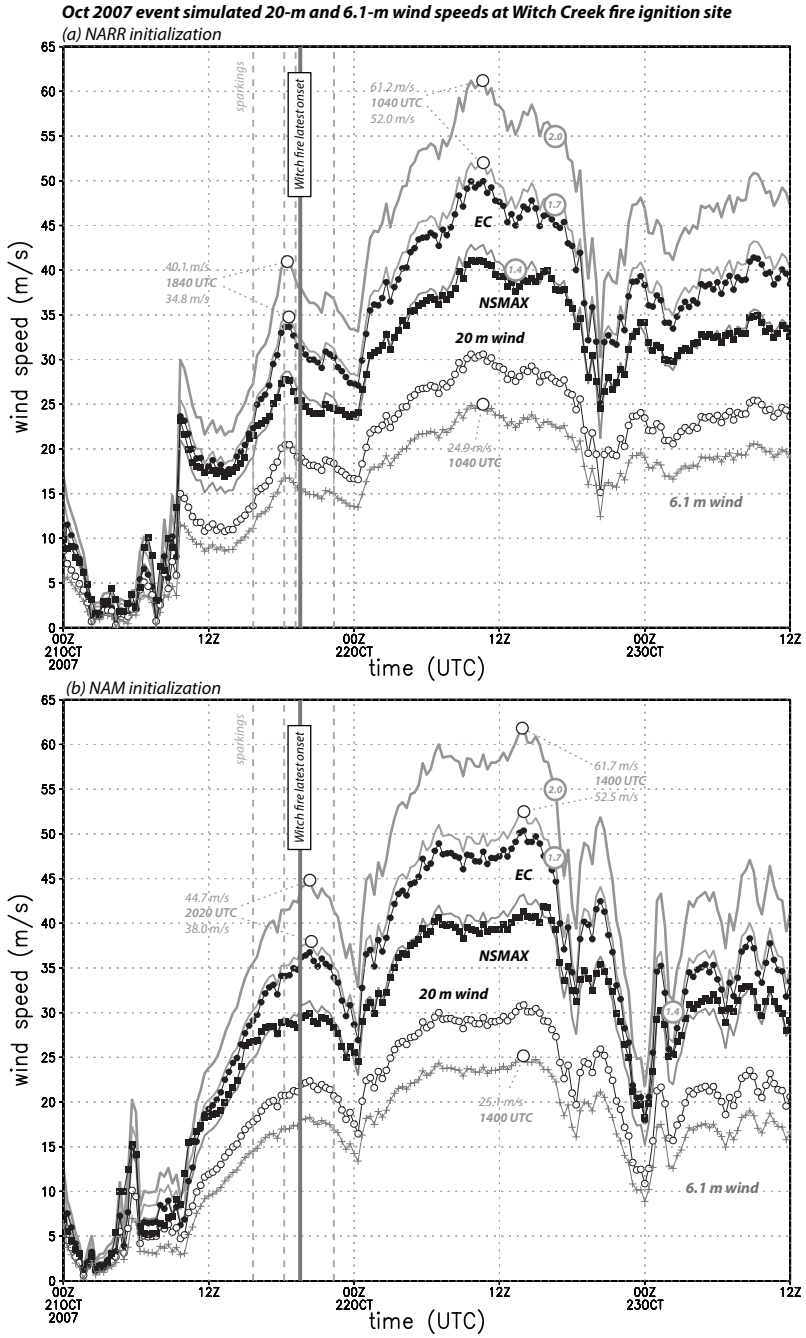

Fig. 18 Time series of 20-m and 6.1-m sustained winds and 20-m estimated gusts (m s^{-1}) employing the EC, NSMAX, and 1.4, 1.7 and 2.0 gust factor metrics at the Witch ignition site over 2.5 days from simulations made with the (a) NARR and (b) NAM initializations. Some maxima highlighted. Vertical grey dashed lines indicate reported power line sparking times, and vertical grey solid line represents the Witch fire latest onset time. Data plotted at 20 min intervals.

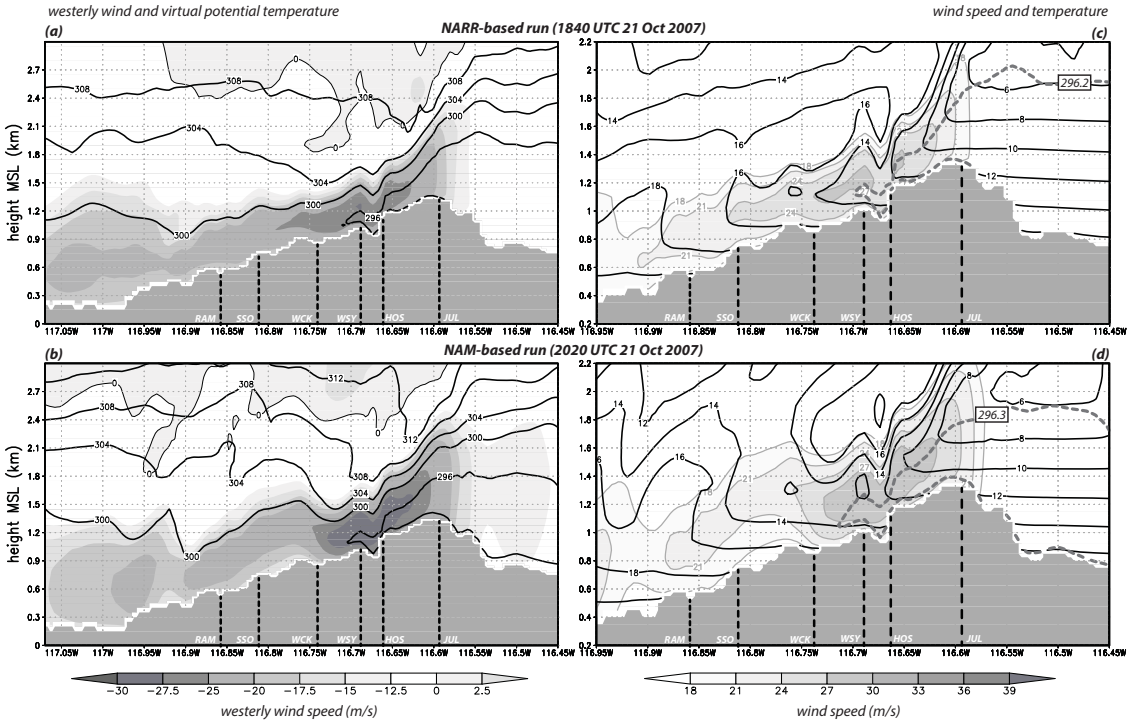

Fig. 19 Similar to Figs. 13 and 14 but for the NARR-initialized and NAM-initialized runs at their respective times of maximum winds at WSY during the sparking period on 21 October 2007.

While they generated relatively comparable winds over the Witch fire site, differing modestly with respect to timing and intensity, the two simulations yielded markedly different flow patterns farther downslope through the event maximum on October 22nd (**Fig. 20**). One run continued to push fast near-surface winds well down the slope, while the other had shifted to more of a lee-wave and/or hydraulic jump behavior in which the strongest winds were lofted. It is appreciated that downslope windstorms can be very sensitive to small shifts in conditions on the upwind side (cf., Durran 1986, Vosper 2004) and Cao and Fovell (2013) and Cao (2015) have demonstrated that in some cases even the infusion of random noise mimicking turbulent perturbations can provoke decidedly different flow structures. During the 2007 event, there were no good observations near the Witch ignition site and, taken together, the results in this study highlight the daunting challenge of inferring wind speeds at specific sites from even high-quality data recorded upwind and farther downwind.

Two additional gust predictions labeled "EC" and "NSMAX" are provided on **Fig. 18**, the former utilizing the equation for non-convective gusts[8] employed by the European Centre for Medium-range Weather Forecasts (ECMWF):

$$V_{gust} \approx V_s + 7.71u_* \tag{3}$$

[8] https://software.ecmwf.int/wiki/display/IFS/CY41R1+Official+IFS+Documentation.

in which V_s is the sustained wind speed and u_* is the friction velocity. This formula was likely developed for the standard anemometer level (10 m AGL) and may not be as applicable farther above the surface. NSMAX (for near-surface maximum) is simply the largest resolved wind speed in the lowest 180 m (the unstable layer top as is shown in **Fig. 15**), based on the assumption this wind could be transported downward to the height of interest by subgrid turbulence [a simple version of Brasseur (2001)]. At the Witch site, the EC gust tracks the reasonable 1.7 GF estimate closely, while NSMAX essentially represents a gust factor of 1.4 so we consider it likely to underpredict the peak winds at that and possibly other locations.

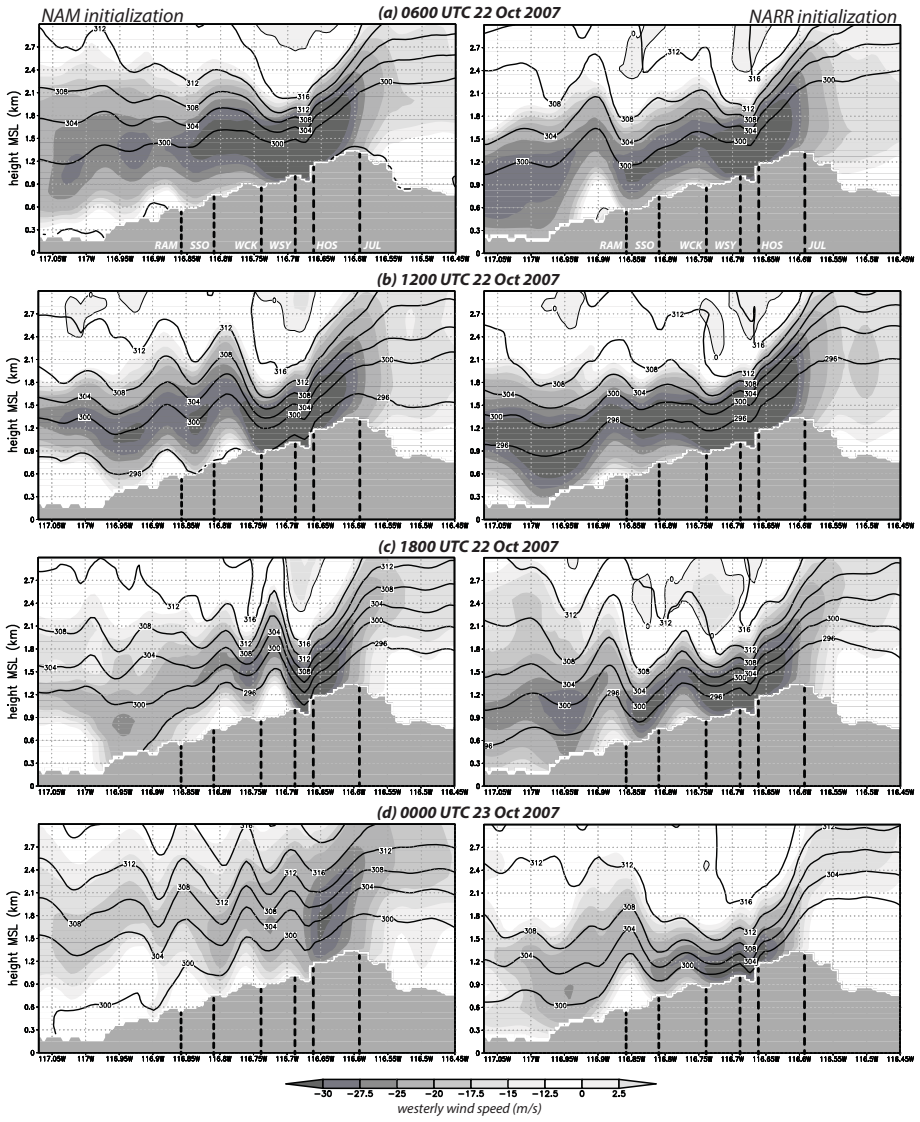

Fig. 20 Similar to Fig. 13, but for four times spanning the peak of the October 2007 event with runs initialized with NAM (left) and NARR (right).

Figure 21 presents the event maximum gusts at the 20-m level computed using the EC formula for the October 2007 (NARR-based run) and April 2014 episodes for part of the SDG&E network. This estimate is not expected to be accurate at every single location, but suffices to illustrate the wind patterns and permit qualitative comparisons among events. The pattern of the two events is very similar, being determined by wind direction and topography, but relative to the April 2014 episode, it is seen that the October 2007 maximum gusts were likely not only more intense, but also more widespread. During the latter, the very strongest winds (exceeding 55 m s^{-1}) appeared in three places: very near the Witch ignition site, at the location of the present SDG&E station Hoskings Ranch (HOS, installed December 2013), and near SIL. The thick black contour highlights gusts ≥ 45 m s^{-1} (100 mph), and during the 2007 event, gusts that strong are also placed close to the ignition point of the Guejito fire, which broke out at 0900 UTC on October 22nd, around the event peak.

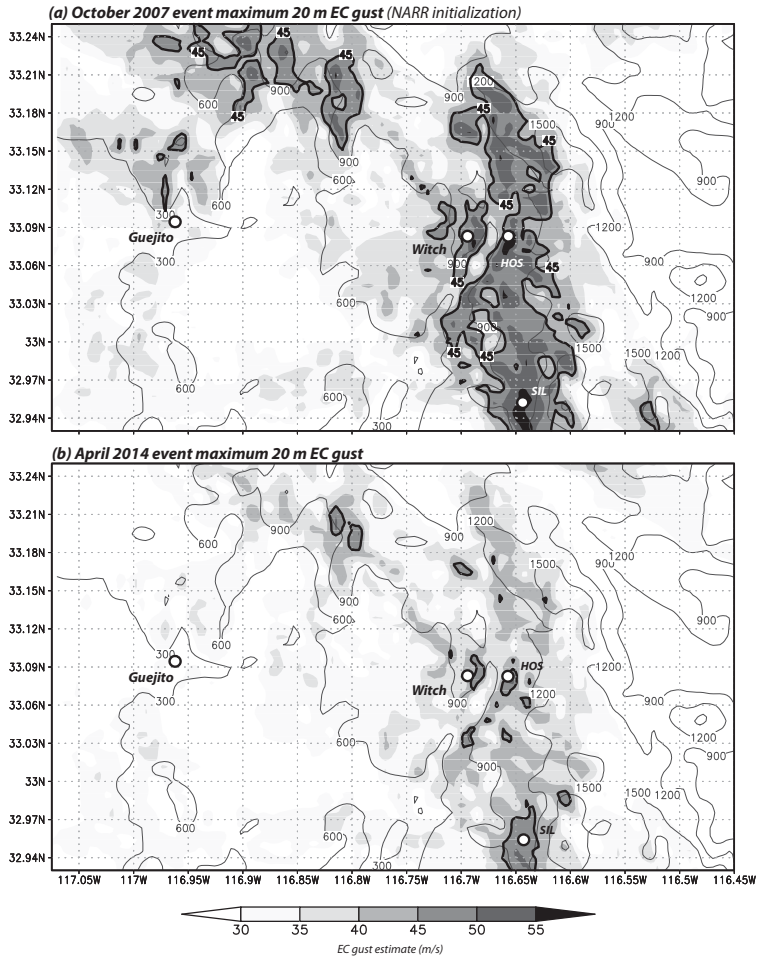

Fig. 21 Maximum simulated 20-m AGL EC gust map (shaded) for the (a) October 2007 (NARR-based run), and (b) April 2014 (NAM-based run) events. Topography (elevation from MSL) is contoured at 300-m intervals (light grey). The thick black contour highlights gusts greater than 45 m s^{-1} (100 mph). Ignition points of October 2007 Witch and Guejito fires are marked.

7. Maximum winds and vertical wind profiles for various Santa Ana wind events

Each Santa Ana wind event produces downslope winds with somewhat different characteristics and intensity, and with considerable temporal variation. A rough gauge of the relative strength of each event may be ascertained from comparisons of maximum winds or gusts (e.g., **Fig. 21**), irrespective of the time at which the maxima actually occurred. In a similar manner, **Fig. 22** presents event-maximum winds in vertical planes oriented west-east across WSY and SIL for five recent Santa Ana wind events, including October 2007 (from the NARR-based run) and four of the strongest episodes since the establishment of the SDG&E mesonet. Vertical profiles for selected stations in these cross-sections are presented in **Fig. 23**.

Among these cases, and in both cross-sections, the October 2007 flow was clearly the fastest nearly everywhere along the lee slope. The largest values (about 41-42 m s^{-1}) are seen immediately above WSY and HOS, and near SIL (**Fig. 22**). Note that, unlike farther up and down the slope, the strong flows at those locations reside fairly close to the surface, and could be expected to be transported relatively easily to the ground by turbulent motions. These wind-favored locations are clearly determined by the terrain profile, as they appear (albeit with weaker wind speeds) consistently among these events.

Recall we previously noted a concern regarding the applicability in complex terrain of the logarithmic wind profile (Eq. 1), which we use to estimate the anemometer-level winds from the lowest model level $z = Z_a$ and, as a consequence, played an important role in our model verification and calibration. Specifically, the log profile is presumed valid within the surface layer, generally regarded as the lowest ~10% of the PBL depth. This is part of a larger issue regarding how well PBL schemes operate in mountainous areas. Boundary layer depths vary with time and among events, but averaged roughly 600 m at the times of maximum winds at WSY and SIL, so 10% of that is 60 m, which exceeds Z_a. It might be instructive to see if the model produces a logarithmic wind profile above $z = Z_a$ and, if so, over what depth.

Figure 24 compares instantaneous profiles of the horizontal wind at WSY and SIL, representing the time at which the near-surface winds were at maximum for several major Santa Ana wind events. Also shown (as dashed curves) are the logarithmic wind profiles (again neglecting the zero-plane displacement) computed using (Eq. 1). The PX LSM employs roughness lengths of 0.18 and 0.87 m, respectively, for the two sites, and static conditions were indeed neutral so ψ_{obs}, $\psi_a \sim 0$. All profiles are scaled with respect to the wind speed at the lowest model level (V_a); this renders the logarithmic profile a function of z_0 only.

Although wind speeds vary substantially, the *normalized* profiles for each station look very similar among the events. For WSY, the log profile fits the simulated winds relatively well, over at least the lowest 100 m. This might suggest that extending the log profile downward from V_a to the anemometer-level wind is reasonable. At SIL, however, the log fit to 6.1 m implies too much vertical shear. This might perhaps suggest that the surface is being treated as too rough at this location[9] and the LSM-assigned roughness value of 0.87 m does appear to be excessive for this

[9] Inclusion of a zero-plane displacement of a few meters would not change the slope of the profile, which is the issue here.

landscape. Recall that the model substantially underforecasts winds at SIL, so employing a less rough surface in this area of the model domain might mitigate the negative forecast bias.

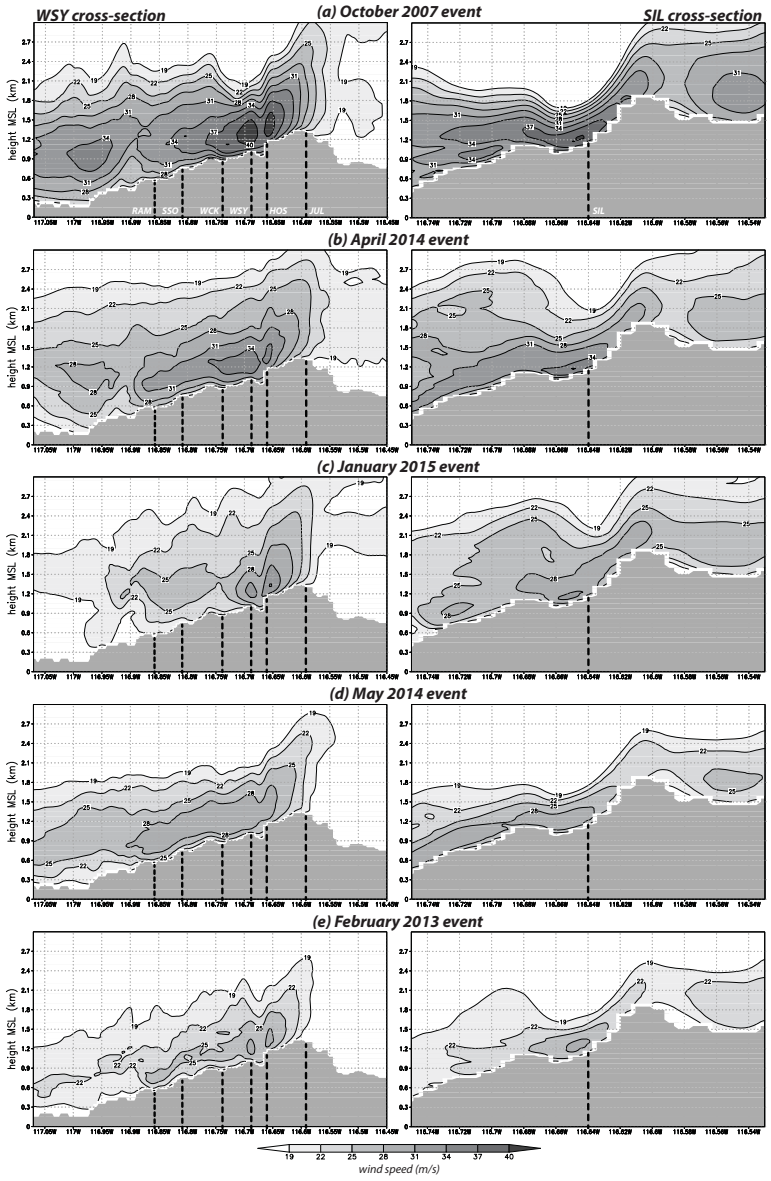

Fig. 22 West-east vertical cross-sections (longitude on abscissa) across WSY (left) and SIL (right) of event maximum winds (m s^{-1}), irrespective of occurrence time, for the (a) October 2007 (NARR-based), (b) April 2014, (c) January 2015, (d) May 2014, and (e) February 2013 events, with topography in grey. Height is above MSL. Some of the locations in the WSY section reside slightly out of the plane depicted. Note the SIL cross-sections span a smaller horizontal distance.

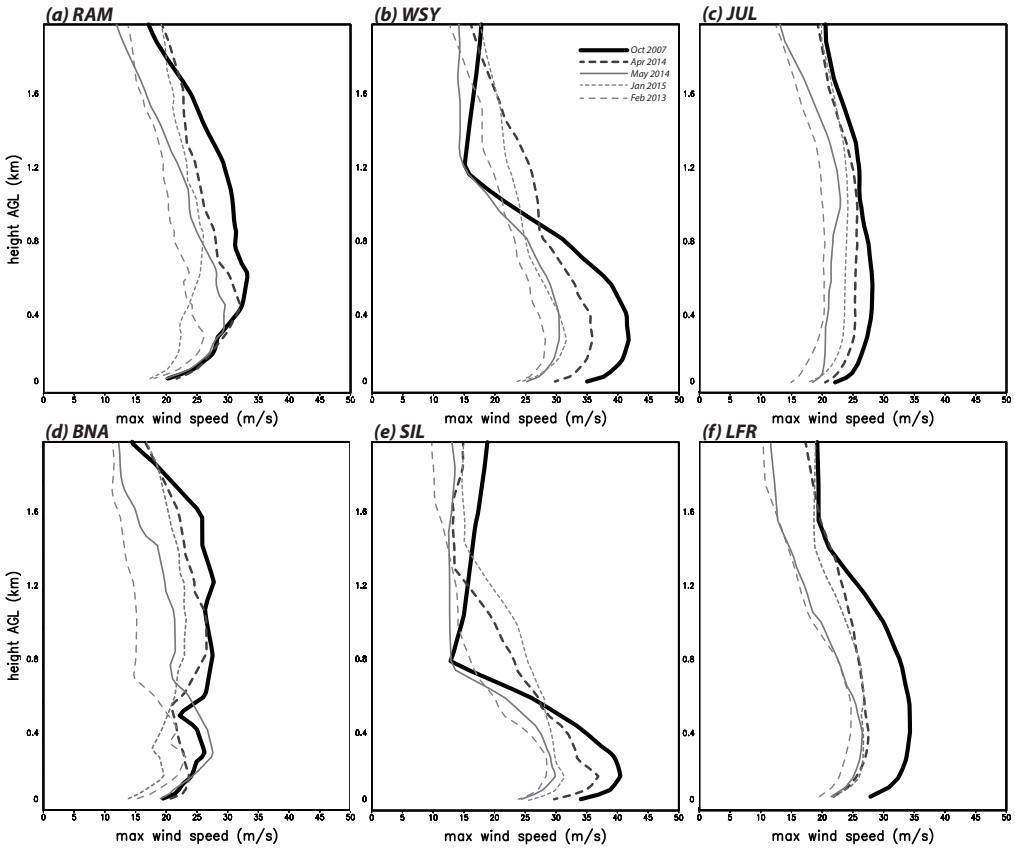

Fig. 23 Vertical profiles over the lowest 2 km AGL of event-maximum horizontal winds at six locations for the October 2007, February 2013, April and May 2014, and January 2015 Santa Ana wind events. As event maxima, the wind speeds shown at each height may not represent a single time for each event and location.

8. Summary and discussion

The Santa Ana winds occur in Southern California between September and May, when high pressure builds in the Great Basin (cf., Raphael 2003, Jones *et a*l. 2010), reversing the normally westerly wind direction so desert air can intrude into the Los Angeles Basin. The winds have characteristics of terrain gap and/or downslope winds at various places through the region (cf. Hughes and Hall 2010, Jackson et al. 2013). We have examined the horizontal, vertical and temporal structure of the winds using a numerical model verified and calibrated against an exceptionally dense network of surface stations in San Diego County, operated by the San Diego Gas and Electric (SDG&E) utility. The model configuration selected did the best job of reproducing the winds at anemometer level (6.1 m AGL) over a variety of Santa Ana wind events (cf., Cao and Fovell 2016).

Three episodes were selected for closer examination herein. Two (occurring during April and May 2014) were motivated by the observational record at SDG&E stations at West Santa Ysabel (WSY) and Sill Hill (SIL), the former sited relatively close to the ignition point of the October 2007 Witch fire, and the latter representing the windiest spot in the mesonet. Along with the February 2013 Santa Ana studied by Cao and Fovell (2016), those cases were among the strongest windstorms that have occurred during the relatively short history of the SDG&E network at WSY and SIL (see **Table 1**). During those events, the sustained winds were strong and gust factors (the ratio between instantaneous gusts and temporally-averaged sustained winds) were higher than average for those stations.

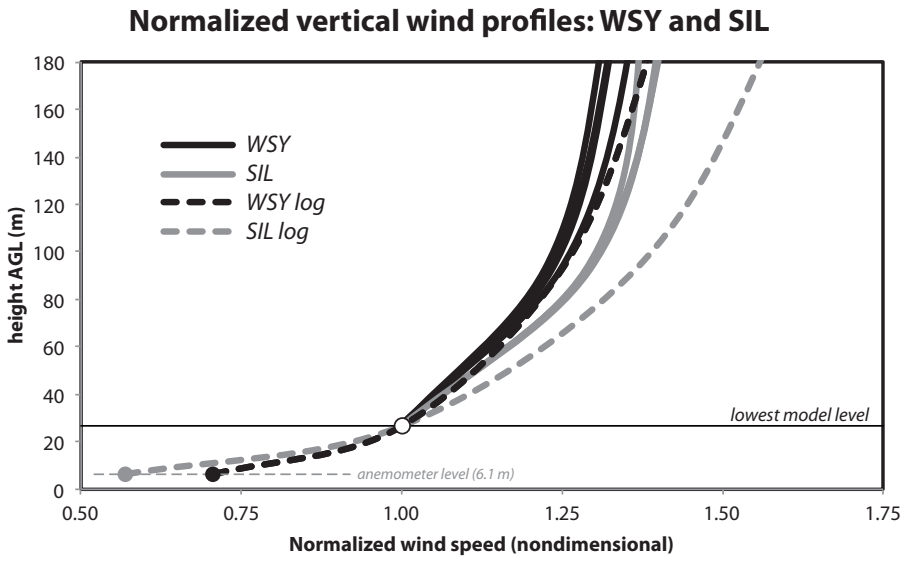

Fig. 24 Vertical profiles of instantaneous horizontal wind speed at WSY (solid black) and SIL (solid grey) for four Santa Ana wind events (October 2007, February 2013, and April and May 2014). Profiles were taken at times representing the maximum wind speed at about 300 m AGL for each event and time. Each profile has been scaled relative to the wind speed at the first model level above the surface (about 27 m AGL). Black and grey circles denote 6.1-m winds estimated using the log wind profile. Dashed curves indicate the logarithmic wind profiles for the two sites, presuming neutral stability and employing surface roughness lengths assigned by the LSM.

Simulations of those and other recent events have been able to capture the network-averaged sustained winds well with respect to strength and temporal variation, albeit with systematic biases at a subset of locations. The sustained winds at both over- and underpredicted stations were likely influenced by landforms that were not resolvable, even on the highest resolution grid (667 m) employed. WSY, located in a well-exposed, largely treeless area, was one of the best-handled sites, while the reconstructed winds at SIL were far too slow. One of the factors that might account for the severe underprediction at SIL is the presence of a steep slope very near the station that does not appear on the model grid; in a similar fashion, there is a sharp terrain depression near the Witch fire site that contrasts with the more level landscape near WSY, 0.6 km away to the northeast.

Statistics for WSY and SIL showed that the frequency of strong gusts is highest between 1500-1800 UTC, which is in the morning hours after sunrise in San Diego. During those hours in the April 2014 episode simulation, an absolutely unstable layer formed over WSY, possibly supporting turbulence that could help generate particularly strong winds and convey them to the surface as gusts. Rather than a consequence of surface heating alone, this instability also resulted from differential cold advection associated with a cold, desert air mass pushing through the terrain gap to the east of the Santa Ysabel area. The unstable layer at WSY was about 200 m deep, extending up to the level where horizontal wind speeds were the highest, and the WSY record gust (still current at this writing) occurred at this time, along with a very large gust factor (> 2.0). One might expect that instability driven by surface heating would be largest during the afternoon hours, but the winds and gusts tended to be weaker then because the temperature difference across the mountains is typically smaller.

The third event was the historically dramatic Santa Ana episode of late October 2007 that produced the Witch fire and over twenty other blazes. The event likely produced the strongest winds in the last half-century or so across a large portion of the region, but available observations were few in number, some questionable in quality (Cao and Fovell 2016, Fovell 2012), and all rather far removed from the fire ignition site. As in the April 2014 episode, and for the same reasons, an absolutely unstable layer formed over the Witch site during the period in which the power lines were observed to be arcing. Based on gust factors observed during April 2014, gusts as large as 45 m s^{-1} could have impacted the sparking power lines, even before considering the potential influence of the aforementioned unresolved terrain depression near the ignition site.

One of the most compelling findings that have emerged from the high-density SDG&E mesonet is how much winds can vary over short distances. This observational dataset, the present study, and our previous work (Cao and Fovell 2016, Cao 2015, Fovell and Cao 2014, Cao and Fovell 2013, and Fovell 2012), combine to demonstrate that great care is required in the estimation of winds and gusts at specific locations from observations at sites located even relatively nearby, and/or from incompletely calibrated simulations, especially those employing coarser resolution. Simulations can also be very sensitive to model physics, initialization, and even small perturbations. This applies not only to winds at particular heights, such as at anemometer level, but also as a function of height.

Acknowledgments

This study was supported by the San Diego Gas and Electric Company. The authors thank SDG&E meteorologists Brian D'Agostino and Steven Vanderburg for assistance, access to data and station sites, and illuminating discussions, and the editor and reviewers for their constructive comments. The authors would also like to acknowledge high-performance computing support from Yellowstone (ark:/85065/d7wd3xhc) provided by the National Center for Atmospheric Research's Computational and Information Systems Laboratory, which is sponsored by the National Science Foundation.

Table 1. Santa Ana episodes ordered by event-maximum gusts at WSY and SIL, for observations ending 31 May 2015. Original measurements were made in miles per hour. Gust rankings are from 197395 and 137368 observations at WSY and SIL, respectively. Fastest sustained winds at both stations occurred on 4/30/2014: 16.5 m s^{-1} at WSY (1610 UTC) and 31.7 m s^{-1} at SIL (1720 UTC).

Date	Time (UTC)	3-sec gust (m/s)	10-min sustained wind (m/s)	Gust factor	Gust observation ranking
WSY					
4/30/14	1600	33.5	15.7	2.14	1
5/14/14	1130	28.2	16.1	1.78	2
12/15/13	1530	27.3	16.1	1.69	6
2/15/13	1800	25.9	15.2	1.71	12 (tie)
1/24/15	1640	25.9	15.2	1.71	12 (tie)
12/9/13	1810	25.0	13.0	1.93	24
SIL					
4/30/14	1710	45.2	29.5	1.53	1
2/15/13	1820	40.7	20.6	1.98	24
1/24/15	1530	39.8	25.0	1.59	35
1/15/14	0530	39.3	22.8	1.73	39
5/13/14	1200	38.9	22.4	1.74	45 (tie)
11/25/14	0710	38.9	27.3	1.43	45 (tie)

References

Arakawa, A., and Lamb, V. R. (1977), "Computational design of the basic dynamical processes of the UCLA general circulation model". *Methods in Computational Physics: Advances in Research and Applications*, **17**, 173–265.

Brasseur, O. (2001), Development and application of a physical approach to estimating wind gusts. Mon. Wea. Rev., **129**, 5–25.

Cao, Y. (2015), "The Santa Ana winds of Southern California in the context of fire weather". Ph.D. dissertation, University of California, Los Angeles, Los Angeles, California, USA.

Cao, Y., and Fovell, R. G. (2013), "Predictability and sensitivity of downslope windstorms in San Diego County. 15th Conference on Mesoscale Processes, Portland, OR, American Meteorological Society. https://ams.confex.com/ams/15MESO/webprogram/Manuscript/Paper228055/cao_fovell_meso_paper.pdf

Cao, Y., and Fovell, R. G. (2016), "Downslope windstorms of San Diego County. Part I: A Case Study". *Mon. Wea. Rev*., **144**, 529-552. http://dx.doi.org/10.1175/MWR-D-15-0147.1

Chang, C.-H., and Schoenberg, F. P. (2011), "Testing separability in marked multidimensional point processes with covariates". *Ann. Inst. Stat. Math.*, **63**, 1103–1122.

Conil, S., and Hall, A. (2006), "Local regimes of atmospheric variability: A case study of Southern California". *J. Climate*, **19**, 4308–4325.

Deacon, E. L. (1955), "Gust variation with height up to 150 m". *Quart. J. Roy. Meteor. Soc*., **81**, 562–573.

Durran, D. R. (1986), "Another look at downslope windstorms. Part I: The development of analogs to supercritical flow in an infinitely deep, continuously stratified fluid". *J. Atmos. Sci.*, **43**, 2527– 2543.

Fovell, R. G. (2012), "Downslope windstorms of San Diego county: Sensitivity to resolution and model physics". 13th WRF Users Workshop, Boulder, CO, Nat. Center for Atmos. Res. https://www.regonline.com/AttendeeDocuments/1077122/43389114/43389114_1045166.pdf

Fovell, R. G., and Cao, Y. (2014), "Wind and gust forecasting in complex terrain". 15th WRF Users Workshop, Boulder, CO, Nat. Center for Atmos. Res. http://www2.mmm.ucar.edu/wrf/users/workshops/WS2014/extended_abstracts/5a.2.pdf

Huang, C., Lin, Y.-L., Kaplan, M. L., and Charney, J. J. (2009), "Synoptic-scale and mesoscale environments conducive to forest fires during the October 2003 extreme fire event in Southern California". *J. Appl. Meteor. Climatol.*, **48**, 553–579.

Hughes, M., and Hall, A. (2010), "Local and synoptic mechanisms causing Southern California's Santa Ana winds". *Clim. Dynam.*, **34** (6), 847–857.

Jackson, P. L., Mayr, G., and Vosper, S., 2013: Dynamically-driven winds. *Mountain Weather Research and Forecasting*, F. K. Chow, S. F. J. D. Wekker, and B. J. Snyder, Eds., Springer-Verlag, 121–218.

Jones, C., Fujioka, F., and Carvalho, L. M. V. (2010), "Forecast skill of synoptic conditions associated with Santa Ana Winds in Southern California". *Mon. Wea. Rev.*, **138**, 4528–4541.

Mesinger, F., and coauthors (2006), "North American Regional Reanalysis". *Bull. Amer. Meteor. Soc.*, **87**, 343–360.

Monahan, H. H., and Armendariz, M. (1971), "Gust factor variations with height and atmospheric stability". *J. Geophys. Res.*, **76**, 5807–5818.

Pleim, J. E. (2007), "A combined local and non-local closure model for the atmospheric boundary layer. Part I: Model description and testing". *J. Appl. Meteor. Climatol.*, **46**, 1383–1395.

Pleim, J. E., and Xiu, A. (1995), "Development and testing of a surface flux and planetary boundary layer model for application in mesoscale models". *J. Appl. Meteor.*, **34**, 16–32.

Raphael, M. N. (2003), "The Santa Ana winds of California". *Earth Interact.*, **7**, 1–13.

Skamarock, W. C., and coauthors (2007), "A description of the Advanced Research WRF Version 2". National Center for Atmospheric Research, Tech. Note NCAR/TN-468+STR, 88 pp.

Small, I. J. (1995), "Santa Ana winds and the fire outbreak of Fall 1993". NOAA Technical Memorandum, National Weather Service Scientific Services Division, Western Region, 30 pp.

Smith, C. M., and Skyllingstad, E. D. (2011), “Effects of inversion height and surface heat flux on downslope windstorms”. *Mon. Wea. Rev.*,**139**, 3750–3764.

Sommers, W. T. (1978), “LFM forecast variables related to Santa Ana wind occurrences”. *Mon. Wea. Rev.*, **132**, 1307–1316.

Stensrud, D. J. (2007), *Parameterization Schemes: Keys to Understanding Numerical Weather Prediction Models*. Cambridge University Press, Cambridge, UK.

Suomi, I., Vihma, T., Gryning, S.-E., and Fortelius, C. (2013), “Wind-gust parametrizations at heights relevant for wind energy: a study based on mast observations”. *Quart. J. Roy. Meteor. Soc*., **139**, 1298–1310.

Verkaik, J. W. (2000), “Evaluation of two gustiness models for exposure correction calculations”. *J. Appl. Meteor.*, **39**, 1613–1626.

Vosper, S. B. (2004), “Inversion effects on mountain lee waves”. *Quart. J. Roy. Meteor. Soc*., **130**, 1723–1748, doi:10.1256/qj.03.63.

Westerling, A. L., Cayan, D. R., Brown, T. J., Hall, B. L., and Riddle, L. G. (2004), “Climate, Santa Ana winds and autumn wildfires in Southern California”. *Eos, Trans. Amer. Geophys. Union*, **85**, 289–296.

Wieringa, J. (1976), “An objective exposure correction method for average wind speeds measured at a sheltered location”. *Quart. J. Roy. Meteor. Soc*., **102** (431), 241–253, doi:10.1002/ qj.49710243119.

Xiu, A., and Pleim, J. E. (2001), “Development of a land surface model. Part I: Application in a mesoscale model”. *J. Appl. Meteor.*, **40**, 192-209.

Appendix 6

APPENDIX 6

The following damage photos were taken on the morning of the 22nd along Highway 78/79 in Wynola. This location is a little more than 2.5 miles upwind (east) of the Witch Fire ignition point. Beneath each photo, there will be information on the location, damage indicator, damage observed, degree of damage, and expected 3-second wind gust. The expected 3-second wind gust is determined by using the National Weather Service's Enhanced Fujita Scale (EF-Scale), which gives a peak wind gust estimate based on 28 damage indicators and 8 degrees (or levels) of damage. http://www.spc.noaa.gov/faq/tornado/ef-scale.html.

Location: Wynola Pizza Express – Highway 78/79 at Wynola Rd.

Damage Indicator: Small barns, farm outbuilding

Damage Observed: Loss of metal roof panels

Expected 3-second wind gust = 74 mph

Location: Highway 78/79 just south of Wynola Rd.

Damage Indicator: Tree - softwood

Damage Observed: Large branches broken (1” – 3” diameter)

Expected 3-second wind gust = 75 mph

Location: Highway 78/79 just south of Wynola Rd.

Damage Indicator: Tree - softwood

Damage Observed: Large branches broken (1” – 3” diameter)

Expected 3-second wind gust = 75 mph

Location: Highway 78/79 just south of Wynola Rd.

Damage Indicator: Tree - softwood

Damage Observed: Large branches broken (1” – 3” diameter)

Expected 3-second wind gust = 75 mph

Location: Highway 78/79 just south of Wynola Rd.

Damage Indicator: Tree - softwood

Damage Observed: Numerous large branches broken (1” – 3” diameter)

Expected 3-second wind gust = 75 mph

Location: Highway 78/79 near Wynola Rd.

Damage Indicator: N/A

Damage Observed: Collapsed shelter/structure

Expected 3-second wind gust = N/A

Just as I did with West Santa Ysabel, I am able to compare wind observations at West Wynola with wind observations at Julian RAWS to estimate the peak wind gust in Wynola during the October 2007 wildfires. For the 42 most recent Santa Ana Wind events since October 2012, peak wind gusts at West Wynola are, on average, 1.27 times stronger than peak wind gust at Julian RAWS. This results in an estimated peak wind gust at West Wynola of 75 mph in October 2007 based on a peak wind gust of 59 mph at Julian RAWS. This estimate matches the expected wind gust based on the EF Scale.

Appendix 7

APPENDIX 7

The following table shows peak wind gusts at Ramona ASOS as compared to peak wind gusts at West Santa Ysabel for 42 Santa Ana Wind Events since October 2012. The offset factor is calculated by dividing the peak wind gust at West Santa Ysabel by the peak wind gust at Ramona ASOS. An offset factor of 1.5 means that the peak wind gust at West Santa Ysabel was 1.5 times stronger than the peak wind gust at Ramona ASOS.

Event Start	Event End	Ramona ASOS Peak Wind Gust (mph)	W. Santa Ysabel Peak Wind Gust (mph)	Offset Factor
4/29/2014	5/1/2014	46	75	1.63
5/12/2014	5/15/2014	40	63	1.58
12/14/2013	12/16/2013	37	61	1.65
2/15/2013	2/16/2013	31	58	1.87
1/22/2015	1/26/2015	42	58	1.38
12/9/2013	12/9/2013	36	56	1.56
1/13/2014	1/17/2014	30	56	1.87
1/15/2013	1/17/2013	36	55	1.53
1/1/2013	1/2/2013	29	52	1.79
11/23/2014	11/25/2014	30	51	1.70
3/5/2015	3/7/2015	29	51	1.76
10/26/2012	10/27/2012	32	49	1.53
2/28/2013	3/1/2013	26	49	1.88
10/4/2013	10/6/2013	41	48	1.17
12/23/2014	12/23/2014	27	48	1.78
2/11/2015	2/13/2015	39	48	1.23
4/14/2014	4/14/2014	23	47	2.04
2/4/2016	2/9/2016	36	47	1.31
4/6/2016	4/6/2016	33	47	1.42
12/26/2014	12/27/2014	21	46	2.19
1/25/2016	1/26/2016	36	45	1.25
11/4/2014	11/5/2014	21	44	2.10
1/21/2016	1/21/2016	28	44	1.57
1/11/2016	1/12/2016	20	43	2.15
5/2/2013	5/2/2013	31	42	1.35
12/26/2015	12/27/2015	20	42	2.10
1/30/2013	1/31/2013	26	41	1.58
1/23/2014	1/24/2014	20	41	2.05
4/16/2015	4/16/2015	21	41	1.95
11/6/2015	11/7/2015	25	41	1.64
11/12/2015	11/13/2015	24	37	1.54
11/20/2015	11/21/2015	23	37	1.61
2/24/2013	2/24/2013	28	36	1.29
4/18/2013	4/19/2013	28	36	1.29
2/14/2016	2/15/2016	17	35	2.06
11/13/2012	11/13/2012	32	34	1.06

1/14/2015	1/15/2015	30	34	1.13
10/2/2014	10/2/2014	23	33	1.43
3/13/2015	3/13/2015	23	32	1.39
3/26/2015	3/26/2015	25	31	1.24
10/14/2012	10/14/2012	20	29	1.45
4/17/2016	4/17/2016	26	25	0.96

Appendix 8

SDG&E DATA REQUEST
SDG&E – UCAN DR-01, Q1-56
A.15-09-010
DATE RECEIVED: October 26, 2016
DATE RESPONDED: November 9, 2016

GENERAL OBJECTIONS

1. UCAN objects generally to each request to the extent that it seeks information protected by the attorney-client privilege, the attorney work product doctrine, statutory mediation confidentiality (see Cal. Evid. Code §§ 1115-28) or any other applicable privilege or evidentiary doctrine. No information protected by such privileges will be knowingly disclosed.

2. UCAN objects generally to each request that is overly broad and unduly burdensome. As part of this objection, UCAN objects to discovery requests that seek "all documents" or "each and every document" and similarly worded requests on the grounds that such requests are unreasonably cumulative and duplicative, fail to identify with specificity the information or material sought, and create an unreasonable burden compared to the likelihood of such requests leading to the discovery of admissible evidence. Notwithstanding this objection,

3. UCAN objects generally to each request to the extent that the request is vague, unintelligible, or fails to identify with sufficient particularity the information or documents requested and, thus, is not susceptible to response at this time.

4. UCAN objects generally to each request that: (1) asks for a legal conclusion to be drawn or legal research to be conducted on the grounds that such requests are not designed to elicit facts and, thus, violate the principles underlying discovery; (2) requires UCAN to do legal research or perform additional analyses to respond to the request; or (3) seeks access to counsel's legal research, analyses or theories.

5. UCAN objects generally to each request to the extent it seeks information or documents that are not reasonably calculated to lead to the discovery of admissible evidence.

6. UCAN objects generally to each request to the extent that it is unreasonably duplicative or cumulative of other requests.

7. UCAN objects generally to each request to the extent that it would require UCAN to search its files for matters of public record such as filings, testimony, transcripts, decisions, orders, reports or other information, whether available in the public domain or through FERC or CPUC sources.

8. UCAN objects generally to each request to the extent that it seeks information or documents that are not in the possession, custody or control of UCAN.

9. UCAN objects generally to each request to the extent that the request would impose an undue burden on UCAN by requiring it to perform studies, analyses or calculations or to create documents that do not currently exist.

10. UCAN objects generally to each request that calls for information that is privileged or otherwise entitled to confidential protection.

SDG&E DATA REQUEST
SDG&E – UCAN DR-01, Q1-56
A.15-09-010
DATE RECEIVED: October 26, 2016
DATE RESPONDED: November 9, 2016

EXPRESS RESERVATIONS

1. No response, objection, limitation or lack thereof, set forth in these responses and objections shall be deemed an admission or representation by UCAN as to the existence or nonexistence of the requested information or that any such information is relevant or admissible.

2. UCAN reserves the right to modify or supplement its responses and objections to each request, and the provision of any information pursuant to any request is not a waiver of that right.

3. UCAN reserves the right to rely, at any time, upon subsequently discovered information.

4. These responses are made solely for the purpose of this proceeding (A.15-09-010) and for no other

5. To the extent that SDG&E is asking for documents such as publications and articles that have already been provided by UCAN as attachments to testimony or that were provided by SDG&E to UCAN in prior data requests, those documents are referenced but not provided in this response.

6. Several of SDG&E's data requests seek publications and presentations from UCAN. In UCAN's responses some are referenced in UCAN's answers with a link to the documents embedded in the response. For those documents in PDF form, UCAN has uploaded them onto SDG&E's Sharepoint website.

SDG&E DATA REQUEST
SDG&E – UCAN DR-01, Q1-56
A.15-09-010
DATE RECEIVED: October 26, 2016
DATE RESPONDED: November 9, 2016

GERSHUNOV'S RESPONSES TO SDG&E'S DATA REQUEST

Request 1:

Please provide copies of all of prior written or oral testimony, in any proceeding.

UCAN's Response 1:

UCAN objects to this question on the grounds set forth in general objections 1 & 10. Subject to the forgoing objection UCAN responds as follows:

Dr. Gershunov was involved in one legal proceeding as a witness five years ago. He is no longer in possession of these documents, which were protected by a confidentiality agreement.

SDG&E DATA REQUEST
SDG&E – UCAN DR-01, Q1-56
A.15-09-010
DATE RECEIVED: October 26, 2016
DATE RESPONDED: November 9, 2016

Request 2:

Has Dr. Gershunov ever provided any opinions, reports or testimony, whether written or oral, in any tribunal or judicial form of any kind that concerned in any way the 2007 San Diego wildfires? If so, please provide a copy of:

a. All such opinions, reports or testimony
b. Any opinions, reports or testimony that either opposed or agreed with all or a portion of Dr. Gershunov's position
c. Any decisions or rulings by such tribunal or judicial forum

UCAN's Response 2:

As per UCAN's meet and confer with SDG&E regarding this question, we understand that SDG&E is only seeking opinions, reports or testimony that was submitted to a judicial forum or tribunal regarding the 2007 San Diego wildfires.

UCAN objects to this question on the grounds set forth in general objections 1 & 10. Subject to the forgoing objection UCAN responds as follows:

Yes. He was involved in a legal proceeding on this issue as an expert witness five years ago.
a. He is no longer in possession of these documents, which were protected by a confidentiality agreement.
b. He is no longer in possession of these documents, which were protected by a confidentiality agreement.
c. He was not privy to decisions or rulings by that tribunal.

SDG&E DATA REQUEST
SDG&E – UCAN DR-01, Q1-56
A.15-09-010
DATE RECEIVED: October 26, 2016
DATE RESPONDED: November 9, 2016

Request 3:

In Appendix 2 to Dr. Coen's testimony (page 30), she indicated "I am submitting this testimony as an individual, not as a representative of the National Center for Atmospheric Research (NCAR) or the National Science Foundation (NSF)." Is Dr. Gershunov submitting his testimony, as a representative of Scripps Institute of Oceanography, University California, San Diego?

UCAN's Response 3:

No. Dr. Gershunov has submitted his testimony as an individual.

SDG&E DATA REQUEST
SDG&E – UCAN DR-01, Q1-56
A.15-09-010
DATE RECEIVED: October 26, 2016
DATE RESPONDED: November 9, 2016

Request 4:

What role, if any, did SIO/USCD have in Dr. Gershunov's testimony, analyses or conclusions?

UCAN's Response 4:

None.

SDG&E DATA REQUEST
SDG&E – UCAN DR-01, Q1-56
A.15-09-010
DATE RECEIVED: October 26, 2016
DATE RESPONDED: November 9, 2016

Request 5:

Please list all persons with whom Dr. Gershunov consulted regarding his testimony.

UCAN's Response 5:

This question has been withdrawn by SDG&E.

SDG&E DATA REQUEST
SDG&E – UCAN DR-01, Q1-56
A.15-09-010
DATE RECEIVED: October 26, 2016
DATE RESPONDED: November 9, 2016

Request 6:

Please list and describe any projects, engagements, analyses or collaborations of any kind in which Dr. Gershunov has been involved that also involved SDG&E.

UCAN's Response 6:

In the Summer of 2012 a colleague, Dr. Rachel Schwartz, had an internship with SDG&E, as a graduate student. Dr. Gershunov was involved as Ms. Schwartz' advisor at SIO/UCSD. The fellowship project focused on the detection and variability of coastal marine layer clouds in San Diego County.

In the past, Dr. Gershunov has had casual conversations with SDG&E personnel on various topics i.e., heat waves, marine layer clouds, Santa Ana Winds, etc. that do not in any way amount to "projects, engagements, analyses or collaborations".

SDG&E DATA REQUEST
SDG&E – UCAN DR-01, Q1-56
A.15-09-010
DATE RECEIVED: October 26, 2016
DATE RESPONDED: November 9, 2016

Request 7:

Please list and describe any projects, engagements, analyses or collaborations of any kind in which Dr. Gershunov has been involved that also involved another utility.

UCAN's Response 7:

This question has been withdrawn by SDG&E.

SDG&E DATA REQUEST
SDG&E – UCAN DR-01, Q1-56
A.15-09-010
DATE RECEIVED: October 26, 2016
DATE RESPONDED: November 9, 2016

Request 8:

Please provide all of Dr. Gershunov's workpapers.

UCAN's Response 8:

There are no workpapers to provide. Dr. Gershunov's analyses were based on the Santa Ana wind catalog of Guzman Morales et al. (2014), which is freely available online: http://cnap.ucsd.edu/ data/janin/. Dr. Gershunov's work involved accessing the requisite data.

The analyses were done in the R statistical software (which is also freely available online) mostly in command-line mode. Estimates of sustained winds were done literally back-of-the-envelope using a calculator and the wind profile power law formula provided in Appendix A. Dr. Gershunov did not save any of those scribbles.

SDG&E DATA REQUEST
SDG&E – UCAN DR-01, Q1-56
A.15-09-010
DATE RECEIVED: October 26, 2016
DATE RESPONDED: November 9, 2016

Request 9:

Please provide a copy of each of the references cited that are listed in Appendix 1 (page 23) of Part I of Dr. Gershunov's testimony.

UCAN's Response 9:

Listed below are the references cited in Appendix 1. Some references were already provided to UCAN by SDG&E in Data Responses and as they are already in SDG&E's possession are not provided here. Others are provided to SDG&E through their Sharepoint website and some are provided for in a link listed below. All of these references are also available online from the appropriate journal web sites.

1. Brasseur, O, 2001: Development and application of a physical approach to estimating wind gusts. Monthly Weather Review, 129, 5-25.
- Uploaded as PDF to SDG&E's Sharepoint site

2. Cao, Y. and R.G. Fovell, 2016: Downslope windstorms of San Diego County. Part 1, a case study. Monthly Weather Review, 144, DOI: 10.1175/MWR-D-15-0147.1.
- Can be accessed online at:
https://www.researchgate.net/publication/293944387_Downslope_Windstorms_of_San_Diego_County_Part_I_A_Case_Study

3. Fovell, R.G. (2012), Downslope Windstorms of San Diego County: Sensitivity to Resolution and Model Physics, 13th WRF Users Workshop, June 2012.
- Provided by SDG&E

4. Fovell, R.G. and Y. Cao, 2016: Santa Ana winds of Southern California: Winds, gusts, and the 2007 Witch Fire. Unpublished manuscript.
- Provided by SDG&E

5. Guzman Morales, J., A. Gershunov, J. Theiss, H. Li and D. Cayan, 2016: Santa Ana Winds of southern California: their climatology, extremes and behavior since 1948. Geophysical Research Letters, 43, doi:10.1002/2016GL067887.
- this article was provided as Attachment 3 (with Supplementary Supporting I Information as Attachment 4) to Dr. Gershunov's testimony, Part 2.

6. Horel J.D. and X. Dong, 2010: An evaluation of the distribution of remote automated weather stations (RAWS). Journal of Applied Meteorology and Climatology, 49, 1563-1578.
- Uploaded as PDF to SDG&E's Sharepoint site

SDG&E DATA REQUEST
SDG&E – UCAN DR-01, Q1-56
A.15-09-010
DATE RECEIVED: October 26, 2016
DATE RESPONDED: November 9, 2016

7. Hughes, M., and A. Hall, 2010: Local and synoptic mechanisms causing Southern California's Santa Ana winds. Climate Dynamics, 34, 847–857, doi:10.1007/s00382-009-0650-4.

- Uploaded as PDF to SDG&E's Sharepoint site

8. Myrick, D.T. and J.D. Horel, 2008: Sensitivity of Surface Analyses over the Western United States to RAWS Observations. Weather and Forecasting, 23, 145-158.

- Uploaded as PDF to SDG&E's Sharepoint site

9. Raphael, M. N., 2003: The Santa Ana winds of California. Earth Interactions, 7.
- Available online at:
http://journals.ametsoc.org/doi/abs/10.1175/1087-3562(2003)007%3C0001%3ATSAWOC%3E2.0.CO%3B2

10. Rolinski, T., S.B. Capps, R.G. Fovell, Y. Cao, B.J. D'Augustino, S. Vanderburg, 2016: The Santa Ana Wildfire Threat Index: Methodology and Operational Implementation. Manuscript in review.

- Provided by SDG&E

11. Westerling, A.L, D.R. Cayan, T.J. Brown, B.L. Hall, L.G. Riddle, 2004: Climate, Santa Ana winds and autumn wildfires in Southern California. Eos, 85, 289-296.

- Uploaded as PDF to SDG&E's Sharepoint site

SDG&E DATA REQUEST
SDG&E – UCAN DR-01, Q1-56
A.15-09-010
DATE RECEIVED: October 26, 2016
DATE RESPONDED: November 9, 2016

Request 10:

Please provide a copy of each of the references cited that are listed in Appendix B (page 29) of Part II of Dr. Gershunov's testimony.

UCAN's Response 10:

1. Cao, Y. and R.G. Fovell, 2016: Downslope windstorms of San Diego County. Part 1, a case study. Monthly Weather Review, 144, DOI: 10.1175/MWR-D-15-0147.1.
   - can be accessed online at https://www.researchgate.net/publication/293944387_Downslope_Windstorms_of_San_Diego_County_Part_I_A_Case_Study

2. Guzman Morales, J., A. Gershunov, J. Theiss, H. Li and D. Cayan, 2016: Santa Ana Winds of southern California: their climatology, extremes and behavior since 1948. Geophysical Research Letters, 43, doi:10.1002/2016GL067887.
   - this article was provided as Attachment 3 (with Supplementary Supporting Information as Attachment 4) to Dr. Gershunov's testimony, Part 2.

3. Hughes, M., and A. Hall, 2010: Local and synoptic mechanisms causing Southern California's Santa Ana winds. Climate Dynamics, 34, 847–857, doi:10.1007/s00382-009-0650-4.
   - Uploaded as PDF to SDG&E's Sharepoint site

4. Kanamitsu M., H. Kanamaru, 2007: Fifty-Seven-Year California Reanalysis Downscaling at 10 km (CaRD10). Part I: System Detail and Validation with Observations, Journal of Climate, 20, 5553-5571.
   - Uploaded as PDF to SDG&E's Sharepoint site

5. Moritz, M.A., T.J. Moody, M.A. Krawchuk, M. Hughes and A. Hall, 2010: Spatial variation in extreme winds predicts large wildfire locations in chaparral ecosystems. Geophysical Research Letters, 37, doi: 10.1029/2009GL041735.
   - Uploaded as PDF to SDG&E's Sharepoint site

SDG&E DATA REQUEST
SDG&E – UCAN DR-01, Q1-56
A.15-09-010
DATE RECEIVED: October 26, 2016
DATE RESPONDED: November 9, 2016

Request 11:

Please provide a complete list of all of Dr. Gershunov's publications and presentations (see Attachment 1).

UCAN's Response 11:

Per UCAN's meet and confer with SDG&E, SDG&E is limiting its request to seek only those publication and presentations that relate to the following topics:

a. Santa Ana winds

b. the climate in Southern California

c. wildfires

d. fire weather

e. mesoscale modeling

f. climate modeling

g. RAWS or ASOS stations

h. katabatic winds

A list of Dr. Gershunov's peer-reviewed publications is provided in his Curriculum Vitae, and the publications relevant to the issues noted in question 11, subsections a-h are provided below.

For non-peer reviewed publications there is nothing relevant to Santa Ana winds and he has stopped updating the list of his presentations years ago. The only presentation he has given that was focused on Santa Ana winds was titled "Santa Ana winds of Southern California: their climatology, extremes, and variability" presented that in November 2012, at the International RSM (Regional Spectral Model) Users Workshop that was held at the Scripps Institution of Oceanography.

Guzman Morales, J., A. Gershunov, J. Theiss, H. Li and D. Cayan, 2016: Santa Ana Winds of southern California: their climatology, extremes and behavior since 1948. *Geophysical Research Letters*, 43, doi:10.1002/2016GL067887.

http://onlinelibrary.wiley.com/doi/10.1002/2016GL067887/abstract

Clemesha, R.E., A. Gershunov, S.F. Iacobellis, D.R. Cayan and A.P. Williams, 2016: The Northward March of Summer Low Cloudiness along the California Coast. *Geophysical Research Letters*, 43, doi:10.1002/2015GL067081.

http://onlinelibrary.wiley.com/doi/10.1002/2015GL067081/full

Guirguis, K., A. Gershunov and D. Cayan, 2015: Interannual variability in associations between seasonal climate, weather and extremes: wintertime temperature over the Southwestern United States. *Environmental Research Letters*, 10, 124023, doi:10.1088/1748-9326/10/12/124023.

http://iopscience.iop.org/article/10.1088/1748-9326/10/12/124023

Cavanaugh, N.R., A. Gershunov, 2015: Probabilistic Tail Dependence of Intense Precipitation on Spatiotemporal Scale in Observations, Reanalyses, and GCMs. *Climate Dynamics*, 45, 2965-2975, DOI:10.1007/s00382-015-2517-1.

http://link.springer.com/article/10.1007/s00382-015-2517-1

Schwartz, R.E., A. Gershunov, S.F. Iacobellis and D.R. Cayan, 2014: North American West Coast Summer Low Cloudiness: Broad Scale Variability Associated with Sea Surface Temperature. *Geophysical Research Letters*. 41, 3307–3314, DOI: 10.1002/2014GL059825.

http://onlinelibrary.wiley.com/doi/10.1002/2014GL059825/full

Polade, S.D., Pierce, D.W., Cayan, D.R., Gershunov, A. & Dettinger, M.D. 2014: The key role of dry days in changing regional climate and precipitation regimes. *Nature Scientific Reports* 4, 4364; DOI:10.1038/srep04364.

http://www.nature.com/articles/srep04364

Guirguis, K., A. Gershunov, A. Tardy and R. Basu, 2014: The Impact of Recent Heat Waves on Human Health in California. *Journal of Applied Meteorology and Climatology*, 53, 3-19.

http://journals.ametsoc.org/doi/abs/10.1175/JAMC-D-13-0130.1

Gershunov, A., B. Rajagopalan, J. Overpeck, K. Guirguis, D. Cayan, M. Hughes, M. Dettinger, C. Castro, R. E. Schwartz, M. Anderson, A. J. Ray, J. Barsugli, T. Cavazos, and M. Alexander. 2013. "Future Climate: Projected Extremes." Chapter 7 in *Assessment of Climate Change in the Southwest United States: A Report Prepared for the National Climate Assessment*, edited by G. Garfin, A. Jardine, R. Merideth, M.

Black, and S. LeRoy, 126–147. A report by the Southwest Climate Alliance. NCA Regional Input Reports. Washington, DC: Island Press. ISBN 9781610914468

http://www.swcarr.arizona.edu/chapter/7

Gershunov A. and K. Guirguis, 2012: California heat waves in the present and future. *Geophysical Research Letters*, 39, L18710, doi:10.1029/2012GL052979.

http://onlinelibrary.wiley.com/doi/10.1029/2012GL052979/abstract

Gershunov, A., D. Cayan and S. Iacobellis, 2009: The great 2006 heat wave over California and Nevada: Signal of an increasing trend. *Journal of Climate*, 22, 6181–6203.

http://journals.ametsoc.org/doi/abs/10.1175/2009JCLI2465.1

Favre, A. and A. Gershunov, 2009: North Pacific cyclonic and anticyclonic transients in a global warming context: possible consequences for Western North American daily precipitation and temperature extremes. Climate Dynamics, 32, 969-987.

http://link.springer.com/article/10.1007/s00382-008-0417-3

Alfaro, E., A. Gershunov, D.R. Cayan, A. Steinemann, D.W. Pierce and T.P. Barnett, 2004: A method for prediction of California summer air surface temperature. Eos. 85. 553, 557-558.

http://onlinelibrary.wiley.com/doi/10.1029/2004EO510001/abstract

Gershunov, A. and D. Cayan, 2003: Heavy daily precipitation frequency over the contiguous United States: Sources of climatic variability and seasonal predictability. *Journal of Climate*, 16, 2752-2765.

http://journals.ametsoc.org/doi/full/10.1175/1520-0442(2003)016%3C2752%3AHDPFOT%3E2.0.CO%3B2

Westerling, A.L., A. Gershunov, T. Brown, D. Cayan, and M. Dettinger, 2003: Climate and wildfire in the western United States. *Bulletin of the American Meteorological Society*, 84, 595-604.

http://journals.ametsoc.org/doi/abs/10.1175/BAMS-84-5-595

Westerling, A.L., A. Gershunov, D.R. Cayan and T.P. Barnett, 2002: Long lead statistical forecasts of area burned in western U.S. wildfires by ecosystem province. *Int. Journal of Wildland Fire*, 11, 257-266.

http://www.publish.csiro.au/WF/WF02009

Gershunov, A., T. Barnett, D. Cayan, T. Tubbs and L Goddard, 2000: Predicting and downscaling ENSO impacts on intraseasonal precipitation statistics in California: the 1997-1998 event. *Journal of Hydrometeorology*, 1, 201-209.

http://journals.ametsoc.org/doi/full/10.1175/1525-7541(2000)001%3C0201%3APADEIO%3E2.0.CO%3B2

SDG&E DATA REQUEST
SDG&E – UCAN DR-01, Q1-56
A.15-09-010
DATE RECEIVED: October 26, 2016
DATE RESPONDED: November 9, 2016

Request 12:

Please provide a copy of each of the Refereed Publications listed in Attachment 1 to Dr. Gershunov's testimony, or of any other publications, that relate to:

a. Santa Ana winds

b. the climate in Southern California

c. wildfires

d. fire weather

e. mesoscale modeling

f. climate modeling

g. RAWS or ASOS stations

a. katabatic winds

UCAN's Response 12:

Attached are the links to Dr. Gershunov's relevant publications. UCAN would note that the links to the publications in this question mirror those provided for Question 11. Besides the first article on Santa Ana winds, these are relevant as they address various aspects of the weather and climate of California, climate modeling, and wildfire, per SDGE's request:

Guzman Morales, J., A. Gershunov, J. Theiss, H. Li and D. Cayan, 2016: Santa Ana Winds of southern California: their climatology, extremes and behavior since 1948. *Geophysical Research Letters*, 43, doi:10.1002/2016GL067887.

http://onlinelibrary.wiley.com/doi/10.1002/2016GL067887/abstract

Clemesha, R.E., A. Gershunov, S.F. Iacobellis, D.R. Cayan and A.P. Williams, 2016: The Northward March of Summer Low Cloudiness along the California Coast. *Geophysical Research Letters*, 43, doi:10.1002/2015GL067081.

http://onlinelibrary.wiley.com/doi/10.1002/2015GL067081/full

Guirguis, K., A. Gershunov and D. Cayan, 2015: Interannual variability in associations between seasonal climate, weather and extremes: wintertime temperature over the Southwestern United States. *Environmental Research Letters*, 10, 124023, doi:10.1088/1748-9326/10/12/124023.

http://iopscience.iop.org/article/10.1088/1748-9326/10/12/124023

Cavanaugh, N.R., A. Gershunov, 2015: Probabilistic Tail Dependence of Intense Precipitation on Spatiotemporal Scale in Observations, Reanalyses, and GCMs. *Climate Dynamics*, 45, 2965-2975, DOI:10.1007/s00382-015-2517-1.

http://link.springer.com/article/10.1007/s00382-015-2517-1

Schwartz, R.E., A. Gershunov, S.F. Iacobellis and D.R. Cayan, 2014: North American West Coast Summer Low Cloudiness: Broad Scale Variability Associated with Sea Surface Temperature. *Geophysical Research Letters*. 41, 3307–3314, DOI: 10.1002/2014GL059825.

http://onlinelibrary.wiley.com/doi/10.1002/2014GL059825/full

Polade, S.D., Pierce, D.W., Cayan, D.R., Gershunov, A. & Dettinger, M.D. 2014: The key role of dry days in changing regional climate and precipitation regimes. *Nature Scientific Reports* 4, 4364; DOI:10.1038/srep04364.

http://www.nature.com/articles/srep04364

Guirguis, K., A. Gershunov, A. Tardy and R. Basu, 2014: The Impact of Recent Heat Waves on Human Health in California. *Journal of Applied Meteorology and Climatology*, 53, 3-19.

http://journals.ametsoc.org/doi/abs/10.1175/JAMC-D-13-0130.1

Gershunov, A., B. Rajagopalan, J. Overpeck, K. Guirguis, D. Cayan, M. Hughes, M. Dettinger, C. Castro, R. E. Schwartz, M. Anderson, A. J. Ray, J. Barsugli, T. Cavazos, and M. Alexander. 2013. "Future Climate: Projected Extremes." Chapter 7 in *Assessment of Climate Change in the Southwest United States: A Report Prepared for the National Climate Assessment*, edited by G. Garfin, A. Jardine, R. Merideth, M. Black, and S. LeRoy, 126–147. A report by the Southwest Climate Alliance. NCA Regional Input Reports. Washington, DC: Island Press. ISBN 9781610914468

http://www.swcarr.arizona.edu/chapter/7

Gershunov A. and K. Guirguis, 2012: California heat waves in the present and future. *Geophysical Research Letters*, 39, L18710, doi:10.1029/2012GL052979.

http://onlinelibrary.wiley.com/doi/10.1029/2012GL052979/abstract

Gershunov, A., D. Cayan and S. Iacobellis, 2009: The great 2006 heat wave over California and Nevada: Signal of an increasing trend. *Journal of Climate*, 22, 6181–6203.

http://journals.ametsoc.org/doi/abs/10.1175/2009JCLI2465.1

Favre, A. and A. Gershunov, 2009: North Pacific cyclonic and anticyclonic transients in a global warming context: possible consequences for Western North American daily precipitation and temperature extremes. Climate Dynamics, 32, 969-987.

http://link.springer.com/article/10.1007/s00382-008-0417-3

Alfaro, E., A. Gershunov, D.R. Cayan, A. Steinemann, D.W. Pierce and T.P. Barnett, 2004: A method for prediction of California summer air surface temperature. Eos. 85. 553, 557-558.

http://onlinelibrary.wiley.com/doi/10.1029/2004EO510001/abstract

Gershunov, A. and D. Cayan, 2003: Heavy daily precipitation frequency over the contiguous United States: Sources of climatic variability and seasonal predictability. *Journal of Climate*, 16, 2752-2765.

http://journals.ametsoc.org/doi/full/10.1175/1520-0442(2003)016%3C2752%3AHDPFOT%3E2.0.CO%3B2

Westerling, A.L., A. Gershunov, T. Brown, D. Cayan, and M. Dettinger, 2003: Climate and wildfire in the western United States. *Bulletin of the American Meteorological Society*, 84, 595-604.

http://journals.ametsoc.org/doi/abs/10.1175/BAMS-84-5-595

Westerling, A.L., A. Gershunov, D.R. Cayan and T.P. Barnett, 2002: Long lead statistical forecasts of area burned in western U.S. wildfires by ecosystem province. *Int. Journal of Wildland Fire*, 11, 257-266.

http://www.publish.csiro.au/WF/WF02009

Gershunov, A., T. Barnett, D. Cayan, T. Tubbs and L Goddard, 2000: Predicting and downscaling ENSO impacts on intraseasonal precipitation statistics in California: the 1997-1998 event. *Journal of Hydrometeorology*, 1, 201-209.

SDG&E DATA REQUEST
SDG&E – UCAN DR-01, Q1-56
A.15-09-010
DATE RECEIVED: October 26, 2016
DATE RESPONDED: November 9, 2016

http://journals.ametsoc.org/doi/full/10.1175/1525-7541(2000)001%3C0201%3APADEIO%3E2.0.CO%3B2

Request13:

Does Dr. Gershunov have any degrees in meteorology?

UCAN's Response 13:

Dr. Gershunov's PhD degree is from a Geography Department and its focus was on meteorology and climatology. Meteorology departments at universities are rare and meteorology is frequently taught by professors who specialize in meteorology (meteorologists) working in departments of Geography, Physics, Environmental Science, and others.

SDG&E DATA REQUEST
SDG&E – UCAN DR-01, Q1-56
A.15-09-010
DATE RECEIVED: October 26, 2016
DATE RESPONDED: November 9, 2016

Request14:

Are there any statements, conclusions or analyses in the testimony of any of the following witnesses in this proceeding with which Dr. Gershunov disagrees? If so, please identify the statement, conclusion or analysis and describe the basis for Dr. Gershunov's disagreement.

d. Mr. Nils Stannik (ORA)

e. Dr. Matthew Rahn (POC)

f. Ms. Jennifer Betts (SDCAN)

g. Dr. Joseph Mitchell (MGRA)

h. Dr. Janice Coen (UCAN)

UCAN's Response 14:

This question has been withdrawn by SDG&E.

SDG&E DATA REQUEST
SDG&E – UCAN DR-01, Q1-56
A.15-09-010
DATE RECEIVED: October 26, 2016
DATE RESPONDED: November 9, 2016

Request 15:

Does Dr. Gershunov have any operational forecasting experience with regards to Santa Ana winds? If so, please describe that experience.

UCAN's Response 15:

No.

SDG&E DATA REQUEST
SDG&E – UCAN DR-01, Q1-56
A.15-09-010
DATE RECEIVED: October 26, 2016
DATE RESPONDED: November 9, 2016

Request16:

Has Dr. Gershunov reviewed Dr. Coen's testimony in this proceeding? If not, why not?

UCAN's Response 16:

Yes.

SDG&E DATA REQUEST
SDG&E – UCAN DR-01, Q1-56
A.15-09-010
DATE RECEIVED: October 26, 2016
DATE RESPONDED: November 9, 2016

Request 17:

Please list each of the RAWS or ASOS stations in San Diego County that Dr. Gershunov has visited in person and when he made that visit.

UCAN's Response 17:

None. I have seen the Ramona Airport ASOS station from a distance several times, including in 2011.

SDG&E DATA REQUEST
SDG&E – UCAN DR-01, Q1-56
A.15-09-010
DATE RECEIVED: October 26, 2016
DATE RESPONDED: November 9, 2016

Request 18:

Please list each of the SDG&E weather stations in San Diego County that Dr. Gershunov has visited in person and when he made that visit.

UCAN's Response 18:

None.

SDG&E DATA REQUEST
SDG&E – UCAN DR-01, Q1-56
A.15-09-010
DATE RECEIVED: October 26, 2016
DATE RESPONDED: November 9, 2016

Request 19:

Please explain and provide all support for the following assertions of Dr. Gershunov (Part I, page 7):

"At locations where anemometers may be obstructed (by nearby tall trees, buildings, etc.), sustained winds are expected to underestimate wind speeds of an otherwise unobstructed flow. Sustained winds mainly represent local wind speeds at the exact location of the anemometer only. However, observed gusts are not as sensitive to obstructions and can be thought of, according to this theory, as being much more representative of the larger-scale flow aloft, with which the gusts are directly linked by turbulence."

UCAN's Response 19:

This statement is supported by theory presented by Brasseur (2001) (article uploaded to SDG&E's Sharepoint website), as explained in Dr. Gershunov's testimony in the paragraph just above the citation in question here, that appears on page 7 in Part 1 of his testimony.

The statement is also consistent with his work (Guzman Morales et al. 2016 – provided as an attachment to his testimony) which shows that gusts are much more consistent with modeled winds, both in terms of temporal evolution and magnitude, which of course are not affected by obstructions.

SDG&E DATA REQUEST
SDG&E – UCAN DR-01, Q1-56
A.15-09-010
DATE RECEIVED: October 26, 2016
DATE RESPONDED: November 9, 2016

Request 20:

How did Dr. Gershunov conclude that "data quality appears excellent at enough [RAWS/ASOS] stations, particularly with respect to observed gusts, and at least adequate at most stations here to resolve SAW?" (Part I, page 13). Please also indicate which stations had excellent data quality and which stations had at least adequate data quality.

UCAN's Response 20:

This conclusion is consistent with the comparison of observed gusts and modeled winds at 85 weather stations as described in Guzman Morales et al. (2016, online supplementary information, also provided in Attachment 4 to Dr. Gershunov's testimony, Part 2) and in detail relevant specifically for the 2007 Wildfires in Part 2 of his testimony. As can be seen on Figures 2 and 3 of his testimony, Part 2, gusts observed at the most relevant stations (Ramona Airport ASOS, Valley Center, Goose Valley, Pine Hills and Alpine RAWS) are consistent with each other and with modeled instantaneous winds. The gust observations appear to be of excellent quality at all these stations even where sustained winds are biased – see for example the dampened sustained wind speeds and variability that result in inflated gust factors at Pine Hills relative to other stations.

Station relevance was taken to be related to both proximity and terrain similarity to Wildfire ignition locations as described in Part 2 of Dr. Gershunov's report.

SDG&E DATA REQUEST
SDG&E – UCAN DR-01, Q1-56
A.15-09-010
DATE RECEIVED: October 26, 2016
DATE RESPONDED: November 9, 2016

Request 21:

Has Dr. Gershunov visited the locations identified by Cal Fire as having been the ignition point of the Witch, Rice and Guejito Fires? If so, please identify the date and time of his visit.

UCAN's Response 21:

Yes. He was in the proximity of the Witch Fire ignition location in December 2011 when he visited CAL FIRE's Witch Creek Fire Station (#87).

SDG&E DATA REQUEST
SDG&E – UCAN DR-01, Q1-56
A.15-09-010
DATE RECEIVED: October 26, 2016
DATE RESPONDED: November 9, 2016

Request 22:

Please identify and describe the source of Dr. Gershunov's statements about the locations (i.e., terrains and slopes) of the Julian RAWS and the WSY weather station (Part I, page 25).

UCAN's Response 22:

His sources include the coordinates of the Julian RAWS and the WSY weather stations and the Digital Elevation Model Data described on page 7 in Part 2 of his Testimony.

SDG&E DATA REQUEST
SDG&E – UCAN DR-01, Q1-56
A.15-09-010
DATE RECEIVED: October 26, 2016
DATE RESPONDED: November 9, 2016

Request 23:

Please explain why Dr. Gershunov chose to use a 10x10 km spatial resolution in his mesoscale modeling.

UCAN's Response 23:

Running mesoscale models is computer intensive and expensive and modelers have to compromise between, for example, spatial resolution and the length of the experiment. Dr. Gershunov used the longest available model data record as the main goal of his work was to describe and understand the long-term behavior of Santa Ana winds at a reasonable (rather than the finest possible) spatial resolution. Validation of winds from this record performed using station observations by Guzman Morales et al. (2016) and more focused comparisons with wind observations at the times and stations most relevant to the Fires (see answer to question 20 above) prove that the 10x10 km resolution mesoscale model produced winds that are locally reasonable, although biased high, as is the case with most mesoscale models regardless of resolution. It is certainly the case with WRF, as Cao and Fovell (2016) clearly state.

SDG&E DATA REQUEST
SDG&E – UCAN DR-01, Q1-56
A.15-09-010
DATE RECEIVED: October 26, 2016
DATE RESPONDED: November 9, 2016

Request 24:

When Dr. Gershunov uses the term "flow aloft" in the statements excerpted below (Part I, page 8), is he referring to the modeled "flow aloft" or the actual "flow aloft?" Please also define the altitude or pressure surface that corresponds to "flow aloft?"

"However, there is a natural connection between observed gusts and modeled (instantaneous) winds, both being representative of the flow aloft. Results of our own research support this reasoning as the model winds are much more in-line with the observed gusts at most meteorological stations over our region than with observed sustained winds. The reason for this two-fold: 1) observed gusts are more representative of the flow aloft and 2) modeled near- surface winds are derived directly from the flow aloft."

UCAN's Response 24:

For these purposes, flow aloft can be defined as flow at the lowest model level where winds are computed prognostically, i.e. dynamically rather than diagnosed by a boundary layer parameterization from winds aloft, as is done for 10m winds. In the CaRD10 configuration of the RSM, this vertical level corresponds to 995mb pressure level. It is worth noting that the 995mb level is roughly consistent with the 250m level from the WRF model chosen by Dr. Peterka for input into his wind tunnel experiments.

SDG&E DATA REQUEST
SDG&E – UCAN DR-01, Q1-56
A.15-09-010
DATE RECEIVED: October 26, 2016
DATE RESPONDED: November 9, 2016

Request 25:

Please explain and provide all support for the following assertions of Dr. Gershunov (Part I, page 9):

"Winds aloft, however, are much less sensitive to model resolution and not at all sensitive to the assumptions involved in parameterizations..."

UCAN's Response 25:

Winds aloft occur far enough above the surface to be less impacted by surface characteristics compared to near surface winds. Such surface characteristics include fine scale terrain features, vegetation and other obstructions. Modeled winds aloft, therefore, are less sensitive to these sub-grid-scale features not resolved on the model grid (any model grid) and should therefore be more realistic than near-surface winds estimated by mesoscale models. Modeled winds aloft do not depend on boundary layer parameterization choice as they are computed prognostically, without the use of boundary layer parameterization.

Support for this view is also provided by Dr. Peterka, who, in his testimony, preferred to use wind tunnel experiments forced with winds at 250m ("aloft") as input into his wind tunnel experiments. Dr. Coen, in her testimony, critiques Dr. Peterka's wind tunnel experiments.

Dr. Gershunov's approach was to put more value in estimating the gusts, which are less sensitive to terrain details and obstructions and small fluctuations in height near the surface.

SDG&E DATA REQUEST
SDG&E – UCAN DR-01, Q1-56
A.15-09-010
DATE RECEIVED: October 26, 2016
DATE RESPONDED: November 9, 2016

Request 26:

Other than the source cited (e.g. Raphael, M. N., 2003), please provide all support for the following assertions of Dr. Gershunov (Part I, page 9):

"This synoptic-scale high pressure centered approximately over the Four Corners region has been traditionally viewed as the only cause of SAWs."

UCAN's Response 26:

UCAN objects to the term "all" support as it is overbroad and unduly burdensome to provide, and UCAN therefore objects to this question on the grounds set forth in general objections 2 & 3. Subject to these objections UCAN answers as follows:

This traditional view is, for example, promulgated by the textbook of Aguado and Burt (2010). It is also explained in the article on Santa Ana winds by Hughes and Hall (2010), which goes on to promote a more nuanced view on the causes of Santa Ana winds, suggesting that a thermodynamic mechanism is prominently at play, which is the reason that SAWs fall under the classification of katabatic winds as opposed to foehn- or Chinook-type winds.

Aguado, Edward, and James E. Burt. Understanding Weather & Climate, 5th edition. Upper Saddle River, NJ: Pearson/Prentice Hall, 2010.

Hughes, M., and A. Hall, 2010: Local and synoptic mechanisms causing Southern California's Santa Ana winds. Climate Dynamics, 34, 847–857, doi:10.1007/s00382-009-0650-4.

SDG&E DATA REQUEST
SDG&E – UCAN DR-01, Q1-56
A.15-09-010
DATE RECEIVED: October 26, 2016
DATE RESPONDED: November 9, 2016

Request 27:

Please provide the results of the following analysis referenced by Dr. Gershunov, but only for those stations that are in San Diego County: "Guzman Morales et al. (2016) validated CaRD10 winds as well as SAWs against observed winds and gusts at 85 available stations." See Part II, page 10.

UCAN's Response 27:

This result was reported in Guzman Morales et al. (2016) and described in the online Supplementary Information to that published article, which was provided as Attachment 4 to Part 2 of Dr. Gershunov's served testimony. See, specifically, Figures S1 and S2 and Section S2.

http://onlinelibrary.wiley.com/doi/10.1002/2016GL067887/abstract;jsessionid=D596DB5ABC1402529546058680C5D15E.f04t01

SDG&E DATA REQUEST
SDG&E – UCAN DR-01, Q1-56
A.15-09-010
DATE RECEIVED: October 26, 2016
DATE RESPONDED: November 9, 2016

Request 28:

Please confirm the data source for each of the blue and green curves in Figure 3 (Part II, page 12). The descriptions of Figure 3 define the blue and green curve as wind observations from Julian RAWS, yet the plots appear to show data from different RAWS.

UCAN's Response 28:

UCAN will be submitting an Errata to this section of testimony as this should have read "at each of the RAWS stations shown" rather than "at the Julian RAWS". The specific RAWS stations are named in the titles to each of the figure panels.

SDG&E DATA REQUEST
SDG&E – UCAN DR-01, Q1-56
A.15-09-010
DATE RECEIVED: October 26, 2016
DATE RESPONDED: November 9, 2016

Request 29:

Do the terrain descriptions given for each RAWS in Figures 3 & 4 by Dr. Gershunov describe the model terrain or the actual terrain (Part II, page 12 & 13)?

UCAN's Response 29:

They describe the actual terrain smoothed to the 10x10 model resolution as described in Part 2 of Dr. Gershunov's testimony. See legend to Figure 1 on page 6.

SDG&E DATA REQUEST
SDG&E – UCAN DR-01, Q1-56
A.15-09-010
DATE RECEIVED: October 26, 2016
DATE RESPONDED: November 9, 2016

Request 30:

Please provide the same plots found in Figures 3 & 4 for the Potrero RAWS (Part II, page 12).

UCAN's Response 30:

UCAN objects to this question on the grounds set forth in general objection #9. UCAN notes that to provide an answer to this question would require Dr. Gershunov to conduct additional analysis to produce a document that does not presently exist.

SDG&E DATA REQUEST
SDG&E – UCAN DR-01, Q1-56
A.15-09-010
DATE RECEIVED: October 26, 2016
DATE RESPONDED: November 9, 2016

Request 31:

Please provide the data used to generate the plots in Figure 5 (Part II, page 17).

UCAN's Response 31:

These data are provided in 2 Attachments to this data response.

SDG&E DATA REQUEST
SDG&E – UCAN DR-01, Q1-56
A.15-09-010
DATE RECEIVED: October 26, 2016
DATE RESPONDED: November 9, 2016

Request 32:

With regards to the estimated peak wind gust of ~57 mph at the location of the Witch Ignition Point, were there any adjustments made to the model output to come up with that estimate? Or does the maximum estimated wind gust of ~57 mph represent the maximum CaD10 instantaneous 10m wind speed for that particular grid cell? (Part II, page 24)

UCAN's Response 32:

No adjustments were made to model output as it was determined that CaRD10 instantaneous 10m winds overestimate sustained near-surface winds by the gust factor. The model instantaneous wind is therefore taken to most closely approximate the observed gusts.

SDG&E DATA REQUEST
SDG&E – UCAN DR-01, Q1-56
A.15-09-010
DATE RECEIVED: October 26, 2016
DATE RESPONDED: November 9, 2016

Request 33:

Is it Dr. Gershunov's opinion that the estimated peak wind gust of ~57 mph at the 10 km grid cell representing the ignition point of the Witch Fire is representative of every physical location within that grid cell (Part II, page 24)? Why or why not?

UCAN's Response 33:

As explained in his testimony, Part 2, this is an approximate estimate. Actual local wind speeds within the area covered by any particular grid cell can vary. The 10 km grid does not resolve local topography, but, as he has demonstrated in Part 2 of his testimony, winds modeled at that resolution do correspond very well to locally observed gusts at the most relevant meteorological stations (see Dr. Gershunov's response to question 20 above) for the Fire Locations. Also, because some locations fall on the edge rather than in the center of a model grid cell, Dr. Gershunov chose among neighboring grid cells to represent specific locations not only because the grid cell contains that location, but for the best topographic similarity among neighboring grid cells with the given location. So it happens with the Witch Fire location, that the best topographic similarity is provided not by the grid cell containing the location, but by its neighboring grid cell to the southwest that provides the best compromise between proximity and the closest topographic similarity with the Witch Fire location. Modeled winds at this location, grid [14,12], chosen to represent the Witch Fire ignition site were faster than those modeled at the grid cell that actually peripherally contained the given location, but that was at its center, more topographically dissimilar to it.

It is Dr. Gershunov's opinion that model winds thus matched by grid cell proximity and topography to given locations and validated at several relevant locations, where observations exist for the Santa Ana event in question, can be reasonably assumed to be a sensible approximation to gusts at unobserved locations within a particular grid cell, especially those on west-facing slopes of significant terrain, including the locations of the Fire ignitions in question. I am also of the opinion that higher resolution without validation does not guarantee a better approximation of local winds. For example, Cao and Fovell (2016), with respect to a different Santa Ana wind event they considered, state of their higher resolution modeling that "WRF has skill in capturing the evolution and magnitude of the event at most locations, although most model configurations overpredict the observed sustained wind and the forecast bias is itself biased."

SDG&E DATA REQUEST
SDG&E – UCAN DR-01, Q1-56
A.15-09-010
DATE RECEIVED: October 26, 2016
DATE RESPONDED: November 9, 2016

Request 34:

Are the estimated return periods given in the Summary Table (Part II, page 3) and Table 2 (Part II, page 24) based entirely on the 1948-2012 CaRD10 dataset?

UCAN's Response 34:

Yes. They are based on the validated CaRD10 data set.

SDG&E DATA REQUEST
SDG&E – UCAN DR-01, Q1-56
A.15-09-010
DATE RECEIVED: October 26, 2016
DATE RESPONDED: November 9, 2016

Request 35:

Please provide the CaRD10 estimated peak wind gust for October 2007 for the grid cell(s) representative of Wynola, CA, particularly along highway 78/79 between Orchard Ln and Williams Ranch Rd.

UCAN's Response 35:

UCAN objects to this question on the grounds set forth in general objection #3. No exact coordinates were provided. Subject to this objection UCAN answers as follows:

The transect on highway 78/79 between Orchard Ln and Williams Ranch Rd appears to be about 3 miles long. The closest CaRD10 grid cell to the midpoint, 33.0780 N, 116.6229 W, is [15,13]. Peak model wind for the event in question at this grid cell was 39.1 mph.

SDG&E DATA REQUEST
SDG&E – UCAN DR-01, Q1-56
A.15-09-010
DATE RECEIVED: October 26, 2016
DATE RESPONDED: November 9, 2016

Request 36:

Please provide the results of the analysis mentioned in the following statement for all stations in San Diego County: "Guzman Morales et al. (2016) validated CaRD10 winds as well as SAWs against observed winds and gusts at 85 available stations." See Part II, page 10.

UCAN's Response 36:

This result was reported in Guzman Morales et al. (2016) and described in the online Supplementary Information to that published article, which was provided as Attachment 4 to Part 2 of Dr. Gershunov's served testimony. See, specifically, Figures S1 and S2 and Section S2.

Should SDG&E be asking Dr. Gershunov to perform additional analysis UCAN objects to this question on the grounds set forth in general objection #9.

SDG&E DATA REQUEST
SDG&E – UCAN DR-01, Q1-56
A.15-09-010
DATE RECEIVED: October 26, 2016
DATE RESPONDED: November 9, 2016

Request 37:

With respect to Dr. Gershunov's CaRD10 analysis of Santa Ana winds, is SDG&E's West Santa Ysabel weather station (WSY) located in the same grid cell as the ignition point of the Witch Fire? For reference, the WSY weather station is located at 33.0868 -116.6897.

UCAN's Response 37:

Yes, technically, they are located within the same model grid, but Dr. Gershunov chose a neighboring grid to represent the Witch Fire location based on topographic similarity. See answer to question 33 above.

SDG&E DATA REQUEST
SDG&E – UCAN DR-01, Q1-56
A.15-09-010
DATE RECEIVED: October 26, 2016
DATE RESPONDED: November 9, 2016

Request 38:

With respect to Dr. Gershunov's CaRD10 analysis of Santa Ana winds, is SDG&E's Dye Mountain weather station (DYE) located in the same grid cell as the ignition point of the Witch Fire? For reference, the DYE weather station is located at 33.068817 -116.709897.

UCAN's Response 38:

Yes, these points are technically located within the same model grid cell, again with the caveat that Dr. Gershunov choose grid cells to represent specific points based on a combination of grid cell proximity and topographic similarity to a given point.

SDG&E DATA REQUEST
SDG&E – UCAN DR-01, Q1-56
A.15-09-010
DATE RECEIVED: October 26, 2016
DATE RESPONDED: November 9, 2016

Request 39:

Has Dr. Gershunov made any attempt to validate the results of his CaRD10 analysis against observations from SDG&E's weather stations for more recent events (since 2010)? If yes, please provide the results. If not, why not?

UCAN's Response 39:

No. The validation presented in Guzman Morales et al. (2016) used public domain stations with the longest records available. The validation he presented in his testimony (Part 2) focused on the relevant stations that were operational at the time of the October 2007 Fires.

SDG&E DATA REQUEST
SDG&E – UCAN DR-01, Q1-56
A.15-09-010
DATE RECEIVED: October 26, 2016
DATE RESPONDED: November 9, 2016
DATA REQUESTS TO DR. JANICE COEN

Request 40:

Please provide copies of all of prior written or oral testimony, in any proceeding.

UCAN's Response 40:

I have not previously provided testimony.

SDG&E DATA REQUEST
SDG&E – UCAN DR-01, Q1-56
A.15-09-010
DATE RECEIVED: October 26, 2016
DATE RESPONDED: November 9, 2016

Request 41:

Has Dr. Coen ever provided any opinions, reports or testimony, whether written or oral, in any tribunal or judicial form of any kind that concerned in any way the 2007 San Diego wildfires? If so, please provide a copy of:
a. All such opinions, reports or testimony
b. Any opinions, reports or testimony that either opposed or agreed with all or a portion of Dr. Coen's position
c. Any decisions or rulings by such tribunal or judicial forum

UCAN's Response 41:

No.

SDG&E DATA REQUEST
SDG&E – UCAN DR-01, Q1-56
A.15-09-010
DATE RECEIVED: October 26, 2016
DATE RESPONDED: November 9, 2016

Request 42:

Please provide all of Dr. Coen's workpapers.

UCAN's Response 42:

Dr. Coen did not generate workpapers outside of her written testimony.

SDG&E DATA REQUEST
SDG&E – UCAN DR-01, Q1-56
A.15-09-010
DATE RECEIVED: October 26, 2016
DATE RESPONDED: November 9, 2016

Request 43:

Please list all persons with whom Dr. Coen consulted regarding her testimony.

UCAN's Response 43:

This question has been withdrawn by SDG&E.

SDG&E DATA REQUEST
SDG&E – UCAN DR-01, Q1-56
A.15-09-010
DATE RECEIVED: October 26, 2016
DATE RESPONDED: November 9, 2016

Request 44:

Please provide a copy of the References listed in Appendix 1 to Dr. Coen's testimony.

UCAN's Response 44:

With the exception of the books by Whiteman and Stensrud and the article by Guzman Morales, which has been provided as an attachment to Dr. Gershunov's testimony, all other references have been uploaded to SDG&E's Sharepoint website

SDG&E DATA REQUEST
SDG&E – UCAN DR-01, Q1-56
A.15-09-010
DATE RECEIVED: October 26, 2016
DATE RESPONDED: November 9, 2016

Request 45:

Please provide a copy of each of the Refereed Publications, Non-Refereed Publications and Invited Presentations listed in Appendix 3 to Dr. Coen's testimony, or of any other publications, that relate to:
a. Santa Ana winds
b. the climate in Southern California
c. Southern California wildfires
d. Southern California fire weather
e. mesoscale modeling
f. climate modeling
g. RAWS or ASOS stations

UCAN's Response 45:

All publications, and Invited Presentations have been uploaded to SDG&E's Sharepoint website

SDG&E DATA REQUEST
SDG&E – UCAN DR-01, Q1-56
A.15-09-010
DATE RECEIVED: October 26, 2016
DATE RESPONDED: November 9, 2016

Request 46:

Has Dr. Coen reviewed Dr. Gershunov's testimony in this proceeding? If not, why not?

UCAN's Response 46:

Yes.

SDG&E DATA REQUEST
SDG&E – UCAN DR-01, Q1-56
A.15-09-010
DATE RECEIVED: October 26, 2016
DATE RESPONDED: November 9, 2016

Request 47:

Are there any statements, conclusions or analyses in the testimony of any of the following witnesses in this proceeding with which Dr. Coen disagrees? If so, please identify the statement, conclusion or analysis and describe the basis for Dr. Coen's disagreement.
a. Mr. Nils Stannik (ORA)

b. Dr. Matthew Rahn (POC)

c. Ms. Jennifer Betts (SDCAN)

d. Dr. Joseph Mitchell (MGRA)

e. Dr. Alexander Gershunov (UCAN)

UCAN's Response 47:

This question has been withdrawn by SDG&E.

SDG&E DATA REQUEST
SDG&E – UCAN DR-01, Q1-56
A.15-09-010
DATE RECEIVED: October 26, 2016
DATE RESPONDED: November 9, 2016

Request 48:

Please explain and provide all support for the following assertion of Dr. Coen (page 13): "However, compared to other flow regimes, it is particularly unlikely to conform to the vertical profiles used by SDG&E witness Peterka as well as Fovell and Cao (2016.)"

UCAN's Response 48:

The idea is that in neutrally stratified air flowing over a flat, frictional surface, air molecules near the surface would be slowed by friction with the surface, with less impact on air higher up. After traveling over the surface, the vertical profile of the air's horizontal velocity would eventually establish a general profile, described by either the log profile or power law. As stated in her testimony, (Lines 196-296), the assumptions made in deriving those vertical profiles "include that there are no underlying trends such as increases or decreases in ambient wind speed (i.e. the flow is "stationary"), that the conditions are horizontally homogeneous (for example, the land surface does not vary in space), and that the terrain is flat." These formula "are only strictly applicable in those conditions" (Lines 227-228). If conditions vary from those that meet these assumptions, the formula may not apply or, if used, not be accurate. As noted, these are widely used in atmospheric science without question where some or all of these conditions may not be satisfied. However, in these conditions, all three conditions are violated - SDG&E witness Peterka's figure in Appendix 13 shows that his mean speed varies depending on the time over which it is averaged suggesting there is such a trend as one would expect as the large-scale weather pattern changes, the land surface varies in space, and the terrain is not flat but very complex. In addition, gustiness in windstorms has been attributed to high energy gusts being driven down to the surface from breaking waves above (rather than moving along a flat frictional surface).

As Dr. Coen wrote, "Overall, one reasonably expects that in a situation where the background conditions are not changing, air moving over a flat, uniform surface may develop a vertical profile where the horizontal wind speed at the surface or at the top of a surface (such as a tree canopy) is zero and it increases with height throughout the boundary layer according to one of these formulas." (Lines 200-204) It is not reasonable to expect such formulas to apply in these very different conditions where none of these criteria were met and where gusts may have descended rapidly to the surface on a trajectory from above.

SDG&E DATA REQUEST
SDG&E – UCAN DR-01, Q1-56
A.15-09-010
DATE RECEIVED: October 26, 2016
DATE RESPONDED: November 9, 2016

Request 49:

Please identify the events in Table 1 (pages 23-24) that correspond to Santa Ana wind conditions.

UCAN's Response 49:

Dr. Coen notes that the data reported in Table 1 were "peak daily wind gusts" which were not provided with a specific time of occurrence. In addition, no accompanying surface station fields indicate whether a Santa Ana was occurring and if one was, whether a particular station was affected. However, the previously referenced work of Guzman Morales et al. (2016) developed an automated methodology to detect Santa Ana winds in hourly data, modeled and observed, based on wind speed and direction. Using their analysis, the data for which extend back to 1948, each entry in Dr. Coen's Table 1 was compared against their regional database. A "Y" in Column 2 – which occurred in 21 of the 34 entries - indicates that, according to Guzman Morales et al.'s database, Santa Ana winds occurred in the region on the day of the listed peak daily gust.

Event	Date (YYYYMMDD)	Does Santa Ana Wind Regional Index indicates Santa Anas were occurring on this date?
1	19950329	Y
2	20070518	N
3	19960723	N
4	19580401	N
5	20041229	Y
6	20070304	Y
7	19950103	Y
8	19880117	N
9	19880117	N
10	19491019	Y
11	20041229	Y
12	19540316	N
13	19590106	Y
14	19830301	Y
15	19581116	Y
16	19540119	N
17	19520307	Y
18	19521114	Y
19	19880217	Y
20	19800129	Y
21	19580403	N
22	19590106	Y
23	19580306	N
24	19800129	Y

SDG&E DATA REQUEST
SDG&E – UCAN DR-01, Q1-56
A.15-09-010
DATE RECEIVED: October 26, 2016
DATE RESPONDED: November 9, 2016

25	19760415	N
26	19780210	N
27	19800306	N
28	19860310	Y
29	19950104	Y
30	19530301	Y
31	19520302	N
32	19521115	Y
33	19911130	Y
34	19871213	Y

SDG&E DATA REQUEST
SDG&E – UCAN DR-01, Q1-56
A.15-09-010
DATE RECEIVED: October 26, 2016
DATE RESPONDED: November 9, 2016

Request 50:

Please identify each Station in Table 1 that is close enough, in Dr. Coen's judgment, to an ignition point to either the Witch, Rice or Guejito Fires to be representative of the wind gusts experienced in the vicinity of those ignition points.

UCAN's Response 50:

The question contains the included assumption that closer locations are more similar. As stated in her testimony, airflow at a point (such as the fires' ignition locations) will vary locally according to the flow parameters and local topography, and so associations between the flow characteristics of two points are not expected to be sound. Thus, she does not believe that there is a meaningful answer to this question.

SDG&E DATA REQUEST
SDG&E – UCAN DR-01, Q1-56
A.15-09-010
DATE RECEIVED: October 26, 2016
DATE RESPONDED: November 9, 2016

Request 51:

How do historical maximum wind gusts along the immediate coast (as provided in Table 1, page 23) measured primarily during winter storms relate to historical wind gusts in the areas where the Witch, Guejito, and Rice fires ignited?

UCAN's Response 51:

Dr. Coen notes that this statement contains the included assertion (provided without supporting evidence) that the peak daily wind gusts primarily occurred during winter storms however, as noted in her response to Question #49, 21 of 34 events occurred on days when Santa Ana winds occurred in the region.

The dataset from which Table 1 was compiled does not contain station data from eastern San Diego County thus there are no similar data on peak daily wind gusts in the areas where the Witch, Guejito, and Rice fires ignited with which to make that assessment.

SDG&E DATA REQUEST
SDG&E – UCAN DR-01, Q1-56
A.15-09-010
DATE RECEIVED: October 26, 2016
DATE RESPONDED: November 9, 2016

Request 52:

What was the resolution of the model Dr. Coen used to investigate the atmospheric conditions associated with the 2012 High Park fire (page 7 & 8)? Why was that resolution chosen?

UCAN's Response 52:

The primary experiment used horizontal grid spacing of 123 m in the innermost of 5 domains. (The five nested, interacting domains had horizontal grid spacing 10 km, 3.33 km, 1.11 km, 370 m, and 123 m.) Using extremely high grid spacing of approximately 100-200 m in her coupled weather-wildland fire modeling studies enables her to better capture fine-scale atmospheric circulations in complex terrain and fire-induced winds that shape the behavior of a wildland fire - in this case, for example, the sharp gradients in potential temperature in the breaking wave and fine-scale circulations within mountain valleys. In additional experiments testing the effect of fuel moisture, 4 nested domains refining horizontal grid spacing only to 370 m were used. These captured some of the wave motion but produced weaker surface winds.

SDG&E DATA REQUEST
SDG&E – UCAN DR-01, Q1-56
A.15-09-010
DATE RECEIVED: October 26, 2016
DATE RESPONDED: November 9, 2016

Request 53:

With respect to the following statement, are there specific downwind locations or weather stations along the Front Range of the Rockies that are known to be prone to gusty winds during downslope wind storms: "While some downwind locations may be prone to gusts, nearby locations may be still or flowing in the opposite direction." See Coen Testimony, page 9. If so, please identify the location(s).

UCAN's Response 53:

As stated in her testimony, a combination of factors determines the airflow downwind of a topographic feature and as the large-scale weather causes the orientation of wind to change with respect to a particular feature, the location of strong winds and gusts (or stagnant locations or wind reversals) is dependent on the event and during that event, will change with time. However, as windstorms occur when ambient winds come from between the west to northwest direction, some locations may more commonly be exposed (or sheltered). Locally, the weather station at the National Center for Atmospheric Research's Mesa Lab is sometimes noted as experiencing strong winds and gusts at times during windstorm events.

SDG&E DATA REQUEST
SDG&E – UCAN DR-01, Q1-56
A.15-09-010
DATE RECEIVED: October 26, 2016
DATE RESPONDED: November 9, 2016

Request 54:

Please explain why Dr. Coen chose an extremely high resolution (~100-200 m) to model the atmospheric conditions associated with the Esperanza wildfire? (page 10)

UCAN's Response:

Using extremely high grid spacing of approximately 100-200 m in her coupled weather-wildland fire modeling studies enabled her to better capture fine-scale atmospheric circulations in complex terrain and fire-induced winds that shape the behavior of a wildland fire.

SDG&E DATA REQUEST
SDG&E – UCAN DR-01, Q1-56
A.15-09-010
DATE RECEIVED: October 26, 2016
DATE RESPONDED: November 9, 2016

Request 55:

Has Dr. Coen ever visited the backcountry of San Diego County? If so, has Dr. Coen ever experienced Santa Ana winds in the backcountry of San Diego County? The "backcountry" in this request refers to all areas east of Valley Center, east of Ramona, and east of Alpine.

UCAN's Response 55:

Yes, She has visited the backcountry of San Diego County. She does not recall the nature of the winds at that time.

SDG&E DATA REQUEST
SDG&E – UCAN DR-01, Q1-56
A.15-09-010
DATE RECEIVED: October 26, 2016
DATE RESPONDED: November 9, 2016

Request 56:

Has Dr. Coen ever experienced downslope windstorms along the Front Range of the Rockies? If so, how often?

UCAN's Response 56:

Yes. When they occur (usually several times per year), they commonly impact Boulder, Colorado, where She has worked and lived since 1992.

Appendix 9

APPENDIX 9

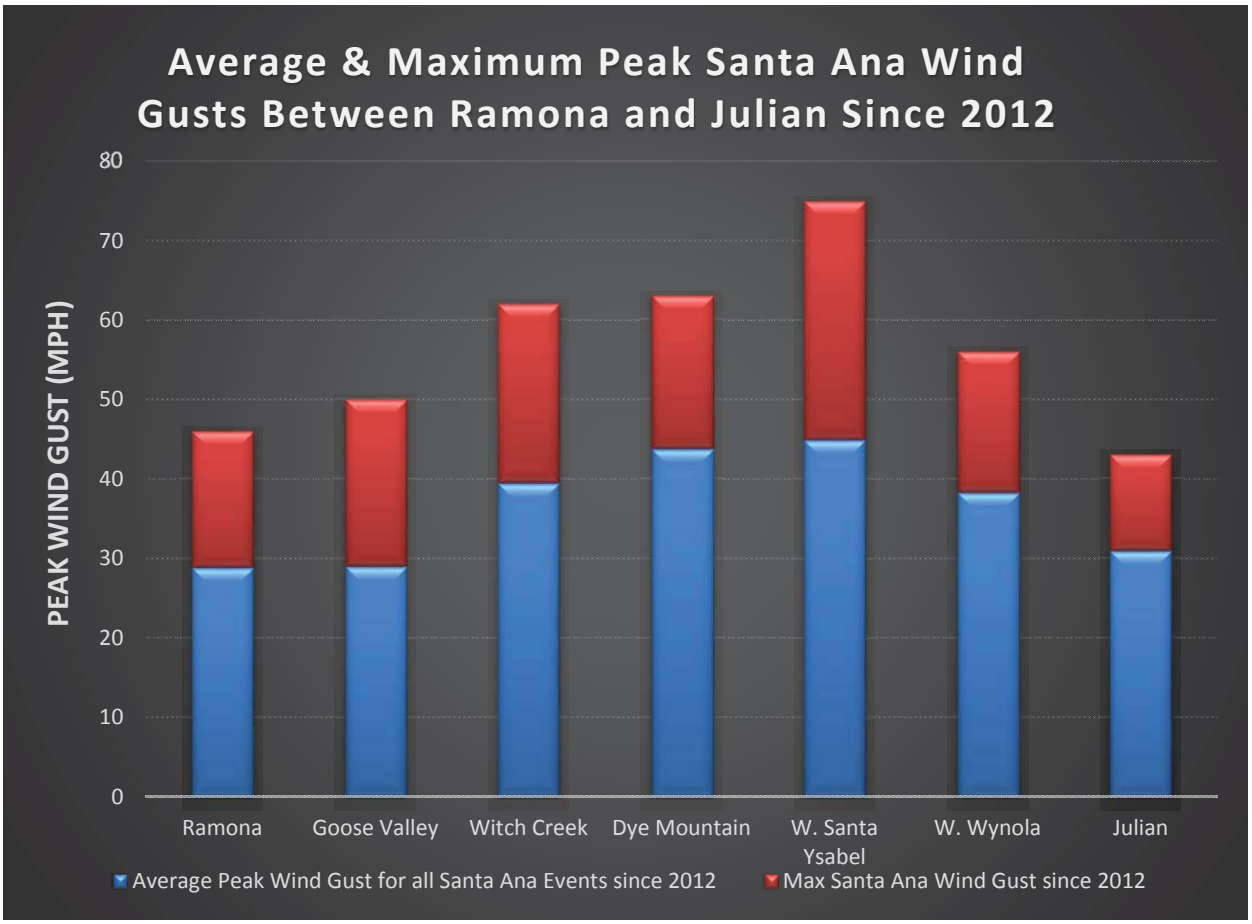

The above bar chart shows the average peak wind gust and maximum peak wind gust for seven weather stations along a line from Ramona ASOS to Julian RAWS for 42 Santa Ana Wind events since 2012. The Witch Fire ignition point is in close proximity to W. Santa Ysabel.

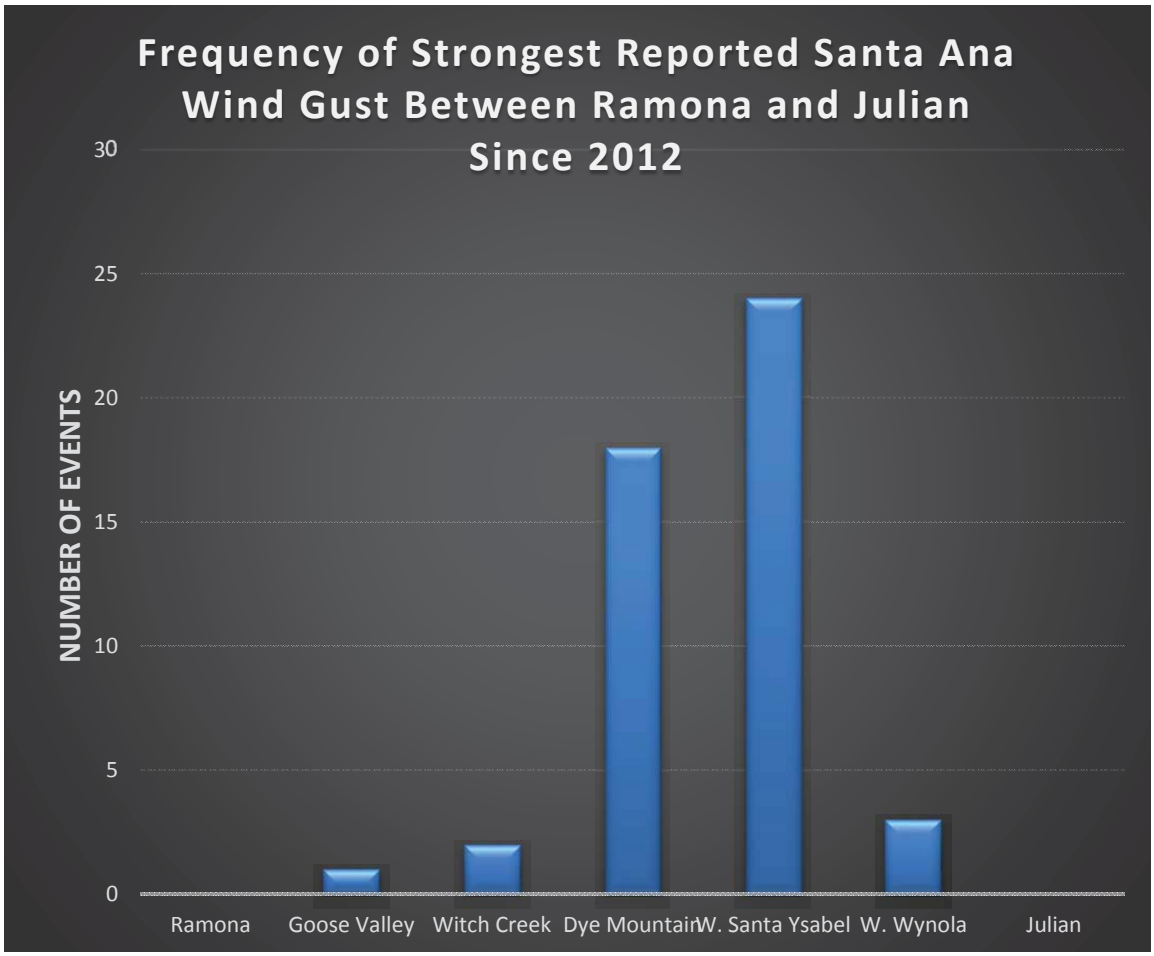

The above bar chart shows the number of times each weather station has recorded the strongest peak wind gust for 42 Santa Ana Wind events since 2012. These seven weather stations are located along a line from Ramona ASOS to Julian RAWS. The Witch Fire ignition point is in close proximity to W. Santa Ysabel and Dye Mountain. If there was a tie for strongest wind gust between stations during a single event, both stations were included in the count.